Nuclear Waste Policy Act
(Section 113)

GEOCHEMISTRY

Consultation Draft

Site Characterization Plan

Yucca Mountain Site, Nevada Research and Development Area, Nevada

Volume II

PART A

January 1988

U.S. Department of Energy
Office of Civilian Radioactive Waste Management
Washington, DC 20585

8802190056   88/01/31   J/928
B4

Chapter 4

GEOCHEMISTRY

INTRODUCTION

This chapter contains geochemical information about the Yucca Mountain site. The chapter references plans for continued collection of geochemical data as part of the site characterization program. Details of these plans are contained in Section 8.3.1.3.

This section provides a brief introduction to the geochemistry chapter. It contains discussions about the following: (1) the concerns that drive the collection of geochemical data, (2) the methods by which data presently available have been collected, (3) concepts of the site that influence geochemical data collection, and (4) the status of present data and models.

In addition to the discussions in this chapter, the following related concerns are addressed in Chapter 7:

1. Anticipated interactions among the waste form, engineered barriers, and environment.

2. The chemical composition and form of the waste.

3. The solubility of the waste form in ground water.

4. The radionuclide species released by leaching from the waste form.

5. Anticipated chemical and mineralogical compositions of natural and engineered barriers.

6. Anticipated interactions among the waste form, water, vapor, gas, and rock.

ISSUES

Geochemical information generated during the characterization of the Yucca Mountain site will play an important role in resolving questions about the ability of the site to isolate radioactive wastes from the accessible environment. This issue is addressed by Key Issue 1 (Will the mined geologic disposal system at Yucca Mountain isolate the radioactive waste from the accessible environment after closure in accordance with the requirements set forth in 40 CFR Part 191, 10 CFR Part 60, and 10 CFR Part 960?) (Section 8.2). Geochemical information is specifically addressed by Characterization Program 8.3.1.3 (geochemistry).

In addition, geochemical data will be used to evaluate the Yucca Mountain site in terms of the siting guidelines outlined in 10 CFR Part 960 and the siting criteria in 10 CFR Part 60. In particular, two issues will require site characterization data for their resolution: Issue 1.8 (Can the demonstrations for favorable and potentially adverse conditions be made as

required by 10 CFR 60.122?) (Section 8.3.5.17) and Issue 1.9 (Can the higher level findings required by 10 CFR Part 960 be made for qualifying conditions on the postclosure system guideline and the disqualifying and qualifying conditions on the technical guidelines for geohydrology, geochemistry, rock characteristics, climate changes, erosion, dissolution, tectonics, and human interference; and can the comparative evaluations be made by 10 CFR 960.3-1-5?) (Section 8.3.5.18).

Specific to the geochemistry task are three favorable conditions and four potentially adverse conditions (10 CFR 60.122):

Favorable conditions:

1. The nature and rates of tectonic, hydrogeologic, geochemical, and geomorphic processes (or any of such processes) operating within the geologic setting during the Quaternary Period, when projected, would not affect or would favorably affect the ability of the geologic repository to isolate the waste.

2. Geochemical conditions that

   a. Promote precipitation or sorption of radionuclides.

   b. Inhibit the formation of particulates, colloids, and inorganic and organic complexes that increase the mobility of radionuclides.

   c. Inhibit the transport of radionuclides by particulates, colloids, and complexes.

3. Mineral assemblages that, when subjected to anticipated thermal loading, will remain unaltered or alter to mineral assemblages having equal or increased capacity to inhibit radionuclide migration.

Potentially adverse conditions:

1. Ground-water conditions in the host rock, including chemical composition, high ionic strength or ranges of Eh-pH, that could increase the solubility or chemical reactivity of the engineered barrier system.

2. Geochemical processes that would reduce sorption of radionuclides, result in degradation of the rock strength, or adversely affect the performance of the engineered barrier system.

3. Ground-water conditions in the host rock that are not reducing.

4. Potential for the movement of radionuclides in a gaseous state through air-filled pore spaces of an unsaturated geologic medium to the accessible environment.

PAST DATA COLLECTION

The Yucca Mountain site was one of a number of sites on and near the Nevada Test Site (NTS) in southern Nevada that was considered as a potential location for a waste repository. Geochemical information had been collected about this area for some time as part of the nuclear testing program at the NTS. The information presently available is a combination of data obtained before Yucca Mountain was considered as a potential waste repository site (before 1977) and data that have been collected as part of the Nevada Nuclear Waste Storage Investigations (NNWSI) Project. Essentially all the data presented here have been collected as part of the NNWSI Project. Information obtained from other sources has primarily been used to aid interpretation or for confirmation of more recent data.

The geochemical data collected as part of the NNWSI Project have been obtained by an examination of samples taken from the surface or at depth from Yucca Mountain and vicinity and by laboratory experiments using these samples and similar materials. Mineralogy and petrology samples have come from drill cores, sidewall samples, drill cuttings, and surface outcrops. Ground-water samples have come from wells that tap the saturated zone at and near Yucca Mountain. Data collected for other aspects of site characterization are also used or referenced in this chapter. This is particularly true of Chapter 3, Hydrology, which is often referenced. Data describing the geochemistry of the Yucca Mountain site and the effects of geochemistry on radionuclide transport are contained in Section 4.1. In addition, assessments of the stability of geochemical conditions (Section 4.4) and of the effects of waste emplacement on geochemical conditions (Section 4.2) are being conducted to ensure that changes in geochemical conditions will not adversely affect the site. These assessments are primarily obtained from experiments that simulate expected conditions and from analyses of the effects of these conditions on the geochemistry of the site. Natural systems and large-scale field tests (Section 4.3) are also being studied to provide information over longer times and larger distances than can be obtained in the laboratory. Data obtained from these studies will be important for confirmation of conceptual models and for validation of mathematical models of important processes.

The geochemical characterization of the Yucca Mountain site is not complete. The discussions presented in this chapter raise a number of questions or identify areas where further information is needed. Specific plans for answering these questions and collecting the information needed are described in Section 8.3.1.3. Specific information needs relevant to geochemistry are also identified in Section 4.5.3 that summarizes the geochemical investigations to be performed during site characterization to address the information needs described in this chapter.

CONCEPTS OF THE SITE THAT INFLUENCE GEOCHEMICAL DATA COLLECTION

A definition of geochemical data needs depends on an understanding of the geochemical processes that affect radionuclide transport from the repository toward the accessible environment. A brief description of the present concepts of the site and of radionuclide transport processes that have influenced data collection is presented here to help orient the reader.

The Yucca Mountain site is composed mostly of ash-flow and ash-fall tuffs in a number of distinct cooling units (Section 4.1.1). The resulting mineralogy primarily reflects the original bulk chemical composition, the extent of devitrification and welding of individual units, and the variable interaction with water during alteration. Where water has contacted vitric tuff, secondary minerals such as zeolites and clays have generally formed from the alteration of glass. Ground water at and near the site is mainly a dilute, near-neutral, sodium-bicarbonate water (Section 4.1.2).

The potential repository location is in the unsaturated zone, in the lower welded and devitrified part of the Topopah Spring Member of the Paintbrush Tuff (Chapter 1). The most likely transport path for radionuclides either in solution or as particulates is in water that might move through the repository and toward the accessible environment. In the presently preferred conceptual model (Montazer and Wilson, 1984), water in the unsaturated zone moves generally downward toward the water table; however, some lateral movement may occur where the lateral permeability greatly exceeds the vertical permeability. Although vertical components of flow occur locally beneath the water table, flow in the saturated zone is dominantly lateral in southerly to southeasterly directions from Yucca Mountain (Section 3.9).

The following geochemical processes that affect the transport or retardation of radionuclides in water have been studied at Yucca Mountain: sorption, precipitation or dissolution, and physical processes like diffusion, dispersion, or filtration of particulates (Section 4.1.3). Sorption of radionuclides provides a potential geochemical barrier at the Yucca Mountain site. Sorption is likely to occur on the highly sorptive minerals, such as the zeolites and clays found between the repository and the water table and below the water table. Understanding sorption processes requires information about the mineralogy (Section 4.1.1) and ground-water chemistry (Section 4.1.2), and knowledge of flow characteristics, particularly the relative importance of matrix (porous) and fracture flow. It is probable that flow in both the matrixes and fractures occurs in the unsaturated zone as well as the saturated zone. However, matrix flow is probably the dominant mechanism in the unsaturated zone and fracture flow is probably dominant in the saturated zone (Chapter 1, DOE, 1986). Therefore, sorption data applicable to both matrix flow and fracture flow are being obtained (Section 4.1.3). Sorption measurements have been determined using Yucca Mountain tuff and ground-water samples for essentially all experiments.

Because the potential repository location is in the unsaturated zone, radionuclides such as carbon-14 and iodine-129 may be transported away from the repository in both the gas phase and the aqueous phase. Exchanges between the gas phase and the aqueous phase present in the rock pores may provide an effective retardation mechanism, and is a topic of investigation (Section 4.1.3.6).

The solubility of waste elements can influence their transport by limiting the concentrations of the elements dissolved in water. Solubility depends primarily on the chemistry of the specific element and the local water chemistry. Solubility measurements under conditions characteristic of the Yucca Mountain site, in combination with chemical equilibrium modeling, are being used to characterize waste element solubility (Section 4.1.3.4).

In addition to being dissolved in water, waste elements can also exist as particulates (colloids) or be sorbed onto particulates that are present in the water. The formation of natural colloids of waste elements is discussed in Section 4.1.3.4; plans to study particulate material that is naturally present in the water from Yucca Mountain and sorption of radionuclides on particulate material are outlined in Section 8.3.1.3.4.

The relative importance of physical processes, such as diffusion, dispersion, or filtration of particulates in the water, that influence radionuclide transport by retarding the radionuclides is also strongly dependent on local flow conditions. As previously noted, the relative importance of matrix flow versus fracture flow is still somewhat uncertain (Section 3.9). Physical processes associated with both matrix and fracture flow are being studied (Section 4.1.3). Matrix diffusion, in which radionuclides being transported by water in fractures can diffuse into water in the surrounding porous rock matrix, is one of the physical processes being given special attention (Section 4.1.3.5). This retardation mechanism may be important if fracture flow is significant along portions of the flow paths.

The concepts presented above will be formalized into a number of conceptual models as data are collected that confirm the physical and chemical descriptions of the site and the operation of the various geochemical processes. The detailed plans for this work are described in Section 8.3.1.3. In particular, geochemical models of the unsaturated and saturated zones (Section 8.3.1.3.7), a conceptual model of mineral evolution at Yucca Mountain (Section 8.3.1.3.3), and a predictive model of sorption as a function of mineral content of the tuff (Section 8.3.1.3.4), are being developed.

PRESENT STATE OF DATA AND MODELS

The development of an understanding of the geochemistry of the Yucca Mountain site is an iterative process in which data collection and analysis are combined with conceptual models. A detailed discussion of questions that still exist and of investigations can be obtained from the remainder of this chapter and from Section 8.3.1.3. However, there are a number of general comments that can be made about the present state of geochemical data and models for the site:

1. The water chemistry in the saturated zone has been well characterized, but ground-water samples are needed from the unsaturated zone. They will be obtained during construction of the exploratory shaft. A qualitative understanding exists of the mineralogical controls on ground-water composition.

2. The mineralogy and petrology, based on data from the existing drillholes, have been well characterized. Future work during construction of the exploratory shaft will provide additional data. However, characterization along flow paths away from the repository is not complete because flow-path definitions are uncertain and because there are few exploratory borings along potential pathways.

3. A conceptual model of mineral evolution is being developed. It must provide credible explanations of the present mineral distribution

and must be capable of predicting future mineral evolution due to natural processes and the thermal loading of the repository.

4. Sorption data have been collected using representative ground water and tuffs. An understanding of the chemistry that controls sorption exists in some cases but is uncertain for many waste elements, such as the actinides, which have complex aqueous chemistry.

5. Solubility data appropriate to Yucca Mountain are being collected. Chemical equilibrium modeling is being done but it is uncertain whether equilibrium models will be adequate. If not, kinetic models will be required.

6. Physical processes (i.e., dispersion, diffusion, advective processes) that affect radionuclide transport are understood qualitatively, but quantitative data are lacking. Radionuclide transport depends strongly on local ground-water flow characteristics, which are presently not well understood.

7. Radionuclide retardation by all processes along the flow paths to the accessible environment is being assessed by performing integrated transport calculations. This includes an analysis of significant interactions among thermal, hydrologic, chemical, and mechanical processes that could have an impact on the geochemistry of the site and the transport of radionuclides as particulates, pseudocolloids, and colloids at Yucca Mountain.

8. The potential for gaseous transport needs to be assessed. No quantitative assessment has been made yet and the mechanism for isotopic exchange and gas and liquid-solid exchange is uncertain at this time.

Experimental methods and measurement techniques used to obtain the data in this chapter are discussed in detail in the references from which the data were taken. Data quality and related data uncertainty are also discussed in the references. The types of data collected range from mineral types and distribution to specific measurements (e.g., sorption ratios and solubility measurements). In the case of measured sorption ratios, the experimental data uncertainty is included in the data tables.

4.1 GEOCHEMISTRY OF THE HOST ROCK AND SURROUNDING UNITS

4.1.1 MINERALOGY AND PETROLOGY

The mineralogic and petrologic characteristics of Yucca Mountain are important for defining the site conditions existing before repository construction and operation, and for predicting the site response to disruption. Mineral distributions as a function of depth and distance from the potential repository are also important for calculating overall radionuclide retardation by sorption. Because sorptive behavior and ground-water chemistry depend on mineralogy, this chapter begins with a description of the site

mineralogy (Sections 4.1.1.1 to 4.1.1.3). Section 4.1.1.4 describes mineral stability at the site.

4.1.1.1 General description of the host rock and surrounding units

The most abundant rock type at Yucca Mountain is ash-flow tuff. The mineralogy of an ash-flow tuff is developed in several episodes of crystallization (Lipman et al., 1966; Byers, 1985). Crystallization from magma occurs primarily within the magma chamber before eruption. During this episode, phenocrysts (most commonly consisting of feldspars, quartz, and biotite) form along with less abundant minor and accessory minerals like hornblende, pyroxene, iron-titanium oxide minerals, sphene, allanite, and zircon. In the second episode of crystallization, glass shards and pumice commonly devitrify to form alkali feldspars and silica minerals. In portions of the ash flow where vapor concentrations are high, vapor-phase crystallization results in the growth of euhedral crystals of tridymite, cristobalite, and alkali feldspars in gas pockets. During vapor-phase crystallization, some rare silicate and oxide minerals are formed (e.g., andalusite and pseudobrookite) (Vaniman et al., 1984; Bish, 1987). Vapor-phase crystallization is common in the proposed host rock, the Topopah Spring Member of the Paintbrush Tuff (Lipman et al., 1966), where several zones develop spherulitic or lithophysal cavities in which pseudobrookite, rutile, manganese-rich augite, pargasite, and biotite have grown from vapor along with the more abundant alkali feldspars, tridymite, and cristobalite. In the third episode of crystallization, many of the initial tuff components may be altered late in the cooling sequence or after the loss of initial heat. It is in this late stage that the most sorptive minerals (i.e., zeolites and clays) are formed. The stratigraphic distribution of these crystallization episodes in the Topopah Spring Member is discussed in Chapter 1.

The petrologic features of ash-flow tuffs are largely determined by cooling history. Simple cooling units deposited at temperatures greater than 500°C (Section 1.2.2.2) typically have compacted or welded interiors between top and bottom zones of partially welded to nonwelded tuff. Compound cooling units occur where eruptive origins are more complex and the welding relations are not so simple; the proposed host rock for the repository in Yucca Mountain is within a compound cooling unit (Lipman et al., 1966). Even within this compound cooling unit, however, the general relationship is preserved in which the core of the cooling unit is more densely welded and the top, bottom, and distal edges of the ash flow are poorly welded or nonwelded. Immediately after the emplacement of an ash-flow tuff, primary glass in the more densely welded interiors of the cooling unit commonly devitrifies to intergrowths of silica minerals and alkali feldspars. The poorly welded or nonwelded margins of the cooling unit, however, often do not devitrify but remain glassy after the ash flow has lost its original heat. It is from the glass in these zones that the most significant intervals of secondary zeolites are formed. Thus, the zeolite intervals at Yucca Mountain (Section 4.1.1.3.2), are roughly correlated with the once vitric stratigraphic intervals that are at the margins of devitrified ash-flows (Vaniman et al., 1984).

Glass, feldspar, and mafic silicates may alter to smectites either within the feldspathic devitrified cores of cooling units or in their glassy margins. It might be expected, therefore, that smectites should occur throughout the tuff cooling units of Yucca Mountain, and in general this is true. In detail, however, the smectite abundances are lower in some zeolitized intervals than in adjacent nonzeolitized intervals; this is particularly true around the zeolitized tuff of Calico Hills (Caporuscio et al., 1982). This relationship is of interest in that the pH and ion concentrations during the hydrous alteration of glass are generally too low for zeolite formation unless the glass alters first to smectite (Hay and Sheppard, 1977). The negative correlation between clay and zeolite abundances at Yucca Mountain suggests that zeolite growth displaces smectite development soon after glass alteration begins along the cooling-unit margins.

Finally, it is important to note that although tuff mineralogy is closely related to cooling-unit petrology, the alteration of tuff to hydrous minerals is coupled with the availability of water. The minerals formed from altered tuff vary with depth. The transition from clinoptilolite to analcime to albite with depth is well documented at Yucca Mountain (Bish et al., 1981) and is discussed in Section 4.1.1.3.

4.1.1.2 Analytical techniques

This section discusses analytical techniques for mineralogic and petrologic analysis, as well as experimental techniques for studying mineral dehydration. Standard petrographic or mineral analysis procedures are used, although the quantitative x-ray technique of powder diffraction (XRD) involves some innovative data-reduction methods (Bish and Chipera, 1986). Special methods employed in the study of fracture minerals are discussed in Carlos (1985). Other techniques, some of which are unique and nonstandard, are described in Section 8.3.1.3.

The basic data on rock textures, mineralogy, and mineral compositions come from drill-core samples, supplemented by sidewall samples and drill cuttings where cores were not available, and samples from outcrops and trenches at Yucca Mountain. Standard optical petrography techniques were used in the study of thin sections made from these samples. Thin sections were used to determine textural relations, the degree of welding, and mineral growth distributions, with emphasis on the potential host rock in the Topopah Spring Member. Percentages of various textures and of phenocrysts were used to determine the stratigraphic position in the Topopah Spring Member (Byers, 1985).

Mineral occurrences and abundances are more generally determined by quantitative XRD. The methods used for quantitative XRD analysis are described by Bish and Vaniman (1985). When estimating the uncertainties of values determined by quantitative XRD, errors due to peak integration, crystalline solution, sample-standard variability, and peak overlap are considered. Relatively high precision is obtained for quartz, calcite, and analcime data (±5 to 10 percent of amount present). Smectite, mica, alkali feldspar, clinoptilolite, and mordenite analyses have precisions that are lower (± 10 to 20 percent of the amount present). Representative XRD tables

can be found in Bish and Vaniman (1985). A new deconvolution technique is being developed to allow greater precision in the feldspar, cristobalite, and tridymite analyses, although feldspar data will still be limited by large amounts of crystalline solution and sample-to-standard variability. This new technique is outlined in Section 8.3.1.3.

For samples with more than 5 percent smectite, the smectites are dispersed and separated by sedimentation and centrifugation techniques. From these separations the type of smectite and the degree of interstratification with other clay minerals are determined by the XRD technique (Bish, 1981).

Mineral compositions for volcanic glasses, zeolites, and authigenic feldspars are determined on an automated Cameca electron microprobe. Instrument parameters for primary-phenocryst analyses are summarized in Caporuscio et al. (1982). Parameters for zeolite analysis are given by Levy (1984a) and Caporuscio et al. (1982). Parameters for the analysis of fine-grained devitrified ground mass are given by Byers (1985).

For zeolite-dehydration experiments, natural clinoptilolites were obtained. Cation-exchanged varieties of clinoptilolite were prepared by suspending 2.5-g portions in 1.0 M solutions of calcium, potassium, and sodium chloride. The treatment was repeated 3 times for 16 h each at about 50°C (Bish, 1984; 1985). The solids were centrifuged and rinsed after each ion exchange. Harsher treatments, such as autoclaving, were not used in the cation exchanges to avoid recrystallization or alteration of the clinoptilolites. Details of these methods are given by Bish (1984).

4.1.1.3 Mineralogical, petrologic, and chemical composition of the host rock and surrounding units

In this section, the topics of mineralogy, petrology, and chemical composition are discussed in two parts. First, the potential host rock within the Topopah Spring Member is described. The description begins with the primary phenocryst, devitrification, and vapor-phase constituents, and ends with a discussion of the secondary mineralogy within fractures. These data are focused on their usefulness in indicating stratigraphic position and in characterizing the mineralogy along potential radionuclide travel paths. The chemistry of the Topopah Spring Member is discussed in Chapter 1. In the second part, the surrounding units are described. This description begins with the primary chemistry and mineralogy and concludes with a discussion of the secondary minerals, emphasizing the sorptive zeolites and clays.

Data on mineral abundances are compiled in Figures 4-1 and 4-2 for drillholes USW G-2, USW GU-3, and USW G-3. The drillhole locations are shown in Section 1.2.1, Figure 1-18. Figures 4-1 and 4-2 represent mineral abundances versus depth in these drillholes from different parts of Yucca Mountain.

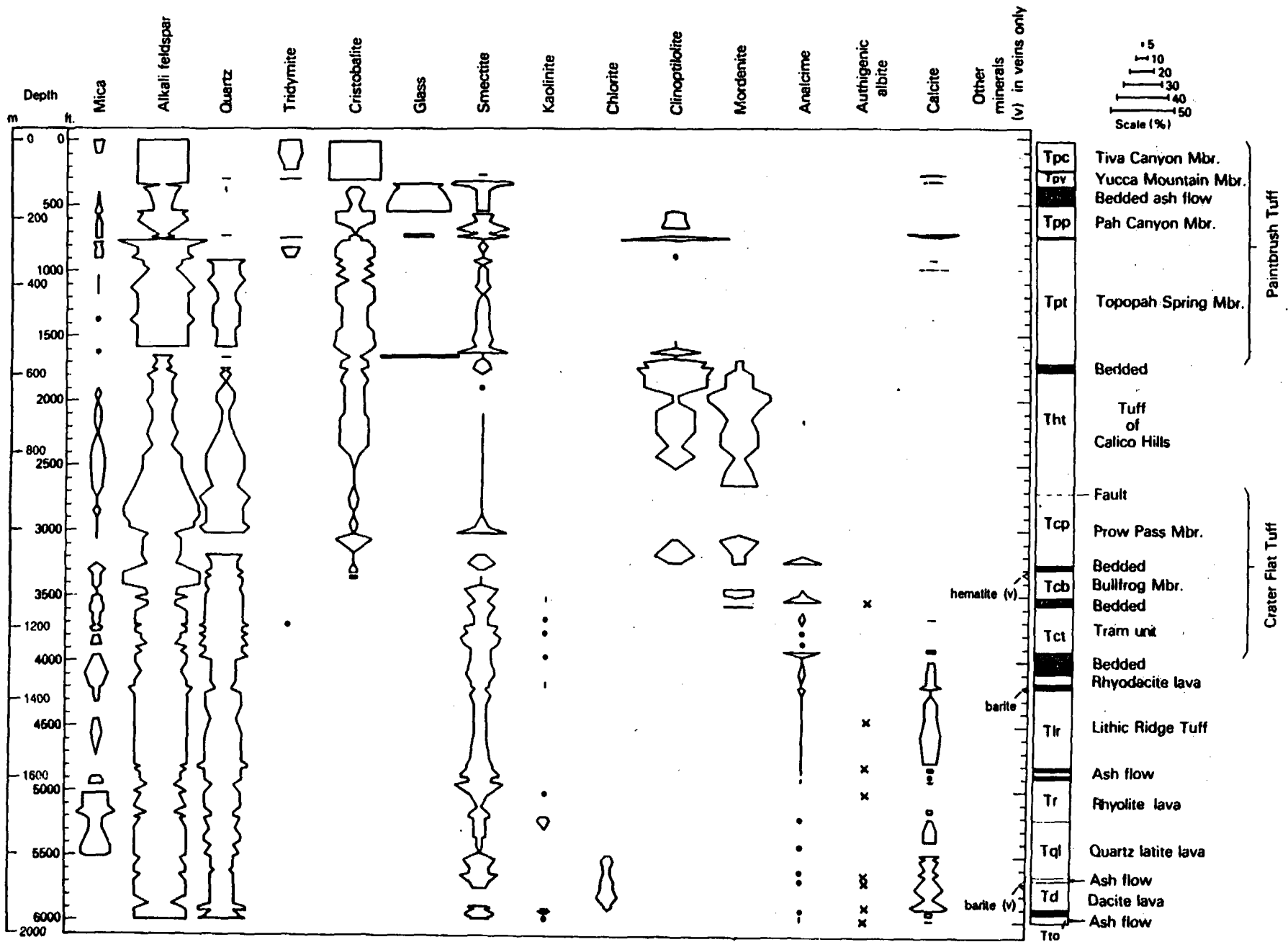**Figure 4-1.** Abundance of minerals as a function of depth from surface; determined by x-ray diffraction for core samples from drillhole USW G-2. Modified from Caporuscio et al. (1982).
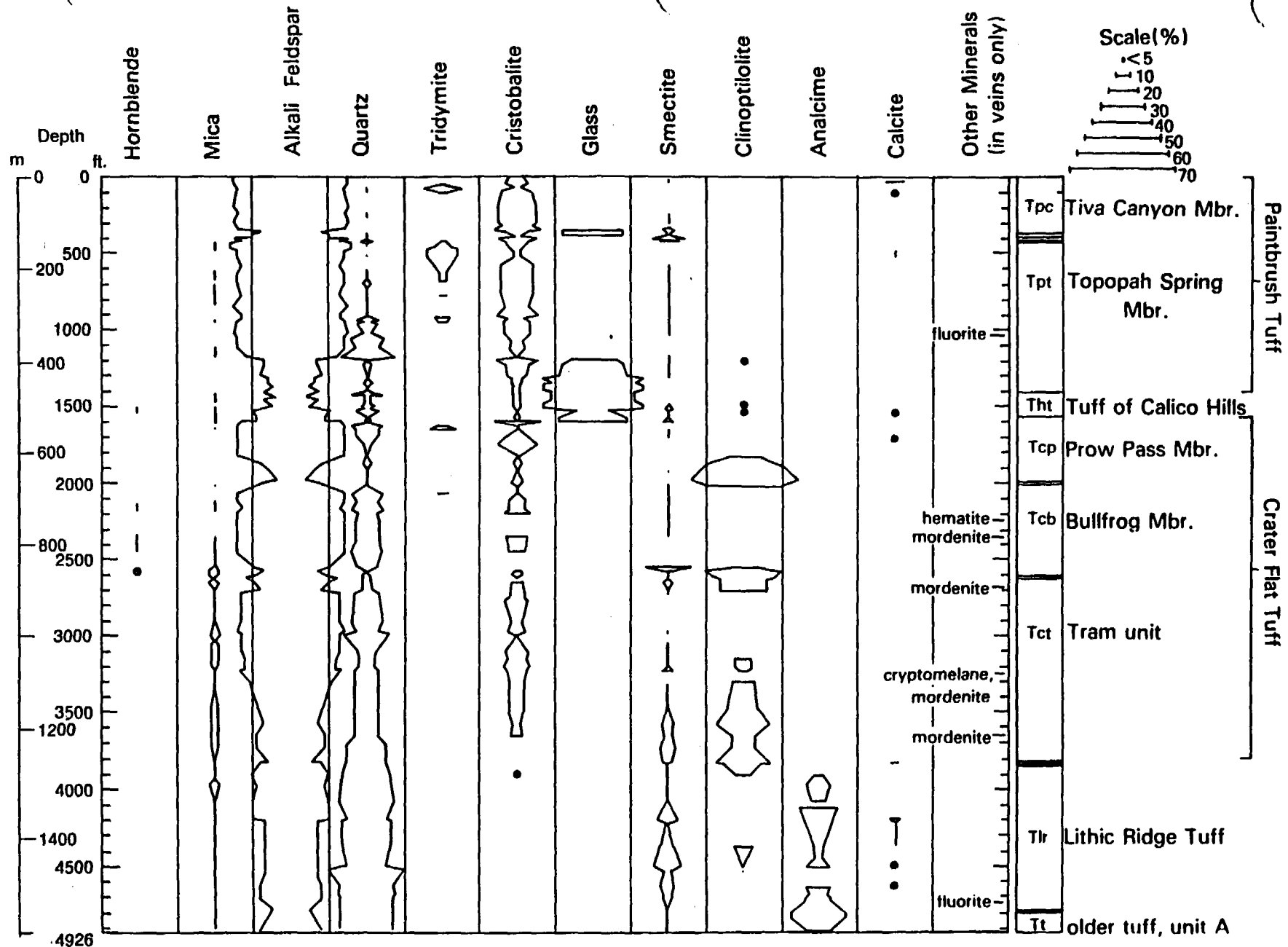
4-10

Figure 4-2. Abundance of minerals as a function of depth from surface: determined by x-ray diffraction for core samples from drillholes USW GU-3 and USW G-3. Modified from Vaniman et al. (1984).

CONSULTATION DRAFT

4.1.1.3.1 The potential host rock

The potential host rock is the lower, rhyolitic portion of the welded devitrified Topopah Spring Member. Present plans do not call for any waste emplacement in the upper, quartz latite portions of the welded devitrified Topopah Spring Member.

4.1.1.3.1.1 Mineralogy of the host rock matrix

The Topopah Spring Member of the Paintbrush Tuff is petrologically complex because it is a thick, compound cooling unit. The unit is compositionally zoned, from nearly aphyric (phenocryst-poor) high-silica (SiO_2) rhyolite (about 77 percent SiO_2) in the lower four-fifths grading upward through a zone of about 20 m into porphyritic (phenocryst-rich) quartz latite (about 69 percent SiO_2). The Topopah Spring Member includes a moderately to densely welded, devitrified interior that is bounded by a thin altered upper vitrophyre and a variably altered lower vitrophyre. The potential host rock for repository emplacement is within the devitrified zone of moderate to dense welding above the basal vitrophyre.

The devitrified high-silica rhyolite matrix above the vitrophyre consists of fine-grained intergrowths of 60 to 80 percent feldspar with 20 to 40 percent silica minerals (quartz and cristobalite with some tridymite). The cryptocrystalline groundmass of the overlying quartz latite is similar, although in most of the quartz latite, tridymite, and cristobalite are more abundant than quartz (Bish et al., 1984). The quartz latite also has higher phenocryst abundances than the high-silica rhyolite (6 to 16 percent versus about 1 percent; Byers, 1985). Phenocrysts throughout the Topopah Spring Member consist predominantly of sanidine and plagioclase; biotite, quartz, and iron-titanium oxide minerals are also common phenocrysts, although biotite is more abundant in the quartz latite and quartz is more abundant in the high-silica rhyolite.

A detailed description of the petrography of different stratigraphic intervals within the Topopah Spring Member, including major mineral variations and phenocryst compositions, and abundances is given in Chapter 1. Plans for more detailed description of petrologic variations are discussed in Section 8.3.1.3. The studies planned will also cover the limits of mineralogic variability in the host rock to help interpret the results of in situ experiments and to help determine the stratigraphic position during repository construction.

4.1.1.3.1.2 Mineralogy of fractures in the host rock

Detailed studies of fracture mineralogy have recently been completed on samples taken from above the static water level (SWL) in drillhole USW G-4 (Carlos, 1985). (The SWL approximates the position of the present-day water table, although it is a composite level affected by differences of hydraulic head in the open section of the hole.) These studies are being pursued because of the possible importance of fracture minerals in cation exchange

during fracture flow. Sequential generations of fracture-related mineral development in the unsaturated zone can be discerned (Figure 4-3), although the absolute ages of fracture formation and mineral deposition are not yet available.

Fractures are common in the moderately to densely welded host rock. Many of the fractures are lined or sealed by silica and feldspars. Fractures sealed by silica and feldspar probably formed by contraction during the cooling of ash flows, with the silica deposited by vapor-phase crystallization during initial cooling after the ash flow was emplaced. All other fracture coatings appear to be younger than the silica- and feldspar-filled fractures. Later fractures that reopened or cut across the early fractures are lined with zeolites (mordenite plus heulandite), sparse smectite, and rarely calcite (Carlos, 1985). Zeolite fracture linings are often discontinuous, and most fractures are only partially sealed. Smectite usually occurs as scattered late overgrowths on the other minerals and rarely fills fractures in the proposed repository horizon.

In Figure 4-3, the fracture mineralogy in tuffs between 770 ft (234.7 m) and the SWL correlate better with lithology than with stratigraphy. The numbers at the top of the figure indicate sequence of deposition, with type 1 (lithophysal type) representing earlier feldspar and silica deposits. The sequence varies between the welded-devitrified, glassy, and zeolitic lithologies. The same fracture minerals may have formed at different times in different units. It can be seen that zeolites occur in fractures throughout the depth interval sampled and are not restricted to the rocks in which the matrix is also zeolitized.

An understanding of fracture mineralogy will also provide information on the past movement of fluids in fractures, which will be important in evaluating the potential for radionuclide movement in the unsaturated zone. The minerals of fractures will also be an important contributor to sorption if fracture flow dominates in the transport of waste elements from the respository. Methods of dating fracture minerals are being investigated. Radiometric dating of smectites and electron-spin-resonance dating of quartz are both being pursued, as described in Section 8.3.1.3.

The information collected on fracture mineralogy and matrix alteration from several drillholes and the exploratory shaft will constrain our models of secondary-mineral formation at Yucca Mountain (Section 8.3.1.3) and models of the mineralogy along potential radionuclide transport paths.

4.1.1.3.2 Surrounding units

The Topopah Spring Member is overlain and underlain by other silicic volcanic units. The mineralogy of these bounding units is summarized briefly below. The stratigraphic framework is discussed in Section 1.2.2.

Above the Topopah Spring Member, the younger members of the Paintbrush Tuff include the Pah Canyon, the Yucca Mountain, and the Tiva Canyon members in order of decreasing age. The Pah Canyon and Yucca Mountain members form thin units (less than 71 m) at the site and are absent throughout much of the
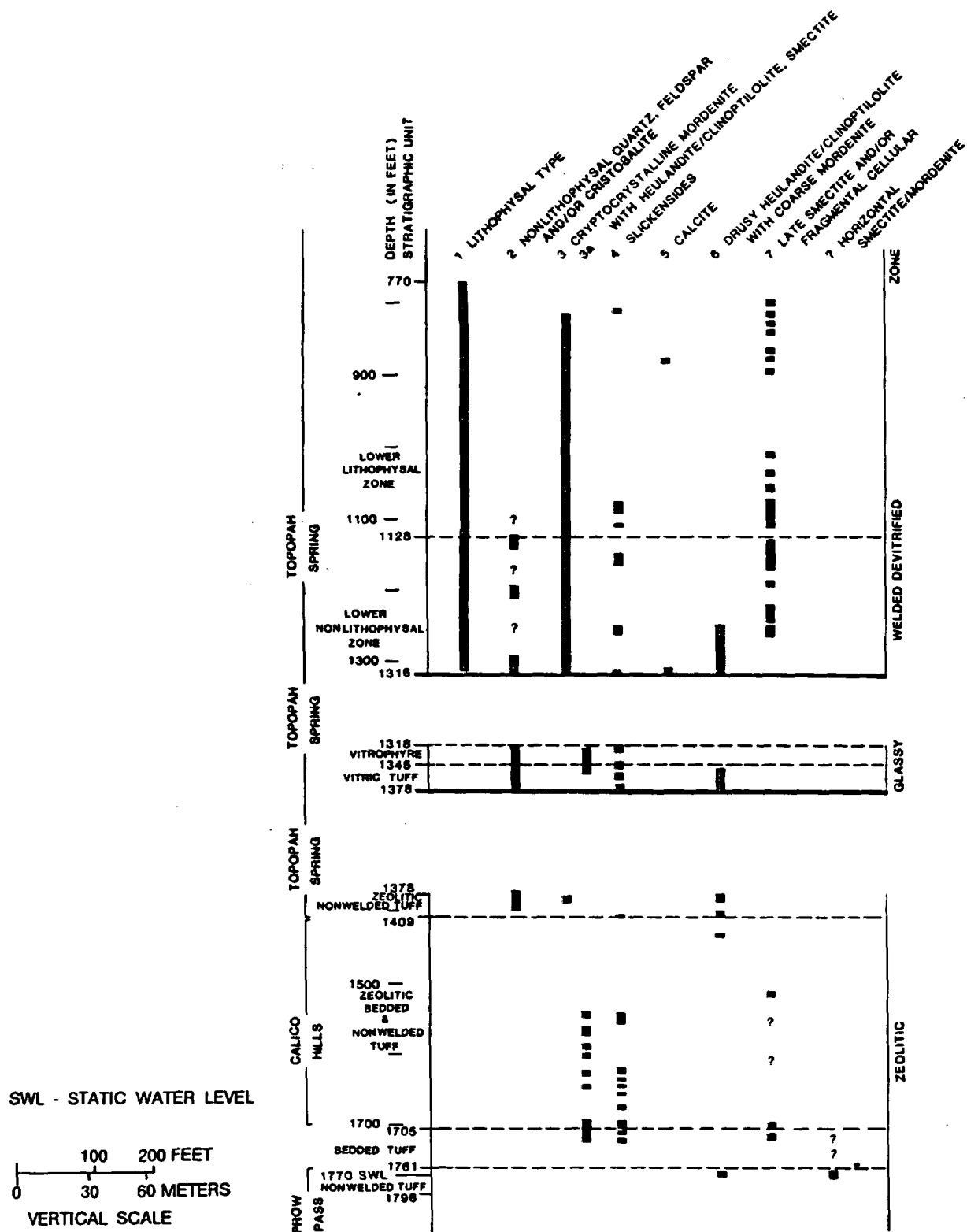
Figure 4-3. Sequence of fracture coatings in the unsaturated zone of drillhole USW G-4. Modified from Carlos (1985). Numbers across the top indicate inferred sequence of mineral growth. determined from overgrowth or cross-cutting relationships. Along the right side of the figure. major lithologic variations in the host rock (welded-devitrified. glassy. and zeolitic) are identified.

exploration block; the Tiva Canyon, however, is about 70 to 150 m thick and forms most of the outcrops on the eastern dip slope of Yucca Mountain (Section 1.2.2.2). These upper members are described in Chapter 1; more detailed descriptions are given by Orkild (1965), Lipman et al. (1966), Byers et al. (1976), and Scott et al. (1983). The mineral constituents and petrography of the upper members are summarized in Section 1.2.2.2.6. Electron-microprobe analyses of phenocrysts are summarized by Broxton et al. (1982), and the compositions of glasses and zeolites are described by Caporuscio et al. (1982). Chemical analyses are yet to be completed (Section 8.3.1.3.2).

The mineralogic compositions of the Topopah Spring Member and of the underlying units are summarized by Warren et al. (1984) and by Bish and Vaniman (1985). Detailed descriptions are published for samples from well J-13 (Heiken and Bevier, 1979; Byers and Warren, 1983; Bish and Chippera, 1986), drillhole UE-25a#1 (Sykes et al., 1979; Carroll et al., 1981; Bish and Chippera, 1986) drillhole USW G-1 (Bish et al., 1981; Bish and Chippera, 1986), drillholes USW G-2 and UE-25b-1H (Broxton et al., 1982; Caporuscio et al., 1982), and drillholes USW GU-3 and USW G-3 (Vaniman et al., 1984). Selected whole-rock compositions are summarized by Zielinski (1983) and cover the range of quartz latitic to rhyolitic tuffs that characterize the volcanic sequence at Yucca Mountain, plus the less common dacitic lavas or flow breccias. Additional chemical data will be obtained during site characterization (Section 8.3.1.3.2).

The petrography and petrology of the Topopah Spring Member were mentioned in Section 4.1.1.3.1 and described in Chapter 1. The symbols used for petrologic units are given in Table 4-1. The petrography of units underlying the Topopah Spring Member is summarized in Table 4-2 based on samples from drillhole USW G-1, and in Table 4-3, which is based on this drillhole and surrounding localities (Warren et al., 1984). Drillhole USW G-1 is centrally located within the site, as shown in Figure 4-4. The tables show that two feldspars, plagioclase and sanidine, plus quartz predominate in the phenocryst assemblages, with biotite forming the most common mafic phenocryst (but note the exceptionally high orthopyroxene content of the Prow Pass Member of the Crater Flat Tuff). Warren et al. (1984) conclude that these petrographic features vary slightly within a given unit, although at the southern end of the site, the tuffaceous beds of Calico Hills contain amphibole, orthopyroxene, and clinopyroxene (Vaniman et al., 1984).

Table 4-3 is a concise summary of the major phenocryst compositions (excluding quartz) in the Topopah Spring Member and in the underlying units. The anorthite content of plagioclase and the potassium and barium content of sanidine have been found to be distinctive for particular units (Warren et al., 1984).

Particular emphasis has been placed on studies of the alteration mineralogy in units surrounding the host rock. The alteration mineralogy is important because (1) it records the history of past chemical transport at Yucca Mountain, and (2) it provides a volumetrically abundant sorptive component to be considered in radionuclide retardation modeling.

Table 4-1. Symbols used for petrologic units, rock types, alteration, and minerals listed in Table 4-2[a] (page 1 of 3)

Unit, rock type, alteration, or mineral	Symbol

PETROLOGIC UNIT

Paintbrush Tuff	TP
Topopah Spring Member	
Upper, mafic-rich portion	TPTu
Lower, mafic-rich portion	TPTl
Tuffaceous beds of Calico Hills	
Upper, mafic-poor portion	TH1
Lower, mafic-poor portion	TH2
Crater Flat Tuff	TC
Prow Pass Member	TCP
Bedded tuff	TCBa
Bullfrog Member	TCB
Upper portion, 2,152 to 2,317.4-ft depth, drillhole USW G-1	TCBu
Middle portion, 2,317.4 to 2,425-ft depth, drillhole USW G-1	TCBm
Lower portion, 2,425 to 2,601.6-ft depth, drillhole USW G-1	TCBl
Bedded tuff	TCTa
Tram Member	TCT
Upper portion, 2,601.6 to 3,083.0-ft depth, drillhole USW G-1	TCTu
Lower portion, 3,083.0 to 3,522.0-ft depth, drillhole USW G-1	TCTl
Flow breccia of drillhole USW G-1	TFB
Rhyodacite lava of drillhole USW G-2	TRD
Bedded tuff between the flow breccia of USW G-1 and the Lithic Ridge Tuff	TLRa
Lithic Ridge Tuff	TLR
Upper portion, 3,920.0 to ≈4,365-ft depth, drillhole USW G-1	TLRu
Lower portion, ≈4,365 to 4,940.2-ft depth, drillhole USW G-1	TLRl
Older tuffs of drillhole USW G-1	TT
Unit A	TTA
Unit B	TTB
Unit C	TTC

Table 4-1. Symbols used for petrologic units, rock types, alteration, and minerals listed in Table 4-2[a] (page 2 of 3)

Unit, rock type, alteration, or mineral	Symbol

ROCK TYPE

Tuff	tf
Bedded tuff	b
Ash-flow tuff	t
Nonwelded	nwt
Partially welded	pwt
Moderately welded	mwt
Densely welded	dwt
Vitrophyric	vt
Lava	l
Intermediate-composition lava (groundmass plagioclase present)	intl
Lava-flow breccia	fb
Tuff breccia	tb
Argillite	ar
Granitoid	gr

ALTERATION[b]

None	
Vitric	gl
Low temperature (secondary)	
Opaline	O
Argillite	Ar
Zeolitic	Z
Clinoptilolite	Zc
Analcime	Za
Calcite	cc
Pyritic	py
Silicic (Chalcedony)	Q
High temperature (secondary)	
Albitic	Ab
High temperature (primary)	
Vapor phase	VP
Granophyric	Gr
Spherulite	Sp
Axiolitic	Ax

Table 4-1. Symbols used for petrologic units, rock types, alteration, and minerals listed in Table 4-2[a] (page 3 of 3)

Unit, rock type, alteration, or mineral	Symbol
MINERALS[c]	
Felsic phenocrysts	
Quartz	Q
Sanidine (+ anorthoclase, if present)	K
Plagioclase	P
Mafic phenocrysts	
Biotite	Biot
Hornblende	Hbld
Clinopyroxene	Cpx
Orthopyroxene	Opx
Accessory minerals	
Sphene	Sph
Allanite	All
Perrierite/cherkinite	Per
Apatite	Ap
Zircon	Zr

[a]Source: Warren et al. (1984). To convert feet to meters, multiply by 0.328.

[b]The symbols m (minor) and μ (micro) are used as modifiers on the alteration symbols.

[c]The mineral volume abundances listed for most samples are for unaltered or partly altered phenocrysts. In some samples, phenocrysts are partly or completely altered. In these samples, the symbol "A" indicates that the accompanying concentration is for partly altered grains only, and the symbol "ps" indicates that the accompanying concentration is based entirely on completely altered (pseudomorphic) forms.

Table 4-2. Summary of petrography for core samples from drillhole USW G-1, determined by point count of glass-covered thin section[a,b] (Page 1 of 2)

Sample depth (ft)[c]	Unit	Rock type	Alteration	Points counted	Major components (volume %)		Felsic phenocrysts (relative %)			Mafic phenocrysts (ppmV)				Fe-Ti oxide (ppmV)	Accessory minerals (grains identified)			
					Lithics	Felsics	Q	K	P	Biot	Hbld	Cpx	Opx		Sph	All	Ap	Zr
1,581.8	TH1	nwt	Zc	3,750	2.8	2.2	43	16	41	270	0	0	0	0	0	0	0	0
1,689.5	TH1	nwt	Zc	8,000	1.8	2.0	51	24	25	375	0	0	0	125	0	0	0	4
1,811.7	TCP	pwt		3,600	0.14	6.2	15	53	32	<280	0(ps)	0	1,900(ps)	560	0	0	0	4
1,943.4	TCP	awt	VP	3,300	0.45	14.4	13	39	48	<280	0	0	910(ps)	610	0	0	0	8
2,009.8	TCP	pwt		3,750	2.6	7.9	15	47	38	<280	<280	0	2,100(ps)	530	0	1	Rare	5
2,124.7	TCP	nwt		3,600	0.6	8.8	6	50	44	280	0(ps)	0	0	1,100	0	2	Rare	7
2,231.0	TCBu	pwt		3,700	0.03	12.2	22	36	42	2,700	1,300(ps)	0	0	810	0	0	Rare	9
2,246.0	TCBu	p-awt		3,000	0.00	11.8	19	45	36	4,300	1,000(ps?)[d]	0	0	1,700	0	0	Gone	7
2,300.4	TCBu	pwt		3,750	0.00	13.6	24	31	45	1,600	2,400(ps)	0	0	1,600	0	0	Rare	13
2,354.6	TCBm	awt	Gr	3,750	0.03	14.6	27	30	43	3,500	2,400(ps)	0	0	1,900	0	0	Rare	10
2,397	TCBm	pwt	VP	3,750	0.2	13.0	23	32	45	5,300	1,300(ps)	0	0	530	0	0	Rare	7
2,461.5	TCB1	awt	VP	3,650	0.9	7.1	5	44	51	2,200	1,600(ps)	0	0	550	0	0	Rare	8
2,470.6	TCB1	pwt	VP	3,700	1.6	8.3	18	29	53	4,900	1,100(ps)	0	0	1,300	0	0	Rare	10
2,478.3	TCB1	pwt	VP	3,750	0.5	10.0	14	39	47	4,000	530(ps)	0	0	270	0	0	Rare	5
2,507	TCB1	awt		3,700	1.2	9.6	13	36	51	4,100	3,200(ps)	0	0	2,400	0	0	Rare-sparse	12
2,555	TCB1	awt	Zc	3,520	0.8	9.9	9	40	51	2,300	2,300	——280(ps?)——		280	0	0	Shot?	5
2,594.2	TCB1	pwt		3,750	2.2	7.1	17	32	51	4,300	270(ps)	0	0	800	0	4	Rare	10
2,678.0	TCTu	pwt		3,980	1.3	7.5	15	34	51	7,300	0	0	0	1,000	2	1	Sparse	6
2,772.6	TCTu	pwt		3,800	2.1	10.2	29	34	37	5,800	——1,600(ps?)——			530	0	0	Sparse	5
2,851.7	TCTu	awt		3,900	4.5	13.6	41	37	22	4,400	0	0	0	1,800	0	0	Rare	11
2,869	TCTu	m-dwt		3,360	3.8	12.1	41	35	24	6,000	0	0	0	890	0	0		7
2,931.4	TCTu	m-dwt		4,000	3.3	12.8	37	32	31	7,000	0	0	0	500	0	0		9
3,013.9	TCTu	pwt		3,500	12.3	12.9	27	44	29	4,900	(ps)	0	0	860	0	10		>2
3,192.8	TCT1	pwt		3,600	23.8	9.4	33	30	37	4,200	0	0	0	280	0	0	Many	3
3,197	TCT1	awt		3,460	22.3	7.4	38	29	33	3,200	0	0	0	<280	0	0	?	3
3,284.5	TCT1	pwt	Ar,cc	3,600	9.0	8.6	35	31	34	3,300	0(ps)	0	0	1,700(py)	0	4	Alt.	>8
3,515.1	TCT1	pwt		3,800	25.8	8.3	34	22	44	2,900	260(ps)	0	0	1,300(py)	0	1	Present	Present
3,724.0	TFB	fb	G1,0	3,700	0.00	8.8	0.0	0.0	100	0	11,100	——15,100(ps)——		8,100	0	0	Large	0
3,908.2	TFB	fb	G1	3,150	0.00	10.0	0.0	0.0	100	0	7,900	2,500	8,200(ps)	5,700	0	0	Large	0
3,956.9	TLR	pwt	Ar	0	0	0	0	0	0					2	2		Present	Present
3,969.9	TLR	awt	Ar	3,300	9.0	17.5	2	34	64	5,500	0(ps?)	0	0	2,400	11	3	Present	Present
3,992	TLR	pwt		3,500	26.5	11.3	4	31	65	9,700	0	0	0	2,000	12	1	Present	Present
4,150.4	TLR	pwt		3,400	13.8	8.5	2	35	63	1,200	0	0	0	600	6	1	Rare	8
4,222.1	TLR	pwt		3,200	42.7	6.1	7	40	53	1,600	0	0	0	1,600	6	0	Sparse	5
4,408.4	TLR	pwt		1,800	11.8	9.2	1	37	62	5,000	0	0	0	1,100	1	1	Rare	7

Table 4-2. Summary of petrography for core samples from drillhole USW G-1, determined by point count of glass-covered thin section[a,b] (Page 2 of 2)

Sample depth (ft)[c]	Unit	Rock type	Alter-ation	Points counted	Major components (volume %)		Felsic phenocrysts (relative %)			Mafic phenocrysts (ppmV)				Fe-Ti oxide (ppmV)	Accessory minerals (grains identified)			
					Lithics	Felsics	Q	K	P	Biot	Hbld	Cpx	Opx		Sph	All	Ap	Zr
4,471.0	TLR	pwt		3,600	26.4	5.1	7	36	57	3,600	0	0	0	560	8(ps)	1	Present	12
4,578.2	TLR	pwt		3,800	23.8	7.6	5	39	56	2,600	0	0	0	530	2(ps)	2	Sparse	9
4,758.4	TLR	pwt		3,900	19.0	9.2	9	38	53	2,600	0	0	0	1,500	6(5ps)	0	Sparse	10
4,849.0	TLR	pwt		3,900	13.0	8.9	10	35	55	3,300	0	0	0	1,000	7(ps)	0	Shot	10
4,917.0	TLR	nwt		3,800	5.9	5.6	14	51	35	3,200	0	0	0	1,800	11(ps)	3	Present	12
4,946.4	TTA	nwt		3,450	4.4	9.8	20	58	22	3,000	0	0	0	300	4(ps)	2	0	12
4,969.0	TTA	pwt		3,700	3.1	11.9	24	31	45	4,900	0	0	0	2,700	5(ps)	0	Partly shot	10
5,002.3	TTA	nwt		3,700	2.5	17.0	32	31	37	5,100	0	0	0	2,400	3(ps)	3	Rare	13
5,045.0	TTA	swt		3,700	8.9	19.9	28	43	29	4,100	0	0	0	1,900	2(1ps)	0	1 ph	19
5,097.9	TTA	swt		3,600	0.58	17.4	28	41	31	2,200	0	0	0	2,000	1(ps)	3	Rare	10
5,115.5	TTA	swt		3,750	3.1	18.3	24	42	34	4,800	0	0	0	1,900	2	11	Sparse	20
5,141.5	TTA	swt		3,700	9.2	14.1	27	33	40	2,100	0	0	0	1,200	4	4	Sparse	15
5,142.2	TTA	pwt		3,750	2.2	19.4	28	36	36	3,700	<270	0	0	1,900	7	5	Present	13
5,187.0	TTA	nwt		3,650	2.1	17.6	24	38	38	1,600	270	0	0	2,200	6	7	Sparse	17
5,265.6	TTA	pwt		3,400	5.4	17.4	35	31	34	2,400	590	0	0	1,800	6	8	Sparse	17
5,316.0	TTA	b		3,600	2.4	21.6	33	36	31	1,400	0	0	0	2,800	4	12	Rare	13
5,373.7	TTB	pwt		3,650	0.69	11.3	13	26	61	9,000	0	0	0	3,300	15	1	Sparse	20
5,400.0	TTB	pwt		3,800	2.3	13.6	12	30	58	4,500	0	0	0	3,200	8	1	Sparse	24
5,416.6	TTB	pwt		3,700	12.8	11.2	11	27	62	2,700	0(ps?)	0	0	3,200	5	1	Rare, shot	20
5,438.2	TTC	pwt		3,900	0.74	12.9	1	3	96	12,000	0	0	0	4,600	0	1	Present	50
5,454.1	TTC	b		3,800	1.9	14.9	16	18	66	7,100	0	0	0	5,000	9	9	Sparse	42
5,496.1	TTC	pwt		3,900	7.5	10.1	1	4	95	21,000	0	0	0	4,900	8	3	Sparse	21
5,517.3	TTC	pwt		3,600	10.3	11.8	2	9	89	11,400	0	0	0	4,500	9	2	Sparse	20
5,540.0	TTC	pwt		3,700	8.5	13.5	0.4	0.0	99.6	19,200	810(ps)	0	0	4,300	1	0	Sparse-common	29
5,558.7	TTC	pwt		3,600	0.64	19.1	4	4	92	16,400	1,100(ps)	0	0	5,300	12	3	Sparse (large)	20
5,600.0	TTC	swt		3,750	8.4	14.8	5	7	88	10,100	800(ps)	0	0	6,400	16	4	Sparse	24
5,642.0	TTC	swt		3,300	5.8	15.4	2	4	94	21,500	1,500(ps)	0	0	5,800	12	3	Sparse	22
5,728.0	TTC	swt		1,650	21.1	21.6	0.0	1	99	18,200	0(ps)	0	0	7,900	4	3	Sparse (large)	24
5,841.0	TTC	swt		1,650	10.8	18.0	0.0	4	96	12,100	600(ps?)	0	0	8,500	3	1	Sparse-common	26
5,894.3	TTC	swt		1,650	7.2	15.5	0.0	4	96	6,100	6,100	0	0	3,600	6	1	Sparse	14
5,929.8	TTC	swt		1,650	5.9	18.2	4	4	92	13,300	5,500(ps)	0	0	6,100	7	8	Sparse-common	24
5,944.9	TTC	m-dwt		1,600	6.3	21.6	1	6	93	6,900	7,500(ps)	0(ps)	0	5,000	8	5	Sparse-common	24
5,980.0	TTC	m-dwt		1,650	3.3	20.9	0.0	0.3	99.7	24,200	7,300(ps)	1,800(ps)	0	7,300	4	1	Sparse-common	24
5,984.7	TTC	m-dwt		1,650	2.3	25.3	0.0	0.0	100	27,200	8,500(ps)	1,200(ps)	0	9,700	1	3	Sparse-common	25

[a] Source: Warren et al. (1984).
[b] ppmv = parts per million. Other symbols are defined in Table 4-1.
[c] To convert feet to meters, multiply by 0.328.
[d] Question marks indicate uncertainty.

Table 4-3. Statistical modes[a] for compositional parameters of phenocrysts for the lower Topopah Spring Member and for underlying units

Unit symbol[b]	Number of samples	Sanidine[c] mole% Or + Cn	Sanidine[c] wt% BaO	Plagioclase[d] mole% An Rim	Plagioclase[d] mole% An Core	Mafic minerals[e] Molecular Mg/(Mg + Fe) Biot	Hbld	Opx	Cpx
TPT1	5	59	0.00	15	17	0.43	--[f]	--	--
TH1	3	68	0.18	19	21	0.37	--	--	--
TH2	1	73	1.0	--	37	0.45	--	--	--
TCP	14	53	0.14	11	11	0.42	--	0.29	--
TCB	22	61	0.56	15	16	0.40	0.44	--	--
TCT	18	67	0.55	21	21	0.42	--	--	--
TFB	4	--	--	61	61	--	0.66	0.70	0.73
TLR	15	65	0.67	18	19	0.59	--	--	--
TTA	8	64	0.55	17	19	0.55	--	--	--
TTB	2	66	0.96	23	29	0.59	--	--	--
TTC	6	72	3.4	29	32	0.62	--	--	--

[a]The median value very closely approximates the statistical mode for compositional parameters of sanidine and mafic minerals and is the value given for these minerals. Sample locations are shown in Warren et al. (1984).
[b]Unit symbols are defined in Table 4-1.
[c]Or = potassium feldspar; Cn = celsian; BaO = barium oxide.
[d]An = anorthite
[e]Biot = biotite; Hbld = hornblende; Opx = orthopyroxene; Cpx = clinopyroxene.
[f]-- = not present.
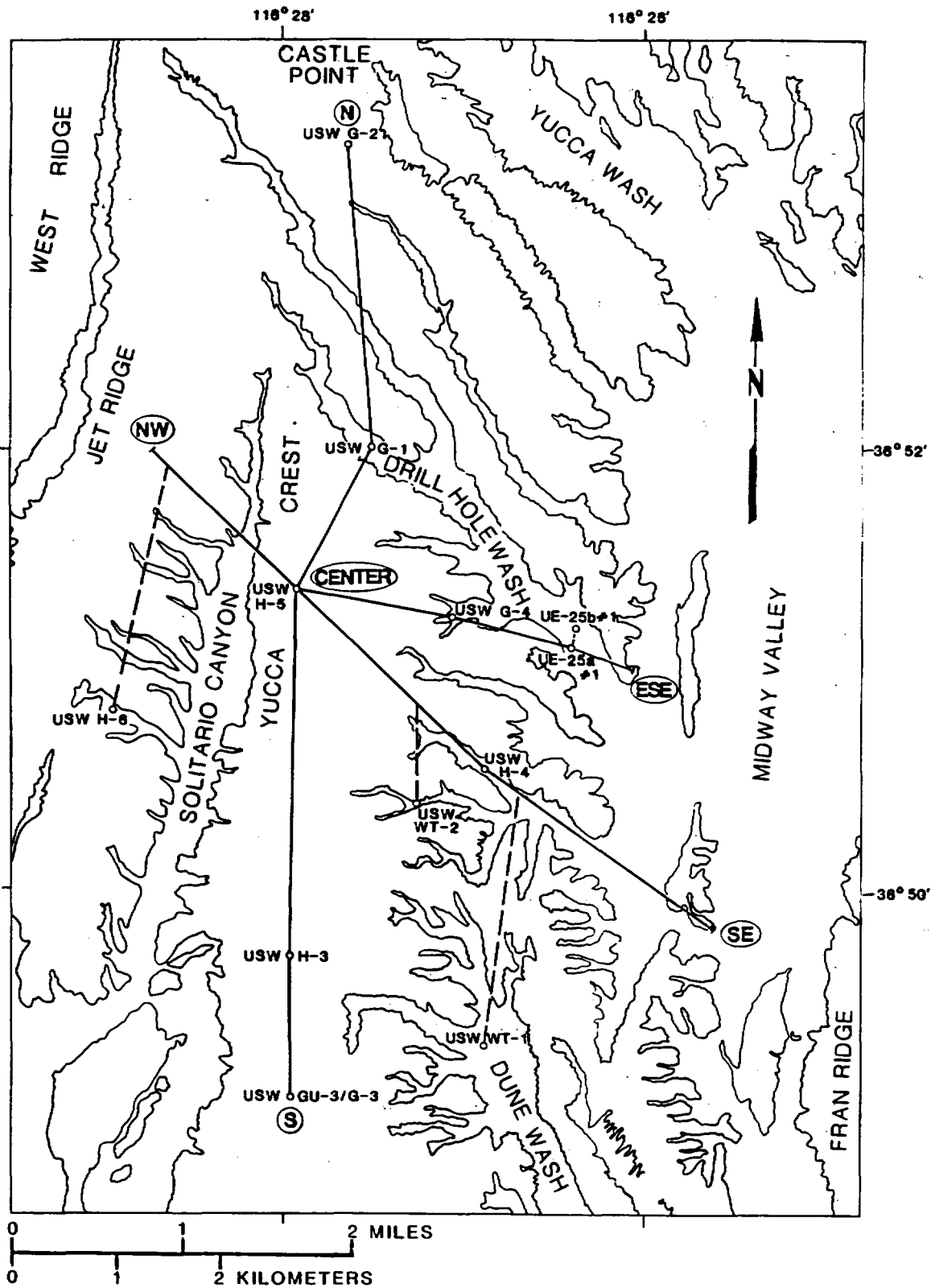
Figure 4-4. Location map for the zeolite cross sections in Figures 4-5, 4-6, and 4-7. This figure and the stratigraphy shown in Figures 4-5 and 4-7 are based on Scott and Bonk (1984).

Distributions of abundant sorptive zeolites in the rock matrix are summarized in cross sections (Figures 4-5 to 4-7) from Bish and Vaniman (1985), which are located on Figure 4-4. The three cross sections transect the exploration block. Only zeolite abundances greater than 10 percent are shown in Figures 4-5 to 4-7, because lesser concentrations may not be laterally continuous and are therefore unreliable for predictions of abundance. From these figures four principal intervals of zeolitization can be identified (Bish et al., 1984). The intervals are as follows:

1. Interval I. This interval is the clinoptilolite-heulandite-smectite zone at the top of the lower Topopah Spring vitrophyre, shown near the base of Tptw. Although thin (generally less than 3 m) and irregularly developed (it is virtually absent in drillhole USW GU-3), this interval is important because it is at the immediate base of the host rock and is everywhere above the water table. This zeolitized interval is unique because it is within the densely welded region of a compound cooling unit, whereas zeolitization is generally restricted to the poorly welded or nonwelded margins of cooling units. Zeolitization in interval I may result from alteration concentrated along the devitrification front at the top of the vitrophyre. Other alteration episodes may be superimposed on this; (see Levy (1984b) for a detailed discussion).

2. Interval II. This interval is the relatively thick zone of clinoptilolite (± mordenite) that may occur in the bedded, nonwelded, and poorly welded tuffs that form the base of the Topopah Spring Member and the underlying tuffaceous beds of the Calico Hills; it often extends into the top of the Prow Pass Member of the Crater Flat Tuff. This zeolitized interval occurs within the "n" unit between Tptw and Tcpw in Figures 4-5 and 4-7. The base of the Topopah Spring Member is the lower margin of a compound cooling unit, providing a predictable locale for zeolitization. The tuffaceous beds of Calico Hills are only partly welded to nonwelded throughout and are thoroughly zeolitized across the northern and eastern part of the exploration block. However, along the crest of Yucca Mountain this interval may be incompletely zeolitized (drillhole USW H-5) or nonzeolitized and vitric (drillhole USW GU-3) (Vaniman et al., 1984).

3. Interval III. This interval contains the partially welded and bedded tuffs at the base of the Prow Pass Member and at the top of the underlying Bullfrog Member compound cooling unit. This interval is consistently zeolitized throughout Yucca Mountain in the vicinity of the exploration block (Vaniman et al., 1984). In Figures 4-5, 4-6, and 4-7, it can generally be traced within the "n" unit between Tcpw and Tcbw.

4. Interval IV. This interval contains the poorly welded and bedded tuffs at the base of the Bullfrog Member compound cooling unit and at the top of an underlying cooling unit within the uppermost Tram Member. This interval also consists of clinoptilolite plus mordenite. In Figures 4-5, 4-6, and 4-7, it can generally be traced within the "n" unit below the Tcbw.
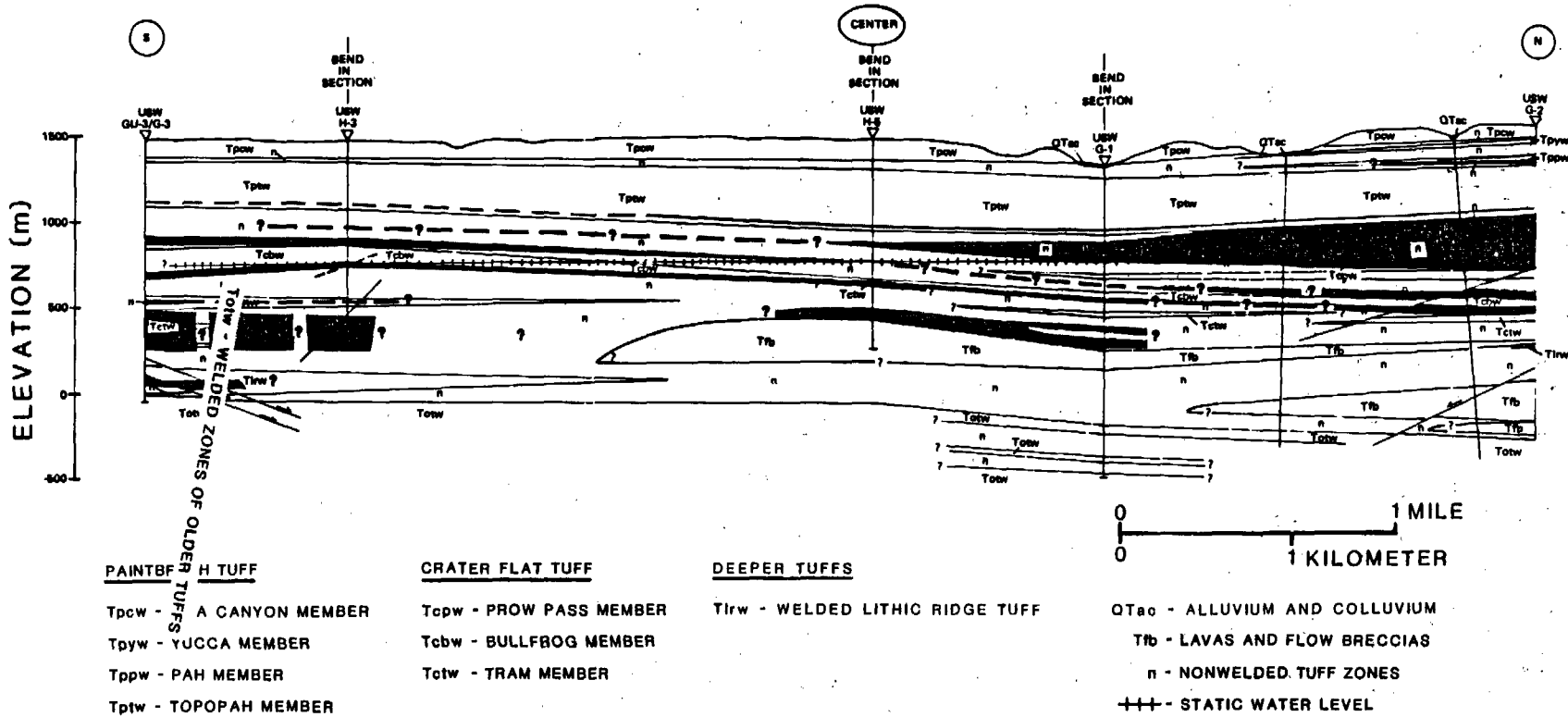
Figure 4-5. Major zeolite distributions (Bish and Vaniman, 1985), north-south cross section, shown as a dark pattern overlying the stratigraphic cross section of Scott and Bonk (1984). Location of cross section is shown on Figure 4-4. Unit designations follow the usage of Scott and Bonk (1984). Tpcw, Tpyw, Tppw, and Tptw represent the welded zones of the Tiva Canyon, Yucca Mountain, Pah Canyon, and Topopah Spring members of the Paintbrush Tuff; Tcpw, Tcbw, and Tctw represent the welded zones of the Prow Pass, Bullfrog, and Tram members of the Crater Flat Tuff; Tfb represents lavas and flow breccias; the Totw represents the welded zones of older tuffs. The symbol n is used for all nonwelded tuff zones. The subhorizontal barred line indicates the water table as inferred from static water levels in the drillholes.

CENTER

NW

ESE

BEND
IN
SECTION

BEND
IN
SECTION

BEND
IN
SECTION

USW
H-6
(projected
2.1 km N)

USW
H-5

USW
G-4

QTac

UE-25a#1
(UE-25b#1
projected
0.1 km S)

QTac

1500

Tpcw

Tpcw

Tpcw

Tpcw

n

n

n

n

n

QTac

1000

Tptw

Tptw

Tptw

Tptw

Tptw

?

?

n

n

n

ELEVATION (m)

?

?

?

n

Tcpw

n

n

Tcpw

500

?

?

?

?

Tctw

n

n

Tcbw

n

?

Tcbw

n

0

0   1 MILE

0   1 KILOMETER

PAINTBRUSH TUFF

Tpcw - TIVA CANYON MEMBER

Tptw - TOPOPAH MEMBER

CRATER FLAT TUFF

Tcpw - PROW PASS MEMBER

Tcbw - BULLFROG MEMBER

Tctw - TRAM MEMBER

QTac - ALLUVIUM AND COLLUVIUM

n - NONWELDED TUFF ZONES

+++ - STATIC WATER LEVEL

Figure 4-6.   Major clinoptilolite-mordenite distributions (Bish and Vaniman, 1985), northwest-southeast cross section. Location of cross section is shown on Figure 4-4. Information on drillhole USW H-5 below 760 m is from Bentley et al. (1983), and information on the central part of the drillhole USW H-6 is from Craig et al. (1983).

CENTER

SE

USW H-5

USW WT-2 (projected 0.7 km N)

BEND IN SECTION

USW H-4

USW WT-1 (projected 2.1 km N)

Tpcw

QTac

Tpcw

Tpcw

Tptw

Tptw

Tptw

Tptw

Tcbw

Tcbw

Tcbw

Tcbw

Tctw

Tctw

Tctw

Tctw

1500

1000

500

0

-500

ELEVATION (m)

1 MILE

0

1 KILOMETER

0

PAINTBRUSH TUFF

Tpcw - TIVA CANYON MEMBER

Tptw - TOPOPAH MEMBER

CRATER FLAT TUFF

Tcbw - BULLFROG MEMBER

Tctw - TRAM MEMBER

QTac - ALLUVIUM AND COLLUVIUM

n - NONWELDED TUFF ZONES

+++ - STATIC WATER LEVEL
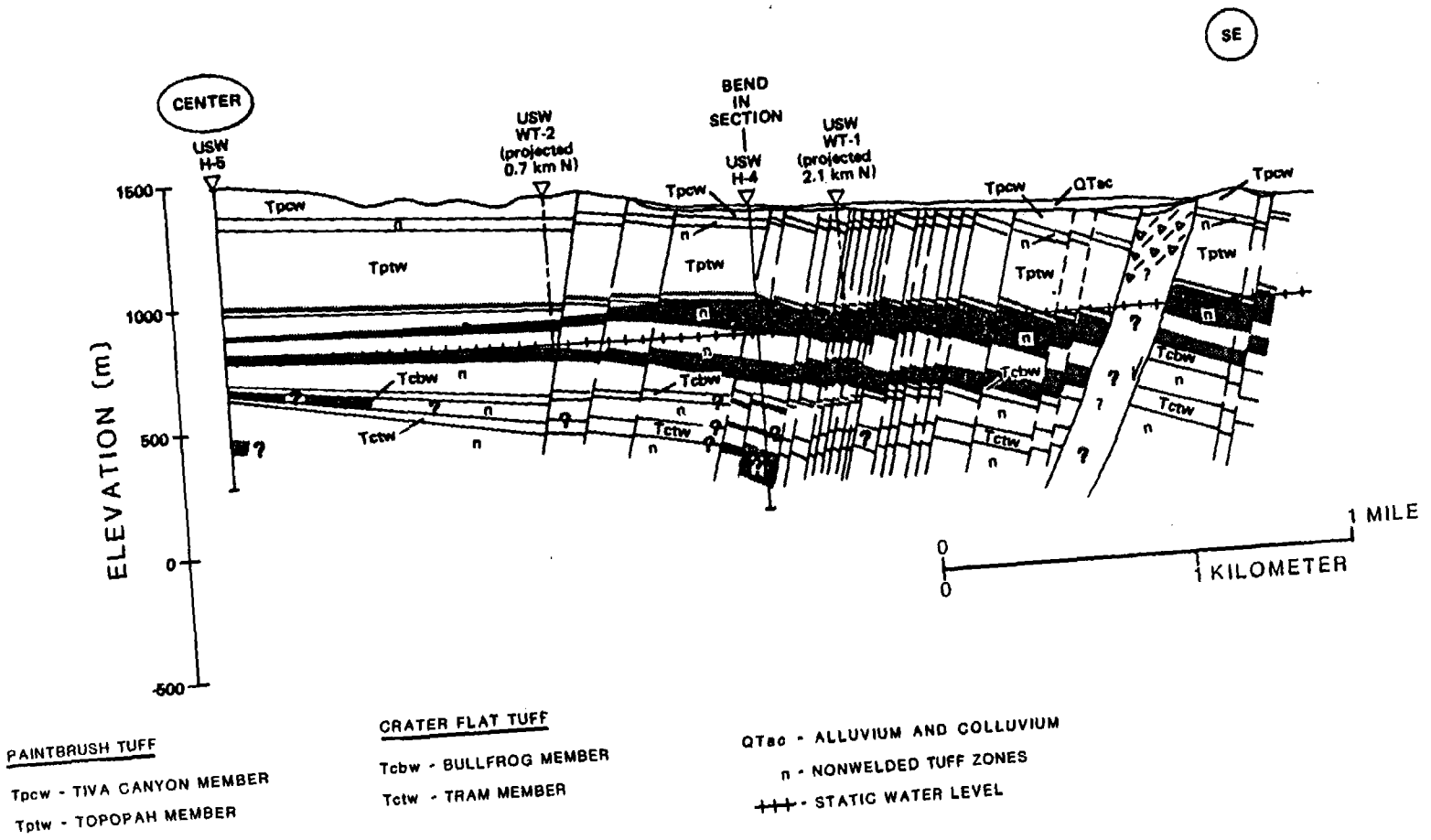
Figure 4-7. Major zeolite distributions (Bish and Vaniman, 1985), center to southeast cross section (Figure 4-5).

The weight percentages of zeolites in the rock in these intervals and the interval thicknesses are summarized in Table 4-4 for drillholes USW G-1, USW H-3, USW H-4, USW H-5, USW GU-3, USW G-3, USW G-4, UE-25a#1, and UE-25b#1 in and around the exploration block. Well J-13 is not included because the drillhole was not continuously cored and samples are lacking from certain critical intervals, particularly interval II within the tuffaceous beds of Calico Hills; well J-13 is also outside the Yucca Mountain exploration block. Drillhole USW G-2 is not included in Table 4-4 because it is 2 km north of the present exploration block and hydrothermal processes may have affected the deep alteration mineralogy at the northern end of Yucca Mountain (Caporuscio et al., 1982; Bish, 1987). The cumulative thicknesses of zeolitized tuff between the host rock and the static water levels in the drillholes are tabulated by Vaniman et al. (1984), and range from 44 to 142 m.

Much work remains to be done on the mineralogy along potential flow paths away from the host rock. Data from several drillholes drilled to the water table within and around the exploration block will be obtained during site characterization (Section 8.3.1.3). Other drillholes may be situated along possible transport pathways away from the exploration block (Section 8.3.1.3). Samples from the exploratory shaft facility will also become available. Present assessment of sorptive minerals along flow paths is still restricted to the unsaturated zone as long as flow paths within the saturated zone are unknown (Section 3.9.3.1). Mineral abundances along possible flow paths will be compiled as more data become available.

Yucca Mountain zeolites and smectites vary in composition, which may control many chemical and physical properties. The properties affected include cation exchange and selectivity (Sherry, 1969; Breck, 1974; Vaughan, 1978), thermal expansion (Bish, 1984), and dehydration behavior (Bish, 1985). Quantitative sorption ratios for different radionuclides as a function of individual clinoptilolite, heulandite, or mordenite composition are lacking, but data will be collected to define the dependence of sorption ratio on individual mineral composition (Section 8.3.1.3). Vaughan (1978) describes selectivity sequences for clinoptilolite in the order potassium>calcium> sodium. This selectivity sequence results in K-clinoptilolite being more difficult to cation exchange than Na- or Ca-clinoptilolite. The distributions and compositions of various zeolite types are being studied to determine their origins and the nature of chemical transportation during alteration, as well as to provide a basis for estimating overall retardation (Sections 4.1.3.3 and 8.3.1.3).

Present data on compositional variations in Yucca Mountain zeolites and clay minerals as a function of depth are summarized in the discussion that follows. The discussion includes consideration of the effects these variations in composition will have on rock properties. The zeolitized intervals I through IV, described earlier in this section and in Table 4-4, are used in the summary of sorptive zeolite compositions.

Sorptive zeolites (clinoptilolite, heulandite, mordenite). Representative compositions for the clinoptilolite-heulandite group minerals from Yucca Mountain are given in Table 4-5. Histograms showing the distribution of silicon-to-aluminum ratios in these minerals are presented in Figure 4-8; consistency in silicon-to-aluminum ratios may be one measure of consistency

Table 4-4. Zeolitized intervals for Yucca Mountain[a,b]

Interval	USW G-1 SWL=577 m	UE-25a#1 UE-25b#1 SWL=471 m	USW G-4 SWL=541 m	USW H-4 SWL=519 m	USW H-5 SWL=704 m	USW H-3 SWL=754 m	USW GU-3 USW G-3 SWL=754 m
I: Above the lower Topopah Spring vitrophyre	Depth: 392-393 m (1 m thick) 15% cpt	Depth: 385-398 m (3 m thick) 7% cpt	Depth: 396-401 m (5 m thick) 10% (±12) cpt	Depth: 357-361 m (5 m thick) No samples	Depth: 485 m 10% cpt	Depth: 367-371 m (4 m thick) No samples	Depth: 360-364 m (4 m thick) Trace cpt
II: Base of the Topopah Spring unit, tuff of Calico Hills	Depth: 425-565 m (140 m thick) 52% (±17) cpt	Depth: 404-556 m (152 m thick) 67% (±6) cpt 17% (±20) mord	Depth: 420-545 m (125 m thick) 50% (±19) cpt 5% (±7) mord	Depth: 400-504 m (104 m thick) 63% (±13) cpt 8% (±12) mord	Depth: 584-594 m (10 m thick) 37%	Vitric (nonzeolitized)	Vitric (nonzeolitized)
III: Between the Prow Pass and the Bullfrog units	Depth: 622-706 m (84 m thick) 45% (±12) cpt 18% (±18) mord	Depth: 636-710 m (74 m thick) 60% cpt & mord	Depth: 600-682 m (82 m thick) 32% (±12) cpt 19% (±10) mord	Depth: 596-698 m (102 m thick) No samples	Depth: 665-689 m (34 m thick) 60% cpt	Depth: 549-610 m (61 m thick) 68% cpt	Depth: 557-613 m (56 m thick) 58% (±18) cpt
IV: Between the Bullfrog and the Tram units	Depth: 779-823 m (44 m thick) 37% (±6) cpt 15% (±11) mord	Depth: 863-890 m (27 m thick) 4% (±4) cpt 16% (±10) mord	Depth: 828-860 m (32 m thick) 9% (±9) cpt 35% (±33) mord	Depth: 765-774 m (9 m thick) No samples	No samples	Depth: 732-760 m (28 m thick) 52% (±17) cpt 18% (±13) mord	Depth: 776-822 m (46 m thick) 36% (±8) cpt

[a]Source: Vaniman et al. (1984).
[b]cpt = clinoptilolite and heulandite; mord = mordenite; and SWL = static water level (given in depth below surface). Percentages represent weight.

CONSULTATION DRAFT

Table 4-5. Representative clinoptilolite analyses for Yucca Mountain[a] (page 1 of 2)

| Mineral | Interval I | | Intervals II, III, and IV and deeper occurring clinoptilolite | | | | | | | | |
| | | | Calcic Suite, Eastern Yucca Mountain | | | | Alkalic Suite, Western Yucca Mountain | | | | |
	Pah Canyon Member (G2-584)	Topopah Spring Member (H5-1666)	Tuff of Calico Hills (25p1-1250)	Prow Pass Member (25p1-1700)	Bullfrog Member (25b1-2879)	Tuff of Lithic Ridge (25p1-3330)	Tuff of Calico Hills (G1-1774)	Prow Pass Member (G3-1874)	Bullfrog Member (G3-2615)	Tram Member (G3-3589)	Tuff of Lithic Ridge (G3-4423)
CONCENTRATION (WT%)											
SiO_2	65.6	65.5	68.6	67.1	56.1	60.6	68.1	68.2	63.9	65.1	65.3
TiO_2	0.00	0.02	0.00	0.00	0.00	0.00	0.00	0.00	0.00	0.00	0.00
Al_2O_3 [b]	13.8	13.3	12.4	12.9	16.9	16.0	12.2	11.9	11.7	11.4	12.6
Fe_2O_3	0.00	0.00	0.00	0.00	0.05	0.00	0.00	0.00	0.00	0.51	0.12
MgO	1.47	0.86	0.07	0.32	0.22	0.08	0.09	0.00	0.00	0.12	0.22
CaO	4.23	5.19	3.59	4.37	6.77	7.22	1.11	1.95	1.57	0.79	2.35
BaO	0.02	0.00	0.00	0.05	0.21	0.19	0.03	0.00	0.00	0.19	0.27
Na_2O	0.18	0.17	1.13	1.55	0.89	0.85	2.84	1.69	2.88	2.23	3.21
K_2O	1.09	0.21	3.01	1.23	1.43	0.41	4.20	5.20	2.71	5.55	1.15
Total	86.3	85.2	88.8	87.5	82.6	85.4	88.6	88.9	82.8	85.9	85.2
CATION CONCENTRATION (%)											
Si	72.60	73.90	73.60	72.90	64.30	67.60	71.90	72.40	72.20	71.20	71.80
Ti	0.00	0.02	0.00	0.00	0.00	0.00	0.00	0.00	0.00	0.00	0.00
Al	18.00	17.70	15.70	16.50	22.80	21.10	15.20	14.90	15.60	14.70	16.40
Fe^{3+}	0.00	0.00	0.00	0.00	0.04	0.00	0.00	0.00	0.00	0.42	0.10
Mg	2.43	1.45	0.11	0.52	0.38	0.13	0.14	0.00	0.00	0.20	0.36
Ca	5.02	6.27	4.13	5.08	8.31	8.64	1.26	2.22	1.90	0.93	2.77
Ba	0.01	0.00	0.00	0.02	0.09	0.08	0.01	0.00	0.00	0.08	0.12
Na	0.39	0.37	2.35	3.26	1.98	1.84	5.82	3.48	6.32	4.73	6.85
K	1.54	0.30	4.12	1.70	2.09	0.58	5.66	7.04	3.91	7.75	1.61

| | Interval I | | Intervals II, III, and IV and deeper occurring clinoptilolite | | | | | | | | |
| | | | Calcic Suite, Eastern Yucca Mountain | | | | Alkalic Suite, Western Yucca Mountain | | | | |
Mineral	Pah Canyon Member (G2-584)	Topopah Spring Member (H5-1666)	Tuff of Calico Hills (25p1-1250)	Prow Pass Member (25p1-1700)	Bullfrog Member (25b1-2879)	Tuff of Lithic Ridge (25p1-3330)	Tuff of Calico Hills (G1-1774)	Prow Pass Member (G3-1874)	Bullfrog Member (G3-2615)	Tram Member (G3-3589)	Tuff of Lithic Ridge (G3-4423)
$(Al + Fe)/(2Mg + 2Ca + 2Ba + Na + K)$
	1.07	1.10	1.05	1.02	1.05	1.05	1.06	1.00	1.11	1.01	1.10
$Si/(Al + Fe)$
	4.03	4.18	4.69	4.42	2.82	3.20	4.73	4.86	4.63	4.71	4.35
RELATIVE ABUNDANCE OF EXCHANGEABLE CATIONS (MOLE %)
K	16	4	38	16	16	5	44	55	32	57	14
Na	4	4	22	31	16	17	45	27	52	35	59
Ca+Mg	80	92	40	53	68	78	11	18	16	8	27

[a]Sample numbers are given in parenthesis under the unit name and consist of abbreviated drillhole designation (G2 = USW G-2, H5 = USW H5, 25p1 = UE-25p#1, 25a1 = UE-25a#1, 25b1 = UE-25b#1, G1 = USW G-1, G3 = USW G-3) followed by sample depth from surface in feet. Data are from Broxton et al. (1986).

[b]Total iron calculated as Fe_2O_3.

INTERVAL I CALCIC CLINOPTILOLITES
AND HEULANDITES
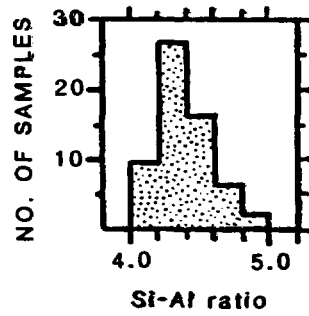
INTERVALS II THROUGH IV
CLINOPTILOLITES ON EASTERN
SIDE OF YUCCA MOUNTAIN
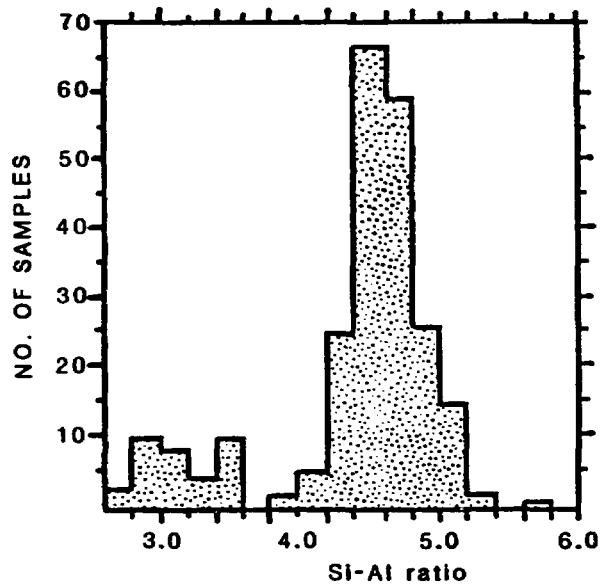
INTERVALS II THROUGH IV
CLINOPTILOLITES ON WESTERN
SIDE OF YUCCA MOUNTAIN
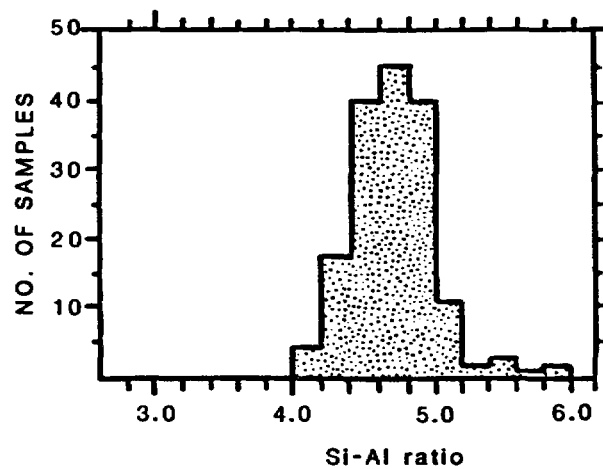
Figure 4-8. Histograms comparing the silicon-to-aluminum ratios for heulandites and calcic clinoptilolites from Yucca Mountain, Nevada. Modified from Broxton et al. (1986).

in sorptive behavior (Rundberg et al., 1985). Triangular plots showing vertical and lateral variations in exchangeable-cation ratios are presented in Figures 4-9 and 4-10. In zeolitized interval I, clinoptilolite and heulandite are calcium rich and have silicon-to-aluminum ratios ranging from 4.0 to 5.0 (Figure 4-8 shows some examples). The magnesium content of these zeolites is generally high, ranging from 0.6 to 1.5 percent magnesium oxide by weight. Using the thermal stability criteria of Mumpton (1960), Levy (1984a) determined that at least some of the calcium-rich clinoptilolite group minerals that occur at the top of the Topopah Spring vitrophyre belong to the heulandite structural group. Clinoptilolite-group zeolites from zeolitized intervals II through IV show more chemical diversity than those in interval I. In these deeper intervals, clinoptilolite compositions are subdivided into an eastern calcic suite of samples and a western alkalic suite of samples based on their exchangeable-cation contents (Figure 4-10). A transitional zone, found in drillholes USW G-4 and USW H-4, has characteristics intermediate between the eastern and western suites. The eastern clinoptilolites show a strong trend toward calcium enrichment with depth. In contrast, the western clinoptilolites become more sodium rich with depth. Silicon-to-aluminum ratios for both suites are similar (Rundberg et al., 1985), falling mostly between 4.0 and 5.2 and clustering around 4.6 (Figure 4-8). However, the silicon-to-aluminum ratios in eastern clinoptilolites have a bimodal distribution with a smaller population of ratios ranging from 2.8 to 3.6. This smaller population of low silicon-to-aluminum ratios correlates with the most calcic clinoptilolite compositions (approximately 70 mole percent calcium plus magnesium) in interval IV.

The other major zeolite type at Yucca Mountain is mordenite. Its chemistry is poorly known because individual mordenite crystals are fine grained and intergrown with other authigenic phases so that analysis by electron-microprobe and mineral-separation techniques is not feasible. The determination of mordenite compositions by bulk-rock techniques is difficult because monomineralic beds of mordenite are extremely rare at Yucca Mountain. In drillhole USW G-4, a bulk-rock sample containing more than 80 percent mordenite contains relatively equal amounts of sodium, potassium, and calcium (Broxton et al., 1986). These mordenites appear to be somewhat more sodic and less calcic than coexisting clinoptilolites.

The data from drillholes (Broxton et al., 1986) show that the first clinoptilolite-heulandites encountered below the repository horizon contain major amounts of calcium and minor amounts of potassium and sodium. Clinoptilolites of this composition will undergo cation exchange more readily than the potassium-rich clinoptilolites below in zeolitized interval II. In addition, the calcic clinoptilolites close to the repository will contract less at elevated temperatures than the deeper sodium-rich zeolites (Section 4.2.2), and fewer rock mechanical problems and permeability changes will be encountered because of this. Below the lower Topopah Spring vitrophyre, in the nonwelded base of the Topopah Spring Member and in the tuffaceous beds of Calico Hills, clinoptilolites contain subequal amounts of potassium and calcium. Below the Prow Pass Member the clinoptilolites are generally sodium rich, and sodium is more easily exchanged than calcium or potassium. Sodium-rich clinoptilolites contract appreciably when temperatures are elevated (Bish, 1985), but these zeolites only occur beyond the anticipated thermally disturbed zone and should pose no mechanical problems. Plans to test this are discussed in Section 8.3.1.3.2.
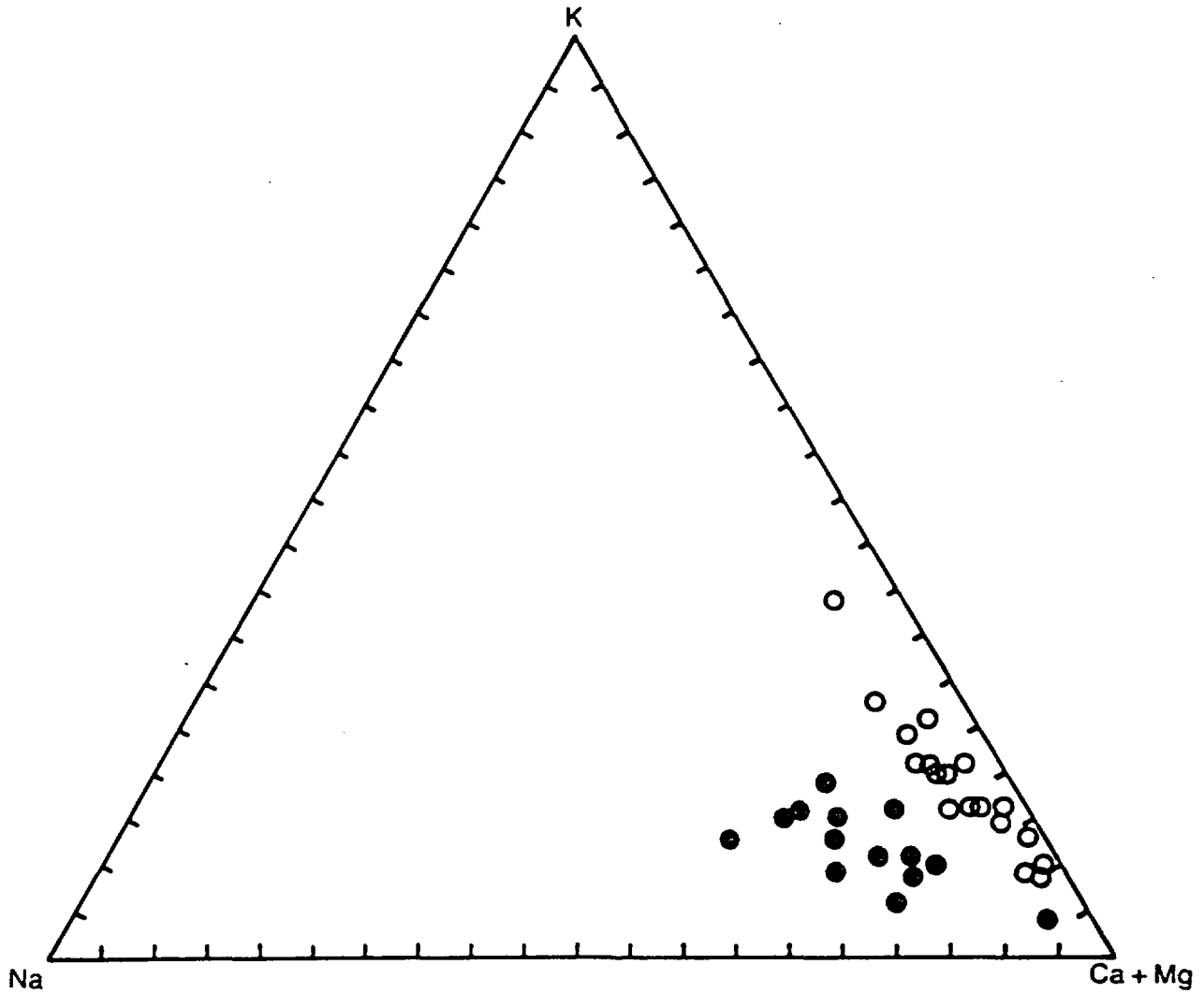
O   COMPOSITIONS FOR PAH CANYON MEMBER FOR DRILL HOLE USW G-2

●   COMPOSITIONS OF THE ZEOLITES THAT OCCUR ON TOP OF TOPOPAH
    SPRING BASAL VITROPHYRE, FOR DRILL HOLES THROUGHOUT YUCCA
    MOUNTAIN

Figure 4-9. Triangular diagram showing the exchangeable-cation ratios in calcic-clinoptilolite and heulandite from zeolitized interval I at Yucca Mountain. Data plotted are in weight percent. Modified from Broxton et al. (1986).
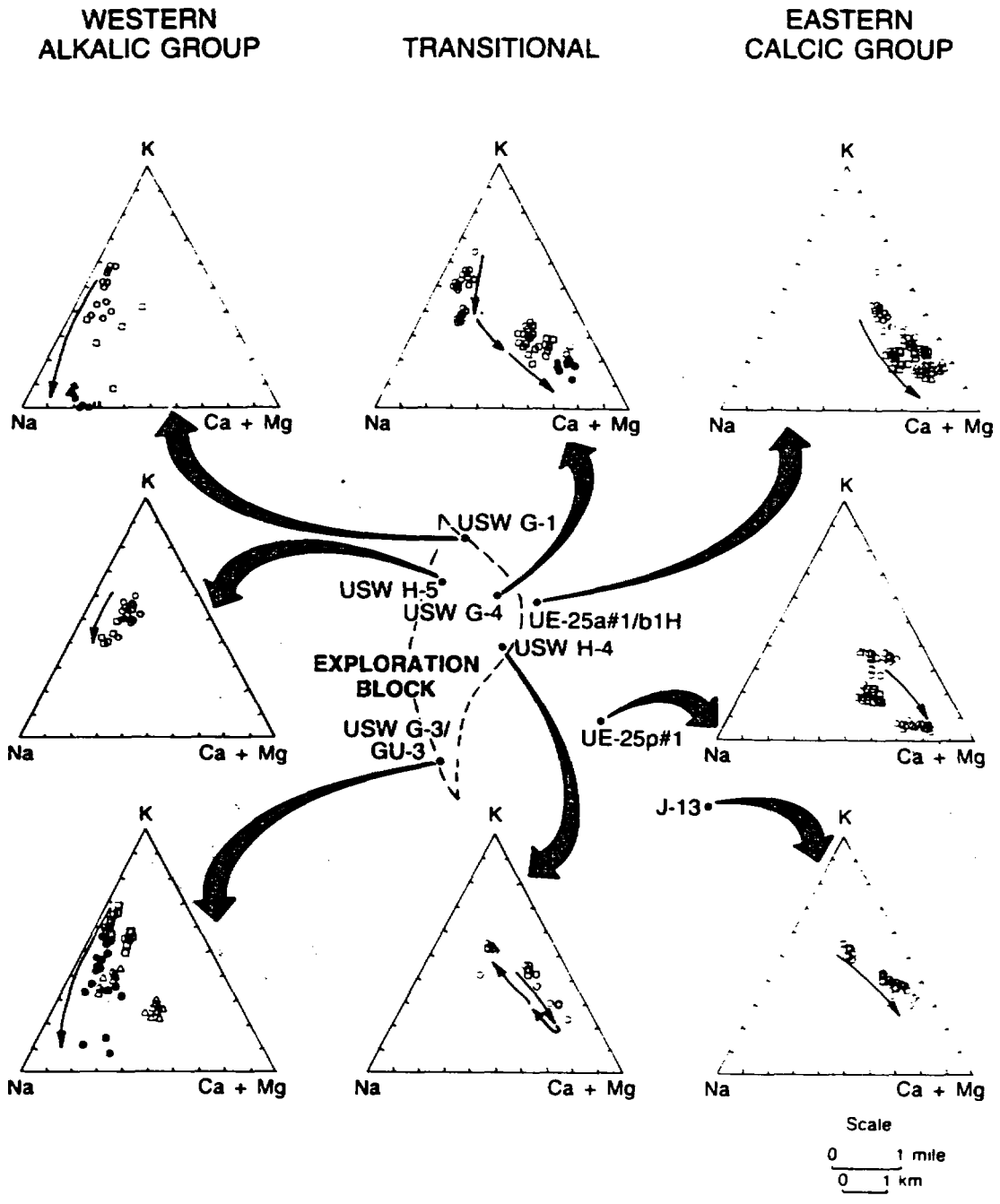
Figure 4-10. Triangular diagrams showing ratios of exchangeable cations in clinoptilolites at Yucca Mountain. Modified from Vaniman (1987).

Smectites. Smectites are widespread throughout the units underlying the
Topopah Spring Member (Bish, 1987) and therefore occur along possible flow
paths. Although smectite abundances are typically 1 to 10 percent, amounts
as high as 50 percent occur in some units (Figures 4-1 through 4-3). The
sorption properties of smectites are not as strong a function of composition
as they are for zeolites, but smectite dehydration under slightly elevated
temperatures (up to 100°C) is determined largely by composition (Bish, 1981).
In addition, information on geologic processes in the past can be obtained
from data on smectite compositions and structures (Bish, 1987). This inform-
ation can aid in the prediction and understanding of the effects of future
elevated temperatures.

Smectites in the host rock unit and along flow paths into the saturated
zone have mixed potassic, sodic, and calcic interlayers. These cations are
easily exchanged by many small and large cations and complexes. There is a
minor increase in the potassium content of smectites with depth throughout
most of the exploration block (Caporuscio et al., 1982). However, potassium
contents of the smectites between the host rock and the Tram Member are still
low enough so that the sorptive properties of the smectites should not
significantly differ from the smectites at shallower depths. Clays below the
Tram Member include a higher content of illite, which will be less sorptive.
Only in the deepest rocks at the northern end of the repository block
(drillhole USW G-2) are the smectites significantly transformed to illite
Caporuscio et al., 1982; Bish, 1987). In the bulk of the repository block,
the smectites retain their highly sorptive nature. As a result of their
minor compositional variations, the smectite sorptive properties should not
vary significantly near a Yucca Mountain repository. Plans to test this are
discussed in Section 8.3.1.3.

In addition to their importance for sorption, the smectites can provide
information on the geologic history of Yucca Mountain. Within and north of
Drill Hole Wash, the data show evidence of hydrothermal alteration at depth,
with large potassium increases and expandability decreases in smectites more
than 1,097 m below the surface (Bish, 1987). Smectites above the Bullfrog
Member in drillhole USW G-2 are not altered, whereas deeper smectites and
interstratified illite-smectites suggest that alteration occurred at temper-
atures as high as 230°C at 1,158-m depth. These data (Caporuscio et al.,
1982) and preliminary potassium-argon radiometric dates for illites from
drillholes USW G-1 and USW G-2 suggest that the hydrothermal alteration
occurred 10.9 ± 0.2 million years ago in the northern end of the exploration
block (Bish, 1987). Smectites at depth in the southern portion of the block
(drillhole USW G-3) do not show evidence of this alteration and remain fully
expandable to the bottom of the drillholes examined. Even in the northern
end of Yucca Mountain, expandable sodium- and calcium-containing smectites
are found at depth, along with potassium-rich, nonexpandable clay. This
suggests that some smectite formation also occurred after hydrothermal
alteration. The use of these deeper tuffs as natural analogs to repository-
induced thermal alteration is discussed by Bish (1987).

4.1.1.4 Mineral stability

    Mineral stability in Yucca Mountain must be considered in two ways. The first is to consider whether the present mineral assemblages in Yucca Mountain are stable under present conditions and, if they are not, what mineralogic changes are probable. The second consideration is what effect repository heating will have on mineral stability, due to both increased temperature and possible dehydration of the rock. This second consideration is covered in Section 4.2.

    The mineralogy of the host rock is primarily quartz, cristobalite, and alkali feldspar with some clays present (Section 4.1.1.3). The stability of clays, cristobalite, glass and zeolites is of concern under present and expected conditions. The cristobalite in these rocks is metastable and will very slowly be converted to quartz. The slow rate of this conversion is evidenced by the persistence of cristobalite in these tuffs, which are about 12 million years old (Kistler, 1968). The disappearance of cristobalite with depth is probably a result of the higher temperatures experienced by tuffs deeper in Yucca Mountain. If the present geothermal gradient (Section 4.1.2.8) is responsible, then repository-induced temperature increases of a few tens of degrees could cause appreciable transformation of cristobalite to quartz. However, there is evidence of increased thermal gradients in at least some parts of Yucca Mountain in the past (Bish, 1987). Thus, the lack of cristobalite lower in the mountain may result in part from past hydrothermal alteration. Plans for obtaining the additional information on silica polymorph stability are outlined in Section 8.3.1.3.3.

    There are two effects when cristobalite transforms to quartz. First, there is a 12-percent volume decrease (using molar volumes for quartz and cristobolite from LePage and Donnay (1976) and Peacor (1973), respectively) that might affect the mechanical and hydrologic properties of the tuff; and second, there is a lowering of the aqueous silica activity. No water compositions are available from the unsaturated zone in which the host rock is located, but water samples taken from below the water table where cristobalite is present show approximate saturation with respect to cristobalite despite the presence of a considerable amount of quartz. This observation suggests that the aqueous silica activity in a particular horizon will remain high until most, if not all, of the cristobalite has converted to quartz. The silica-activity evolution is of particular concern because silica activity appears to be important in controlling the stability of clinoptilolite (Keith et al., 1978).

    Clays are present in small quantities in the host rock and occur throughout Yucca Mountain as late-stage alteration minerals (Caporuscio et al., 1982). Clays are also observed as alteration products of Topopah Spring tuff in hydrothermal experiments (Section 7.4.1.3). On the basis of these observations and on reaction-path studies of glass alteration (Kerrisk, 1983) it seems possible that clays may be continuing to crystallize in Yucca Mountain. The stability of clays is of concern because they are highly sorptive minerals. At present it seems likely that the amount of clays will remain constant or increase in Yucca Mountain. The possibility of clay dehydration or breakdown due to repository-induced heating is discussed in Section 4.2.2.

The smectites at or above the stratigraphic level of the Tram Member in Yucca Mountain have interlayer water that can be driven out with minor temperature increases or with minor changes in the partial pressure of water, causing a decrease in volume (Bish, 1981). This volume reduction is reversible at low temperatures. The implications of irreversible collapse are discussed in Section 4.2.2.

Below the host-rock horizon, successive zones of glass, heulandite and smectite, clinoptilolite, analcime, and authigenic albite are found in addition to devitrified zones dominated by alkali feldspar and silica phases. The stability of clinoptilolite is of particular concern because it has been identified as an important sorptive phase (Section 4.1.3.3).

Smyth (1982) has summarized the diagenetic zones beneath Yucca Mountain. This diagenesis begins with unaltered glass. Unaltered glass occurs in many rocks above the water table, including the vitrophyre of the host rock (where devitrification is not extensive). The next zone contains clinoptilolite or mordenite or both (Calico Hills and the upper zeolitic Crater Flat Tuff). Below these zeolites, analcime occurs, replacing clinoptilolite and mordenite. Finally, authigenic albite is typical of the deepest tuff units examined. This generalized zonation can be seen in Figures 4-1 and 4-2.

There are varying hypotheses to explain this diagenetic zonation. Smyth and Caporuscio (1981) give a plot of sodium-ion concentration versus temperature appropriate for the zeolite transition in this diagenetic sequence. Increases in sodium concentration appear to decrease the temperatures at which these reactions occur. Because the present ground water has a low sodium content (37 to 171 mg/L, Ogard and Kerrisk, 1984), the analysis of Smyth (1982) would predict that the clinoptilolite-to-analcime transformation, if it occurred, would be expected at temperatures of about 100 to 120°C.

There are, however, other factors that must be considered in this analysis. First, the stoichiometry of clinoptilolite and analcime does not suggest that the concentration of the sodium ion should affect the relative stability of the two phases. Second, the transition from clinoptilolite to analcime is also characterized by the disappearance of cristobalite, which suggests that silica activity with analcime is lower than that with clinoptilolite. Because silica evolves in the transformation of clinoptilolite to analcime, a lowering of the silica activity would move the system toward analcime stability relative to clinoptilolite. Reaction-path modeling for temperatures up to 175°C (Kerrisk 1983) indicates that increase in temperature alone does not account for the transition from clinoptilolite to analcime; rather, this transition can probably be accounted for by the change in silica activity that occurs with the change from cristobalite to quartz saturation. Field observations (Keith et al., 1978) also indicate that silica activity, rather than temperature, may be a factor controlling the transformation of clinoptilolite to analcime. Keith et al. (1978) observed clinoptilolite and analcime in drillhole Y-8 in Yellowstone National Park. Clinoptilolite was observed in a temperature interval from about 70°C to slightly above 150°C. However, throughout this interval, clinoptilolite zones were interlayered with analcime-bearing zones, indicating that temperature was not a controlling factor in determining whether clinoptilolite or

analcime was present. There was, however, an excellent correlation between the presence of clinoptilolite and that of cristobalite and between analcime and quartz (Figure 4-1), suggesting that silica activity was the controlling variable in determining the presence of clinoptilolite or analcime.

The observations on which the conclusions of Smyth (1982) were based probably reflect the effects of temperature on the kinetics of the transition from cristobalite to quartz more than an equilibrium temperature for the transformation of clinoptilolite to analcime. The apparent dependence of transition temperature on the sodium content of the solution may arise from two sources. The generally higher pH high-sodium solutions may increase the rate of transition from cristobalite to quartz. Also, as the sodium concentration increases, the activity of water is lowered by the increasing salinity of a solution, which would favor formation of the less hydrous phase, analcime.

Thus, it seems likely that the stability of clinoptilolite in Yucca Mountain is determined largely by the silica activity. If that activity in a particular horizon is at or above cristobalite saturation, the clinoptilolite is probably stable to at least 150°C. If clinoptilolite breaks down after the emplacement of waste in a repository at Yucca Mountain, it will probably be because repository heating will have increased the rate of cristobalite conversion to quartz. Plans to obtain the information to assess the likelihood of cristobalite transformation are discussed in Section 8.3.1.3.

The effects of composition on thermal expansion and thermal stability have been determined for several cation-exchanged clinoptilolites (Bish, 1984). It is known that sodium- and potassium-rich clinoptilolites are stable to higher temperatures than the calcium-rich clinoptilolites (Shepard and Starkey, 1966) that commonly occur above the basal vitrophyre in the Topopah Spring Member. However, the potassium-rich clinoptilolites in the base of and slightly below the Topopah Spring Member contract less with increased temperature than do the sodium-rich clinoptilolites farther along flow paths (Bish, 1984).

Glass is another phase in Yucca Mountain that is certainly metastable. The distribution and compositions of glass are discussed by Caporuscio et al. (1982), Vaniman et al. (1984), Bish and Vaniman (1985), and Broxton et al. (1986). Glass exists in the vitrophyre in the lower Topopah Spring Member and in parts of the tuffaceous beds of Calico Hills (Figures 4-1 and 4-2). Alteration of the glass originally present in the tuffaceous beds of Calico Hills in the northeastern part of Yucca Mountain has led to the extensive development of clinoptilolite (Section 4.1.1.3). The persistence of glass in the southwest area of Yucca Mountain may be due to the lack of water for hydration because the glasses are above the water table. However, since considerable pore water is present, the general lack of clinoptilolite formation may also be due to lack of reaction because of low temperature. There is a possibility that glass would react to form appreciable clinoptilolite in response to moderate heating from the repository, or to increased hydration that would result from a rise in the water table. Future glass stability studies are outlined in Section 8.3.1.3.3.

4.1.2 GROUND-WATER CHEMISTRY

The composition of water in the Yucca Mountain exploration block is an important parameter for evaluating the suitability of the site for the containment and isolation of radioactive waste. The water composition will affect the rate at which the waste containers corrode, the leach rate of the waste form, and the rate of radionuclide transport to the accessible environment. A reference ground water (i.e., water from well J-13) similar in composition to the water of Yucca Mountain is needed to conduct transport and retardation experiments.

Because the composition of ground water is controlled by a number of variables both internal and external to the repository horizon, it is necessary to define the range of ground-water compositions, in both the saturated and the unsaturated zones, from the exploratory block to the accessible environment. In addition, it is necessary to identify the main factors that would determine how changes in the natural (e.g., increased recharge) and man-induced conditions would affect the ground-water compositions.

At present, the only water available for chemical analysis has come from saturated-zone wells on and near Yucca Mountain. When the exploratory shafts are constructed, water from the pores in unsaturated tuff, any water flowing in fractures in unsaturated tuff, and water from any perched water zones in Yucca Mountain will be sampled, where possible, and analyzed. Plans for further analyses of the saturated-zone ground water can be found in Section 8.3.1.2. The remainder of this section discusses ground water from the saturated zone. Plans for studying the unsaturated-zone water chemistry can be found in Section 8.3.1.2.2.

4.1.2.1 General description of the hydrochemistry

Analyses of ground water from drillholes that penetrate the host rock and surrounding units in the area of the exploration block indicate that they are principally sodium bicarbonate waters (Benson et al., 1983; Ogard and Kerrisk, 1984) with low contents of total dissolved solids (200 to 400 mg/L). However, water from the carbonate aquifer (Drillhole UE-25p#1) contains over 1,000 mg/L total dissolved solids. Tables 4-6 and 4-7 summarize the geochemical data reported on ground-water samples from Yucca Mountain and its vicinity. The data are consistent with the data reported in Section 3.9.1.3, but include additional species (dissolved iron, manganese, aluminum, nitrite, nitrate, and oxygen) not reported there. The analytical techniques and sampling procedures by which these data were obtained are reported by Ogard and Kerrisk (1984). The locations of wells are shown in Figure 4-11.

4.1.2.2 Major inorganic content

The content of major and minor inorganic constituents of ground water from Yucca Mountain and vicinity are listed in Tables 4-6 and 4-7 and are discussed in the following paragraphs.

Table 4-6. Element concentrations in ground water from the
vicinity of Yucca Mountain

Well[b]	Field pH	concentrations (mg/L)								
		Ca	Mg	Na	K	Li	Fe	Mn	Al	Si
USW VH-1[c]	7.5	10	1.5	80	1.9	0.090	--[d]	--	--	23
USW H-6	7.4	5.5	0.22	74	2.1	0.10	0.12	0.04	0.12	20.0
USW H-3	9.4	0.8	0.01	124	1.5	0.22	0.13	0.01	0.51	16.9
USW H-5	7.1	1.1	0.03	54	2.3	0.04	0.01	--	0.17	17.4
USW G-4	7.1	9.2	0.15	56	2.5	0.08	0.04	0.02	0.02	19.6
USW H-1[c]	7.5	6.2	<0.1	51	1.6	0.04	--	--	--	19
USW H-4	7.4	10.8	0.19	84	2.6	0.16	0.03	0.005	0.04	25.9
UE-25b#1	7.7	19.7	0.68	56	3.3	0.28	0.04	0.004	0.03	31.5
UE-25b#1[e]	7.2	18.4	0.68	46	2.5	0.30	0.69	0.36	0.04	28.7
UE-25b#1[f]	7.3	17.9	0.66	37	3.0	0.17	0.08	0.07	0.06	28.8
J-13	6.9	11.5	1.76	45	5.3	0.06	0.04	0.001	0.03	30.0
UE-29a#2	7.0	11.1	0.34	51	1.2	0.10	0.05	0.03	0.04	25.8
J-12[c]	7.1	14	2.1	38	5.1	-	-	-	-	25
UE-25p#1[g]	6.7	87.8	31.9	171	13.4	0.32	<0.1	<0.01	0.1	30

[a]Concentrations from Ogard and Kerrisk (1984) unless otherwise noted.
All samples are integral water samples unless otherwise noted.
[b]See Figure 4-11 for locations.
[c]Data from Benson et al. (1983).
[d]--indicates the element was not detected.
[e]Bullfrog zone, 4th day of pumping.
[f]Bullfrog zone, 28th day of pumping.
[g]From dolomite aquifer.

Table 4-7. Anion concentrations and other measurements for ground
water from the vicinity of Yucca Mountain

Well[b]	Concentration[a] (mg/L)								
	F^-	Cl^-	SO_4^{2-}	HCO_3^-	NO_2^-	NO_3^-	O_2	Detergent	Eh[c]
USW VH-1[d]	2.7	11	44	167	--	--	--	--	--
USW H-6	4.1	7.7	27.5	--	--[e]	5.3	5.6	--	395
USW H-3	5.4	8.3	31.2	245	<0.10	0.2	<0.1	<0.02	-123
USW H-5	1.3	5.7	14.6	--	--	8.6	6.3	<0.005	353
USW G-4	2.4	5.5	15.7	--	--	5.5	6.4	--	402
USW H-1[d]	1.0	5.8	19	122	--	--	--	--	--
USW H-4	4.5	6.2	23.9	--	--	4.7	5.8	>2	216
UE-25b#1	1.2	7.1	20.6	--	--	0.6	1.8	--	220
UE-25b#1[f]	1.5	9.8	21.0	--	0.5	2.2	<0.1	2.7	-18
UE-25b#1[g]	1.2	6.6	20.3	--	--	4.5	1.8	0.02	160
J-13	2.1	6.4	18.1	143	--	10.1	5.7	--	--
UE-29a#2	0.56	8.3	22.7	--	--	18.7	5.7	--	305
J-12[d]	2.1	7.3	22	119	--	--	--	--	--
UE-25p#1[h]	3.5	37	129	698	--	<0.1	--	<0.2	360

[a]Concentrations from Ogard and Kerrisk (1984) unless otherwise noted.
All samples are integral samples unless otherwise noted.
[b]See Figure 4-11 for location.
[c]mV versus H_2 electrode.
[d]Data from Benson et al. (1983).
[e]--indicates the element was not detected.
[f]Bullfrog zone, 4th day of pumping.
[g]Bullfrog zone, 28th day of pumping.
[h]From dolomite aquifer.
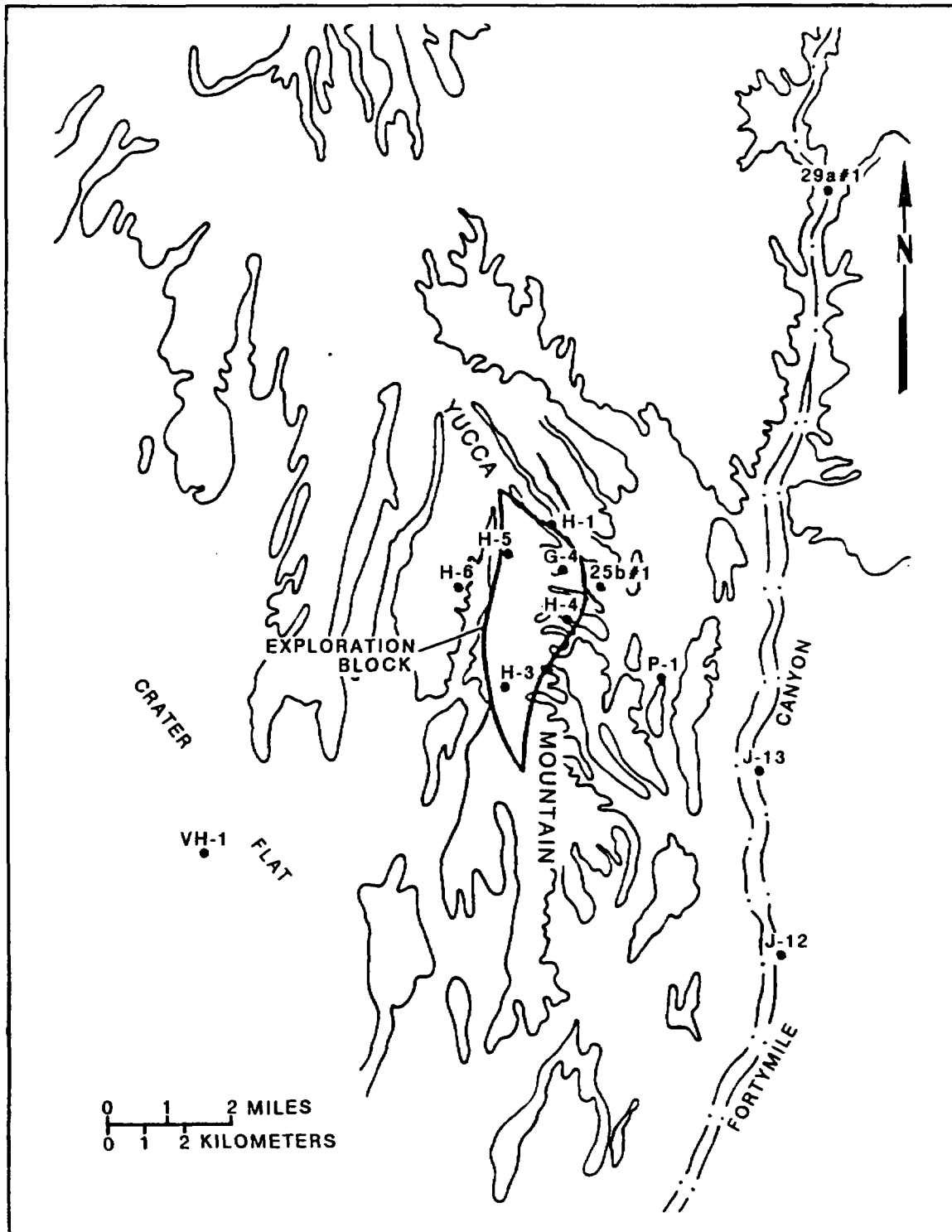
Figure 4-11. Selected drillhole and well locations on and near Yucca Mountain exploration block (the names of the wells and drillholes have been shortened for clarity; for example, drillhole USW H-6 is listed as H-6 and drillhole UE-25p#1 as P-1, etc.). Modified from Ogard and Kerrisk (1984).

The data presented in Tables 4-6 and 4-7 are representative of the chemistry of the ground waters at Yucca Mountain. Kerrisk (1987) is a more recent review of the water chemistry at Yucca Mountain and in the surrounding area. This report references and compiles hundreds of analyses representing a large data base for the saturated zone water chemistry. More hydro-chemistry work is planned in Section 8.3.1.2 for the saturated zone and and more importantly the unsaturated zone. Section 8.3.1.3.1 will synthesize the present and future data into a ground-water chemistry model.

The dominant cations in the Yucca Mountain ground water are sodium, calcium, potassium, and magnesium. Sodium is the most abundant, accounting for 65 to 95 percent of the cations present. The relative concentrations of cations are shown in a ternary diagram in Figure 4-12. Data from three other wells are also shown on these figures; wells UE19e and U20a-2 are in tuff-aceous rocks on Pahute Mesa (Claassen, 1973), and well 9 is in the Amargosa Desert (Claassen, 1985).

The additional wells were included because ground water at Yucca Mountain is probably derived by subsurface flow from recharge areas at higher altitudes to the north such as Pahute Mesa (Winograd and Thordarson, 1975), and because the southern Amargosa Desert is considered a discharge area for water moving beneath Yucca Mountain (Winograd and Thordarson, 1975). The shaded areas in Figure 4-12 represent the ranges of compositions of inter-stitial and fracture waters in ash-flow tuffs at Rainier Mesa north of Yucca Mountain (White et al., 1980). Wells on Yucca Mountain and just to the west (USW H-3, USW H-5, and USW H-6; Figure 4-11) plot nearest the sodium apex of Figure 4-12. Wells on the eastern slopes and washes (USW H-1, USW H-4, USW G-4, J-13, and UE-25b#1) show increasing levels of calcium. The carbonate aquifer well (UE-25p#1) and the well from the Amargosa Desert (well 9) show the highest relative calcium contents. The two wells on Pahute Mesa (wells UE19e and U20a-2) are similar to the wells on and just east of Yucca Mountain; this is consistent with a relation in actual recharge or recharge mechanisms between the two areas. The data for the wells plot in a band that is generally parallel to the sodium-calcium axis in Figure 4-12, which indi-cates that the relative potassium content of the waters is nearly constant.

The concentrations of iron and manganese are generally low (Table 4-6). The elevated concentrations in drillhole UE-25b#1 after the fourth day of pumping may reflect contaminants from the drilling operation because the concentrations dropped down to more typical values after 28 d. Both iron(III)/iron(II) and manganese(IV)/manganese(II) as well as nitrate/nitrite have been considered as oxidation-reduction (redox) couples that reflect the redox potential of the ground waters (Rundberg et al., 1985). Analytical data are available only for the nitrate/nitrite couple in drillhole UE-25b#1 water. The redox potential, Eh, calculated from these data (100 to 400 mV) is substantially different from the Eh measured in this water with a platinum electrode (80 to 170 mV) (Rundberg et al., 1985). Such differences are commonly observed in ground water (Lindberg and Runnells, 1984) and may indicate a lack of equilibrium due to slow reaction kinetics among the redox couples in the water. The positive Eh values and dissolved-oxygen content of waters listed in Table 4-7 indicate that most of the waters are oxidizing. The reducing character of the drillhole UE-25b#1 water collected on the fourth day after pumping was initiated probably reflects an initial disturb-ance of the producing horizon due to completion of the drillhole. The

Na

LEGEND

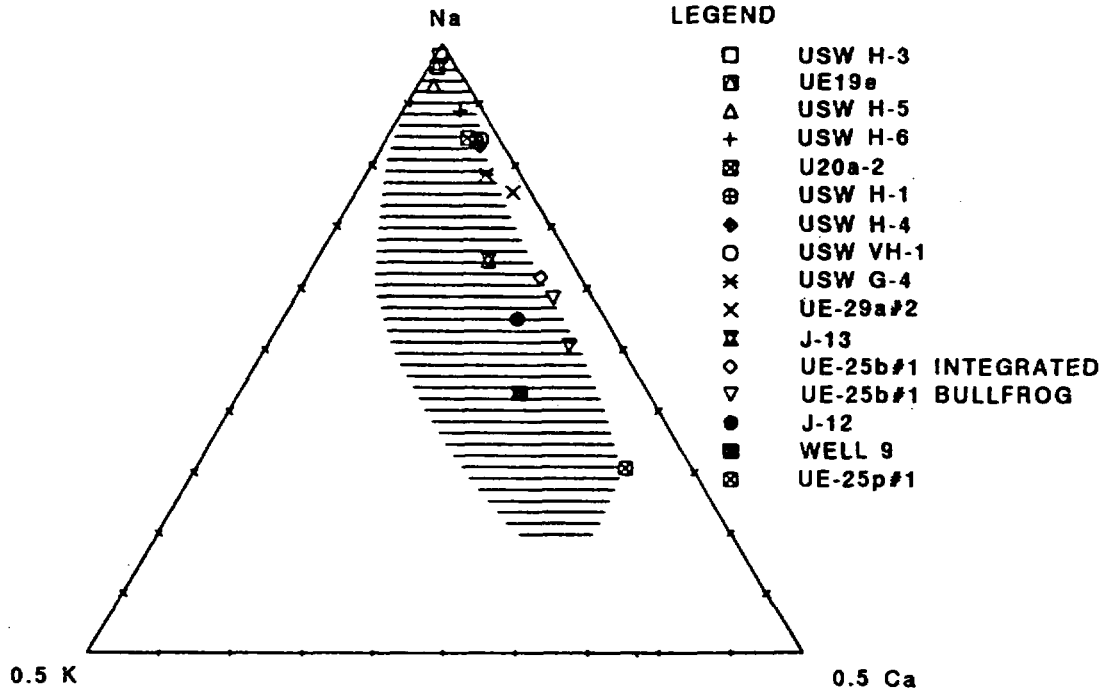|	
☐	USW H-3
◨	UE19e
△	USW H-5
+	USW H-6
⊠	U20a-2
⊕	USW H-1
◆	USW H-4
○	USW VH-1
✳	USW G-4
✕	UE-29a#2
⊠	J-13
◇	UE-25b#1 INTEGRATED
▽	UE-25b#1 BULLFROG
●	J-12
■	WELL 9
⊠	UE-25p#1

0.5 K   0.5 Ca

Figure 4-12.   Relative sodium-potassium-calcium concentration in Yucca Mountain water (Ogard and Kerrisk. 1984). Shaded area represents range of compositions of interstitial and fracture waters at Rainier Mesa. Modified from White et al. (1980). Data shown are in mole percent.

reducing character of the drillhole USW H-3 water has not been fully explained but may reflect a reduction of recharge waters by organics during the last pluvial (Ogard and Kerrisk, 1984).

The anionic constituents of the ground water show a relatively uniform distribution in all the wells, with about 80 percent bicarbonate and the remainder as sulfate and chloride (usually present in nearly equal molar concentrations) and fluoride (in varying concentrations). The carbonate ion is a major complexing agent for the actinide elements, with the hydroxide ion (Section 4.1.3.4) and the fluoride ion being of less importance under oxidizing conditions (Ogard and Kerrisk, 1984).

Spatial variations in ground-water composition are implicit in Tables 4-6 and 4-7 because the ground waters listed are from wells surrounding the repository block. Overall, there is only minor variation in ground-water compositions in and adjacent to Yucca Mountain.

4.1.2.3 Trace elements

The trace elements detected in Yucca Mountain ground water are barium, bromine, lithium, phosphorus, strontium, titanium, and vanadium. The observed ranges in concentration (in mg/L) are less than 0.001 to 0.011 for barium, less than 0.2 to 14.5 for bromine, 0.04 to 0.95 for lithium, less than 1.2 for phosphorus, less than 0.001 to 0.07 for strontium, less than 0.012 to 0.03 for titanium, and less than 0.004 to 0.03 for vanadium (Daniels et al., 1983; Ogard et al., 1983b).

Because lithium was added to the drilling fluid as a tracer to monitor contamination of ground water by the fluid (Daniels et al., 1983), the high end of the range reported here may not represent natural concentrations.

4.1.2.4 Organic content

The in situ organic contents of the waters from drillhole UE-25b#1 and well J-13 were measured by Means et al. (1983). The total organic carbon contents were 0.14 ± 0.05 mg/L in well J-13 water and 0.58 ± 0.06 mg/L in drillhole UE-25b#1 water, respectively. The lower carbon content in well J-13 water is probably representative of the in situ content because the well is a producing well for the Nevada Test Site and all drilling fluids have been removed by extensive pumping. Because of the low concentrations, little can be said about the individual organic compounds other than that organics with high molecular weight (higher than 1,000) constitute 50 percent of the organics present in J-13 water and 33 percent in UE-25b#1 water. The low organic content in the saturated zone suggests that complexing of waste elements americium, neptunium, plutonium, and uranium with naturally occurring organic ligands will be insignificant.

4.1.2.5 Dissolved gas

Measurements of the concentrations of dissolved gases in Yucca Mountain ground waters are very limited. The presence of carbon dioxide in saturated-zone water is indicated by the change in pH (from 7 to 8.5) of ground water that is pumped from deep wells and allowed to stand at atmospheric pressure. A change in dissolved carbon dioxide from $10^{-2.5}$ to the normal $10^{-3.5}$ atmospheres would explain this shift in pH (Daniels et al., 1982). A direct measurement of the carbon dioxide content of the lowest zone of well UE-25p#1 produced a value of 242 mg/L (Bryant and Vaniman, 1984).

The dissolved-oxygen contents of several saturated-zone ground waters are shown in Table 4-7 (Ogard and Kerrisk, 1984). The presence of dissolved oxygen in the water indicates oxidizing conditions.

4.1.2.6 Background radioactivity

Well J-13 is the only well in the vicinity of Yucca Mountain for which data on radionuclide activity are available. The activities of radionuclides present in well J-13 water have been measured (EPA, 1976); results are shown in Table 4-8. Plans for obtaining additional data on the concentration of naturally occurring radionuclides in Yucca Mountain ground water are outlined in Section 8.3.1.2. These data will provide baseline values for future reference in monitoring the ground water at Yucca Mountain.

4.1.2.7 Particulates and colloids

It is necessary to measure the ambient concentration of particulates because particulate material in ground water at a repository site may be significant as a means of transport of radionuclides by sorption on the particulate material. At Yucca Mountain there are no springs or other accessible sources of flowing ground water. Therefore, well J-13, a water well adjacent to Yucca Mountain, was pumped and sampled for particulates by filtering 9,300 L of water through a 0.4-micrometer filter, and 5,300 L of water through 0.05-micrometer Nuclepore filters (Kerrisk, 1987). Material that was present on the filters ranged in diameter from tens of micrometers down to less than 0.01 micrometer, the resolving power of the microscope. A total quantity of 0.25 g of solid material was obtained, corresponding to a sediment concentration of about 2.7×10^{-5} g/L. The composition of individual particles varied considerably. The detectable cations in the >0.4 micrometer fraction were (in weight percent) silicon (60), iron (20), calcium (11), and aluminum (4), while analysis of the smaller size fraction gave somewhat different results: sodium (44), silicon (42), calcium (8), and iron (4) with no detectable aluminun. Because the amount of iron in the Yucca Mountain tuffs and ground waters is low, it is possible that the iron-rich particulates could have been contamination from the steel piping and pumping system. Filter samples also were obtained from two other wells at the NTS, both drawing from an aquifer in alluvial soil. The results were similar to those from well J-13. Because the samples were derived from water flowing in

Table 4-8. Background radioactivity

Number of samples analyzed	Radionuclide	Radioactivity concentration 10^{-9} μCi/ml		
		Maximum	Minimum	Average
5	H-3	8	<7	<8
1	Sr-89	<2	<2	<2
1	Sr-90	<0.9	<0.9	<0.9
1	Ra-226	0.067	0.067	0.067
1	U-234	1.7	1.7	1.7
1	U-235	<0.02	<0.02	<0.02
1	U-238	0.22	0.22	0.22
1	Pu-238	<0.03	<0.03	<0.03
1	Pu-239	<0.04	<0.04	<0.04

[a]Data extracted from Table 8, EPA (1976) for five water samples collected from Nevada Test Site well J-13.

an artificially created gradient, it can be argued that the particulate content is not that of natural water. However, pumped well water may provide a worst-case situation. Plans for obtaining data on the sorption of radionuclides on colloids and particulates are outlined in Section 8.3.1.3.4.

4.1.2.8 Temperature and pressure

The temperatures in drillholes and wells on and near Yucca Mountain are shown in Figure 4-13. The temperature gradient varies between approximately 20° and 40°C/km at depths of less than or equal to 3 km. The variance suggests that the temperature in the repository horizon should be 25° to 35°C and it also provides a baseline range of temperatures for modeling the perturbation of the temperature gradient produced by the emplacement of the waste. This topic is discussed in Section 1.7 and the discussion here is taken from Sass and Lachenbruch (1982).
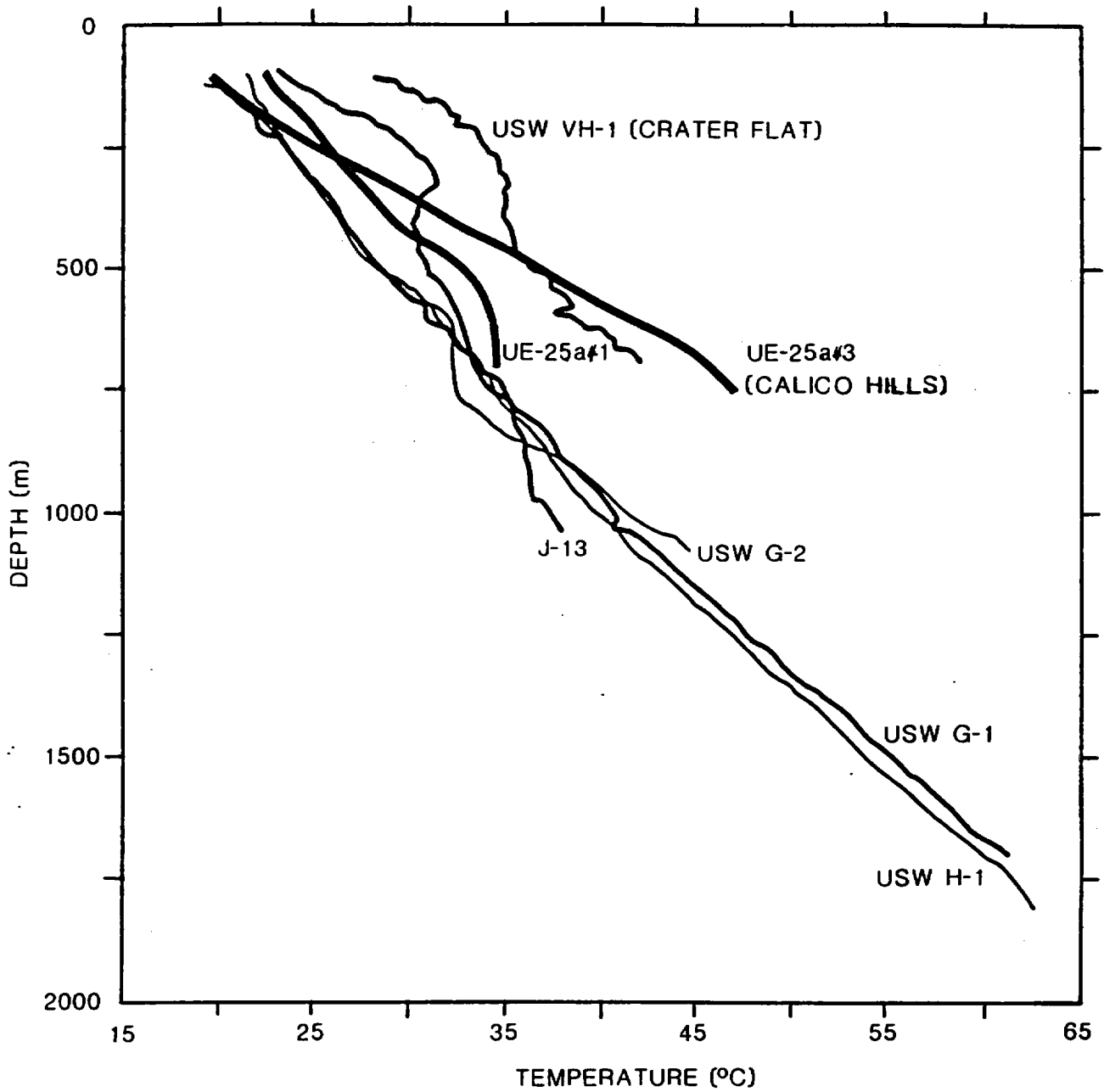
Figure 4-13. Plot of temperature versus depth in drillholes deeper than 600 m for Yucca Mountain and nearby areas. Modified from Sass and Lachenbruch (1982).

Because the repository horizon is in the unsaturated zone, the pressure on ground water in this horizon will be close to atmospheric at the appropriate elevation above sea level. Below the water table and along pathways to the accessible environment, the pressure of the ground water will correspond roughly to depth below the water table.

4.1.2.9 Mineralogical controls on water composition

The composition of ground water in the exploratory block and between the repository block and the accessible environment is determined by various factors, including the composition of water infiltrating from the surface, the composition of saturated zone water upgradient from the repository block, and interactions between ground water and the rocks through which it may flow. Ground-water interactions with rock and models describing these interactions are discussed in this section. These interactions between ground water and rock consist primarily of the dissolution of primary silicate phases contained in the volcanic rocks, the precipitation of secondary phases, and sorption and ion-exchange reactions with primary and secondary phases. Primary silicate phases include volcanic glass and various mineral types formed at high temperatures (higher than 500°C). Secondary phases include minerals such as clays, carbonates, and zeolites as well as amorphous solids such as amorphous silica and semiamorphous oxides (e.g., manganese-iron, oxyhydroxides). The models describing ground-water interactions with rock have not considered precipitation and ion-exchange reactions with these minerals.

Because reactions between ground water and silicate phases are generally slow at the temperatures and water-flow rates likely to prevail in rocks between the repository block and the accessible environment, models that assume chemical equilibrium between ground waters and host rocks may not be appropriate. Models of ground-water interactions with rock must incorporate reaction with rock kinetics. Because reaction kinetics cannot be reliably predicted on the basis of theoretical considerations alone, experimental data on the kinetics of appropriate interacting systems (ground water and rock) are required (Chapter 7 and Section 8.3.1.3.3).

White and Claassen (1979; 1980) have presented experimental data and discussed mechanisms for the dissolution of volcanic glass by water. Their glass samples were obtained from the Timber Mountain Tuff exposed on Rainier Mesa at the NTS. White et al. (1980) presented experimental data on the dissolution of glassy and nonglassy tuffs from Rainier Mesa. Using the data, they derived rate constants that were used to extrapolate the experimental results to longer time scales. White et al. (1980) concluded that the composition of interstitial and fracture waters obtained from the Rainier Mesa area could be explained on the basis of a glass-dissolution model. However, the model does not explain all the water compositions obtained by White et al. (1980), such as the highly sodic waters. In addition, the model does not attempt to explain the detailed variations in the pH and the Eh of the ground water. These two parameters are particularly important to radionuclide-transport calculations. Nonetheless, two important aspects of these studies are clear: (1) water composition varies with stratigraphic

position in the tuffs of Rainier Mesa, suggesting local control, and
(2) experimental data suggest that the variations are the result of
dissolution of the tuffs through which the water flows.

The overall similarity of the rock types and alteration minerals in
Yucca Mountain and Rainier Mesa (Byers et al., 1976) suggests that the con-
trols on ground-water compositions in these two areas might be similar. This
is supported by the overlap in the relative cation concentrations of Rainier
Mesa and Yucca Mountain ground waters shown in Figure 4-12. Note that the
overlap does not extend to ground water from the Paleozoic limestone aquifer
(drillhole UE-25p#1) beneath Yucca Mountain (Figure 4-12). The concentra-
tions of other cations, anions, and uncharged species in Yucca Mountain
waters also overlap those in Rainier Mesa waters.

Although the work of White and Claassen (1979, 1980) has provided impor-
tant data on the possible influence of glass dissolution on ground-water com-
positions in tuffaceous aquifers, further work is required to adequately
understand the controls on the composition of Yucca Mountain saturated- and
unsaturated-zone waters. This additional work is discussed in Section
8.3.1.3.

4.1.2.10 Reference ground-water composition

Many of the processes taking place in the transport and retardation of
waste elements along pathways from the repository to the accessible environ-
ment will be investigated in a laboratory and then the results will be used
in modeling the entire pathway. To conduct such experiments, a reference
ground water or ground waters that will represent ground-water conditions
that will be experienced along such a pathway is needed. The reference
ground water for the NNWSI Project was chosen on the basis of meeting the
following criteria:

1. It should be readily available because many laboratory experiments
    will use the reference ground water.

2. It should have a composition that is representative of compositions
    estimated for the interstitial and fracture waters in the Topopah
    Spring Member tuff in the unsaturated zone (the potential repository
    horizon).

3. It should have a composition that is representative of ground waters
    along the potential flow paths away from the repository.

4. It should be a natural ground water rather than synthetic water.

The ground water from well J-13 has been chosen as best meeting these
requirements.

Well J-13 is a producing well located in Jackass Flats southeast of the
Yucca Moutain site (Figure 4-11) which has been pumped since 1962. Because
of the large amount of water produced to date, the well should be clear of

any drilling fluids that may have been used in the original drilling. The main producing zone in well J-13 is in the Topopah Spring Member of the Paintbrush Tuff, which corresponds to the potential repository horizon at Yucca Mountain. This aspect of well J-13 water makes it a useful reference water.

The compositions of interstitial and fracture waters in the unsaturated zone of Yucca Mountain are not yet available, plans for obtaining them are outlined in Section 8.3.1.3. However, White et al. (1980) have determined the composition of interstitial and fracture waters in the tuffaceous aquifers of Rainier Mesa. Because Rainier Mesa and Yucca Mountain are composed of similar rock types, the ground-water compositions in these two areas should reflect similar rock-water interactions. As shown in Figure 4-12, the composition of well J-13 water plots in the field of the Rainier Mesa interstitial and fracture waters reported by White et al. (1980), and may be representative of interstitial and fracture waters in the unsaturated zone of Yucca Mountain. Data for waters from the saturated zone beneath the Yucca Mountain area are also plotted in Figure 4-12. Because the data for well J-13 water plot near the middle of the range of compositions, this water should be adequate for use as a reference water. Other constituents in well J-13 waters (e.g, dissolved silica, bicarbonate, chloride, and sulfate) also show concentrations similar to those of Rainier Mesa interstitial and fracture waters.

4.1.3 GEOCHEMICAL RETARDATION PROCESSES

Under present baseline conditions, the expected flow mechanism in the unsaturated zone is matrix flow through the tuff. This does not exclude the possibility that fracture flow may be important under some potential conditions. In addition, it is possible that future hydrologic research may find that fracture flow under present conditions is also important. Fracture flow is important in the saturated zone where it is the significant flow mechanism. The flow of water through the unsaturated zone is driven by the hydrostatic head and by capillary suction. The expected flow path in the unsaturated zone is downward through the welded and highly fractured Topopah Spring Member tuff and then through the zeolitized bedded tuff of the Calico Hills. The median pore size for tuff reported by Walter (1982) is between 1.2 and 0.1 μm. The unsaturated flow will be drawn to smaller pores by capillary suction. Much of the smallest diameter porosity is intracrystalline pore space in the zeolites and clay minerals. This is particularly true in the nonwelded zeolitic tuff. The intracrystalline porosity of the zeolite clinoptilolite is about 36 percent based on the crystallographic structure. Zeolitic tuff, with 80 to 90 percent clinoptilolite, has a total porosity of 40 to 50 percent, and hence, in zeolitic tuff more than half the porosity is intracrystalline. Furthermore, the channels in the clinoptilolite framework are only 3.6 angstroms in diameter, and it is, therefore, expected that there would be good contact between water containing radionuclides and the strongly adsorbing zeolites and clays in the unsaturated zone.

The transport of contaminants by flow through either a porous matrix or a fracture system in a porous matrix will in each case be affected by various

geochemical and mechanical processes. Among the chemical processes considered in this section are adsorption on mineral surfaces (both internal and external to the crystal structure), including the kinetics of adsorption, and processes leading to precipitation. The mechanical processes considered are dispersive effects (hydrodynamic dispersion, channeling) and diffusion.

In the saturated zone, the flow is believed to be mainly through fractures in welded-tuff units, such as the upper part of the Prow Pass Member. The transport of radionuclides through such fractured units will be affected by sorption on fractured surfaces, but probably not to the same degree as sorption in matrix pore spaces. Since fluid velocities in fracture flow can be much higher than in matrix flow, local chemical equilibrium may not be attained and kinetics becomes an important consideration. Evidence from laboratory experiments shows that sorption reaction rates are fast and equilibrium could be achieved for quite high flow rates (Rundberg, 1985). An additional process that will affect transport through fracture systems is matrix diffusion into the adjacent matrix pore spaces. This process may be limited by channeling, which effectively reduces the surface area through which solutes diffuse from fracture flows to the matrix. Channeling also acts as a dispersion mechanism--that is, it broadens the pulse of solute concentrations.

4.1.3.1 General description of geochemical retardation

The most likely mechanism for the release of radionuclides from a repository is transport in the aqueous or vapor phase from the repository to the accessible environment. This transport can be retarded by three geochemical processes:

1. Sorption--the sorption of chemical species on mineral surfaces such as ion exchange, chemisorption, van der Waals attraction, etc., or ion exchange within the crystal structure.

2. Precipitation--the formation of less soluble compounds by chemical reaction with chemical entities present in the ground water.

3. Exchange between the vapor phase and the aqueous or solid phases.

Sorptive mineral phases, particularly zeolites and clays, along potential flow paths are expected to delay the rate at which radionuclides are released to the accessible environment. Flow paths from the repository to the saturated zone are through bedded tuff at the bottom of the Topopah Spring Member and through the tuffaceous beds of Calico Hills, both of which contain significant quantities of zeolites and clays (Section 4.1.1.3). Other formations that might be part of the flow path are the Prow Pass, the Bullfrog, and the Tram members of the Crater Flat Tuff; zones containing zeolites and clays in variable abundances are present in these units (Section 4.1.1.3).

Precipitation processes (i.e., solubility) will limit the concentration of radionuclides in water that moves from the repository toward the accessible environment. Solubility depends on the composition of the solution;

that is, formation of complexes can retain species in solution in greater amounts than would otherwise exist. Yucca Mountain ground water is primarily a sodium-bicarbonate water (Section 4.1.2.1); carbonate, bicarbonate, and hydroxyl are the most prevalent anions that form complexes with radionuclide cations. However, for some radionuclides, such as cesium or strontium, the solubility limits may not limit radionuclide transport. Quantitative data for the hydroxyl and carbonate complexes of most waste elements are insufficient and need to be determined. Plans for obtaining this information are outlined in Section 8.3.1.3.

Vapor-phase transport is generally in the opposite direction from aqueous transport and may proceed more quickly since the pores that are not filled with water are the larger pores and have a higher permeability than the water-filled pores. In the unsaturated zone, volatile elements, such as iodine, can be transported in the vapor phase. The vapor-transport process is impeded, however, by exchange between the slower moving aqueous phase and the solubility in the aqueous phase, which lowers the partial pressure of the volatile species.

There are physical processes such as matrix diffusion that are driven by advective forces in which radionuclides diffuse into water in the pores and may retard the transport of all species, including nonsorbing or low-sorbing species (Section 4.1.3.5). In general matrix diffusion can be regarded as the movement of dissolved species from water in connected pore spaces to water in "dead-end" pore spaces as a result of gradients in species concentrations. In particular, the connected pore spaces may be fracture networks in which flow is rapid, and the dead-end pore spaces may be the matrix pores in which flow is relatively slow. Dissolved species may also be transferred from matrix flow to fracture flow (and vice versa) by advective forces arising from pressure differences; however, advective transfer is not considered in this chapter.

The modeling of radionuclide transport requires that the reactions of radionuclides that occur between the solid phase (minerals, or precipitates) and aqueous phase (fracture or pore water) be coupled with the hydrologic flow and physical processes like diffusion and dispersion. Much of the basis for transport modeling has origins in chemical engineering and specifically the modeling of chromatographic columns. Chromatographic columns, however, are constructed so that dispersion is minimized. Moreover, the column is homogeneous and hence channeling is minimized. Homogeneity also prevents any effects that would be analogous to matrix diffusion and fracture flow. The columns are run at flow rates that do not exceed mass transfer kinetics and under chemical conditions (i.e., controlled pH, complexing agents, etc.) which ensure well-behaved adsorption. Thus, for column chromatography the coupling between chemistry and flow is simple and can be successfully modeled. The transport of tracers in geohydrologic systems, however, is not simple and simplifying assumptions must be tested by laboratory and field studies (Sections 8.3.1.3.6 and 8.3.1.3.4). In addition, transport by colloids must be examined because colloids may not interact with the stationary solid phase.

4.1.3.1.1 Key radionuclides

The importance of the various radionuclides present in the waste can vary depending on time scales of interest, site conditions, transport mechanisms, health physics concerns, or waste types. A list of important waste elements has been developed for the Yucca Mountain site (Kerrisk, 1985) from the following criteria:

1. The quantity of various radionuclides present in the waste.

2. The release limits established by the EPA for the radionuclides (40 CFR Part 191).

3. Preliminary estimates of the solubility and sorption of waste elements.

4. Special problems that may arise for certain waste elements.

The following types of waste were considered: spent fuel and high-level waste (HLW) from pressurized water reactors (PWR) or boiling water reactors (BWR), and defense high-level waste (DHLW). Data for spent fuel and HLW were obtained from a compilation by Croff and Alexander (1980). The radionuclides include fission products, actinides and their decay products, and activation products present in the fuel, cladding, and subassembly hardware. Data for PWR waste (spent fuel and HLW) were used as characteristic of both PWR and BWR waste because the radionuclide inventories are similar (Kerrisk, 1985). Data for DHLW were obtained from calculations by Foweler and Boersma of the Waste Solidification Technology Division of the Savannah River Laboratory (Boersma, 1984). These calculations give radionuclide inventories that are characteristic of waste from the future Defense Waste Processing Facility and include radionuclides present in the waste glass only. The results compiled by Croff and Alexander (1980) are in curies per metric tons heavy metal (Ci/MTHM), where MTHM is metric ton of heavy metal (uranium and plutonium) originally charged to the reactor. The results can be directly compared with the EPA standards, where the release limits are given in terms of curies per 1,000 MTHM. The results for DHLW are in curies per container. For this assessment, the equivalent loading of DHLW containers was estimated as 0.5 MTHM per container based on a comparison of the total activity of PWR HLW and DHLW canisters.

A general criterion for the importance of the various radionuclides in waste in terms of the EPA standards can be obtained from the ratio of the quantity of the radionuclide in the waste to the EPA release limit for that radionuclide, where both are expressed in curies per 1,000 MTHM. Tables 4-9 through 4-11 list radionuclides ordered by this ratio along with the ratios for PWR spent fuel, PWR HLW, and DHLW, respectively (Kerrisk, 1985). Radionuclides near the top of the lists in the tables have larger values of this ratio. Thus, larger fractions of these radionuclides must be contained by the repository to meet the EPA standard. At 100 yr after discharge from the reactor, isotopes of cesium, strontium, americium, and plutonium head the lists. In the 1,000- to 10,000-yr range, isotopes of the actinides (americium, plutonium, neptunium, and uranium) head the lists. By 100,000 yr after discharge, the lists are headed by actinides as well as radionuclides in the actinide decay chains, but a few other radionuclides, such as isotopes of

Table 4-9. Radionuclides ordered by ratio of inventory to U.S. Environmental Protection Agency limit for PWR spent fuel for various decay times[a]

1×10^2 yr		1×10^3 yr		1×10^4 yr		1×10^5 yr	
Am-241	3.8×10^4	Am-241	9.0×10^3	Pu-239	2.4×10^3	Pu-239	1.8×10^2
Pu-238	1.1×10^4	Pu-240	4.8×10^3	Pu-240	1.8×10^3	Th-230	1.0×10^2
Cs-137	1.0×10^4	Pu-239	3.1×10^3	Am-243	6.7×10^1	U-234	1.6×10^1
[b]Ba-137m	9.8×10^3	Am-243	1.6×10^2	U-234	1.9×10^1	Pu-242	1.5×10^1
Sr-90	6.8×10^3	U-234	2.0×10^1	Pu-242	1.7×10^1	Np-237	1.1×10^1
[c]Y-90	6.8×10^3	Pu-242	1.8×10^1	Th-230	1.7×10^1	[d]Ra-226	1.0×10^1
Pu-240	5.3×10^3	[e]Np-239	1.6×10^1	Np-237	1.2×10^1	U-233	4.1
Pu-239	3.1×10^3	C-14	1.4×10^1	[e]Np-239	6.7	U-236	4.0
Pu-241	1.0×10^3	Np-237	1.0×10^1	Ni-59	4.8	Th-229	3.7
Cm-244	3.3×10^2	Pu-238	9.7	C-14	4.6	U-238	3.2
Ni-63	3.1×10^2	Ni-59	5.2	U-236	3.5	Ni-59	2.2
Am-243	1.7×10^2	U-238	3.2	U-238	3.2	Zr-93	1.9

[a]Source: Kerrisk (1985), PWR = pressurized water reactor.
[b]Short-lived daughter of Cs-137.
[c]Short-lived daughter of Sr-90.
[d]Decay products of Ra-226 are in secular equilibrium. Each alpha emitter in the decay chain has the same ratio of inventory to EPA limit; others have a ratio that is 10 times lower. The Ra-226 decay products are generally short-lived.
[e]Short-lived daughter of Am-243.

Table 4-10. Radionuclides ordered by ratio of inventory to the U.S. Environmental Protection Agency limit for high-level waste from pressurized water reactors for various decay times

1×10^2 yr		1×10^3 yr		1×10^4 yr		1×10^5 yr	
Cs-137	1.0×10^4	Am-241	1.8×10^3	Am-243	1.6×10^2	Pu-239	5.1
[b]Ba-137m	9.8×10^3	Am-243	1.7×10^2	Pu-239	4.0×10^1	Np-237	3.4
Sr-90	6.8×10^3	Pu-240	6.3×10^1	Pu-240	2.4×10^1	Th-230	2.4
[c]Y-90	6.8×10^3	Pu-239	2.1×10^1	[d]Np-239	6.7	Ni-59	2.2
Am-241	2.0×10^3	[d]Np-239	1.6×10^1	Ni-59	4.8	Zr-93	1.7
Pu-238	5.2×10^2	C-14	1.4×10^1	C-14	4.6	[e]Nb-93m	1.6
Cm-244	3.3×10^2	Ni-59	5.1	Np-237	3.5	U-233	1.2
Ni-63	3.1×10^2	Np-237	3.5	Zr-93	1.8	[f]Th-229	1.1
Am-243	1.7×10^2	Zr-93	1.8	[e]Nb-93m	1.7	Tc-99	9.4×10^{-1}
Sm-151	1.7×10^2	[e]Nb-93m	1.7	Tc-99	1.3	Sn-126	3.9×10^{-1}
Pu-240	6.8×10^1	Tc-99	1.3	Nb-94	9.1×10^{-1}	U-234	3.6×10^{-1}
Cm-242	2.0×10^1	Nb-94	1.2	Sn-126	7.3×10^{-1}	[g]Pa-233	3.4×10^{-1}

[a]Source: Kerrisk (1985).
[b]Short-lived daughter of Cs-137.
[c]Short-lived daughter of Sr-90.
[d]Short-lived daughter of Am-243.
[e]Short-lived daughter of Zr-93.
[f]Decay products of Th-229 are in secular equilibrium. Each alpha emitter in the decay chain has the same ratio of inventory to EPA limit; others have a ratio that is 10 times lower. The Th-229 decay products are generally short lived.
[g]Short-lived daughter of Np-237.

Table 4-11. Radionuclides ordered by ratio of inventory to the U.S. Environmental Protection Agency limit for defense high-level waste for various decay times

1×10^2 yr		1×10^3 yr		1×10^4 yr		1×10^5 yr	
Pu-238	8.7×10^3	Am-241	1.9×10^2	Pu-239	1.3×10^2	Th-230	7.5×10^1
Sr-90	7.8×10^3	Pu-239	1.7×10^2	Pu-240	3.8×10^1	U-234	1.1×10^1
[b]Y-90	7.8×10^3	Pu-240	9.9×10^1	U-234	1.4×10^1	Pu-239	9.7
Cs-137	7.4×10^3	U-234	1.5×10^1	Th-230	1.3×10^1	[c]Ra-226	7.4
[d]Ba-137m	7.0×10^3	Pu-238	7.1	Ni-59	3.3	Zr-93	1.9
Am-241	7.8×10^2	Ni-59	3.5	Zr-93	2.0	[e]Nb-93m	1.9
Ni-63	4.3×10^2	Zr-93	2.0	[e]Nb-93m	2.0^c	Ni-59	1.4
Sm-151	2.1×10^2	[e]Nb-93m	2.0	[c]Ra-226	9.7×10^{-1}	U-236	6.3×10^{-1}
Pu-239	1.7×10^2	Th-230	1.2	U-236	6.2×10^{-1}	Np-237	2.6×10^{-1}
Pu-240	1.1×10^2	U-236	6.0×10^{-1}	Tc-99	3.3×10^{-1}	Tc-99	2.4×10^{-1}
Pu-241	2.4×10^1	Tc-99	3.4×10^{-1}	Np-237	2.7×10^{-1}	U-238	1.5×10^{-1}

[a]Source: Kerrisk (1985).
[b]Short-lived daughter of Sr-90.
[c]Decay products of Ra-226 are in secular equilibrium. Each alpha emitter in the decay chain has the same ratio of inventory to EPA limit; others have a ratio that is 10 times lower. The Ra-226 decay products are generally short lived.
[d]Short-lived daughter of Cs-137.
[e]Short-lived daughter of Zr-93.

nickel (present in subassembly hardware) and zirconium (present as a fission product and cladding activation product), are near the top.

Two of the most important retardation mechanisms available in a geologic repository are precipitation and sorption. Radionuclides that are present in significant quantities in waste and have high solubility and low sorption must be considered important because they could pose problems in meeting release limits. A review of the waste inventories, the sorption data presented in Section 4.1.3.3 and the solubility data presented in Section 4.1.3.4 indicates that three waste elements (carbon, technetium, and iodine)

may have high solubility and low sorption at the Yucca Mountain site. The radionuclides of these waste elements are not present in large quantities relative to the EPA limits, but they deserve consideration because they may not be strongly retarded by sorption or precipitation. Waste elements with moderately high solubilities and intermediate sorption coefficients are neptunium and uranium. The estimated solubility of nickel is relatively high; sorption data for nickel have not been measured as yet, but it probably should be considered in this category as well (Sections 4.1.3.4.2.3 and 8.3.1.3.4).

Radionuclides that can be released as gases must be given special consideration at Yucca Mountain. Most gaseous radionuclides are short-lived or are present in such small quantities that they do not represent problems. However, two radionuclides that may be transported in the gas phase and will be present for long periods of time are carbon-14 and iodine-129. The likely gaseous forms of both these radionuclides (carbon dioxide and iodine gas) are soluble in water. Carbon-14 as carbon dioxide (CO_2) may also undergo isotopic exchange with natural carbon in the surrounding rocks. Thus, for both waste elements, an exchange between the gas, aqueous, and solid phase may be possible.

On the basis of the quantity of radionuclides in the waste, the EPA release limits, solubility, sorption, the potential for vapor transport, and the potential for colloid transport, the following radionuclides should be considered important (Kerrisk, 1985):

1. Isotopes of the elements americium, plutonium, neptunium, and uranium are the most important because they are present in the largest quantities in waste relative to their EPA release limits and because of their potential for colloid transport. Solubility and sorption measurements for these elements should be of utmost importance.

2. Isotopes of the elements carbon, nickel, zirconium, technetium, thorium, radium (barium used as an analog), and tin are present in lesser amounts at most times, but are also important for solubility and for their transport potential.

3. Isotopes of the elements carbon, technetium, and iodine are important because these elements appear to have high solubility and low sorption at Yucca Mountain. This should be confirmed experimentally by determining their transport potential.

4. Isotopes of the elements carbon and iodine are important because they could be transported in the gas phase at Yucca Mountain. Studies of gas-phase transport should concentrate on these elements. Detailed discussions of the various retardation processes and the radionuclides considered for these processes are contained in Sections 4.1.3.3 through 4.1.3.8.

4.1.3.2 Analytical techniques

This section discusses the methods and procedures used to investigategeochemical retardation in the experiments reported here. (Results are reported in Sections 4.1.3.3. through 4.1.3.5.) The discussion emphasizes the retardation mechanism of sorption, but it also provides basic dynamic- transport information and includes the coupling of adsorption to dynamic processes. The procedures, and estimates of the attendant uncertainties, are discussed in detail by Daniels et al. (1982). The analytical techniques are discussed in Sections 4.1.3.2.1 through 4.1.3.2.5, but a general overview of the techniques and their interrelationships is given in this introduction.

The simplest mathematical approach to adsorption is to use the distribution coefficient, K_d, which is the approach used routinely by analytical chemists to model separations on chromatographic columns. The measurement of K_d allows the characterization of tuffs with different mineralogies. In a manner similar to chromatographic columns, the samples are crushed to a predetermined size fraction (typically between 75 and 500 micrometers) and carefully mixed to ensure homogeneity (on a small scale) of the column. The crushed sample will allow rapid equilibration. The heterogeneity of the tuff strata at Yucca Mountain requires a significant number of measurements to characterize the sorptive properties. The limitations of the distribution-coefficient approach to geologic investigations are as follows:

1. The assumption of a linear sorption isotherm. The terms "sorption isotherm," "Freundlich isotherm," or "Langmuir isotherm" are generally used to define the relationships between sorption and the concentration of the element being sorbed at a constant temperature.

2. The distribution between the solid phase and the aqueous phase may include precipitation or irreversible reaction or both.

3. The aqueous-phase species are not well known for many of the important radionuclides.

4. The assumption of equilibrium (i.e., rapid kinetics).

These limitations do not necessarily apply to all of the radionuclides of importance. For example, the solution chemistry of the alkali metals and the alkaline earths is well known, and the aqueous-phase species can be predicted with certainty. Average values are calculated for measured sorption ratios since measurements are made in duplicate. The uncertainties associated with averages of sorption data are the standard deviations of the means. When measured sorption values are very high or very low, the range of individual measurements may be quite large, resulting in a large standard deviation of the mean. This large range arises as a result of counting statistics. A very high or very low K_d means one phase, either the solution or the solid, has very little activity and, therefore, very few counts giving rise to counting errors larger than those obtained with sorption ratios close to unity.

Often, the surface area of the geologic media is thought to be important to total sorption. As a result, a surface-area sorption coefficient (K_a) is

used. However, for tuff, surface area does not appear to correlate with cation exchange capacity or particle size (Wolfsberg et al., 1979; Daniels et al., 1982). Furthermore, the data presented by Daniels et al. (1982) in their Appendix A show that particles in the size range of 75 to 500 micrometers have no effect on measured sorption ratios, yet the surface area is changing, therefore, K_a is not used for this size range. Other supporting evidence for the lack of correlation of surface area with cation exchange capacity can be found in Meyer et al. (1986). Analyses with neptunium (V) on crushed tuff to test effects of particle size resulted in only a slight increase in sorption. If the phenomena were controlled by surface area, a much larger effect of particle size would have been observed.

Three different sorption procedures were used: batch, crushed tuff column and circulating columns. These three sorption procedures are discussed in Sections 4.1.3.2.2, 4.1.3.2.3, and 4.1.3.2.4. Batch sorption methods approach equilibrium distribution coefficients for long-time experiments and yield information on kinetics for short-term experiments and on reversibility by desorption experiments. They are easy to conduct, but "equilibrium" sorption values may not be representative of a flowing system. The batch technique, in spite of its simplicity, is not without experimental pitfalls. To ensure that discrepancies between laboratory experiments are not due to experimental errors, the following must be carefully controlled:

1. Phase separation. When distribution coefficients (K_d) are high, the experiments are susceptible to contamination of the aqueous phase with colloidal material containing radionuclides leading to erroneously low K_d values.

2. Water composition. Comparison between experiments using radically different water compositions leads to large discrepancies.

3. Crushing and sieving. The rock must not be crushed below mineral crystal size. The samples should be sieved to ensure uniformity.

4. Mineral fractionation. This can occur either in the process of sieving or in the course of an experiment, such as a crushed tuff column, because the adsorption minerals (clays and zeolites) in tuff generally have small crystal sizes that will enrich in the smaller size fractions.

5. Speciation. The results of experiments where the complexing agents or oxidation-reduction conditions are not identical will show discrepancies for some radionuclides.

The above parameters must be controlled to study the distribution of geochemical properties in the geologic system. Where these parameters cannot be made to coincide exactly with the conditions in the field, compromises are made in a conservative direction for the purpose of applying the result to predictions in the field. For example, the smallest-size fractions are discarded, oxidizing conditions are used, etc. To systematically study which simplifying assumption may be valid and to experimentally examine the coupling of adsorption to dynamic processes the following types of experiments have been performed:

1. Crushed-tuff columns. The experiments allow the comparison of batch to transport through nearly identical material; they allow the study of kinetic effects, speciation, and other physical and chemical effects, such as anion exclusion. The advantage in using crushed tuff is that the results are free of ambiguities in the interpretation which would occur if the effect of heterogeneity and dispersion was not minimized.

2. Recirculating columns. The experiments were performed to test whether self-grinding, which might produce extremely small particles when stirred, had occurred in batch measurements. The technique is otherwise subject to nearly the same pitfalls as batch measurements.

3. Solid-tuff columns. The experiments have been and will continue to be performed to examine the validity of batch sorption measurements on tuff where homogeneity and dispersion are not controlled. The hydrologic flow is more constrained than that in the field. The filtration of colloids will also be studied to examine the potential for particulate migration.

4. Fractured-tuff columns. The experiments represent the most complex transport system that can be simulated in the laboratory.

5. Diffusion in solid tuff. The experiments are ancillary to the fractured-tuff columns but provide fundamental data for modeling diffusion in the tuff matrix. The experiments will also provide some kinetic data.

6. Solubility. The experiments are primarily directed toward understanding actinide solution chemistry in near-neutral solution. The understanding of actinide chemistry under near-neutral conditions is growing at a very slow pace because the low solubility of these elements does not allow the direct determination of oxidation state and molecular structure at present. Without a firm knowledge of the aqueous chemical species, the interpretation of the above transport experiments is hampered.

The major isotopes chosen for study come from the EPA critical element list. Additional radionuclides have been investigated when warranted (Section 4.1.3.3.1).

4.1.3.2.1 Preparation of ground-water samples for use in laboratory experiments

Before use, reference ground water from well J-13 is pretreated by putting it in contact with samples of tuff from individual strata in the vicinity of Yucca Mountain to obtain water chemistries representative of steady-state equilibrium for each tuff sample. After contact for at least 2 wk, the water is filtered through 0.05 micrometer Nuclepore membranes. Then, the water is analyzed and used in the sorption experiments. In general, after pretreatment sodium increases up to 50 percent and magnesium decreases by 50 percent probably due to ion exchange; chloride, fluoride, and

sulfate remain unchanged; and the pH (8.1 to 8.4) increases slightly. The changes, however, do not greatly affect sorption.

The spiked-feed solutions for each tuff sample were prepared by adding measured concentrations of radionuclide tracers to the pretreated water. Spiked-feed solutions are prepared as described by Daniels et al. (1982) for separate radionuclides. The final concentrations of the feed solutions generally range from 10^{-6} to 10^{-9} M; plutonium concentrations as low as 10^{-11} M have been studied.

4.1.3.2.2 Batch sorption methods

In batch measurements of sorptive properties, the distribution of a radionuclide is measured between ground water and crushed tuff as a function of contact time, the concentration of sorbing species, particle size, temperature, oxidation-reduction conditions, ground-water components, and lithology. In the batch procedure, a 1-g sample of crushed tuff is pretreated by contact with 20 ml of well J-13 ground water for at least 2 wk. The ground water used to prepare the solution containing radionuclides (spiked-feed solution) is also pretreated by contact for at least 2 wk with a crushed-tuff sample from the same section of core. The solids are separated from the liquid by centrifuging after the pretreatment period.

A sorption measurement starts when 20 ml of spiked-feed solution is added to the 1-g sample of tuff treated with ground water. The concentration of the spiked element ranges from 10^{-6} to 10^{-13} M, except in isotherm measurements where concentrations approaching the solubility limit are investigated. Care is taken to ensure that the spike concentration is well below predicted solubility limits in standard experiments. Except for the highest concentrations used in the isotherm studies (generally greater than 10^{-4} M), no significant change in sorption ratio has been observed with changing spike concentrations covering six to seven orders of magnitude (Wolfsberg et al., 1981; Daniels et al., 1982; Rundberg et al., 1985). Next, the two phases are thoroughly mixed and the sample is placed in a shaker to be agitated at about 200 rpm for selected times. At the end of the sorption period, the sample is removed from the shaker and the solids are separated by centrifuge. Tracer (spike) activity in the separated solid and liquid phases then is determined and the pH of the liquid is measured. The analytical techniques for each element are discussed by Daniels et al. (1982), who also discussed the technique used to completely separate the solids from the aqueous phase and to calculate the sorption ratios. The standard sorption and desorption times were 6 wk each. The data in Appendix A of Daniels et al. (1982) show that sorption either increases with time or remains unchanged. The choice of 6 weeks (or a total of 12 wk for both sorption and desorption measurements) was a compromise between reaching equilibrium, if that were even possible, and completing the measurements within a reasonable amount of time.

After the radioactivity of a solid phase has been measured, a desorption measurement is started. Tuff-pretreated ground water (20 ml) without tracer is added to the remaining solid phase. The sample is agitated again to ensure a thorough mixing of the two phases. The rock sample is separated

from the pretreated water and analyzed for radioactivity in the same manner as that used for the sorption sample.

The results are reported as sorption ratio, R_d, for each radionuclide as a function of the lithology of the crushed-tuff sample and various experimental conditions, where

$$R_d = \frac{\text{activity of radionuclide on solid phase per unit mass of solid}}{\text{activity of radionuclide in solution per unit volume of solutions}} \quad (4\text{-}1)$$

The sorption ratio, R_d, is equivalent to the distribution coefficient, K_d, only under equilibrium conditions. Sorption ratios determined by the batch method measure the distribution of an element between the solid and the liquid phases under specific conditions and do not necessarily represent equilibrium values. Uncertainties in the average sorption ratios reported for each set of test conditions are given as the standard deviation of the mean.

4.1.3.2.3 Crushed-tuff column method

The transport behavior of nuclides in columns of crushed tuff has been studied to characterize retardation in a flowing system. The column method is sensitive to speciation and also to reaction kinetics. The method will enable improvements to the transport model or empirical adjustments to the retardation data base so that the calculated bounds will encompass any reduced retardation from speciation or kinetics. Column studies are conducted to determine the retardation factor, R_f, rather than the sorption ratio, R_d. The velocity of a radionuclide is measured directly and then compared with the ground-water velocity as measured with nonreacting tracers like tritiated water or iodine-131. The retardation factor is related to the sorption ratio by the expression

$$R_f = 1 + \frac{R_d \, (\text{density})(1 - \text{porosity})}{\text{porosity}} \quad (4\text{-}2)$$

where density equals the rock-column density (2.5 g/cm^3).

A thorough discussion of the crushed-tuff column methodology is given by Treher and Raybold (1982).

Crushed-tuff columns are limited by the time required to observe the elution of adsorbing species. For example, cesium and strontium elutions require approximately 1 yr at flow rates of 11 to 60 m/yr—a long time to keep a mechanical system operating without failure. Crushed tuff has the potential to create or expose surfaces that would not be exposed in situ. In addition, there can be a coupling between flow and mineralogy such that adsorbing minerals are either avoided or preferentially contacted in intact tuff.

4.1.3.2.4 Circulating system method

The circulating system for determining sorption ratios incorporates features of the batch and column methods. In the circulating system the solid phase remains stationary and thus is not subject to possible self-grinding during agitation. Also, the solution-to-rock ratio in the column itself is considerably lower than the 20 ml/g ratio used in batch experiments and is, therefore, closer to that in the true geologic setting; but the ratio in the entire system, including the reservoir, is the same as in the batch system. A description of the circulating-system technique is given by Wolfsberg et al. (1981) and Daniels et al. (1982).

4.1.3.2.5 Solubility

Solubility measurements that provide upper limits on the concentrations of waste elements were made by preparing oversaturated solutions of radionuclides and monitoring radionuclide concentrations as a function of time (Nitsche and Edelstein, 1985). During the equilibration time, the temperature and the pH of the solutions were controlled. For measurements in well J-13 water, the pressure of carbon dioxide over the water was also controlled. Solids that precipitated were identified by x-ray diffraction; some of the solids were amorphous and could not be identified in this manner (Section 4.1.3.4.2; Nitsche and Edelstein, 1985). At this time there is a lack of firm knowledge of aqueous chemical species (actinides) under near-neutral conditions. Further work is planned in Section 8.3.1.3.

4.1.3.3 Sorption

Ion exchange and sorption (chemical or physical) are surface processes by which ions or other solution species can be removed from ground water by rock. The measured sorption ratios (defined in Section 4.1.3.2.2) are primary data for the assessment of retardation along the flow path. An understanding of these processes may permit extrapolation of laboratory data to field experiments and will aid in estimates of uncertainty limits. Plans for obtaining the additional information required are outlined in Section 8.3.1.3.4. The sorption of radionuclides on colloidal material will be studied as discussed in Section 8.3.1.3.4.

Several parameters directly affect sorption measurements as they relate to Yucca Mountain. Among these are the composition of the ground water used in the sorption experiments, the cation-exchange capacity of the minerals, the pH, the temperature, the oxidation-reduction conditions, the waste element being sorbed, and the concentration of the waste element. Additionally, three primary experimental methods (batch, crushed-rock column, or circulating systems) are used for measuring sorption coefficients as discussed in Sections 4.1.3.2.2 through 4.1.3.2.4. Relevant data that characterize the ion-exchange and sorption capacities of the tuff at Yucca Mountain are taken primarily from Daniels et al. (1982).

4.1.3.3.1 Sorption data for tuff

Daniels et al. (1982, 1983), Ogard et al. (1983b), Wolfsberg et al. (1983), Wolfsberg and Vaniman (1984), Crowe and Vaniman (1985), Ogard and Vaniman (1985), Rundberg et al. (1985) present data concerning sorption on tuff and list the results of all previous experiments. These sorption data were obtained from samples representative of Yucca Mountain strata from well J-13 (JA samples) and drillholes UE-25a#1 (YM samples), USW G-1 (G1 samples), USW G-2, and USW GU-3. Variables include time, temperature, particle size, oxidation-reduction conditions, element concentration, ground-water composition, and test method (batch, column, or circulating system). The radionuclides investigated were americium, cesium, neptunium, plutonium, uranium, thorium, strontium, technetium, tin, barium, radium, cerium, europium, and selenium. Strontium and cesium, while being shorter lived than many potentially hazardous waste elements, were studied first because of their relatively simple sorption behavior. These elements continue to be used to help validate the experimental techniques because their behavior can be predicted fairly well. Barium is included as a chemical analog for radium to reduce the number of experiments with radium. A great deal of care must be taken in handling radium-226 samples to prevent the release of daughter element radon-222 which could contaminate low-level counting facilities. Uranium and thorium are long-lived parents of radium; cerium and europium have been studied as analogs of rare-earth radionuclides. Selenium was studied as a potentially important waste element.

4.1.3.3.2 Sorption data from batch experiments

Average sorption ratios (R_d) from batch sorption and desorption experiments on tuff samples for strontium, cesium, barium, radium, cerium, europium, americium, plutonium, uranium, selenium, technetium, and neptunium are given in Tables 4-12a, 4-12b, 4-13a, and 4-13b. Each sample is assigned a depth equivalent in drillhole USW G-1 on the basis of the relative position of the sample in the major stratigraphic units so that sorption results on samples from one drillhole can be compared with samples from another. Data are for contact times greater than one week and particle sizes greater than 75 micrometers in an air environment at 25°C unless otherwise noted. Mineral abundance data determined by x-ray diffraction and petrologic characterization of these samples (as well as for finer fractions) are given in Table 4-14.

The R_d values from sorption experiments are often significantly lower than those from desorption experiments. Although the differences in R_d are unexplained at present, they suggest that, at least for some elements, sorption is not readily reversible. The sorption of cesium, strontium, and barium, which are noncomplexed cations that probably sorb by ion exchange, appears reversible because the R_d values from sorption and desorption experiments generally agree within a factor of 2. The R_d values from desorption experiments for technetium, the lanthanides, and the actinides are as much as 10 times greater than R_d values from sorption experiments. The latter elements all have multivalent species, some of which are sparingly soluble, hydrated, or form colloids and complexes (Section 4.1.3.4.1), which can alter the sorption processes. Differences in sorptive behavior may be caused by

4-66

CONSULTATION DRAFT

Table 4-12a. Average sorption ratios from batch sorption experiments on crushed tuff for strontium, cesium, barium, radium, cerium, and europium[a,b] (page 1 of 2)
(See footnotes at the end of Table 4-12b)

Strati-graphic unit[c]	Sample	Depth (ft)	Sorption ratios (ml/g)					
			Strontium	Cesium	Barium	Radium	Cerium	Europium
Tpc	JA-8	606	270(5)	2,700(400)[d]	45(15)			2,100(300)[d]
	YM-5	251	280(80)	5,800(800)[d]	1,100(200)		450,000(240,000)[d]	2,300,000(40,000)[d]
Tpp	G2-547	547	265(10)[f]	13,300(1,500)	3,490(30)[f]			340(30)[f]
	G2 723	723	290(40)[f]	4,100(600)[f]	3,500(400)[f]			>10,000[f]
	GU3-433	433	45(9)[g]	630(20)[g]	810(100)[g]			100(14)[g]
	GU3-855	855						
Tpt	YM-22	848	53(4)	290(30)	900(30)		1,270(40)	1,390(110)
	GU3-1203	1,203	42(1)[f]	350(30)[f]	640(40)			190(2)
	G1-1292	1,292	200(6)[f]	430(28)[f]	2,100(300)	1,500(100)	68(8)[f]	140(14)[d]
	GU3-1301	1,301	28(4)[g]	160(40)[g]	570(60)[g]			45(12)[g]
	YM-30	1,264	260(80)	855(5)	3,400(1,500)		230,000(100,000)	160,000(50,000)[e]
	JA-18	1,420	17,000(3,000)	16,000(1,000)	38,000(18,000)		2,800(1,400)[e]	1,400(200)[e]
Th	G1-1436	1,436	36,000(3,000)	7,800(500)	150,000(24,000)		59,000(7,000)	30,000(2,000)
	G2-1952	1,952	2,200(400)[f]	63,300(1,100)	25,000(4,000)[f]			89(14)[f]
	GU3-1436	1,436						
Bt	GU3-1531	1,531						
	YM-38	1,504	17,000(2,000)	13,000(2,000)	100,000(10,000)		760(140)	1,600(200)
	YM-42	1,824	3,900(600)	17,000(1,000)	94,000(14,000)		49,000(7,000)	52,000(4,000)
Tcp	G1-1854	1,854	60,000(14,000)	13,000(2,000)	45,000(7,000)			15,000
	YM-45	1,930	195(14)	520(90)	1,200(100)		730(100)	1,600(200)
	G1-1883	1,883	22(0.2)	187(3)	183(12)		1,420(20)	
	YM-46	2,002	190(60)	840(6)	14,000(6,000)		310,000(110,000)	307,000(110,000)
	G1-1982	1,982	55(4)	1,120(110)	700(50)		560(40)[f]	970(150)
	YM-48	2,114	2,100(400)	9,000(4,000)	18,000(6,000)		1,400(500)	2,200(500)
	YM-49	2,221	3,200(300)	36,000(3,000)	42,000(8,000)		550(100)	1,200(100)
	JA-26	1,995	95(35)	1,500(600)	800(300)			

Table 4-12a. Average sorption ratios from batch sorption experiments on crushed tuff for strontium, cesium, barium, radium, cerium, and europium[a,b] (page 2 of 2) (See footnotes at the end of Table 4-12b)

Strati-graphic unit[c]	Sample	Depth (ft)	Sorption ratios (ml/g)					
			Strontium	Cesium	Barium	Radium	Cerium	Europium
Tcb	JA-28	2,001	94(20)	1,640(210)	820(50)			2,100(1,000)
	G1-2233	2,233	48,000(3,000)[f]	13,500(800)	250,000(30,000)		1,400(300)	900(200)
	G1-2289	2,289	7,300(500)	37,000(13,000)	66,000(9,000)	46,000(20,000)		797(10)
	YM-54	2,491	62(12)	180(40)	400(150)		150(40)	470(40)
	G1-2333	2,333	180(20)	1,400(130)	1,500(200)			2,300(400)
	G1-2363	2,363	64(3)	470(40)	235(9)	540(60)		730(50)
	G1-2410	2,410	169(1)	1,250(50)	1,780			440(80)
	JA-32	2,533	57(3)	123(4)	380(30)		82(14)	90(20)
	G1-2476	2,476	41(1)	700(40)	385(11)			3,200(100)
Tct	G1-2698	2,698	42,000(3,000)[f]	7,700(400)[f]	63,000(5,000)[f]		240(30)[f]	200(30)[f]
	G1 2840	2,840	860(1)	2,200(200)	2,070(70)			4,900(400)
	G1-2854	2,854	94(1)	1,080(120)	1,000(50)			1,300(200)
	G1-2901	2,901	68(1)[f]	1,290(110)[f]	1,600(200)[f]		42,000(3,000)[f]	160,000(50,000)[f]
	G1-3116	3,116	2,400(17)[f]	6,600(500)[f]	12,000(4,000)[f]		100(10)[f]	760(60)[f]
	JA-37	3,497	287(14)	610(40)	760(150)			6,000(800)
Tl	G1-3658	3,658	13,000(0)	4,950(50)	13,500(500)		1,000(200)[f]	530(40)
Tba	G2-3933	3,933	240(60)[f]	2,500(1,000)[f]	1,700(500)[f]			1,500(700)[f]

Table 4-12b. Average sorption ratios from batch sorption experiments on crushed tuff for americium, plutonium, uranium, selenium, technetium, and neptunium[a,b] (page 1 of 3)

Stratigraphic unit[c]	Sample	Depth (ft)	Sorption ratios (ml/g)					
			Americium	Plutonium	Uranium	Selenium	Technetium	Neptunium
Tpc	JA-8	606						
	YM-5	251						
Tpp	G2-547	547	13,000(110)[f]	1,200(120)	9.4(0.1)	2(2)	0[f]	
	G2-723	723	890,000(40,000)	>4,500	2.4(0.6)	19(2)	0[f]	
	GU3-433	433	3,400(200)[d]	330(60)[g]	0	15(3)	0	7.9(0.1)
	GU3-855	855			10.0(0.7)	10(0.4)		
Tpt	YM-22	848	1,200(130)[d,e]	64(20)[d]	1.8(0.2)[d]		0.3(0.14)[d]	7.0
	GU3-1203	1,203	1,100(120)[g]	360(40)[g]	0	(1)	0	2.7(0.1)
	G1-1292	1,292						
	GU3-1301	1,301	1,800(160)[g]	290(40)[g]	0	7(2)	0.03(0.001)	5.0(0.1)
	YM-30	1,264						
	JA-18	1,420	180(30)	120(20)	2.5(0.4)			
Th	G1-1436	1,436						
	G2-1952	1,952	1,700(70)[f]	66(6)[f]	0	2(1)		2.7(0.1)
	GU3-1436	1,436			20.0(2)	3(10)		
Bt	GU3-1531	1,531			54.0(9)	5(1)		
	YM-38	1,504	14,600(1,000)	140(30)	5.3(0.2)			11.0
	YM-42	1,824						

4-69

CONSULTATION DRAFT

Table 4-12b. Average sorption ratios from batch sorption experiments on crushed tuff for americium, plutonium, uranium, selenium, technetium, and neptunium[a,b] (page 2 of 3)

Strati-graphic unit[c]	Sample	Depth (ft)	Sorption ratios (ml/g)					
			Americium	Plutonium	Uranium	Selenium	Technetium	Neptunium
Tcp	G1-1854	1,854						
	YM-45	1,930						
	G1-1883	1,883	470(300)					
	YM-46	2,002		77(11)				6.4
	G1-1982	1,982						
	YM-48	2,114						
	YM-49	2,221	4,300(1,400)				0.15(0.02)	
	JA-26	1,995		230(50)[e]			0.21(0.02)	9.0(3)
Tcb	JA-28	2,001						
	G1-2233	2,233						
	G1-2289	2,289				9(1)		
	YM-54	2,491	153(6)	80(20)	1.3(0.3)		4.2(0.5)[h]	
	G1-2333	2,333						
	G1-2363	2,363		110		25(5)		
	G1-2410	2,410			2.2(0.9)			
	JA-32	2,533	130(30)					
	G1-2476	2,476						
Tct	G1-2698	2,698						
	G1-2840	2,840						
	G1-2854	2,854						
	G1-2901	2,901		400(70)[e]	4.6(0.3)			
	G1-3116	3,116						
	JA-37	3,497	28,000(10,000)[e]					24

Table 4-12b. Average sorption ratios from batch sorption experiments on crushed tuff for americium, plutonium, uranium, selenium, technetium, and neptunium[a,b] (page 3 of 3)

Strati-graphic unit[c]	Sample	Depth (ft)	Sorption ratios (ml/g)					
			Americium	Plutonium	Uranium	Selenium	Technetium	Neptunium
Tl	G1-3658	3,658						
Tba	G2-3933	3,923	6,600(400)		1,600.0(30)	0	0.0(1)	0.1(0.006)

[a]Sources: Daniels et al. (1982); Ogard et al. (1983b); Wolfsberg et al. (1983). If no footnote is indicated, the sorption ratio in parentheses represents the standard deviation of the mean.
[b]Ambient conditions, air, $20 \pm 4°C$; fractions do not contain particles smaller than 75 micrometers in diameter except in fractions designated by footnote (f). Sorption times greater than 1 week.
[c]Stratigraphic units are as follows: Tpc = Tiva Canyon Member; Tpp = Pah Canyon Member; Tpt = Topopah Spring Member; Th = tuffaceous beds of Calico Hills; Bt = bedded tuff; Tcp = Prow Pass Member; Tcb = Bullfrog Member; Tct = Tram Member; Tl = older tuffs; Tba = bedded tuff.
[d]Nonweighted average; value in parentheses is the standard deviation of the mean.
[e]Some data were rejected in averaging.
[f]Average of data for the fraction with particles smaller than 500 micrometers in diameter (contains some particles smaller than 75 micrometers).
[g]Nonweighted average of samples taken in two different positions.
[h]Performed under controlled atmospheric conditions of nitrogen with less than or equal to 0.2 parts per million O_2 and less than or equal to 20 parts per million CO_2.

Table 4-13a. Average sorption ratios from batch desorption experiments on crushed tuff for strontium, cesium, barium, cerium, and europium[a,b] (page 1 of 2)
(See footnotes at the end of Table 4-13b)

Stratigraphic unit[c]	Sample	Depth (ft)	Sorption ratios (ml/g)				
			Strontium	Cesium	Barium	Cerium	Europium
Tpc	JA-8	606	311(3)[d]	4,600(400)[d]	480(50)[d]		10,000(3,000)
	YM-5	251	320(30)[d]	8,900(600)[d]	1,200(120)[d]	31,000(30,000)[d]	36,000(14,000)
Tpp	G2-547	547	210(10)[f]	8,700(550)[f]	2,900(200)[f]		1,700(600)[f]
	GS-723	723	330(4)[f]	4,300(4)[f]	4,200(10)[f]		>10,000[f]
	GU3-433	433	40(10)[g]	520(20)[g]	460(20)[g]		140(10)[g]
Tpt	YM-22	848	59(2)	365(7)	830(100)	6,500(800)	3,500(200)
	GU3-1203	1,203	47(1)[f]	340(10)[f]	720(30)		650(50)
	G1-1292	1,292	120(5)[f]	510(20)[f]	1,500(100)	600(200)[f]	600(70)
	GU3-1301	1,301	80(20)[g]	185(20)[g]	675(60)[g]		100(20)[g]
	YM-30	1,264	210(30)	1,500(100)	3,100(600)	170,000(15,000)	11,000(700)
	JA-18	1,420	15,000(2,000)	17,500(700)	280,000(50,000)	1,600(500)[e]	2,400(300)[e]
Th	G1-1436	1,436	87,000(12,000)	24,000(2,000)[f]	340,000(90,000)[f]	6,700(600)	5,300(600)
	G2-1952	1,952	4,200(200)[f]	46,000(1,400)[f]	40,000(1,000)[f]		1,600(200)
	YM-38	1,540	22,000	13,000	260,000	2,600	7,300
	YM-42	1,842	4,100(1,000)	21,000(2,000)	90,000(30,000)	44,000(5,000)	64,000(3,000)
Tcp	G1-1854	1,854	72,000(13,000)[e]	14,000(2,000)	150,000(40,000)		4,800(700)
	YM-45	1,930	210(20)	620(110)	1,310(60)	5,800(600)[f]	7,300(900)
	G1-1883	1,883	59(1)[f]	430(4)	440(10[f]	2,200(100)[f]	1,350(50)[f]
	YM-46	2,002	260(20)	1,800(300)[f]	210,000(3,000)	300,000(50,000)	31,000(2,000)[f]
	G1-1982	1,982	322(8)[f]	2,300(200)[f]	2,780(120)[f]	7,000(800)[f]	6,370(130)[f]
	YM-48	2,114	2,700(200)	27,000(4,000)	34,000(7,000)	128,000(300)	8,100(1,200)
	YM-49	2,221	4,400(100)	39,000(1,000)	65,000(7,000)	1,040(40)	2,100(500)
	JA-26	1,995	39(3)	1,580(90)	450(13)		2,900(200)

Table 4-13a. Average sorption ratios from batch desorption experiments on crushed tuff for strontium, cesium, barium, cerium, and europium[a,b] (page 2 of 2)
(See footnotes at the end of Table 4-13b)

Stratigraphic unit[c]	Sample	Depth (ft)	Sorption ratios (ml/g)				
			Strontium	Cesium	Barium	Cerium	Europium
Tcb	JA-28	2,001	114(3)	2,400(100)[f]	1,160(20)[f]		12,300(500)[f]
	G1-2233	2,233	90,000(40,000)[f]	23,000(6,000)[f]	40,000(80,000)[f]	20,000(13,000)[e]	5,000(2,000)[f]
	G1-2289	2,289					
	YM-54	2,491	97(9)	310(20)	660(20)	1,000(200)	1,840(110)
	G1-2333	2,333	140(13)	1,230(100)	1,460(130)		9,900(1,200)
	G1-2363	2,363	150(6)[f]	1,200(30)[f]	820(20)	130,000(6,000)[f]	6,100(300)
	G1-2410	2,410	140(14)	1,120(100)	1,760(150)		6,000(3,000)
	JA-32	2,533	53(3)	175(11)	490(40)	530(120)	850(130)
	G1-2476	2,476	200(4)	1,520(0)			
Tct	G1-2698	2,698	210,000(50,000)	17,000(1,100)	190,000(80,000)[f]	2,000(400)[f]	
	G1-2840	2,840	1,540	2,300(130)	2,500(200)		9,000(1,100)
	G1-2854	2,854	96(1)	1,160(20)[f]	1,300(0)		5,000(200)
	G1-2901	2,901	67(1)[e,f]	1,380(30)[f]	1,980(30)	39,000(1,000)[f]	210,000(50,000)
	G1-3116	3,116	24,000(13,000)[f]	11,000(3,000)[f]	160,000(80,000)	3,000(1,000)[f]	8,000(3,000)[f]
	JA-37	3,497	312(9)	850(50)	920(40)		11,000(2,000)
T1	G1-3658	3,658	12,000(3,000)[f]	12,000(2,000)[f]	10,000(4,000)	9,000(4,000)[f]	9,000(3,000)[f]
Tba	G2-3933	3,933	140(20)[f]	1,400(350)[f]	1,100(200)[f]		3,000(1,100)[f]

Table 4-13b. Average sorption ratios from batch desorption experiments on crushed tuff for americium, plutonium, uranium, technetium, and neptunium[a,b] (page 1 of 3)

Strati-graphic unit[c]	Sample	Depth (ft)	Sorption ratios (ml/g)				
			Americium	Plutonium	Uranium	Technetium	Neptunium
Tpc	JA 8	606					
	YM-5	521					
Tpp	G2-547	547	17,000(1,400)	1,200(170)[f]			
	G2-743	723	2.8×10^{6} (2.6×10^{4})	>47,000			
	GU3-433	433	9,300(1,780)[g]	920(40)[g]			
Tpt	YM-22	848	2,500(400)[d]	1,330(140)[d]	5(2)[d]	1.2(0.3)[d]	33(5)[d]
	GU3-1203	1,203	1,300(200)[g]	920(15)[g]			
	G1-1292	1,292					
	GU3-1301	1,301	2,500(600)[g]	1,300(460)[g]			
	YM-30	1,264					
	JA-18	1,420	1,100(300)	350(140)	9.4(1.4)		
Tht	G1-1436	1,436					
	G2-1952	1,952	5,800(1,100)[g]	350(45)[g]			
	YM-38	1,540	7,100(1,200)	1,600(300)	14.8(1.0)		24(2)
	YM-42	1,824					

Table 4-13b. Average sorption ratios from batch desorption experiments on crushed tuff for americium, plutonium, uranium, technetium, and neptunium[a,b] (page 2 of 3)

Strati-graphic unit[c]	Sample	Depth (ft)	Sorption ratios (ml/g)				
			Americium	Plutonium	Uranium	Technetium	Neptunium
Tcp	Gl-1854	1,854					
	YM-45	1,930					
	Gl-1883	1,883	7,200(900)	890(60) = (61-1883)			36(10)
	YM-46	2,002					
	Gl-1982	1,982					
	YM-48	2,114				1.6(0.2)	
	YM-49	2,221	3,400(400)[e]	720(90)		2.0(0.3)	12(4)
	JA-26	1,995					
Tcb	JA-28	2,001					
	Gl-2233	2,233					
	Gl-2289	2,289					
	YM-54	2,491	550(80)	720(40)	12(8)	38(-)[h]	
	Gl-2333	2,333					
	Gl-2363	2,363					
	Gl-2410	2,410			8(2)		
	JA-32	2,533	2,200(600)				
	Gl-2476	2,476					
Tct	Gl-2698	2,698					
	Gl-2840	2,840					
	Gl-2854	2,854					
	Gl-2901	2,901					
	Gl-3116	3,116					
	JA-37	3,497	32,000(10,000)	1,400(300)	9.9(0.4)		170(50)

Table 4-13b. Average sorption ratios from batch desorption experiments on crushed tuff for americium, plutonium, uranium, technetium, and neptunium[a],[b] (page 3 of 3)

Strati-graphic unit[c]	Sample	Depth (ft)	Sorption ratios (ml/g)				
			Americium	Plutonium	Uranium	Technetium	Neptunium
T1	G1-3658	3,658					
Tba	G2-3933	3,933	1,200(410)	530(130)			

[a]Sources: Daniels et al. (1982); Ogard et al. (1983b); Wolfsberg et al. (1983). If no footnote is indicated, the sorption ratio in parentheses represents the standard deviation of the mean.
[b]Ambient conditions, air, 20 ± 4°C; fractions do not contain particles smaller than 75 micrometers in diameter except in fractions designated by footnote f. Sorption times greater than 1 week.
[c]Stratigraphic units are as follows: Tpc = Tiva Canyon Member; Tpp = Pah Canyon Member; Tpt = Topopah Spring Member; Th = tuffaceous beds of Calico Hills; Tcp = Prow Pass Member; Tcb = Bullfrog Member; Tct = Tram Member; T1 = older tuffs; Tba = bedded tuff.
[d]Nonweighted average; value in parentheses is the standard deviation of the mean.
[e]Some data were rejected in averaging.
[f]Average of data for the fraction with particles smaller than 500 micrometers in diameter (contains some particles smaller than 75 micrometers).
[g]Nonweighted average of samples taken in two different positions.
[h]Performed under controlled atmospheric conditions of nitrogen with less than or equal to 0.2 ppm O_2 and less than or equal to 20 ppm CO_2.

Table 4-14. Petrologic characterization of tuff samples from drillholes J-13, UE-25a#1, USW G-1, USW G-2, and USW GU-3[a] (Page 1 of 4)

Unit[b]	Sample	Depth (ft)	USW G-1 depth (ft)[c]	Particle size (μm)	Abundance (weight %)								Degree of welding[e]	Oxidation state[f]	Crystals (%)	Lithics (%)
					Smectite	Illite Muscovite	Clinop-tilolite	Quartz	Cristob-alite	Alkali feldspar	Glass	Other[d]				
Tpt	JA-8	806	172	All[g]	25-50	--[h]	--	--	10-20	tr[h]	25-50	--	M	(h)	8.9	8.7
Tpt	JA-8	806	172	75-500	30-60	--	--	<5	10-20	--	20-50	--				
Tpt	JA-8	606	172	75	30-60	--	--	--	10-20	--	30-60	--				
Tpc	YM-5	251	221	All	10	--	--	<5	<5	10-20	70	--	M		10.9	4.3
Tpp	G-2-547	547		<500	5-15	<5	--	--	5-15	10-20	40-60	--				
Tpp	G-2-547	547		75-500	14-84	--	--	3-7	2-8	43-63	--	6-16T				
Tpp	G-2-723	723		<500	5-15	<5	--	--	<5	5-10	15-30	30-70C				
Tpp	G-2-723	723		75-500	2-8	1-5	--	--	1-5	15-35	9-21	40-60C				
Tpt	GU-3-433	433	245	75-500	--	2-6	--	2-6	8-16	60-100	--	--				
Tpt	GU-3-855	855	758	<500	1-3	--	--	16-24	4-10	50-90	--	--				
Tpt	YM-22	480	868	All	5-10	--	--	40-60	--	40-60	--	--	0	C6(2-7)	1.0	0.4
Tpt	VII-22	848	868	106-500	<5	<2	--	30-50	--	30-50	--	--				
Tpt	VII-22	848	868	38-106	<2	tr	--	30-50	--	30-50	--	--				
Tpt	VII-22	848	868	<38	<5	<2	--	30-50	--	30-50	--	--				
Tpt	GG-3420[i]	1,000	1,100	75-500	1	1	--	2-7	8-16	35-55	20-60	000				
Tpt	G1-1292	1,292	1,292	All	tr	--	--	--	5-10	10-20	80-90	--	V	C1		
Tpt	G1-1292	1,292	1,292	75-500	--	--	--	--	15-30	10-20	10-60	--				
Tpt	GU-3-1201	1,201	1,298	75-500	1-3	2-6	--	4-8	9-21	15-55	20-60	--				
Tpt	YM-30	1,264	1,318	All	5-10	5	5-10	40-60	5-15	30-50	--	--	0	C5(2-7)	2.1	21.6
Tpt	YM-30	1,264	1,318	75-100	--	--	15	30	20	35	--	--				
Tpt	YM-30	1,264	1,318	<75	--	--	15	30	20	35	--	--				
Tpt	JA-18	1,420	1,339	All	5	5	5-10	--	15-25	15-25	50	--	N	C3(2-5)	1.8	11.9
Tpt	JA-18	1,420	1,339	355-500	5	--	10-20	--	30-50	30-50	40	--				
Tpt	JA-18	1,420	1,339	106-150	5	5	10-20	--	30-50	30-50	40	--				
Tht	G1-1436	1,436	1,436	75-500	<5	<5	75-90	5-10	--	5	--	--		C6(5-7)	5.2	3.2
Tht	G2-1952	1,952	1,493	<500	--	1	25-45	3-7	3-7	20-40	--	15-35	M			
Tht	G2-1952	1,952	1,493	75-500	--	1	10-30	5-9	5-11	25-46	--	20-40				
Tht	G43-1436	1,436	1,504[j]	<500[k]	--	1	--	2-6	3-9	30-70	20-60	--				
Tht	YM-3d	1,504	1,538	106-500	5-10	<2	30-50	15-30	10-20	5-15	--	A,tr	N	C5(4-6)	4.0	7.7
Tht	YM-3d	1,504	1,538	38-106	5-10	<5	40-60	2-10	10-20	5-15	--	--				
Tht	YM-3d	1,504	1,538	<38	5-15	<5	40-60	2-10	10-20	10-10	--	A,tr				
Tht	VII-42	1,824	1,802	75-500	tr	<5	20	35-40	--	40	--	--			15.6	46.6
Tht	V14-42	1,824	1,802	<75	tr	tr	20	40	--	40	--	--				
Tba	GU3-1531	1,531		<500[k]	--	3-7	--	15-25	3-9	20-60	10-50	--				

Table 4-14. Petrologic characterization of tuff samples from drillholes J-13, UE-25a#1, USW G-1, USW G-2, and USW GU-3[a] (Page 2 of 4)

Unit[b]	Sample	Depth (ft)	USW G-1 depth (ft)[c]	Particle size (μm)	Abundance (weight %)								Degree of welding[e]	Oxidation state[f]	Crystals (%)	Lithics (%)
					Smectite	Illite Muscovite	Clinop-tilolite	Quartz	Crist-ob-alite	Alkali feldspar	Glass	Other[d]				
Tcp	G1-1854	1,854	1,854	75-500	5-10	--	30-50	5-15	15-30	20-40	--	--				
Tcp	G1-1854	1,854	1,854	<75	5-10	--	40-60	20-40	15-30	10-30	--	--				
Tcp	YM-45	1,930	1,873	All	1-5	--	--	40-60	tr	30-50	--		M	C4(3-5)	13.5	0.6
Tcp	G1-1883	1,883	1,883	75-500	<2	<5	--	30-50	--	50-70	--	--	P	C4(3-5)	16.6	1.0
Tcp	G1-1883	1,883	1,883	106-500	<2	<2	--	20-40	0-10	40-60	--	--				
Tcp	G1-1883	1,883	1,883	38-106	<2	<5	--	30-50	0-10	30-50	--	--				
Tcp	G1-1883	1,883	1,883	<38	2-5	<2	--	20-40	0-10	40-60	--	--				
Tcp	VII-46	2,002	1,926	All	<5	<5	--	40-60	--	35-55	--	--	0		12.7	0.3
Tcp	G1-1982	1,982	1,982	All	tr	<5	--	5-15	40-60	30-50	--	--	N	C2	13.2	0.4
Tcp	G1-1982	1,982	1,982	75-500	5-10	<2	--	--	--	70-90	--	--				
Tcp	G1-1982	1,982	1,982	38-106	<2	--	--	--	40-60	40-60	--	--				
Tcp	G1-1982	1,982	1,982	<38	10-20	--	--	--	30-40	20-40	--	C,<2				
Tcp	YM-48	2,114	2,019	All	tr	--	10-20	--	--	20-30	40-60	--				
Tcp	YM-48	2,114	2,019	106-500	<2	--	20-40	5-10	5-15	20-40	10-30	--				
Tcp	YM-49	2,221	2,090	All	tr	tr	10-20	--	--	20-30	40-60	--	P	C6(5-7)	8.0	1.4
Tcp	JA-26	1,995	2,173	All	--	--	tr	30-50	tr	10-20	--	A,30-50	N		18.3	1.0
Tcb	JA-28	2,001	2,178	All	tr	2.5	--	30-50	--	10-20	--	A,30-50			20	5
Tcb	G1-2233	2,233	2,233	<500	<5	<5	20-40	11-20	10-20	10-20	--	B,20-40	N	C6(6-7)	15.4	0.4
Tcb	G1-2233	2,233	2,233	75-500	<5	5-15	15-30	5-10	--	40-60	--	B,<5				
Tcb	G1-2233	2,233	2,233	38-106	<5	5	20-40	15-30	10-20	10-20	--	B,20-40				
Tcb	G1-2289	2,289	2,289	75-500	--	5-10	30-50	<5	--	30-50	--	B,10-20	N	C6(5-7)	15.8	1.0
Tcb	YM-54	2,491	2,330	All	tr	tr	--	50-70	--	20-40	--	--	W	C5(4-7)	17.8	0
Tcb	YM-54	2,491	2,330	106-500	5-10	2-5	--	30-50	--	25-45	--	--				
Tcb	YM-54	2,491	2,330	38-106	5-10	5-10	--	30-50	--	30-50	--	--	M	C6(5-7)	20.4	0.2
Tcb	YM-54	2,491	2,330	<38	5-10	2-10	--	15-30	--	40-60	--	--				
Tcb	G1-2333	2,333	2,333	75-500	2-5	2-5	--	15-30	10-30	50-70	--	--				
Tcb	G1-2333	2,333	2,333	<75	5-10	<5	--	15-30	20-40	20-40	--	--				
Tcb	G1-2363	2,363	2,363	All	10-20	5-10	--	30-50	--	30-50	--	--				
Tcb	G1-2363	2,363	2,363	106-500	5	<2	--	30-50	0-10	30-50	--	--				
Tcb	G1-2363	2,363	2,363	38-106	5	<2	--	30-50	0-10	30-50	--	--				
Tcb	G1-2363	2,363	2,363	<38	5-10	<2	--	20-40	0-10	40-60	--	--				

Table 4-14. Petrologic characterization of tuff samples from drillholes J-13, UE-25a#1, USW G-1, USW G-2, and USW GU-3[a] (Page 3 of 4)

Unit[b]	Sample	Depth (ft)	USW G-1 depth (ft)[c]	Particle size (μm)	Abundance (weight %)								Degree of welding[e]	Oxidation state[f]	Crystals (%)	Lithics (%)
					Smectite	Illite Muscovite	Clinop-tilolite	Quartz	Cristob-alite	Alkali feldspar	Glass	Other[d]				
Tcb	G1-2410	2,410	2,410	75-500	5-10	<2	--	20-40	0-10	30-50	--	--				
Tcb	G1-2410	2,410	2,410	<75	5-10	<5	--	20-40	5-15	30-50	--	--				
Tcb	JA-32	2,533	2,467	106-500	<5	5-15	--	30-50	--	30-50	--	--				
Tcb	JA-32	2,533	2,467	355-500	--	5-10	--	40-50	--	30-40	--	--				
Tcb	JA-32	2,533	2,467	150-180	--	10-15	--	35-50	--	40-65	--	--				
Tcb	JA-32	2,533	2,467	106-150	<5	5-15	--	30-50	--	30-50	--	--				
Tcb	JA-32	2,533	2,467	38-106	<2	tr	--	30-50	--	30-50	--	--				
Tcb	JA-32	2,533	2,467	<38	5-10	--	--	20-40	--	40-60	--	A, tr				
Tcb	G1-2476	2,476	2,476	75-500	<2	2	--	30-50	5-15	40-60	--	--				
Tcb	G1-2476	2,476	2,476	<75	2-5	2	--	30-50	5-15	40-60	--	--				
Tct	G1-2698	2,698	2,698	All	<5	10-15	30-50	<5	--	30-50	--	H, 5	M	C6(5-7)	S13.2	1
Tct	G1-2840	2,840	2,840	75-500	2-5	2-5	--	40-60	0-10	30-50	--	--				
Tct	G1-2840	2,840	2,840	<75	2-5	2-5	--	40-60	0-10	30-50	--	--				
Tct	G1-2854	2,854	2,854	75-500	<2	5-10	--	30-50	0-10	30-50	--	--				
Tct	G1-2854	2,854	2,854	<75	<2	5-10	--	30-50	0-10	30-50	--	--				
Tct	G1-2901	2,901	2,901	All	5-10	5-10	--	20-40	--	40-60	--	--	W	C6(6-7)	4.0	21.4
Tct	G1-3116	3,116	3,116	All	5-10	5-10	5-15	20-40	--	20-40	--	A,10-30				
Tct	JA-37	3,497	3,286	All	20-40	5	5	30-60	--	15-30	--	--				
Tct	JA-37	3,497	3,286	355-500	10-15	--	tr	40-50	--	30-40	--	C,tr				
Tct	JA-37	3,497	3,286	106-150	5-10	--	--	40-50	--	30-40	--	C,tr				
TI	G1-3658	3,658	3,658	75-500	40-60	--	--	--	--	40-60				C3	23.4	0
TI	G1-3658	3,658	3,658	106-500	40-60	--	--	--	--	40-60						
TI	G1-3658	3,658	3,658	38-106	30-50	--	--	--	--	50-70						
TI	G1-3658	3,658	3,658	<38	50-70	--	--	--	--	30-50						

Unit[b]	Sample	Depth (ft)	USW G-1 depth (ft)[c]	Particle size (μm)	Abundance (weight %)									Degree of welding[e]	Oxidation state[f]	Crystals (%)	Lithics (%)
					Smectite	Illite Muscovite	Clinop- tilolite	Quartz	Cristob- alite	Alkali feldspar	Glass	Other[d]				
Tba	G2-3933	3,933		<500	10-20	--	--	20-40	--	20-40	--	10-40,A				
Tba	G2-3933	3,933		75-500	40-10	--	--	29-39	--	34-54	--	10-20,A				

[a] Analyses were performed by ESS division of the Los Alamos National Laboratory; methods are discussed in Caporuscio et al.,1982. Data from Daniels et al., (1982). To convert from feet to meters, multiply by 0.328.

[b] Tpc = Tiva Canyon Member of the Paintbrush Tuff; Tpt = Topopah Spring Member of the Paintbrush Tuff; Tht = Tuffaceous beds of Calico Hills; Tcp = Prow Pass Member of the Crater Flats Tuff; Tcb = Bullfrog Member of the Crater Flat Tuff; Tct = Tram unit of the Crater Flat Tuff; TI = lava flow and flow breccia; Tba = bedded tuff; and Tpp = Pah Canyon Member.

[c] Equivalent depth in drillhole USW G-1 according to relative position in stratigraphic unit. The thickness of the Bullfrog and Tram units in drillholes UE-25a#1 and J-13, respectively, are assumed to be of the same thickness as the corresponding units in drillhole USW G-1.

[d] A = analcime; C = calcite; M = mordenite; and T = tridymite.

[e] N = nonwelded; P = partly welded; M = moderately welded; D = densely welded; V = very densely welded (vitrophyre); and W = intermediately welded.

[f] The empirical stage of oxidation of iron-titanium exsolution oxide phases; C1 denotes unoxidized and C7 denotes completely oxidized. See Caporuscio for a discussion of oxide mineral alteration trends.

[g] Starting with whole rock.

[h] A blank indicates that an analysis was not performed; dashes indicate that the mineral was not detected, and tr = trace (<1%).

[i] Topopah Spring vitrophyre.

[j] Mineralogy in Tht in USW GU-3 is not similar to that in Tht in USW G-1. Stratigraphic equivalence is not valid.

[k] Sorption work was done with 75-500 μm fraction. Analysis still in progress.

differences in aqueous speciation or sorption reactions with the solid phases. Further studies are described in Section 8.3.1.3.4.

Only limited data are available on the effect of elevated temperature on sorption behavior in tuff. Data obtained at 70° and 85°C (Table XVII, Ogard et al., 1983b) suggest that higher temperatures will generally increase slightly the sorptive capacity of the tuff samples for all elements studied (Daniels et al., 1982; Ogard et al., 1983a). Samples studied for temperature effects were Topopah Spring Member tuffs containing equal amounts of cristobalite and alkali feldspar; Topopah Spring Member tuff largely composed of alkali feldspar; Topopah Spring Member tuff with equal amounts of glass and alkali feldspar; Bullfrog Member tuff containing equal amounts of quartz and alkali feldspar and a small amount of illite; and Tram Member tuff containing equal amounts of quartz, alkali feldspar, and a small amount of smectite.

The sorptive behavior of some multivalent radionuclides may depend on in situ oxidation-reduction conditions of the ground-water environment in the tuff. Data are available on sorptive behavior under conditions less oxidizing than atmospheric conditions (Daniels et al., 1982). These experiments were performed in a nitrogen atmosphere with less than 0.2 parts per million (ppm) oxygen and less than 20 ppm carbon dioxide. These conditions are somewhat different from those in deep geologic environments because of the low carbon dioxide content in the laboratory experiment and the possible influence on complex formation. The inert atmosphere environment should bracket the subsurface oxidation-reduction conditions. The results showed the absence of oxygen and carbon dioxide had little effect on sorption for most elements (Daniels et al., 1982). However, plutonium and technetium showed higher sorption ratios in these experiments (plutonium up to 800 ml/g and technetium up to 14 ml/g as compared with approximately 100 ml/g and less than 1 ml/g, respectively, under oxidizing conditions). Experiments performed under conditions that maintained the solution pH at 6 to 7 by varying the carbon dioxide content of the atmosphere also showed little changes in the sorption ratio in comparison with ambient experiments (Ogard and Vaniman, 1985; Rundberg et al., 1985).

It is important to determine the range of linearity of the sorption isotherms for several reasons. First, the concentration of waste elements will change considerably from a dilute solution at the repository to an even more dilute solution when the dissolved waste element becomes mixed with ground water. To model such a change in concentration in the transport process, the variation of sorption with concentration is needed. In the case of nonlinear sorption, the variation data may help to establish bounds on sorption. Second, mechanisms like those that lead to irreversible sorption are studied by measuring desorption ratios. Third, diffusion into the tuff matrix as would occur in fracture flow is interpreted and modeled. If diffusion is occurring, then the sorption mechanism is not a simple ion exchange.

In most transport codes, the sorption ratio does not depend on concentration. This assumption should be valid for ion-exchange equilibrium at tracer-level concentrations within zeolitized tuffs, but it may not be true for welded nonzeolitized tuffs. Therefore, the dependence on concentration must be determined. Sorption isotherms have been determined (Wolfsberg et al., 1981; Daniels et al., 1982) for three tuff samples from drillhole UE-25a#1 (YM-22, YM-38, and YM-49), and on a sample from drillhole USW G-1

(G1-2840) (Wolfsberg et al., 1982a) (Table 4-14 for sample descriptions). Sample YM-22 is a densely welded tuff from the Topopah Spring Member; sample YM-38 is a highly zeolitized tuff from the tuffaceous beds of Calico Hills; sample YM-49 is a partially zeolitized and partially welded vitric tuff from the lower Prow Pass Member; and sample G1-2840 is a devitrified tuff similar to YM-22. Sorption isotherms for strontium, cesium, barium, and europium were determined for samples YM-22 and YM-38 (Wolfsberg et al., 1981). Sorption isotherms were also determined for cesium for sample G1-2840 (Daniels et al., 1983). The experimental data were fitted to a Freundlich isotherm, an empirical formula of the form

$$q = kc^n \qquad (4-3)$$

where q is the solute concentration on the solid phase, c is the solute concentration in the aqueous phase, and k and n are constants (n = 1 for a linear isotherm).

This isotherm can be used to summarize large amounts of data. The results by Wolfsberg et al. (1981, 1982a) and Daniels et al. (1983) for strontium, cesium, barium, and europium indicate a nonlinear isotherm (n = 0.71 to 0.92) for the coarse size fraction of sample YM-22 (welded tuff) and for sample G1-2840, both of which are nonzeolitized tuffs. With the possible exception of strontium (n = 0.87), a linear isotherm (n = 0.98 to 1.1) is indicated for the coarse-size fraction of sample YM-38 (zeolitized tuff). This latter result is expected because the sorption of these elements on zeolitized material should occur predominantly by ion exchange. The results of this study indicate that isotherms can be used to interpret the studies of sorption on both zeolitized and nonzeolitized tuff.

Sorption isotherms were determined for plutonium on tuff samples YM-22 and YM-49 for 10 concentrations from 2.9×10^{-6} to 5.9×10^{-13} M (Daniels et al., 1982). Except for the highest plutonium concentration, which generally exhibits the lowest R_d value, there was little correlation between sorption ratio and element concentration in the range studied. The Freundlich isotherm for tuff sample YM-22 (welded) indicates nonlinear sorption (n = 0.84 to 0.88), whereas sorption for tuff sample YM-49 (partially zeolitized and vitric) is approximately linear (n = 0.96 to 1.0). This is consistent with the results of measurements using strontium, cesium, barium, and europium. The sorption-isotherm studies are being extended to include the other waste radionuclides to fully model the retardation process. Plans for obtaining the additional information are outlined in Section 8.3.1.3.4.

The saturation of sorption sites can cause a sorption isotherm to be nonlinear, as observed in samples YM-22 and G1-2840. Some experimentally determined values for cation-exchange capacity (CEC), which is the measure of available sorption sites, are presented by Wolfsberg and Vaniman (1984). High concentrations (higher than 10^{-5} M) of sorbing species were used in these experiments to obtain the CEC. Sample YM-22 tuffs have a relatively low CEC while exhibiting nonlinear sorption isotherms; however, the zeolitized tuffs (YM-49, YM-38) have a relatively high CEC and exhibit linear sorption isotherms. However, it was determined that a simple retardation factor is valid for the alkali metals and alkaline earths at concentrations as high as 10^{-5} M for strontium and cesium and 10^{-8} M for barium and plutonium.

4.1.3.3.3 Sorption data from experiments with crushed-tuff columns

The sorptive behavior of radionuclides in elution experiments with columns of crushed tuff has been described by Treher and Raybold (1982). Several observations can be made based on data reported from approximately 40 column experiments. Sorption ratios (R_d) for strontium, cesium, and barium measured by the column method generally fall within the range of values measured with the batch technique when both column and batch measurements are made with crushed tuff washed free of fine particles (less than 35 μm). Wolfsberg et al. (1981) had indicated that the R_d values inferred from column studies were two to five times smaller than those from batch studies, but the comparisons were made with batch measurements on material containing fine particles, which are predominantly highly sorbing clays. Column-elution curves for uranium-237 result in an R_d value of 0.72 ml/g, in good agreement with the batch measurement of 1.5 ml/g. Experiments with actinide elements are planned (Section 8.3.1.3).

4.1.3.3.4 Sorption data from circulating-system experiments

Average sorption ratios determined by both the batch and the circulating-system methods are shown in Table 4-15 for strontium, cesium, barium, americium, and plutonium. Considering the spread of experimental values, the agreement between the two methods is acceptable. In most cases the results fall within the spread of individual experimental values reported by Daniels et al. (1982).

Devitrified tuffs give slightly higher sorption ratios in the batch method than in the circulating-system method. The R_d values for the smectite-bearing devitrified tuff and for the zeolite-bearing vitric tuff show no consistent pattern.

4.1.3.3.5 Comparison of sorption ratios from batch, circulating system, and column measurements

Batch and both types of column experiments on various tuffs with the same particle-size distribution yield sorption ratios for strontium, barium, cesium, americium, and plutonium that are within a factor of 2 (americium on sample JA-37, a devitrified tuff containing smectite, was an exception). This agreement means that self-grinding of the tuff in batch experiments is probably not a problem. The experiments with crushed-tuff columns show that batch sorption measurements are a valid representation of flowing experiments when the crushed tuffs are free of fine particles less than 35 micrometers in diameter.

4.1.3.3.6 Sorptive behavior as a function of stratigraphic position and mineralogy

This section discusses sorption ratios as a function of stratigraphic

Table 4-15. Average sorption ratios from batch, circulating-system, and crushed-tuff column sorption measurements at room temperature[a]

Element	Sample	Petrologic character[b]	Batch[c]	Sorption ratio (ml/g) Circulating system	Column
Sr	YM-22	D	53 (3)[d]	27 (2)[c]	22
	YM-54	D	62 (12)	45 (3)	43
	JA-37	D + S	287 (14)	390 (10)	123
Cs	YM-22	D	290 (30)	490 (50)	363
	YM-54	D	180 (40)	120 (10)	130
	JA-37	D + S	610 (40)	1,800 (10)	1390
Ba	YM-22	D	900 (30)	120 (10)	137
	YM-54	D	410 (150)	130 (10)	149
	JA-37	D + S	760 (150)	860 (40)	--[e]
Am	YM-49	V + Z	4,300 (1,400)	2,200 (300)	--
	JA-37	D + S	28,000 (10,000)	3,400 (600)	--
	G1-1883	D	4,700 (300)	3,300 (100)	--
Pu	YM-49	V + Z	230 (50)	570 (170)	--
	JA-37	D + S	400 (70)	290 (170)	--
	G1-1883	D	77 (11)	56 (11)	--

[a]Sources: Daniels et al. (1982); Treher and Raybold (1982).
[b]D = devitrified, V = vitric, S = contains smectite, Z = contains zeolite.
[c]From Tables 4-12 and 4-13.
[d]Value in parentheses is the absolute-value standard deviation of the means of duplicate measurements.
[e]-- = no data.

position and mineralogy. These analyses are important for calculations of retardation along possible travel paths to the accessible environment.

Average sorption ratios determined from ambient-temperature batch sorption experiments on crushed-tuff samples from well J-13 and drillholes UE-25a#1, USW G-1, USW G-2, and USW GU-3 are presented in Table 4-12. In Figure 4-14, the data are plotted against equivalent sample depths in drill-hole USW G-1 for well J-13 and drillholes UE-25a#1 and USW G-1 by Daniels et al. (1982).
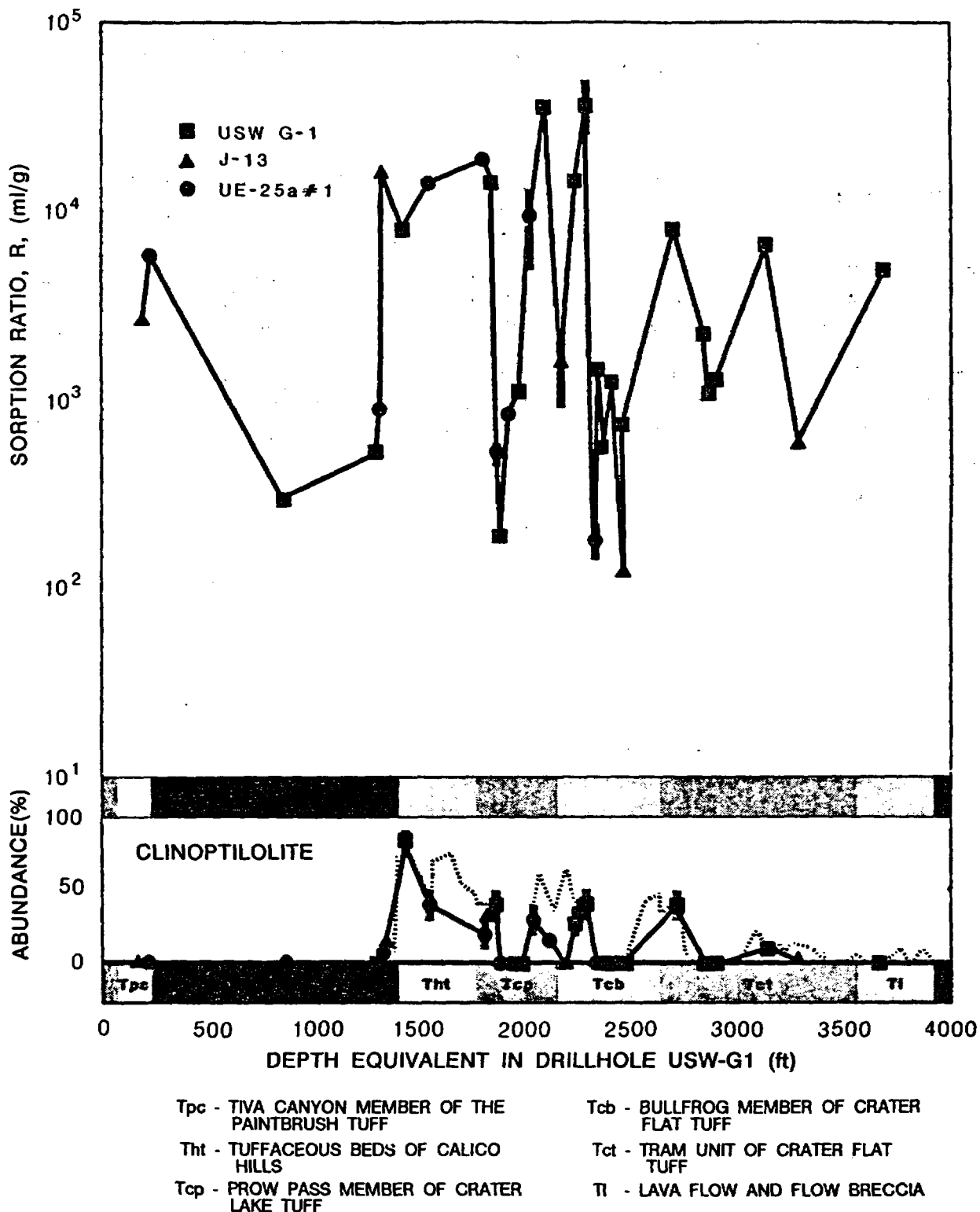
Figure 4-14. Variations in the sorptive behavior of strontium and cesium with the abundance of clinoptilolite and stratigraphic depth. Modified from Daniels et al. (1982). Dashed lines are data for a more complete set of samples from Bish et al. (1981).

Variations in the sorptive behavior of strontium and cesium with the abundance of the zeolite clinoptilolite are shown in Figure 4-14. The relative abundances of the minerals found at various depths given in Figures 4-1 and 4-2. The correlations are quite striking, showing an essentially direct correlation between an increase in strontium and cesium sorption ratios and an increase in clinoptilolite abundance. A similar correlation can be made for the sorption of barium and radium (Daniels et al., 1982; Ogard et al., 1983b). The correlations are even better when the abundances of clinoptilolite and mordenite are considered together. The increase in sorption for cesium, strontium, and barium on sample G1-3658 from the flow breccia below the Tram Member appears to be directly related to the high content of smectite clay in the sample (30 to 70 percent); the sample contains no detectable quantities of zeolite (Table 4-14) (Daniels et al., 1982; Ogard et al., 1983a). Section 8.3.1.3 describes plans for examining the sorption data using various statistical analyses, with emphasis on correlating sorption with mineralogy.

For cerium and europium, variations in the sorption ratios with stratigraphic position are not as regular as those for strontium, cesium, and barium. In broad outline, the stratigraphic positions of the maximum and minimum sorption ratios for cerium and europium coincide closely with the maxima and minima in R_d for cesium, strontium, and barium in units in the unsaturated zone and downward to the contact between the Bullfrog and Tram members. The Tram Member shows little correlation, with samples having the highest R_d for cerium and europium often giving the lowest R_d for cesium, strontium, and barium (and vice versa). The difference may be explained by mineralogic differences and will be investigated on that basis (Section 8.3.1.3). It may be difficult to correlate statistically this difference with mineralogic differences due to other processes that may be affecting the sorption; however, it is known that the analytical error inherent in these experiments is not the source of the difference.

Apparently there is a correlation between the sorption of cerium or europium and the presence of zeolites in the lower Topopah Spring Member, in the tuffaceous beds of Calico Hills, and in the upper Prow Pass Member (Table 4-14). The high sorption ratios in the upper Topopah Spring Member and the lower Tiva Canyon Member may be associated with the high content of smectite (10 to 60 percent) in the samples studied. The high sorption ratio measured for sample G1-2901 from the middle portion of the Tram Member unit does not appear to be correlated with mineralogic variations in drillhole USW G-1.

Sorption data for the actinides uranium, neptunium, plutonium, and americium are limited. The sorption ratios for uranium and neptunium are below 10 ml/g for most samples (Table 4-12b); sorption ratios for plutonium are near 100 ml/g (Table 4-12b) for all samples. However, there are no strong correlations with the mineralogy of the test samples. Sample JA-37 from the lower portion of the Tram Member and sample G2-723 from the lower portion of the Pah Canyon Member of the Paintbrush Tuffs generally give the highest R_d values for these actinides. The high R_d values may be due to the relatively high smectite content of sample JA-37 (10 to 40 percent), or the high calcite content (30 to 40 percent) of sample G2-723. The sorption ratios for americium may be mineralogically controlled, being generally higher than 1,000 ml/g in the zeolite tuffs of Calico Hills and the Prow Pass Member and decreasing to about 100 ml/g in the nonzeolitized lower Topopah

Spring and the middle Bullfrog members. The sorption ratio for sample JA-37 from the Tram Member is again the highest and may result from the presence of smectites.

The sorption ratios for plutonium are generally between 50 and 1,000 ml/g, independent of sample position and lithology (Daniels et al., 1982). In samples from nonwelded to partially welded zeolitized or vitric tuffs from the tuffaceous beds of Calico Hills, the Prow Pass, the Pah Canyon, the Topopah Spring, and the Tram members have R_d values for americium higher than 1,000 ml/g, whereas samples with lower R_ds are generally associated with welded and devitrified units. The sorption ratio for americium is highest in sample G2-723 from the lower Tram Member unit.

The sorption ratios for technetium are very limited. In most experiments under atmospheric conditions, the sorption ratios are less than unity and in some cases are zero. Because the sorption ratios for technetium are so low, long-term (12 mo) sorption experiments approaching equilibrium have been done and they show no change in R_d with time (Ogard and Vaniman, 1985). At these low sorption levels, correlation with stratigraphic position may not be valid or useful.

Very limited data for thorium and tin (Rundberg et al., 1985) do not show a correlation with mineralogy. The sorption ratios for thorium were higher than 140 ml/g, and those for tin were 150 ml/g or higher.

As described in Section 8.3.1.3, current studies will provide a more complete understanding of the sorption of the radionuclides listed in 40 CFR Part 191, Appendix A, including technetium, tin, and neptunium. Uranium and thorium are also being studied because they are the parents of radium. Regression analysis is being employed to determine the correlation of sorption with tuff mineralogy.

Because tuff samples may be composed of more than one sorbing mineral, a method has been developed to predict sorption ratios for samples of known mineralogy by combining the effects of several minerals. The combined effect is tentatively defined as a weighted sum called the SMC. Thus,

$$SMC = \Sigma W_i X_i, \qquad (4-4)$$

where W_i is the weighting factor for each mineral phase relative to that of clinoptilolite and X_i is the abundance in percent of each phase. Further details are given in Daniels et al. (1982). Studies of sorption on pure minerals and selected core samples will be performed to quantify expected sorption along transport pathways using the SMC concept (Section 8.3.1.3.4).

The following correlations of mineralogy with sorptive behavior of radionuclides have been identified and can be summarized as follows:

1. The sorption of alkali metals (e.g., cesium) and alkaline earths (strontium, barium, and radium), which probably exist in ground water as uncomplexed ions (Section 4.1.3.4.2) and probably sorb by ion exchange, is directly related to the presence of minerals with exchangeable cations: the zeolite clinoptilolite and potentially the smectite clays. The sorption ratios on these minerals are from

1,000 to higher than 10,000 ml/g. Because of the large quantities of the zeolite clinoptilolite in the Calico Hills and Prow Pass units lying below the repository horizon, the waste elements cesium, strontium, and radium would be strongly sorbed and their movement greatly retarded if the flow path is through these units.

2. The correlation of sorption of cerium, europium, plutonium, and americium with mineralogy also exists, but the relation is not as clear as for the alkali metals. However, sorption ratios are high for the elements previously listed (from 100 to higher than 1,000 ml/g) and, therefore, the lack of correlation is not critical. The sorption of these elements, though, is undoubtedly influenced by the formation of hydroxyl and carbonate complexes.

3. It appears that sorption on tuff will not offer much retardation for such anionic species as oxidized technetium species (i.e., TcO_4^-).

4.1.3.3.7 Sorptive behavior as a function of ground-water composition

The composition of the ground water and matrix mineralogy controls the oxidation state and speciation of radionuclides as well as their solubility, while at the same time providing competing ion and species for sorption sites, all of which can affect sorption of the radionuclides by tuff. Because ground-water composition may vary between the repository and the accessible environment, studies have been performed to determine what effect changes in ground-water composition have on measured sorption ratios.

Three ground waters are being investigated: water from well J-13, located in Jackass Flats; water from drillhole UE-25p#1 and from drillhole USW H-3, both of which are located on Yucca Mountain. Water from well J-13 has been used as the reference ground-water composition partly because the approximate production region of the well is the Topopah Spring Member; which, at Yucca Mountain, lies in the unsaturated zone and is the proposed repository horizon, and because, at the time studies on ground water began, well J-13 was the nearest producing well to Yucca Mountain. Comparisons are now being made of sorption ratios obtained with J-13 water to those from drillholes UE-25p#1 and USW H-3. The composition of these waters is given in Tables 4-7 and 4-8. Water from drillhole UE-25p#1 has the highest ionic strength, whereas drillhole USW H-3 water has the highest pH measured thus far at Yucca Mountain and was measured as slightly reducing in the field. A thorough discussion of water chemistry at Yucca Mountain is contained in Ogard and Kerrisk (1984). Distilled water was also studied (in some instances) as a representative of an extreme in ground-water composition.

Elements studied thus far include strontium, cesium, barium, europium, and tin. Plans for studying the sorption of actinides as a function of ground-water chemistry is found in Section 8.3.1.3.4. The selection of tuff samples used was based on their predominant mineralogy. Sample GU3-1301 is a vitric tuff from the Topopah Spring Member; G1-2233 is a zeolitized tuff from the Bullfrog Member; G4-1504 is a zeolitized tuff from the Calico Hills; and G1-2901 is a devitrified tuff from the Tram Member. Sorption ratios were measured using standard batch technique (Section 4.1.3.2.2).

Tables 4-16a and 4-16b give the results obtained for well J-13, drill-hole UE-25p#1, and distilled water (where available). Data from drillhole USW H-3 have not yet been published. For those elements presumed to sorb by an ion exchange mechanism (such as strontium, barium, and cesium), the lower ionic strength waters gave the highest sorption ratios. This is probably due to decreased competition for sorption sites. The exception appears to be barium in distilled water on sample G1-2233; however, the well J-13 results may be too high due to the inclusion of particles finer than 75 micrometers in that experiment. In contrast to these single oxidation state elements, europium and tin exhibit higher sorption ratios for the same initial concen-trations in the higher ionic strength drillhole UE-25p#1 water than in the more dilute waters. It is postulated that europium and tin are precipitating out of solution in the drillhole UE-25p#1 water, perhaps as sulfates or fluorides. Plans for studying solubility and precipitation of the radio-nuclides are discussed in Section 8.3.1.3.5.

From the data presented, it is evident that ground-water composition can affect sorption ratios. The ground waters studied represent extremes in the water composition found so far at Yucca Mountain. When information on the vadose water composition (unsaturated-zone water) is available, studies will be made to characterize its effect on sorption ratios. Plans for obtaining the additional required information are outlined in Section 8.3.1.3.

4.1.3.4   Processes affecting radionuclide concentrations and speciation in solution

The solubility of the waste elements can influence their transport by limiting the maximum concentration of the elements dissolved in the aqueous phase. Speciation, defined as the formation of various complexes and oxida-tion states in the aqueous phase, in turn affects the solubility. Speciation and solubility of individual waste elements depend on the chemical properties of the waste element, on the state of the local water (composition, pH, oxi-dation state, and temperature), and, if nonequilibrium processes are impor-tant, on factors such as precipitation and dissolution kinetics, oxidation-reduction kinetics, the identity of the solids present, water-flow condi-tions, and colloid formation. The following discussion of solubility and speciation is in terms of waste elements rather than radionuclides because these processes are controlled by the total concentration of an element in solution--that is, the sum of the concentrations of all its isotopes. The concentrations of individual radionuclides depend on the isotopic composition of the element.

At this time it is possible to estimate the solubilities of many important waste elements under repository conditions. The estimates are primarily based on literature data interpreted in terms of a chemical-equilibrium model. However, solubility calculations alone will not be sufficient for determining the concentration limits of waste elements (NRC, 1984). For this reason, solubility data for important waste elements have been and will continue to be obtained by laboratory experiments under conditions that are characteristic of a Yucca Mountain repository. The experiments are just beginning, and only a few results are available. A combination of site-specific solubility and speciation data will be used

Table 4-16a. Sorption ratios for cesium and strontium in different waters[a,b,c]

Core[d]		Cesium			Strontium		
		J-13	UE-25p#1	Distilled water	J-13	UE-25p#1	Distilled water
GU3-1301 (vitric)	Sorption	160(35)	46(5)	NA[e]	32(8)	10(2)	NA
	Desorption	180(40)	55(4)	NA	90(20)	32(1)	NA
G1-2233 (zeolitized)	Sorption	13,500(800)	7,500(1,100)	13,000(1,600)	48,000(3,000)	2,000(330)	56,000
	Desorption	23,000(6,000)	8,800(900)	8,700(3,400)	90,000(40,000)	3,000(500)	21,000(12,000)
G1-2901 (devitrified)	Sorption	1,290(110)	900(250)	3,350(170)	68(1)	44(13)	136(1)
	Desorption	1,380(30)	850(76)	3,800(670)	67(1)	35(4)	105(13)
G4-1502 (zeolitized)	Sorption	ND[g]	ND	ND	ND	ND	ND
	Desorption	ND	ND	ND	ND	ND	ND
G1-2840	Sorption	ND	ND	ND	ND	ND	ND
	Desorption	ND	ND	ND	ND	ND	ND

[a] Sorption ratios in ml/g.
[b] Numbers in parenthesis represent the standard deviation of the mean.
[c] Crowe and Vaniman (1985); Daniels et al. (1982); Ogard and Vaniman (1985); and Rundberg et al. (1985).
[d] The cores are described in the text.
[e] NA = Not applicable.
[f] Particle size was <500 m rather than the standard 75 to 500 μm.
[g] ND = No data.
[h] Only one measurement.

Table 4-16b. Sorption ratios for barium, europium and tin[a,b,c]

Core[d]		Barium			Europium			Tin	
		J-13	UE-25p#1	Distilled water	J-13	UE-25p#1	Distilled water	J-13	UE-25p#1
GU3-1301	Sorption	570(60)	82(18)	NA	75(12)	>17,000	NA	160(8)	4,000(520)
(vitric)	Desorption	660(100)	140(30)	NA	110(40)	>20,000	NA	1,280(180)	6,750[h]
G1-2233	Sorption	250,000(30,000)[f]	41,000(6,300)	55,000(5,300)	900(200)	>5,600	516(100)	ND[g]	ND
(zeolitized)	Desorption	240,000(80,000)[f]	59,000(6,000)	34,000(23,000)	5,000(2,000)	>7,900	1,400(600)	ND	ND
G1-2901	Sorption	1,600(200)	1,400(520)	7,200(100)	160,000(50,000)	38,000(16,000)	37,000(400)	22,000(5,000)	35,800(900)
(devitrified)	Desorption	1,980(30)	1,100(90)	6,100(900)	210,000(50,000)	69,000(20,000)·	27,500(6,200)	38,000(8,000)	52,500(1,900)
G4-1502	Sorption	ND	ND	ND	ND	ND	ND	215(56)	800(110)
(zeolitized)	Desorption	ND	ND	ND	ND	ND	ND	500(8)	300(130)
G1-2840	Sorption	ND	ND	ND	ND	ND	ND	283(160)	20,000(2,700)
	Desorption	ND	ND	ND	ND	ND	ND	780(130)	18,400(6,900)

[a] Sorption ratios in ml/g.
[b] Numbers in parenthesis represent the standard deviation of the mean.
[c] Crowe and Vaniman (1985); Daniels et al. (1982); Ogard and Vaniman (1985); and Rundberg et al. (1985).
[d] The cores are described in the text.
[e] NA = Not applicable.
[f] Particle size was <500 m rather than the standard 75 to 500 μm.
[g] ND = No data.
[h] Only one measurement.

together with literature data to develop solubility models. The modeling effort is basically an attempt to understand within a theoretical framework the parameters that control solubility and speciation. Thus, chemical-equilibrium (thermodynamic) models will be used wherever possible.

Section 4.1.3.4.1 gives brief discussions of speciation, solubility, natural colloid formation, and radiolysis, processes important in understanding the concentration limits of elements in solution. Section 4.1.3.4.2 discusses the results of solubility measurements conducted for this program as well as solubility and speciation data that are available in the literature. Section 4.1.3.4.3 briefly discusses the modeling program that is being conducted in conjunction with the solubility and speciation experiments. Section 4.1.3.4.4 lists estimates of the solubility of a number of important waste elements in well J-13 water. Plans for obtaining additional solubility data are outlined in Section 8.3.1.3.5.

4.1.3.4.1 Processes affecting waste element concentrations in solution

4.1.3.4.1.1 Speciation

Elements dissolved in water can exist as various chemical species such as different oxidation states or complexes with other ions in the water (Garrels and Christ, 1965; Baes and Mesmer, 1976; Stumm and Morgan, 1981). Solubility generally increases as the variety and concentration of complexes of an element increase; thus, the solubility is influenced by the tendency of a given element to form complexes and the concentrations of species with which it can complex. Sorptive behavior depends on the size and charge of the sorbing species; both of these quantities vary among the complexes of a given element. Thus, speciation can influence sorption. Aqueous species can be experimentally detected in solution by a number of techniques; spectroscopy is most commonly used (Rossotti and Rossotti, 1961). However, concentrations of aqueous species are normally calculated from a knowledge of the overall composition of the solution (total concentrations of the elements in solution) and the formation constants of possible aqueous species using equilibrium thermodynamic methods. Equilibrium thermodynamic methods work well (given the proper data) for the various complexes of a particular oxidation state, but may yield inaccurate results for the distribution of the element among possible oxidation states (Lindberg and Runnells, 1984).

4.1.3.4.1.2 Precipitation

Solubility, like speciation, depends on the composition, pH, and temperature of the water (Garrels and Christ, 1965; Sposito, 1981; Stumm and Morgan, 1981). If an element can also exist in various oxidation states, variables that control oxidation-reduction behavior also influence solubility. Unlike complex formation, which is essentially always an equilibriumprocess, precipitation processes are often not in equilibrium or in metastable equilibrium (Stumm and Morgan, 1981). If dissolution and precipitation kinetics are fast on the time scale of interest, equilibrium

behavior can be assumed. If kinetics are very slow, a metastable equilibrium
may exist where the aqueous phase is in metastable equilibrium with some
solid other than the most stable (least soluble) one. In some intermediate
cases, the dissolution or precipitation rates may be comparable to the time
scale of interest; for these cases, kinetic data are required to accurately
describe aqueous concentrations.

Coprecipitation refers to a group of processes whereby more than one
compound precipitates at one time (Sposito, 1981). Three examples are mixed-
solid formation, adsorption during precipitation, and inclusion during preci-
pitation. The importance of coprecipitation for waste-element solubility at
Yucca Mountain is uncertain at this time.

4.1.3.4.1.3 Natural-colloid formation

A number of actinides, plutonium in particular, can form natural col-
loids under certain conditions (Avogadro and DeMarsily, 1984; Kim et al.,
1984a; Olofsson et al., 1984). The questions of primary importance for a
waste repository are whether natural colloids can form under the conditions
expected at the repository or along flow paths to the environment--and
whether the colloids would be transported by the aqueous phase. This section
addresses only the question of natural-colloid formation; colloid transport
is discussed in Section 4.1.3.6. Related, but different phenomena, the
sorption of waste elements on particulate material normally present in the
water and colloid formation during waste-form or waste-package dissolution,
are discussed in Sections 4.1.2 and 4.1.3.3, and Section 7.4, respectively.

Plutonium(IV) readily forms colloids under conditions that are similar
to Yucca Mountain water (Olofsson et al., 1984) near-neutral solutions of low
ionic strength (about 10^{-3} mole/L) (Newton and Rundberg, 1984). These col-
loids are solution like sols that are optically clear, show a characteristic
absorption spectrum, and do not settle out of solution. Colloidal plutonium
shows x-ray diffraction patterns similar to crystalline plutonium dioxide;
higher-order lines are missing, indicating small crystalline size (20 to 30
angstroms). There is also some indication that americium(III) may form
colloids under similar conditions (Olofsson et al., 1984). Neither element
has been studied to the extent that colloid properties (particle size and
stability) can be predicted for known solution conditions. Colloid pro-
perties are, however, being examined. Plans for obtaining this information
are outlined in Section 8.3.1.3.5.

4.1.3.4.1.4 Radiolysis

Radiation can affect the solubility of waste elements by altering the
composition of the water or by influencing the crystallinity of the solids
that form (Ausloos, 1969). The primary effect of gamma radiation will be a
reduction of water pH and a trend toward more oxidizing conditions as long as
air is present; secondary effects will be the production of nitrate (or
nitrite) anions. Gamma radiation will be most important early in the life of
the waste and will affect only the water near the waste. By 300 yr after

discharge from the reactor, the total gamma flux (in watts) of spent fuel is about 500 times less than the flux at 10 yr after discharge (Croff and Alexander, 1980). Because containment would not be significantly breached before 300 yr (10 CFR 60.113(a)(1)(ii)(A)), the effects of gamma radiation will be reduced considerably. The effects of gamma radiation on the far field is negligible; however, the effects on waste element dissolution are discussed in Section 7.4.3.

Alpha radiation can affect water compositions in ways that are similar to the effects of gamma radiation. The primary effects of alpha radiation are a decrease in pH and a trend toward more oxidizing conditions in the water. Solids composed of alpha emitters tend to show self-irradiation damage to their crystal structure; the solubilities of solids like the actinide oxides and hydroxides are affected in that amorphous solids, which are generally more soluble than crystalline solids, are more likely to be the natural precipitation products (Rai et al., 1983; Nitsche and Edelstein, 1985).

4.1.3.4.2 Solubility and speciation data

Solubility and speciation data are available for a number of important waste elements. Although most of the data have not been measured under conditions that are characteristic of a Yucca Mountain repository, thermodynamic models of solubility and speciation allow solubility estimates for these conditions. This section describes data that can be used to estimate waste element solubilities at Yucca Mountain.

4.1.3.4.2.1 Solubility of americium, plutonium, and neptunium in well J-13 water

Preliminary measurements of the solubility of americium, plutonium, and neptunium in a neutral electrolyte and in water from well J-13 have been completed (Nitsche and Edelstein, 1985). The measurements were made from oversaturation at 25°C and a pH of 7. For plutonium and neptunium, measurements were started with different oxidation states that might exist under natural conditions. Table 4-17 summarizes the results.

Under the conditions of the measurements, neptunium(V) was the only oxidation state finally observed in the aqueous phase, for neptunium(V) or neptunium(VI) as the initial aqueous oxidation state. Measurements were done starting with plutonium(IV), plutonium(V), and plutonium(VI) aqueous species; the final aqueous species were predominantly plutonium(V) plus plutonium(VI) (over 90 percent), with plutonium(V) ranging from about 40 to 80 percent. Some difficulties were encountered in identifying the solid phases that precipitated in the experiments. For americium solubility in well J-13 water, both americium(III) hydroxy carbonate ($AmOHCO_3$) and americium (III) carbonate-2-hydrate ($Am_2(CO_3)_3 \cdot 2H_2O$) were found. For neptunium in well J-13 water, sodium neptunyl carbonate-n-hydrate ($Na_3NpO_2(CO_3)_2 \cdot nH_2O$) was tentatively identified as the solid. For plutonium, the solids could not be identified.

Table 4-17. Analytical results of solutions in equilibrium with their solid phase (supersaturated starting conditions) in 0.1 M $NaClO_4$ and well J-13 ground water at pH = 7.0 ± 0.1, 25 ± 1°C

Test no.	Initial species	Solubility (M)		Final oxidation state of soluble species[a]		Solid	
		$NaClO_4$	Well J-13	$NaClO_4$	Well J-13	$NaClO_4$	Well J-13
1	NpO_2^+	$(4.4 \pm 0.1) \times 10^{-4}$	$(1.6 \pm 0.6) \times 10^{-3}$	+V = 100%	+V = 100%	Amorphous	Crystalline $Na_3NpO_2(CO_3)_2$ x nH_2O
2	NpO_2^{2+}	$(3.5 \pm 0.1) \times 10^{-4}$	$(7.2 \pm 0.7) \times 10^{-4}$	+V = 100%	+V = 100%	Crystalline unidentified	Crystalline unidentified
3	Am^{3+}	$(3.0 \pm 0.1) \times 10^{-4}$	$(1.1 \pm 0.2) \times 10^{-6}$	+III = 100%	+III = 100%	Mostly amorphous	Crystalline $Am_2(CO_3)_3$ x $2H_2O/AmOHCO_3$
4	Pu^{4+}	$(3 \pm 2) \times 10^{-8}$	$(1.6 \pm 0.2) \times 10^{-6}$	III + IV + p = 3 ± 2% V + VI = 95 ± 4% V = 68 ± 9%	III + IV + p = 2 ± 3% V + IV = 98 ± 3% V = 40 ± 5%	Amorphous	Amorphous
5	PuO_2^+	$(2 \pm 1) \times 10^{-9}$	$(8 \pm 3) \times 10^{-6}$	III + IV + p = 5 ± 4% + VI = 95 ± 4% V = 70 ± 17%	III + IV + p = 0 ± 2% V + VI = 100 ± 2% V = 64 ± 6%	Amorphous	Crystalline unidentified
6	PuO_2^{2+}	$(1.0 \pm 0.5) \times 10^{-7}$	$(3 \pm 2) \times 10^{-5}$	III + IV + p = 3 ± 2% V + VI = 97 ± 2% V = 82 ± 16%	III + IV + p = 2 ± 2% V + VI = 98 ± 2% V = 67 ± 6%	Amorphous	Crystalline unidentified

[a] p = Pu(IV) polymer (Nitsche and Edelstein, 1985).

The results from these experiments are being reviewed in terms of a chemical equilibrium model of solubility. They will be incorporated into the solubility models for Yucca Mountain.

4.1.3.4.2.2 Solid waste dissolution experiments

In addition to direct solubility measurements, dissolution experiments on spent fuel and other high-level waste forms such as borosilicate glass are also being performed. The measurements are described in Section 7.4.3 (see also Bazan and Rego, 1985; Wilson and Oversby, 1985). The experiments expose bare spent fuel or glass to well J-13 water and other water compositions and essentially approach steady state from undersaturation. Many of the experiments contain other materials such as zircaloy cladding, stainless steel, or tuff. Thus, the experimental data may be more difficult to interpret in terms of fundamental mechanisms than simple solubility experiments.

Waste-dissolution experiments under conditions characteristic of Yucca Mountain will be reviewed and the data will be used, where appropriate, to help define solubility limits. Plans for this work are outlined in Section 8.3.1.3.5.

4.1.3.4.2.3 Literature data for waste elements

The measurement of solubilities and other thermodynamic properties of important waste elements is an active field of study. Thus, the literature contains data that are useful for understanding and modeling solubility and speciation. Although these data were not obtained under conditions that are characteristic of a Yucca Mountain repository, solubility models for repository conditions can be tested and validated using literature data.

Americium. The behavior of americium in natural waters is somewhat simpler than that of the other actinides (e.g., plutonium or uranium) because americium(III) is the only stable oxidation state observed under these conditions. There have been a number of recent measurements of the solubility of americium(III) in a neutral electrolyte and with carbonate present (Kim et al., 1984b; Rai et al., 1983; Silva and Nitsche, 1983; Bernkopf and Kim, 1984; Rai and Ryan, 1984; Nitsche and Edelstein, 1985). The studies have also been used to define or support formation constant data for a number of important americium(III) complexes. Experiments by Lundqvist (1982) and Bidoglio et al. (1983) were aimed at defining formation constants for carbonate complexes with americium(III). Experimental data indicate that in a neutral electrolyte at 25°C and pH 7, americium has a solubility of about 10^{-4} to 10^{-6} mole/L, and in well J-13 water, its solubility is about 10^{-6} mole/L.

Americium thermodynamic data have been reviewed by Kerrisk (1984a). A thermodynamic data base for the EQ3/6 chemical-equilibrium computer model (Wolery, 1983) was developed. However, the review did not include a number of the more recent publications cited above. Two problems identified in the review were a conflict in the identity and formation constants of americium

complexes with carbonate and a lack of data above 25°C. The americium data base is being updated and will be reissued in the near future. The review and comparison with experimental data as they become available will continue as described in Section 8.3.1.3.5. The solubility calculations reported in this section have used the data base prepared by Kerrisk (1984a).

Plutonium. The solubility of plutonium in a neutral electrolyte and in carbonate solutions has been studied by a number of investigators (Rai et al., 1980; Rai and Swanson, 1981; Rai and Ryan, 1982; Kim et al., 1984b, 1984; Ogard et al., 1983b; Rai, 1984; Crowe and Vaniman, 1985; Nitsche and Edelstein, 1985). In a neutral electrolyte, the solid that appears to control solubility is hydrous plutonium dioxide (sometimes called amorphous plutonium dioxide or plutonium(IV) hydroxide). The solubility is much higher than that calculated for crystalline plutonium dioxide and may be an example of metastable equilibrium because crystalline plutonium dioxide, the most stable solid under the experimental conditions, does not precipitate from solution. Under oxidizing conditions, plutonium(V) and plutonium(VI) are the primary aqueous species. Thus, oxidation-reduction reactions are important in determining plutonium solubility. There is evidence that with sufficient concentrations of plutonium in solution, the plutonium(V)/plutonium(VI) concentrations are in equilibrium with a stronger oxidizing agent than dissolved oxygen (Rai, 1984); this may result from alpha radiolysis of the water and formation of significant amounts of hydrogen peroxide or some other radiolysis product. In a neutral electrolyte in contact with air, measured total plutonium concentrations in solution at pH 7 are in the range of 10^{-6} to 10^{-8} M.

From solubility measurements with carbonate present, Kim et al. (1984b) have proposed the existence of solid plutonium(IV) dihydroxide carbonate $(Pu(OH)_2 CO_3)$ and a very stable complex, plutonium(IV) carbonate ion $(PuCO_3^+)$. Their value of the formation constant for the reaction $Pu^{4+} + CO_3^- = PuCO_3^+$, is $\log(K) = 47.1$. This is similar to a value of $\log(K)$ of 41 or less at 25°C for the same reaction reported by Lemire and Tremaine (1980). If the formation constant of the plutonium(IV) carbonate ion $(PuCO_3^+)$ is this large, the solubility of plutonium in water from Yucca Mountain could be quite high (Wolfsberg et al., 1982a). However, estimates of the formation constant based on analogies with other actinides give a $\log(K)$ value of about 10 (Wolfsberg et al., 1982a). A recent experiment by Silva and Nitsche (1985), designed to find evidence of the existence of plutonium(IV) carbonate ion $(PuCO_3^+)$, placed an upper limit on $\log(K)$ of 13. Analysis of data taken during the preparation of solutions of plutonium in well J-13 water for sorption measurements indicates an upper limit of plutonium solubility in well J-13 water of 10^{-6} mole/L (Ogard et al., 1983b). This limit is consistent with the measurements of Nitsche and Edelstein (1985) noted above and with recent calculations of plutonium solubility in well J-13 water using $\log(K) = 10$ for the formation constant of plutonium(IV) carbonate ion $(PuCO_3^+)$ and hydrous plutonium dioxide as the solid controlling solubility (Ogard and Kerrisk, 1984). Although some evidence has been published for the existence of a stable plutonium(IV)-carbonate complex, more recent data seem to be contradictory. The question will continue to be investigated as described in Section 8.3.1.3.5.

Another question that has been raised about plutonium is the stability of the hydrolysis product plutonium(IV) pentahydroxide ion $(Pu(OH)_5^-)$ (Allard,

1983). The complex has not been observed, but was assigned a formation constant by analogy with uranium (Baes and Mesmer, 1976). Plutonium(IV) pentahydroxide ion becomes important at high pH; if it is stable, plutonium solubility could increase with increasing pH beyond a pH of about 7 or 8. It is not clear at this time whether this problem is of concern at Yucca Mountain. It will continue to be reviewed, as described in Section 8.3.1.3.5.

Uranium. The solubility of uranium has been studied extensively both in neutral electrolytes and also with carbonate present (Gayer and Leider, 1955; Blake et al., 1956; Miller, 1958; Robins, 1966; Sergeyeva et al., 1972; Silva and Yee, 1981; Krupka et al., 1984). In a neutral electrolyte under oxidizing conditions, uranium(VI) is the predominant aqueous oxidation state and schoepite ($UO_2(OH)_2 \cdot H_2O$) is the most stable solid phase at 25°C. At higher temperatures beta-uranium dioxide may be more stable (Robins, 1966). Some of the early solubility measurements were difficult because of a problem with precipitation of sodium uranates at high pH because sodium hydroxide was used to control solution pH. Measured uranium solubilities are in the range of 10^{-3} to 10^{-6} mole/L at 25°C and pH 7; however, the higher solubilities probably result from inadequate phase separation.

Uranium solubility under oxidizing conditions with sufficient carbonate present results in rutherfordine (UO_2CO_3) as the precipitate (Blake et al., 1956; Sergeyeva et al., 1972). The experiments were conducted under much higher carbonate concentrations than those existing in Yucca Mountain water and thus these data are not indicative of uranium solubility at Yucca Mountain. They are, however, useful for testing solubility models with carbonate present.

Experiments on spent fuel dissolution in well J-13 water showed uranium concentrations in solution that are less than about 2×10^{-5} mole/L (Wilson and Oversby, 1985). At present it is not clear what solid phase is controlling uranium solubility at this concentration. Although the test solutions are exposed to air, uranium in spent fuel is primarily as uranium(IV), that is as uranium dioxide; thus, it is possible that a uranium solid other than schoepite controls solubility. This measured concentration limit is about a factor of 100 below the calculated solubility of uranium in well J-13 water assuming schoepite as the controlling solid (Ogard and Kerrisk, 1984). The calculations indicate that one polynuclear complex, uranyl(VI) trihydroxide carbonate ion $((UO_2)_2CO_3(OH)_3)^-$, incorporates almost all the aqueous uranium. An experimental determination of uranium solubility in well J-13 water may be needed to resolve this difference. Plans for obtaining the information are outlined in Section 8.3.1.3.5.

Thermodynamic data for uranium(VI) have recently been reviewed by Tripathi (1984). The thermodynamic data base for EQ3/6 is being updated using this review as a basis.

Neptunium. Solubility data for neptunium were discussed in Section 4.1.3.2.1 and in the work of Nitsche and Edelstein (1985). Other literature data on the solubility of neptunium under oxidizing conditions will be reviewed as part of the incorporation of neptunium data. Plans for the work are outlined in Section 8.3.1.3.5.

Other waste elements. A number of waste elements are likely to have high solubilities in water from Yucca Mountain. They include carbon, cesium, iodine, and technetium (Rai and Serne, 1978; Allard and Torstenfelt, 1983; Apps et al., 1983; Ogard and Kerrisk, 1984). The solubility of technetium, which can exist in a number of oxidation states, should be high because of the likelihood of oxidizing conditions in Yucca Mountain water (Section 4.1.2). Solubility measurements for the elements listed above are not planned under repository conditions, because there is little expectation that solubility will limit their concentrations.

Carbon (carbon-14) can be released as carbon dioxide gas or directly as a carbonate under certain circumstances. In either case, there is an equilibrium between carbonate in the aqueous phase and carbon dioxide gas. There is also a large reservoir of natural carbon as carbonate dissolved in the aqueous phase that must be considered. Solubility data for the most likely carbonate solids (calcite or dolomite) are well known (Stumm and Morgan, 1981). Based on these data it is unlikely that solubility will limit carbon-14 concentrations in water from Yucca Mountain. Thus, no solubility measurements are planned for carbon. Two alkali-metal waste elements, strontium and radium, have similar chemistries but radium is expected to have a much lower solubility than strontium in water from Yucca Mountain (Ogard and Kerrisk, 1984; Crowe and Vaniman, 1985). Solubility measurements are planned for radium, whose sulfate solid may provide a useful limit on the aqueous concentration. No solubility measurements are planned for strontium. The solubilities of tin and thorium are also expected to be low in Yucca Mountain water (Apps et al., 1983); solubility measurements are planned for these elements because they are in large quantities and because they are considered as important radionuclides (Section 4.1.3.1.1). Radioisotopes of nickel are present as waste elements in subassembly hardware from light water reactors and in defense high-level waste glass. No solubility data were found for nickel that could be applied to water from Yucca Mountain; solubility measurements are planned as outlined in Section 8.3.1.3.5.

4.1.3.4.3 Solubility modeling

A program to model solubility and speciation data is an important part of any effort to assess the concentration limits of elements in solution. It is necessary to model experimental data in terms of some theoretical frame-work: to test the data for inconsistencies; to assess the sensitivity of the data to variations in independent parameters; and to allow interpolation and some extrapolation of solubilities beyond the specific conditions used in the experiments. A chemical equilibrium (thermodynamic) model, EQ3/6, is being used to model solubility and speciation data (Wolery, 1983).

Past efforts in modeling have concentrated on assessments of thermo-dynamic data and calculations that highlight the importance of particular aqueous species or solids for solubility in water from Yucca Mountain (Wolfsberg et al., 1982b; Ogard et al., 1983b; Rard, 1983; Kerrisk, 1984a; Crowe and Vaniman, 1985; Isherwood, 1985). Calculated solubilities and important aqueous species have been reported (Ogard and Kerrisk, 1984) and used for further analyses (Kerrisk, 1984b). This effort is expected to continue as described in Section 8.3.1.3.5.

It is uncertain whether nonequilibrium or kinetic models will be required to model the solubility and speciation of waste elements at Yucca Mountain. Colloid formation and rapid fracture flow are areas where such modeling may be needed. Until the formation of waste element colloids is better understood, the requirement for the models will remain an open question. Plans to review this question are outlined in Section 8.3.1.3.5.

4.1.3.4.4 Solubilities of waste elements in Yucca Mountain water

The solubilities of a number of waste elements in well J-13 water have been estimated from some experimental measurements and some equilibrium-thermodynamics calculations. Table 4-18 lists the estimates along with their source. The water was assumed to be at pH 7, 25°C, and oxidizing.

Ogard and Kerrisk (1984) reported calculated solubilities for six waste elements (uranium, plutonium, americium, strontium, radium, and technetium) in well J-13 water. The solubilities of two of these elements (americium and plutonium) were subsequently measured in well J-13 water by Nitsche and Edelstein (1985). The measured solubility of americium was about 100 times higher than the calculated solubility. The EQ3/6 thermodynamic data base for americium is presently being revised. The measured solubility of plutonium varied with the starting material but the average value was about five times higher than the calculated solubility. For uranium, Table 4-18 shows the value calculated by Ogard and Kerrisk (1984) for uranium(VI). This solubility is about 100 times higher than measured uranium concentrations in the same water over spent fuel (Section 7.4.3 and Wilson and Oversby, 1985). The reason for this difference is uncertain. At this time there are no other direct measurements of waste-element solubilities in well J-13 water.

Ogard and Kerrisk (1984) also reported calculated solubilities of the same six elements in waters from two other drillholes in the vicinity of Yucca Mountain (UE-25p#1 and USW H-3). The water from these drillholes has somewhat different compositions than water from well J-13 (Tables 4-6 and 4-7); the calculated solubilities were significantly different in a number of cases. Particularly, the water from drillhole USW H-3 was assumed to be reducing. No waste element solubility measurements have yet been made in waters from drillholes UE-25p#1 and USW H-3. Future experimental solubility measurements are described in Section 8.3.1.3.5.

4.1.3.5 Matrix diffusion

Moving ground water would provide the principal means of transporting radionuclides from the repository. Consequently, an understanding of water movement through tuff formations is vital. The diffusion of radionuclides from fracture water into the pore water in the rock matrix is important for retarding the transport of dissolved radionuclides through fractures in tuff, particularly for nonsorbing or low-sorbing soluble species. The apparent diffusion coefficient for a given radionuclide in tuff matrix depends on properties that are intrinsic to the chemical species (e.g., ion mobility) and properties of the tuff (such as porosity, tortuosity, and sorption

Table 4-18. Solubility of waste elements in well J-13 water[a]

Waste element	Solubility (moles/L)	Source of data
Americium	1×10^{-6}	Nitsche and Edelstein, 1985
Plutonium	1×10^{-5}	Nitsche and Edelstein, 1985
Neptunium	1×10^{-3}	Nitsche and Edelstein, 1985
Uranium	4×10^{-3}	Ogard and Kerrisk, 1984
Curium	[b]1×10^{-6}	Apps et al. 1983
Thorium	[b]1×10^{-9}	Apps et al. 1983
Strontium	8×10^{-4}	Ogard and Kerrisk, 1984
Radium	3×10^{-7}	Ogard and Kerrisk, 1984
Carbon	High[b,c]	Kerrisk, 1984b
Cesium	High[b,c]	Rai and Serne, 1978
Technetium	High[b,c]	Ogard and Kerrisk, 1984
Iodine	High[b,c]	Apps et al. 1983
Tin	[b]1×10^{-9}	Apps et al. 1983
Zirconium	[b]1×10^{-10}	Rai and Serne, 1978
Samarium	[b]2×10^{-9}	Benson and Teague, 1980
Nickel	[b]1×10^{-2}	Benson and Teague, 1980

[a]At pH of 7, 25°C, and oxidizing conditions.
[b]Estimated data.
[c]Solubility of these waste elements is expected to be high enough so that solubility will not limit concentration at a Yucca Mountain site.

ratio). It is therefore necessary to measure the diffusion coefficient of waste-element species in various unsaturated and saturated fractured tuff units. Preliminary results from experiments on radionuclide diffusion in tuff matrix are described in detail by Daniels et al. (1982). The information presented here is based on that report. Further work on the dynamic transport of radionuclides is planned in Section 8.3.1.3.6. This work will encompass diffusion studies in saturated and unsaturated fractured tuff.

4.1.3.5.1 Diffusion into the rock matrix

In the current conceptual model of the hydrology of Yucca Mountain, water is believed to flow predominantly in the matrix of the tuffs in the unsaturated zone, and predominantly in the fracture networks of the tuffs in the saturated zone. The effective diffusion coefficient of a dissolved species in the tuff matrices is an important quantity in determining the rates at which that species is transported through the rock units of either zone. If the flux through unsaturated rocks is small (less than 0.05 mm/yr), ordinary diffusion will be the dominant transport mechanism, and measurements of the effective diffusion coefficient will be needed in order to model the transport of radionuclide-bearing compounds to the accessible environment. For the flows through the fracture networks of the saturated zones, the effective diffusion coefficient in the matrix is one of several quantities that determine the rate at which radionuclides dissolved in rapidly flowing fracture water can enter the pore water of the matrix, where chemical retardation is generally most pronounced; this is the "matrix diffusion" mechanism alluded to earlier in this section. Thus, the effectiveness of retardation in the transport of solutes through fracture networks also depends on the effective diffusion coefficient.

Diffusion through the liquid-filled pore spaces of the matrix may proceed so rapidly that the assumption of local chemical equilibrium is not valid. Thus, knowledge of the rates of the chemical reactions involved in sorption on the solid phases of the matrix is necessary to determine experimentally effective diffusion coefficients for dissolved species. The kinetics of the sorption reactions are also of intrinsic interest in determining the circumstances under which assumptions of chemical equilibrium (and therefore constant geochemical retardation) are valid.

Experiments were performed (Rundberg, 1985) to determine the diffusion coefficients and rate constants for the sorption of strontium, cesium, and barium in samples of Yucca Mountain tuff from drillhole USW G-1. The uptake of radionuclides with time was determined for tuff disks 2.54 cm in diameter and 2.0 mm thick. The data were then fitted to the one-dimensional diffusion equation for a plane sheet coupled to a linear reversible reaction with the solid phase, defined as follows:

The diffusion is governed by the equation

$$\frac{\partial C}{\partial t} = D \frac{\partial^2 C}{\partial x^2} - \frac{\partial S}{\partial t} \qquad (4\text{-}5)$$

with the simultaneous reaction of the type

$$\frac{\partial S}{\partial t} = k_1 C - k_2 S \qquad (4\text{-}6)$$

where

C = the concentration of the solute free to diffuse within the sheet
S = the concentration of the immobilized solute
D = the diffusion coefficient
x = the position in the disk
t = the time
k_1, k_2 = the rate constants of the forward and backward reactions.

The effect of slow reaction on the diffusion of a sorbing species into tuff is demonstrated in Figure 4-15. The uptake of cesium with a R_d of 230 ml/g and a diffusion coefficient of 8.33 x 10^{-8} cm^2/s, assuming instantaneous or diffusion-limited sorption, is given by the broken line. The solid line is the best fit to the experimental data, using the solution to equations 4-5 and 4-6 given by Crank (1975). It is evident that the conventional treatment (instantaneous sorption) is inadequate. The shape of the curve does not match the experimental uptake well on a log-log plot, so varying the diffusion coefficient or the R_d value will not improve the fit. The solution with slow kinetics, however, appears to give an excellent fit to the experimental uptake. At early times, the discrepancy between the slow kinetics and the conventional treatment becomes quite large.

The rate constants for the sorption of cesium-137, strontium-85, and barium-133 are summarized in Table 4-19 with the diffusion coefficients determined by fitting the data to the Crank (1975) solution. The diffusion coefficients are all smaller than the ionic diffusion coefficient calculated from ionic mobilities. This is as expected because the pores in the tuff matrix represent a tortuous path that also may have constrictions to slow the diffusion of ions through the matrix. Details of the above analysis are given by Rundberg (1985). Plans for obtaining additional information are outlined in Section 8.3.1.3.6.

4.1.3.5.2 Retardation by matrix diffusion during fracture flow

Experiments comparing radionuclide transport by fracture flow in tuff (Daniels et al., 1982) with that in granite have provided a test of the validity of simple matrix- diffusion models. The principal purpose of the studies was to determine the degree of radionuclide retardation provided by geochemical processes (sorption) coupled to matrix diffusion along the flow path in a single fracture. The results provide information about the effectiveness of both diffusion and sorption processes in retarding radionuclides in rapidly flowing single-fracture systems. These results have been compared with transport-model predictions to partially validate the models.

The experiments employed artificial fractures induced in tuff and granite core samples. Artificial fractures are hydraulically smooth; thus, the
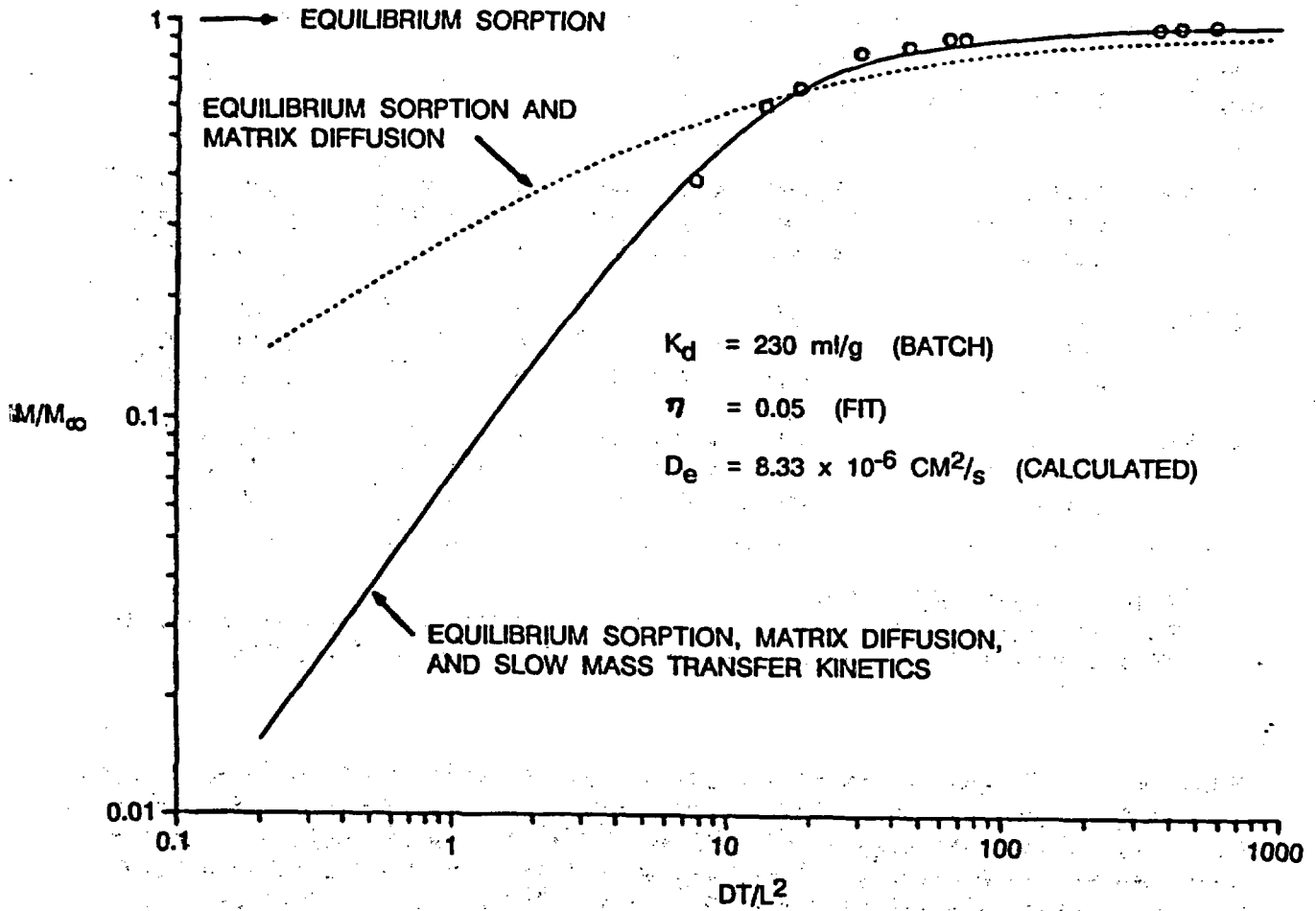
Figure 4-15. Cesium diffusion with slow sorption (tuff sample number G1-1883). Modified from Rundberg (1985).

Table 4-19. Sorption rate constants for tuff from drillhole USW G-1[a,b]

Tuff sample	Radionuclide	K_d (ml/g)	k_1 (s^{-1})	k_2 (s^{-1})	D (cm^2/s)
G1-1436	Cesium	7,790	6.3×10^0	1.4×10^{-4}	2.78×10^{-6}
	Strontium	36,300	3.5×10^0	2.0×10^{-5}	2.11×10^{-6}
	Barium	148,000	1.2×10^1	1.7×10^{-5}	3.38×10^{-7}
G1-1883	Cesium	230	5.9×10^{-2}	4.2×10^{-5}	1.33×10^{-6}
	Strontium	27	1.1×10^{-3}	6.7×10^{-6}	1.33×10^{-5}
	Barium	210	5.7×10^{-2}	4.4×10^{-5}	8.89×10^{-6}
G1-1982	Cesium	1,000	4.0×10^{-1}	4.7×10^{-5}	9.44×10^{-6}
	Strontium	88	9.5×10^{-3}	1.4×10^{-5}	1.37×10^{-5}
	Barium	800	2.6×10^{-1}	4.4×10^{-5}	8.89×10^{-6}

[a]Source: Rundberg (1985).
[b]K_d = retardation coefficient; k_1 = rate constant for forward reaction; k_2 = rate constant for reverse reaction; D = diffusion coefficients.

pieces mate well and do not have fracture-fill material that would complicate the surface chemistry and diffusion process. Experiments were performed on partially welded tuff samples G1-2335 and G1-2840 from the Bullfrog and the Tram members, respectively. Water was pumped through the fractures at the relatively high velocity of 2.8×10^{-2} cm/s. The fracture apertures were estimated by applying Darcy's law to a series of permeability measurements (Freeze and Cherry, 1979). The effective apertures in both tuff samples were approximately 30 micrometers. The effective aperture in the granite sample was 16 micrometers. Water containing strontium-85 and cesium-137 tracers was monitored as it passed through the fractures.

The analytical solution proposed by Neretnieks (1979) for a one-dimensional fracture with matrix diffusion was applied to the data from the experiments. The granite data fit the solution with experimentally determined R_d values. However, the results of the fracture-flow experiments on tuff did not agree with those of flow calculations that used experimentally determined R_d values. The R_d values that gave the best fits to the breakthrough portion of the strontium elution in the fracture-flow experiments were 30 and 16 ml/g for samples G1-2335 and G1-2840, respectively. The R_d values from batch sorption measurements were 148 and 160 ml/g for the same samples. The shape of the elution curve calculated for the tuffs also does not agree with the observed elution data. The radionuclide activity desorbs more slowly than would be expected for reversible diffusion-controlled sorption. This observation is consistent with previous measurements of batch desorption on tuff.

The two important conclusions that can be drawn from these fracture-flow

studies are as follows:

1. Matrix diffusion is an important mechanism contributing to the retardation of radionuclides in fracture flow; however, simple analytic models may not be adequate to predict the transport of waste elements in tuff fractures.

2. Because matrix diffusion is directly related to porosity, it should more effectively retard the movement of soluble species in porous tuffs than in low-porosity crystalline rock like granite or densely welded, devitrified tuff.

Plans for further work on matrix diffusion coupled with fracture flow are given in Section 8.3.1.3.6.

4.1.3.6 Radionuclide transport

Ground water can carry material along in solution or as suspended solids. The rate at which the transported material moves is affected by a variety of factors, the most important being the velocity of the flowing water, and the partitioning of the material between liquid and solid phases. Other factors include:

1. Chemical species in the water flowing in fractures diffuse into the water contained in rock pores.

2. The negative charge that is present on many rock surfaces can restrict the approach of anions. The exclusion may limit the diffusion of anions into the matrix thereby allowing the anions to move at the higher velocity of the water flowing in the center of the fractures, or channels, away from the surface film. The same phenomenon can restrict the entry of anions into the smaller pores.

3. A somewhat similar effect, called hydrodynamic chromatography, can result in particles flowing along pores at velocities somewhat greater than the average water velocity. Filtration in rock pores, however, can remove or retard the flow of suspended particulates.

4. Dispersion can result from diffusion, channeling, and turbulent flow, but dispersion by itself does not affect the average rate at which the transported material moves.

Gaseous phase transport is another means of transporting radionuclides. Volatile elements such as iodine-129 and carbon-14 can be transported in the gaseous phase in the unsaturated zone.

Previous portions of Section 4.1.3 have discussed radionuclide transport in terms of the retardation processes of sorption, precipitation, and diffusion. The remainder of this section will discuss radionuclide transport by suspended solids and by gaseous transport.

4.1.3.6.1 Transport of suspended solids

A possible mode of transport involves the movement of radioactive particles suspended in the ground water. Colloidal particles (less than a few micrometers in diameter) remain suspended for long periods and hence may migrate with the ground water. As the solid waste form is leached, particles containing radionuclides may form by the sorption of dissolved radionuclides on nonradioactive particles. At this time it is believed that plutonium and americium are likely to contribute most to transport as colloids.

To estimate the amount of radionuclides that could be transported by colloidal suspension, it is necessary to determine whether colloidal-sized particles that could be sorption sites for waste elements exist in the ground water of Yucca Mountain. Then, the sorption ratios for waste elements on these particles must be measured or estimated from the composition of the particles. In addition, the conditions under which colloids could form from the waste elements or from the waste and their stability after formation must be determined (Section 4.1.3.4.1). Finally, the conditions necessary for filtration of the particles by the tuff itself must be defined.

Matter in the colloidal state has a large surface area ($300 \, m^2/g$), thus it is not surprising that the most important properties of colloids are those that depend on surface interactions, such as adsorption. Drever (1982) discusses the nature and geochemistry of colloids, with emphasis on the charge surrounding colloids and its effect on suspension stability.

Olofsson et al. (1981, 1982a,b) classify radiocolloids (colloids containing radionuclides) as true colloids or pseudocolloids depending on their formation process. True colloids are formed by condensation of molecules or ions as a result of hydrolytic or precipitation processes. Colloids consist mostly of hydroxides or polymers formed by hydrolysis, and they have a very rapid formation rate. Pseudocolloids, on the other hand, are formed as a result of adsorption on impurities in the solution and tend to be much larger than true colloids (up to 5,000 angstroms). Pseudocolloids can be of two types, reversible and irreversible. The formation rate of pseudocolloids is basically determined by the sorption rate on colloidal impurities (Olofsson et al., 1982a,b).

In the event of a repository failure, radiocolloids are believed to be a significant factor for the transport of radionuclides, and might actually accelerate their transport away from the repository (Avogadro and Lanza, 1982; Avogadro and De Marsily, 1984). Radiocolloids may arise from a variety of sources. The corrosion of canister material can lead to the formation of absorbent colloids. Degradation of engineered backfills at the end of a repository's active life may also lead to colloid formation. If the waste form is leached by ground water, naturally occurring colloids derived from smectites, vermiculites, illites, kaolinite, and chlorite present in ground water may also adsorb radionuclides. Champ et al. (1982) have demonstrated experimentally the existence and rapid transport of plutonium colloids using core samples and ground water. Fried et al. (1975), in their 1975 laboratory studies, observed a fast migrating form of plutonium in their column experiments on Bandelier Tuff. Retardation of this polymeric form of plutonium was only one-tenth of the ionic form. A discussion of radiocolloid formation is found in Section 4.1.3.4.1.3.

Transport of particulates in geologic media will depend on aqueous flow rate, on pore and fracture size in the rock, on ions carried with the water, and on the nature of the particulate matter. Several mechanisms may remove colloidal particulates from ground water such as mechanical filtration by the rock matrix, sorption on the surface of rock pores (van der Waals), and neutralization of the repulsive charges on the colloids thus allowing them to coagulate.

Filtration will be an effective barrier to transport in the tuff matrix. Pore size is an important element in filtration. Pseudocolloids will not flow through pores that are smaller than the pseudocolloid carrier particles. In very small pores, true colloids will have a high probability of entering boundary layers around matrix particles, where they can be captured in the small pores. Pore-size distributions have been measured (Daniels et al., 1982) for several Yucca Mountain tuff samples. Mercury porosimetry data on a sample of Topopah Spring tuff show that most of the pores are less than 1.0 micrometer in diameter. There is a small percentage larger than 1.0 micrometer, but they should be dry because the amount of Topopah Spring saturation is less than 90 percent. More than 50 percent of the pore volume is made up of pores 0.1 micrometer in diameter or smaller. For samples from the Calico Hills, 50 percent of the pores are smaller than 0.05 micrometer, but there are somewhat more of the largest pores (4 micrometers). The data indicate that to pass through pores in the tuff matrix, colloids must be on the order of 0.1 micrometer or less.

Pore-water velocities, assuming matrix flow, are estimated to be less than 1.0 cm/yr (Travis and Nuttall, 1987). It is not clear whether such low velocities can provide sufficient momentum to allow bulk colloid movement. If fracture flow is significant, then colloid transport may be likely. If fracture flow is dominant in the Topopah Spring tuff, the average fracture-flow rate would be roughly 2 m/yr (Travis and Nuttall., 1987); this is still only on the order of transfer rates by molecular diffusion. If fracture flow is episodic, corresponding to a few intense rainfalls per year, flow rates in fractures might be much larger (tens of meters per year) but of shorter duration.

In addition, colloids will be subject to gravitational settling (Travis and Nuttall, 1987) for particles larger than about 0.1 micrometer. The transporting ability of very small colloids will be diminished by diffusion of radionuclides out of the carrier particles. Diffusion in solid phases is small, but not zero. Solid phase diffusion for some radionuclides on several Yucca Mountain minerals has been measured at about 10^{-16} to 5×10^{-13} cm^2/s (Rundberg, 1985). A characteristic diffusion time (T) from 0.1 micrometer diameter particles is given by

$$D \approx \frac{R^2}{T} = \frac{L^2}{4T} \longrightarrow T \approx \frac{L^2}{4D} \approx \frac{(10^{-5})^2}{4 \times 10^{-16}} = 2.5 \times 10^5 \text{ s} \approx 3 \text{ days} \qquad (4\text{-}7)$$

where

D = diffusion coefficient
T = diffusion time
L = particle diameter
R = particle radius.

Small pseudocolloids, in fluids of low ionic concentrations, should not be able to retain absorbed radionuclides for more than a few days. Very small true colloids may be able to migrate rapidly if fracture flow is occurring; however, more experimental work is needed to determine the importance of true colloid transport. Plans for obtaining the additional information required are outlined in Section 8.3.1.3.

One additional mechanism that might allow transport of some radionuclides are microbes (West and McKinley, 1984). Studies measuring the uptake of radionuclides by bacteria and studies determining the mobility and radionuclide transport capability of bacteria in tuff are detailed in Section 8.3.1.3.

Because natural particulate material in ground water at a repository site may be significant as a means of transport of radionuclides by sorption on the particulate material, it is necessary to measure the ambient concentration of such particles. At Yucca Mountain there are no springs or other accessible sources of flowing ground water. Therefore, well J-13, a water well adjacent to Yucca Mountain, was pumped and the water was sampled for particulates by filtering several hundred liters of water through 0.05 micrometer Nuclepore filters, then examining the filters with a scanning electron microscope. An abundance of material was present on the filters, ranging in size from tens of micrometers in diameter down to less than 0.01 micrometer, the resolving power of the microscope. The composition of individual particles varied considerably, although most contained potassium, aluminum, and silicon as major constituents. Filter samples also were obtained from two other wells at the Nevada Test Site, both drawing from an aquifer in alluvial soil. The results of subsequent filter tests were similar to those from well J-13. Because the samples were derived from water flowing in an artifically created gradient, it can be argued that the particulate content is not that of natural water. However, pumped well water may provide a worst-case situation. Future experimental work is planned to determine whether particulates in well J-13 water can sorb a significant amount of dissolved radioactive material and whether these particulates are readily transported through crushed and fractured tuff. Plans for obtaining the additional information required are outlined in Sections 8.3.1.3.4 and 8.3.1.3.6.

4.1.3.6.2 Gaseous transport

A limited number of radionuclides can form volatile species that are capable of being transported in a moving vapor or gas. Among these are tritium, carbon-14, and iodine-129. In the far field, factors that affect transport in flowing ground water also affect transport in flowing gas, (i.e., the velocity of the gas determines the potential for advective transport). In the absence of flow, diffusion is the only mechanism for transport in the gaseous state. The processes of partitioning of the volatile species between the gaseous, liquid, and solid state and isotopic exchange must also be considered when assessing the impact of gaseous transport.

The probability of gaseous transport will be investigated to determine its applicability to Yucca Mountain. Presently, no work is actively being

done on gaseous transport; however, plans for obtaining information required to assess the probability of gaseous transport and the processes of exchange (i.e., gaseous phase and aqueous/solid) are outlined in Section 8.3.1.3.8.

4.1.3.7 Geochemical retardation in the host rock and surrounding units-- anticipated conditions

In the previous sections the principal processes that affect and retard radionuclide transport in ground water were discussed. Through the use and application of numerical models the data on sorption properties, matrix diffusion, flow rates (advection), radioactive decay, colloids speciation, and precipitation and dissolution can be synthesized with numerical models. Numerical models use the data concerning the processes as input and then calculate the total radionuclide transport and retardation through Yucca Mountain.

Currently available computer models can account for most of the known physical and geochemical transport processes (advection, diffusion, dispersion, matrix flow, fracture flow, and equilibrium sorption). More complex geochemical processes, such as speciation, dissolution and precipitation, and colloid formation have only very recently been incorporated into transport models. Plans for refining and improving already developed models, and for developing models that will incorporate all significant processes is outlined in Section 8.3.1.3.7. The development of such models is dependent upon results obtained from Investigations 8.3.1.3.1 through 8.3.1.3.6 and the geohydrology program (Section 8.3.1.2). In turn, the models can be used to interpret results arising from these information needs and to validate the assumption made in constructing the systems models for Information Needs 1.1.4 and 1.6.2; the models may also be useful in establishing the presence of favorable and potentially adverse conditions (Issue 1.8), and making the higher-level findings required by 10 CFR Part 960 (Issue 1.9).

One model that can be used to simulate the transport of radionuclides from the repository to the water table is TRACR3D (Travis, 1984; Perkins et al., 1985). As an example of model calculations under anticipated conditions, the transport of technetium-99 and uranium-238 was calculated (Vaniman, 1987). The processes assumed to affect transport in this example are advection, sorption, dispersion, matrix diffusion, and radioactive decay.

The relative importance of these processes is shown in Figures 4-16a, -16b and 4-17a, -17b. Figures 4-16a and 4-16b show the results of TRACR3D calculations after a 10,000-yr pulse of technetium-99 is introduced into a uniform vertical flow field of (1) 4.5 mm/yr and (2) 0.5 mm/yr. The normalized mass flux entering the water table is plotted against time. The expected flux has been shown to range from 0.1 to 4.5 mm/yr (Montazer and Wilson, 1984). If simple advection is the only transport process operating, the technetium-99 pulse will arrive at the water table without attenuation (the square pulses). Technetium-99 has a long half-life and is only slightly sorbed onto the Yucca Mountain tuffs. Dispersion will be an important attenuating mechanism (by spreading out the pulse and reducing amplitude) followed by matrix diffusion. In the calculations, a dispersivity of 10 cm was used. Comparison of Figures 4-16a and 4-16b show the magnitude of this effect. So
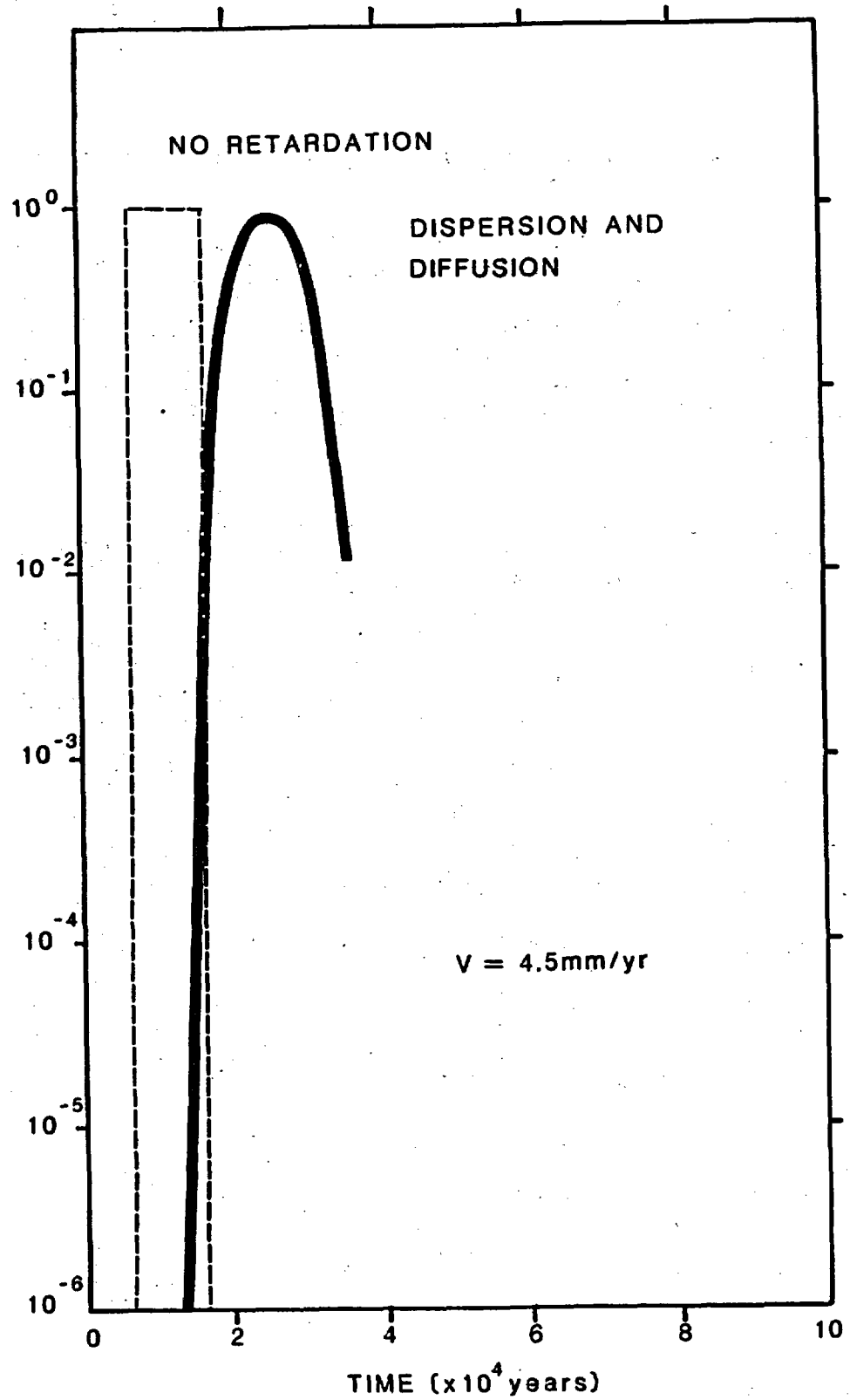
Figure 4-16a. The movement of a 10,000-yr pulse of technetium-99 for V = 4.5 mm/yr. Modified from Vaniman (1987).
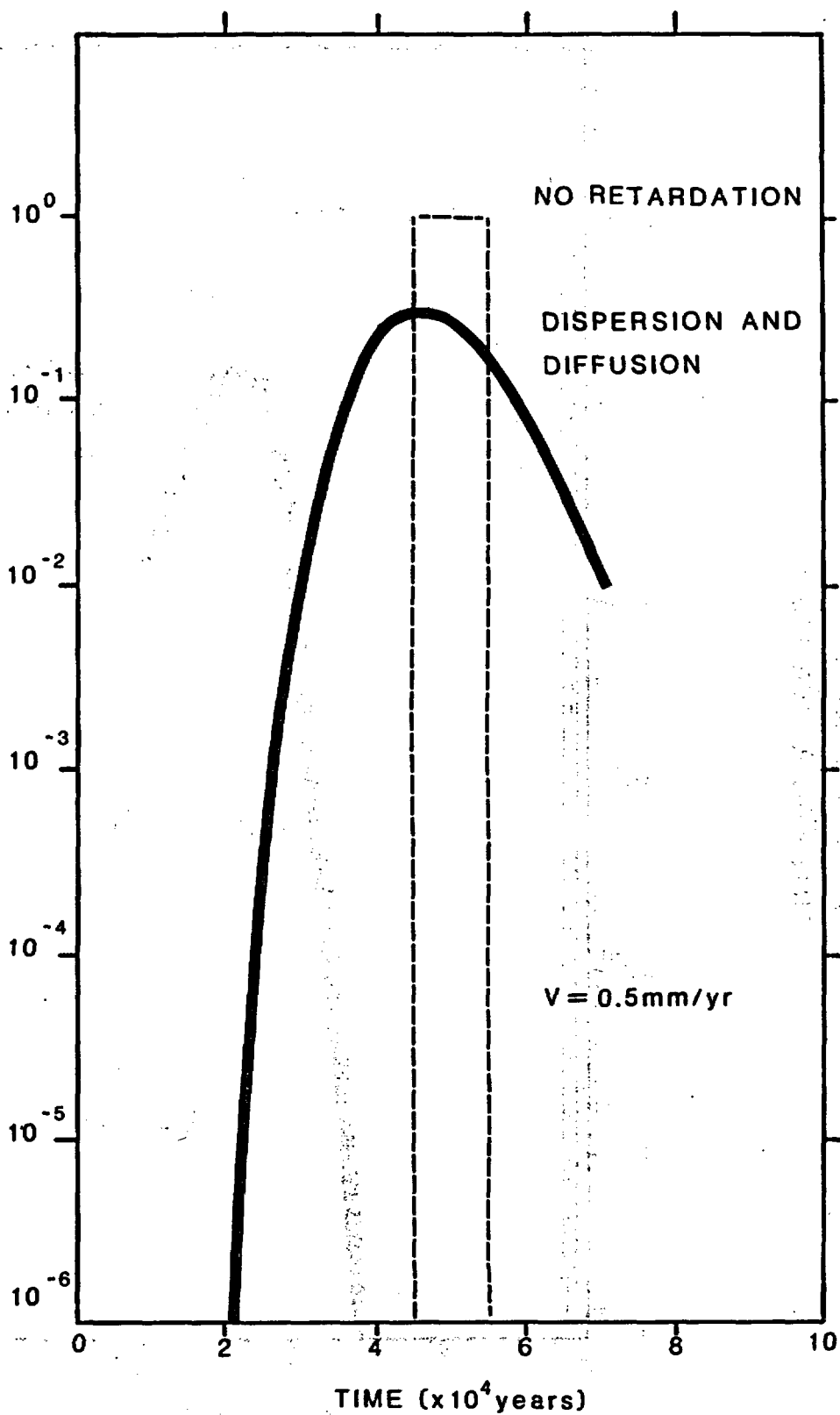
Figure 4-16b. The movement of a 10,000-yr pulse of technetium-99 for V = 0.5 mm/yr. Modified from Vaniman (1987).
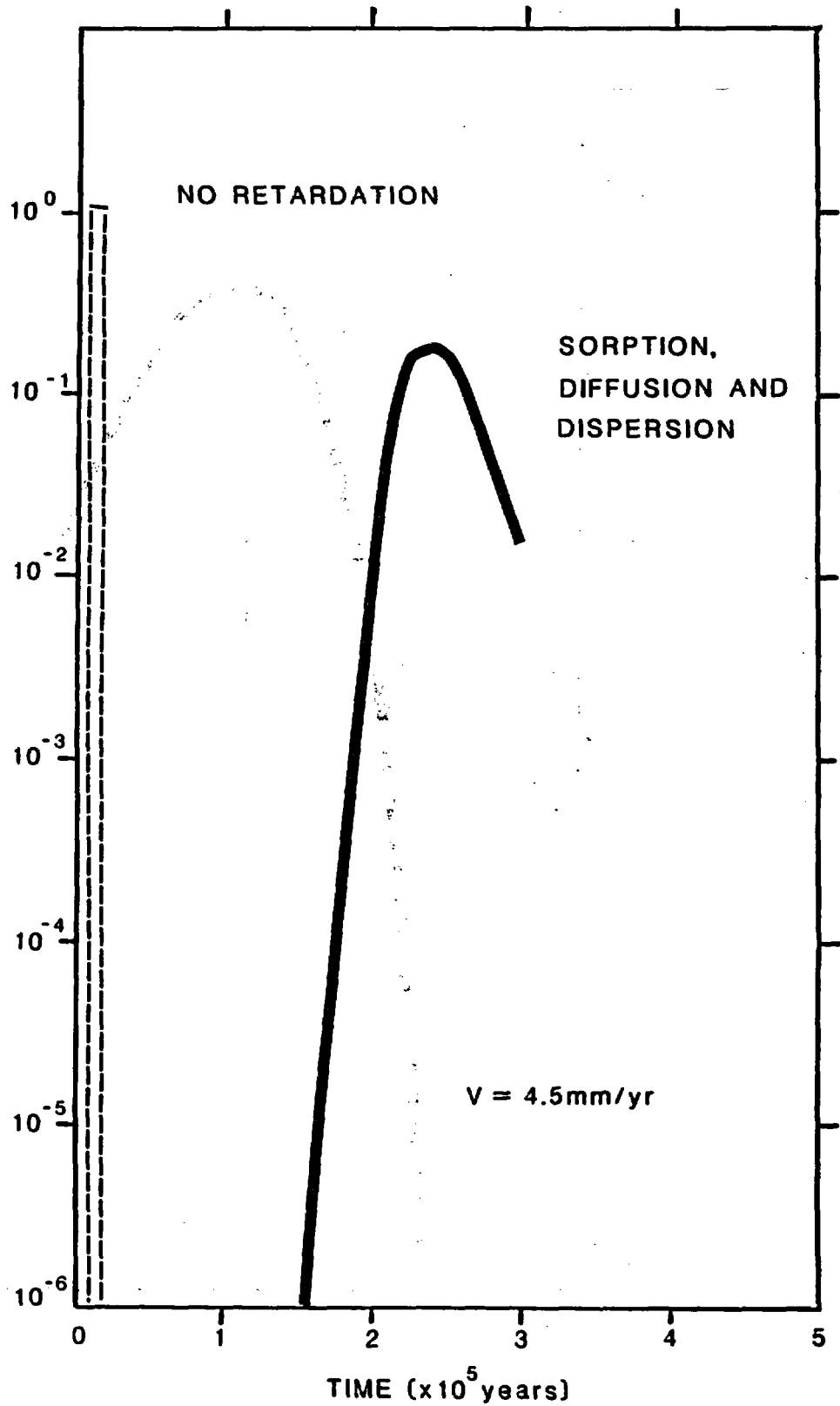
Figure 4-17a.   Uranium-238 normalized mass flux entering water table for V = 4.5 mm/yr. Modified from Vaniman (1987).
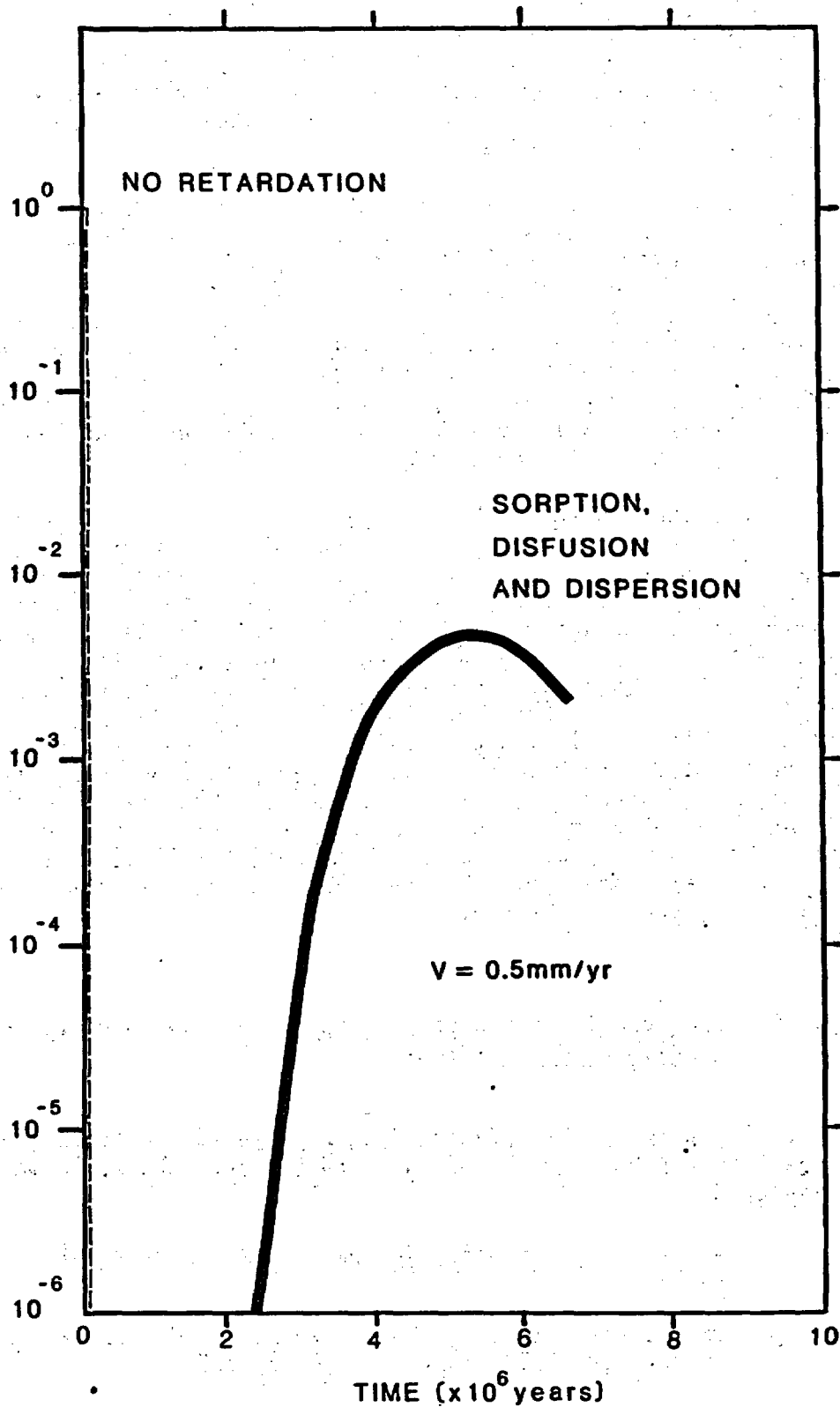
Figure 4-17b. Uranium-238 normalized mass flux entering water table for V = 0.5 mm/yr. Modified from Vaniman (1987).

even where a small dispersivity is used, attenuation occurs. Also, in Figure 4-16b for the case of a slower flow rate, dispersion has a greater effect in attenuating the pulse because of the longer travel time. Therefore, for a conservative, nonsorbing radionuclide such as technetium-99, a slower flow rate will result in a longer travel time to the water table and a more attenuated, broadened pulse.

Figures 4-17a and 4-17b show the effects of sorption, dispersion, and diffusion on the transport of uranium-238. Again a 10,000-yr pulse is introduced in a uniform vertical flow field of (1) 4.5 mm/yr and (2) 0.5 mm/yr. Uranium-238 adsorbs readily to the Yucca Mountain tuffs. In Figure 4-17a, with the larger flow rate, sorption, dispersion, and diffusion act to delay the arrival of the peak by a factor of 10 and decrease the peak concentration by almost a factor of 10. When the flow rate is decreased as in Figure 4-17b, sorption, dispersion, and diffusion act to delay the arrival of the peak to the water table by a factor of 200 and decrease the peak concentration by more than a factor of 100.

It has been shown in this example calculation that under anticipated conditions the combined processes of sorption, dispersion, and diffusion have a significant effect on the transport of sorbing and nonsorbing radionuclides. Therefore, it is extremely important that these processes and their relative parameter values are well-defined. As the processes and their relative parameter values become updated more calculations similar to the examples given above will be done to investigate the sensitivity of radionuclide transport to sorption, dispersion, and diffusion as outlined in Section 8.3.1.3.7. The investigation into the sensitivity of radionuclide transport calculations to speciation, precipitation/dissolution, and colloid formation is planned and outlined in Section 8.3.1.3.7. Estimates of total radionuclide releases to the accessible environment based on transport calculations can only be completed after the sensitivity of radionuclide transport to geochemical processes is better known and more information concerning parameter values is obtained.

4.1.3.8 Geochemical retardation in the host rock and surrounding units-- unanticipated conditions

To investigate the effects of unanticipated events on geochemical retardation into the hiost rock and surrounding units the following questions must be answered:

1. What is the potential for and likely magnitude of the unanticipated events?

2. What is the effect of these unanticipated events on such processes as sorption, diffusion, and dispersion?

3. What is the impact on the overall integrated transport due to the changes in the transport processes?

Examples of unanticipated events are an increase in water-transmission rates, changes in the water chemistry, changes in the water table, transformations of zeolites and clays to less sorptive minerals, and changes in permeability. Plans for obtaining the additional information required to determine the effects of these and other unanticipated conditions on transport processes are outlined in Section 8.3.1.3.

An example is given below to illustrate the interactions between the unanticipated condition, the effect on transport processes, and the effect on radionuclide migration. Preliminary calculations have been conducted to investigate the effect of an increase in water transmission rates on radionuclide transport. An increase in water transmission rate could occur, for example, from increased precipitation or by an elevation of the water table.

An increase in the water-transmission rate might result in fracture flow in the unsaturated zone, but in the absence of fractures, flow and transport will be diffusive. At the recharge rate in Yucca Mountain of a few millimeters per year (assuming current climatic conditions), radionuclides would not reach the water table via vertical porous flow for roughly 10,000 to 20,000 yr or more after the release (Travis et al., 1984). Computer simulations of transport in simple fracture systems using extreme values for flow rates (full saturated permeability applied constantly rather than intermittently) show that to get a travel time of less than 10,000 yr requires a water flux at least 100 times greater than the present water flux (Travis et al., 1984).

For radionuclide transport through fractures, more information is needed on fracture flow in Yucca Mountain tuffs. For example, additional information is needed to establish whether the recharge water moves vertically through unfractured layers and then enters fractures, or if water moves through fractures as a film on the fracture surface or as a pulse fully saturating the fracture. Film flow would be very much slower than slug flow (Travis et al., 1984). Plans for obtaining this information are outlined in Section 8.3.1.3.6.

Other factors that cannot be evaluated at present because of the lack of data are the connectivity of fractures and the dimensions of fracture apertures. If fractures are present but not connected or intersecting, their impact on flow and transport will be greatly diminished. If fractures are a connected network, the path that a water slug will travel will probably be tortuous and might involve branching into cracks in other directions. In regard to the dimensions of apertures, fracture flow depends on fracture permeability, which varies roughly as the cube of the aperture, a strong sensitivity. Plans for obtaining the required information about fracture aperture and fracture permeability are outlined in Section 8.3.1.3.6, and plans for obtaining such information for a hydrologic model are given in Section 8.3.1.4.

Given fracture flow, the contaminant will diffuse into the pore spaces of the rock. Because of this diffusion into the matrix, the effective flow rate for radionuclides must be modified (Sudicky and Frind, 1982). The modification introduces a retardation factor due to a matrix diffusion from fractures. One can then calculate an equivalent retardation value, applicable only when fracture flow is occurring, combining retardation through

sorption with retardation through diffusion. The calculated equivalent retardation factors are a factor of 10 to 100 larger than those retardation factors based on sorption alone (Travis et al., 1984).

From the preceding discussion it is evident that a change in one condition such as the water-transmission rate leads to a change in flow characteristics. The characteristics of the flow in turn will affect retardation processes such as sorption and finally the overall retardation. Plans for obtaining the impact on the overall, integrated transport due to the changes in the transport processes are outlined in Section 8.3.1.3.7.

Factors that may affect radionuclide transport include: (1) fracture fill, (2) nonequilibrium sorption, (3) radionuclide sorption in fractures, (4) colloid transport, and (5) geometric dispersion. Plans for obtaining this information are outlined in Section 8.3.1.3.

4.2 GEOCHEMICAL EFFECTS OF WASTE EMPLACEMENT

The thermal pulse from waste emplacement and its effects on water displacements and geochemistry must be characterized for intervals extending tens of meters away from the waste containers emplaced in a repository. Discussions of the interactions within the engineered barrier system are presented in Chapter 7.

This section describes the time-dependent temperature profiles for a reference repository in unsaturated devitrified tuff, with the attendant phenomena of drying near the waste containers and water condensation at boundaries that move inward as the thermal pulse from waste emplacement decays. Also discussed is the possible hydrothermal alteration due to the thermal pulse--a prospect that is not critical to the devitrified host rock but may be important to the hydrous alteration minerals and glasses beneath the host rock. Desiccation and rehydration of the hydrous alteration minerals, as well as other phase transitions that may affect permeability, rock strength, and radionuclide retardation, must be studied as well. Water chemistry as a function of temperature must also be known; therefore, an assessment of thermal effects on unsaturated-zone pore water and on recharge water is important. Finally, this section discusses the thermal dependence of factors important on constraining radionuclide migration--namely, sorption, precipitation, dispersion, diffusion, and advection on unsaturated tuff.

4.2.1 ANTICIPATED THERMAL CONDITIONS RESULTING FROM WASTE EMPLACEMENT

This section discusses the impact of expected thermal conditions resulting from waste emplacement. Waste emplacement leads to heat buildup due to radioactive decay. This heat influences the rate of the waste container degradation, and the compositions of the surrounding tuff due to hydrologic changes.

The magnitude of the effects resulting from the thermal pulse depends on (1) heat content of the waste, (2) rate of decay of the waste, (3) amount of pore water, (4) effective permeability of the tuff, (5) waste emplacement geometry, and (6) presence or absence of venting. These factors are discussed in detail in Section 7.4.1. However, time-temperature calculations described in the sources only extend out to 1 m from the borehole wall.

The following is an example of the type of calculation that can be done to investigate the qualitative behavior of the anticipated thermal conditions resulting from waste emplacement. Preliminary numerical calculations using a flow and transport code (WAFE) that incorporates a thermal component (Travis, 1985) have been made. Using a heat load of 50 kW/acre, Figure 4-18 shows a fluid temperature profile around a 2 by 6 m room after 50 yr. The absolute numbers shown should be considered preliminary because of the uncertainties in the rock property values. However, in these calculations, as heat diffuses away from the source, water vaporizes. The water vapor is then driven outward until it reaches cooler rock and then condenses. Temperatures are buffered by the boiling process because energy is going into vaporizing water rather than raising the rock temperature. Peak temperatures at the wet edge of the boiling region are only about 140°C, considerably lower than peak waste temperature. After a century or so, temperature and saturation profiles decay back to ambient. A temperature increase of 5°C or more extends to at least 30 m (Travis et al., 1984).

This same heat loading or thermal scenario can in turn influence the rate of breakdown of the waste container. For example, if heat loading were to cause vaporization of pore water near each container, the atmosphere surrounding a container could change from wet air to a dry-steam, oxygen-poor atmosphere, which would affect the degradation of the container. The problem is discussed in Section 7.4.

The presence of fractures in the rock can alter the thermally induced flow patterns and make the interpretation of the effects of anticipated thermal conditions on the natural environment more complicated. Many small cracks will increase the overall permeability, making a convective or circulating flow pattern more likely. However, few large cracks that promote conduction may prevent convective circulation, and more likely provide a path for a fairly rapid movement of water, vapor, and air. Other factors could also be important, such as the thermomechanical behavior of cracks. Heat may close cracks or open them depending on the mechanical properties of the host rock. Plans for obtaining the additional results on these scenarios are outlined in Section 8.3.1.3.7.

The sections that follow discuss the effects of the thermal pulse on rock alteration, water chemistry, and radionuclide retardation. As future experimental results are obtained, the data below will be updated. Plans for obtaining the information required for evaluating anticipated thermal conditions are outlined in Section 8.3.1.3.
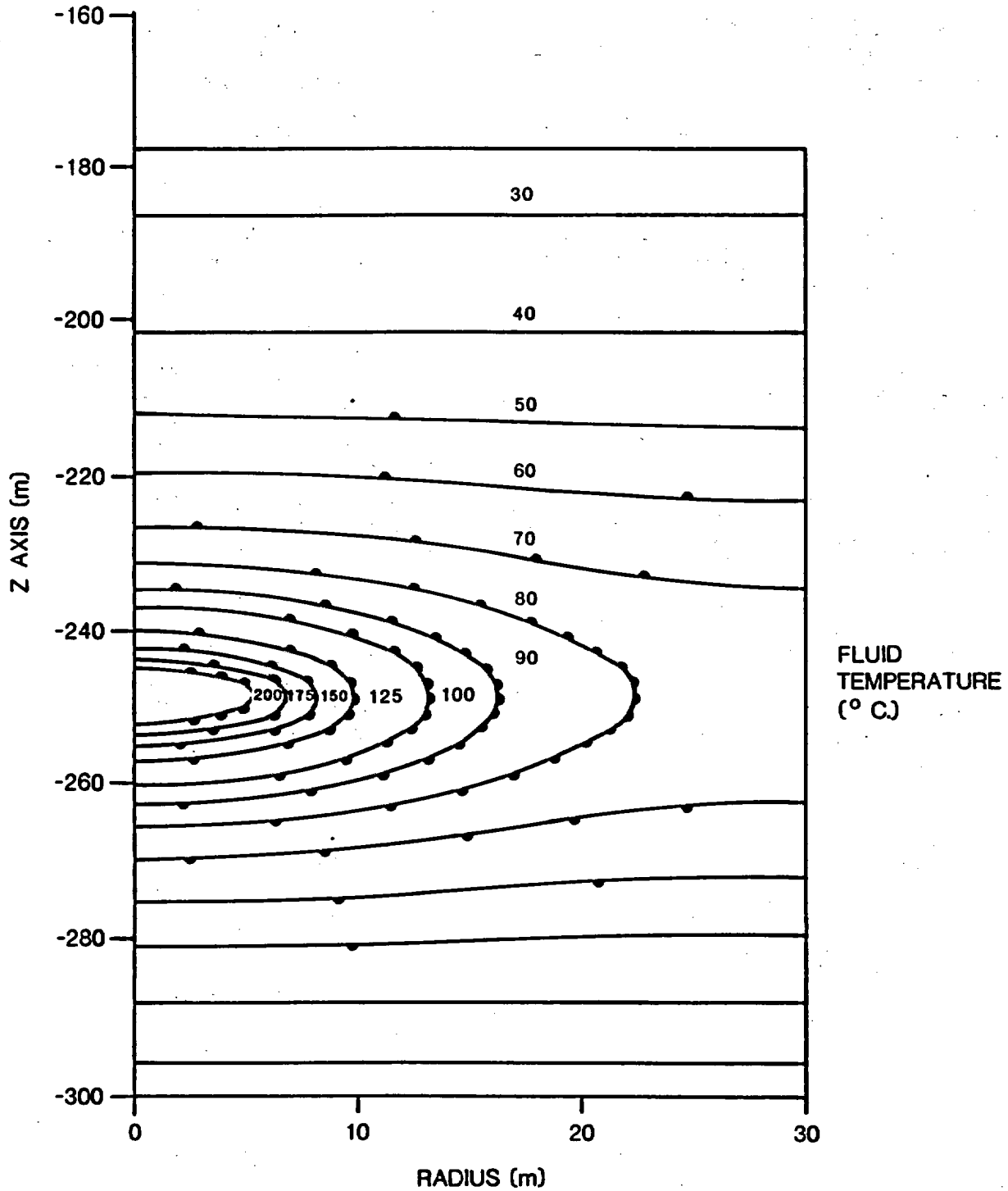
Figure 4-18. Fluid temperature profile showing temperature contours 50 yr after emplacement of a 50 kw/acre heat load using the WAFE code. Dots generated by plotter indicate the direction of the gradient. Modified from Travis et al. (1984)

4.2.2 HYDROTHERMAL ALTERATION DUE TO THE THERMAL PULSE

Flow paths near the repository will pass through a zone in which temperatures are elevated above the ambient geothermal gradient. The elevated geothermal gradient may give rise to temperature-induced reactions that have the potential for altering various chemical and physical properties of the rocks in Yucca Mountain. In the repository environment, little alteration is anticipated among the abundant devitrified silica minerals and alkali feldspars because they are anhydrous and stable to high temperatures. Cristobalite may transform to quartz with about a 12-percent volume decrease. Opal may also dehydrate, with a comparable loss in volume. The abundances of cristobalite and opal range from 0 to 30 percent, indicating maximum whole-rock volume decreases can be expected to be less than 4 percent. The thermal influence of the repository, however, may extend to regions where zeolites, smectites, and glasses are abundant. The hydrous phases have much lower thermal stabilities and can be affected by a temperature rise of tens of degrees Celsius. Two major effects of temperature on the hydrous phase are contraction due to water loss and the alteration of sorptive minerals to minerals that are less sorptive.

When tuff that contains hydrous phases is heated, various processes may occur. A reversible dehydration of smectites and zeolites involving significant volume reductions (Bish, 1981; Bish, 1984) may possibly reduce rock strength and alter permeability. Irreversible dehydration of smectites, zeolites, and volcanic glass reduces both volume and cation exchange capacity. Glass devitrification is of particular interest because of the proximity of the host rock to the vitrophyre in the lower Topopah Spring Member and to the nonwelded, nonzeolitized tuffs at the base of the Topopah Spring Member and in the underlying tuffs of Calico Hills in the southern portion of the Yucca Mountain exploration block. Alteration of glass may have four important effects: (1) changing the volume, causing changes in rock property such as permeability; (2) maintaining a high silica activity; (3) raising the pH of acidic water; and (4) forming sorptive secondary phases like smectite and zeolites (Kerrisk, 1983). Finally, the alteration of minerals to less-sorptive phases (i.e., the alteration of clinoptilolite to analcime) can affect the zeolitic rocks influenced by the heat of the repository (Bish et al., 1982; Bish, 1987).

Since mineral reactions at repository temperatures may occur at rates comparable to the isolation period (thousands of years), an understanding of kinetics is also important. Also, because many of the effects of elevated temperatures on hydrous minerals result from mineral dehydration, the effect of the partial pressure of water on the dehydration reactions must be known in order to predict the differences between unsaturated-zone and saturated-zone mineral dehydration. The plans for obtaining information about these processes are outlined in Section 8.3.1.3.

4.2.2.1 Hydrothermal alteration of zeolites

Data on the kinetics of zeolite reactions at slightly elevated temperatures are very limited because of experimental difficulties; reactions occur very slowly at temperatures below 200°C. Hydrothermal experiments have been

conducted on zeolitic, vitric, and welded tuff at temperatures of 80 to 180°C (the temperatures necessary to make observable changes in short times) for several weeks to several months (Daniels et al., 1982; Knauss and Beiriger, 1984; Blacic et al., 1986). The results of the experiments pertinent to the near-field environment are discussed in Section 7.4.1.3; some zeolites have been formed during the experiments but the products require further characterization.

Assuming a water composition similar to well J-13 water, the geologic data from the deeper portions of drillholes in Yucca Mountain and the experimental data described by Smyth and Caporuscio (1981) indicate that reaction of clinoptilolite to analcime will occur above 85°C in the tuffaceous beds of Calico Hills, although silica activity may more directly control the reaction than temperature (Section 4.1.1.4).

Although the clinoptilolite-to-analcime reaction is not anticipated in most zeolitic tuffs, experiments in progress suggest that water loss with volume decrease (up to 10 percent) in clinoptilolite will begin below 50°C when the water-vapor pressure is low. The volume loss could occur in the first major zeolite horizon under the thermal influence of the waste emplaced in the repository. The opening of new flow paths in a zeolite horizon barrier is possible, but they will probably expand again and close during rehydration. The effects of temperature on number of natural clinoptilolites and sodium-, calcium-, and potassium-exchanged clinoptilolites have been examined by x-ray powder diffraction (Bish, 1984). The molar volumes of all clinoptilolites decreased, with sodium-clinoptilolite undergoing the greatest decrease and potassium-clinoptilolite undergoing the least. Calcium-clinoptilolite and the natural clinoptilolite samples underwent intermediate decreases in volume. Most of the volume contraction in most samples occurred on evacuation at room temperature, demonstrating the strong effect of water-vapor pressure upon dehydration. Samples heated under 1-atm water-vapor pressure underwent significantly less volume decrease at a given temperature than those heated in ambient air or in a vacuum. All samples showed the ability to rehydrate upon cooling.

The data of Bish (1984) show that heat effects on volume change of clinoptilolite are strongly related to the exchangeable-cation content. The volumes of natural, mixed sodium-potassium-calcium clinoptilolites in rocks could be reduced in a repository environment, particularly if the clinoptilolites occur in the rock being dehydrated by the thermal pulse. However, tests now in progress suggest that clinoptilolites occurring in partially saturated rocks at temperatures below 100°C should not decrease in volume. Thermogravimetric and differential scanning calorimetric experiments on natural and cation-exchanged clinoptilolites also demonstrate the strong dependence of dehydration on exchangeable-cation composition (Bish, 1985). The results show that clinoptilolites can yield water on heating and rehydrate on cooling if the dehydration process is reversible after long-term heating (more than 1 yr). The volume decreases observed for clinoptilolite were completely reversible over short heating periods (less than 1 week). However, long-term heating of clinoptilolite can cause modifications, including irreversible collapse and reduction in cation-exchange capacity. Sodium-rich clinoptilolites are most susceptible to large volume reductions and exchange-capacity modifications, and they can alter to a phase analogous to heulandite-B. Further experiments are examining both the dependence of

dehydration temperature on water vapor pressure and the possibility of irreversible dehydration at 100°C (Section 8.3.1.3).

4.2.2.2 Hydrothermal alteration of smectites

Although smectites are not as abundant as zeolites, they occur in small amounts in virtually all core samples from Yucca Mountain examined to date (Bish et al., 1982). The smectites are important to radionuclide retardation because they selectively sorb certain cations (cesium, strontium, barium, and some actinides) (Section 4.1.3.3). Bish (1981) reviewed the effects of changes in relative humidity and temperature on smectites and noted that decreases in ambient humidity alone can cause dehydration and large decreases in volume when the ambient humidity drops below 20 to 50 percent. Smectites typically undergo reversible crystal structure collapse with attendant volume decrease at about 100°C with humidities of less than 100 percent. However, Koster van Groos and Guggenheim (1984, 1986) showed for Na- and K-montmorillonite that an increase in water pressure significantly raises the temperature of dehydration and layer collapse. Thus, collapse as a result of dehydration will probably be unimportant except where temperatures are high and the partial pressure of water is low. Smectites will remain in an expanded state along the flow paths in the saturated zone where the clays will not be dehydrated. An expanded state may not, however, be the case for clays exposed to a steam environment; the ability of bentonite to swell osmotically has been shown to be greatly reduced after exposure to a steam environment (Couture, 1985).

With increasing temperature over extended times under unsaturated conditions such as those predicted for the near field, smectite dehydration and collapse become irreversible (MacEwan, 1972; Bish et al., 1982). Once the smectite layers have irreversibly collapsed, their sorption capacity is greatly decreased, although selectivity for cesium is dramatically increased (Bish et al., 1982). The dehydration reaction is very likely controlled by the diffusion of the interlayer cation into the silicate layers and can occur over short periods at temperatures as low as 150°C. However, the actual dehydration temperature for any given smectite is controlled by interlayer cation composition and kinetics and can be as high as 500°C under unsaturated conditions in the presence of large divalent cations (Bish et al., 1982). Experiments are under way to determine whether the kinetics of the irreversible-collapse reaction are fast enough for the reaction to be important in the thermally disturbed zone (Section 8.3.1.3.3). If smectites do collapse irreversibly in the thermally disturbed zone near the repository, the consequence could alter the physical properties of the rocks and decrease the cation exchange capacity in the near field. The effects should be on the very near field, and rocks farther along the flow paths will retain their expandability and sorptive capacity.

4.2.2.3 Hydrothermal alteration of rhyolitic glasses

Data in the literature indicate that volcanic glass naturally alters to zeolites, but the phases resulting from this alteration depend greatly on the

glass and the ground-water composition (Hay, 1978). Moreover, the alteration of glass to smectite is suggested by the smectites that occur in perlitic fractures in the basal vitrophyre of the Topopah Spring Member and supported by reaction-path modeling (Kerrisk, 1983). The alteration of glass to smectites or zeolites increases the sorptive capacity of the rock; this would be beneficial along flow paths. Alteration of glass to nonhydrous phases will probably lower the permeability along flow paths but the overall sorptive capacity along the flow path will not be significantly affected. The vitrophyre underlying the host rock contains approximately 3.5 percent water, and dehydration or recrystallization of the vitrophyre could produce significant amounts of water. The vitrophyre is also one of the few sources of reduced iron in Yucca Mountain, although it is doubtful whether the small amounts of ferrous iron available would result in less oxidizing conditions which could enhance actinide retardation (Caporuscio and Vaniman, 1985). Plans for further investigation of these topics are given in Sections 8.3.1.3.2 and 8.3.1.3.3.

4.2.3 CHANGES IN WATER CHEMISTRY DUE TO THE THERMAL PULSE

The heating of fluids in and adjacent to the repository will cause increased reaction with the host rock, changing the compositions of both. Experimental results on the interaction of well J-13 water with crushed and solid samples of devitrified Topopah Spring tuff at 90, 150, and 250°C are discussed in Section 7.4.1.3. Briefly, tests at 150°C for 66 days showed changes from 0.01 to 0.5 parts per million (ppm) for aluminum, from 38 to about 120 ppm for silicon, from 12 to 6 ppm for calcium, from 1.9 to near 0 ppm for magnesium, from 5.1 to 4.4 ppm for potassium, and a pH change from 7.1 to 6.8. The concentrations of sodium ion, fluoride, chloride, nitrate, and sulfate showed no significant changes. The dissolved-carbonate content decreased slightly. These changes were associated with the appearance of secondary phases, including a potassium-rich clay or zeolite; clays rich in magnesium, calcium, and/or iron gibbsite; calcite; and a pure silicon dioxide phase (possibly cristobalite). The total amount of secondary phases was quite small, with clay being dominant. Tests run at 90°C showed only minor changes in water composition for durations of 66- and 300-days.

The modeling of hydrothermal reactions with the EQ3/6 reaction-path code is also reported in Section 7.4.1.3. This code, unlike the experiments, allows the modeling of open system behavior. Open system behavior is expected at least for gases such as carbon dioxide in the unsaturated zone in Yucca Mountain. The results of modeling the interaction of Topopah Spring tuff with well J-13 water at 150°C over long reaction times are shown in Table 7-10. The differences between the long-term open-system model and the short-term experiments are as follows: (1) the degassing of carbon dioxide with a concomitant change in pH, (2) very high aluminum concentrations, (3) higher sodium concentrations, and (4) very low calcium and dissolved carbon concentrations in the model. The modeling results could be improved with the following: (1) better data on dissolution kinetics, (2) more data on precipitation kinetics, (3) better high-temperature data on aluminum hydroxide complexes, and (4) experimental data on the reaction of tuff with water in the presence of gamma radiation. Plans for obtaining the needed

data on hydrothermal interactions are outlined in Section 8.3.4.2 and
Section 8.3.1.3.

4.2.4 EFFECTS OF THE THERMAL PULSE ON RADIONUCLIDE MIGRATION

The preceeding sections discussed the anticipated thermal conditions,
the hydrothermal alteration due to a thermal pulse, and the effects of the
thermal pulse on ground-water chemistry. To date little work has been done
on investigating the effects of the thermal pulse on overall radionuclide
migration. To affect radionuclide migration the thermal pulse must alter the
characteristics of the host rock which in turn would alter the character-
istics of the transport processes, such as matrix diffusion, colloid form-
ation, and advection (e.g., matrix flow, fracture flow).

One preliminary investigation into the effects of the thermal pulse on
radionuclide migration has shown that silica mobility and redistribution is
expected. A heat alteration study described by Daniels et al. (1982) reports
that, particularly for the vitrophyre (G1-1292), a great amount of silica was
dissolved at elevated temperatures (152°C) and then was precipitated upon
cooling globules analyzed as pure SiO_2. In addition, greatly increased
amounts of clays or other fine grained sheet silicates were deposited on
glass edges (examined by scanning electron microscope). The placement of
waste containers will lead to the development of a temperature gradient in
the surrounding host rock which will induce a solubility gradient. If water
also flows, silica will be redistributed and depending on the magnitude and
duration of the heat-induced flow, silica may accumulate in cooler regions.
This deposition will result in reduced pore size which subsequently will
lower permeability. A region of reduced permeability around a waste con-
tainer will tend to isolate the container from infiltrating water. Thus the
infiltrating water will be deflected away from the container, thereby
reducing the transport of radionuclides from the waste container.

The scenario described above was qualitatively investigated by a
numerical study (Travis and Nuttall, 1987) with the WAFE computer code. The
WAFE code (Travis, 1985) can calculate heat and mass transport in porous
media. Silica and chloride were included in the study. The inclusion of
chloride is conservative because it does not adsorb and is not present, to
any significant extent, in tuff minerals; thus, its potential source is from
the surface. With an initial buildup of the pressure and temperature, the
results of the study predicted an outward migration of silica. A narrow
elevated saturation region developed with silica dissolving in a region near
the container and migrating outward where it precipitated upon reaching a
cooler environment. Some silica returned to the initially hot region, but a
net outward flux of dissolved silica occurred. Figures 4-19 and 4-20 show
the calculated transient dissolved silica concentration distribution and the
total (dissolved and precipitated) silica concentration distribution at 10
and 100 yr. Note that in Figure 4-19 there is a zone of no dissolved silica
where x = 4 m. This corresponds to a region where the silica has precipi-
tated. The sum of the dissolved and the precipitated silica is responsible
for the peaks shown in Figure 4-20.
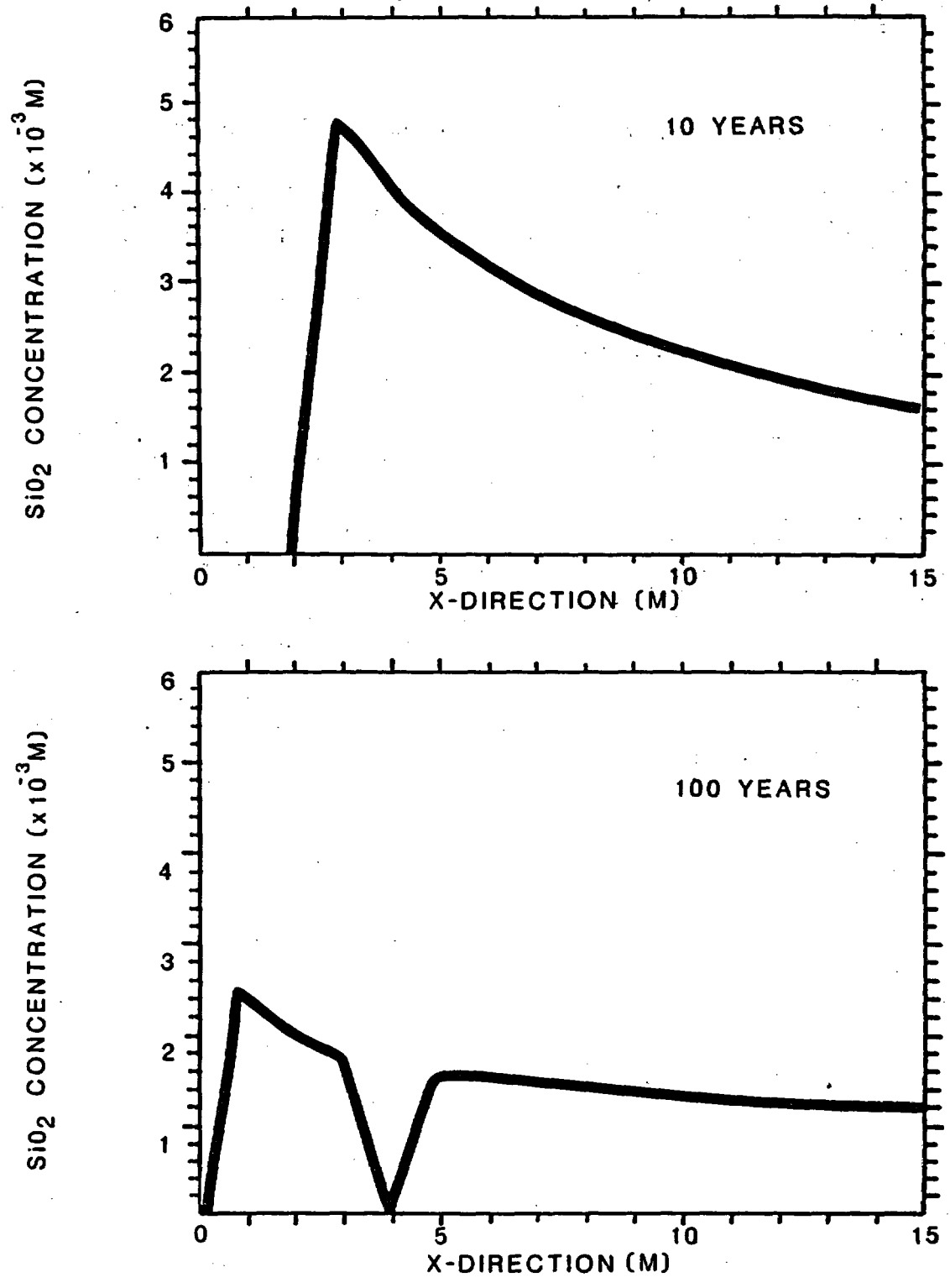
Figure 4-19.   Calculated dissolved silicon dioxide distribution at selected times. Modified from Travis and Nuttall (1987).
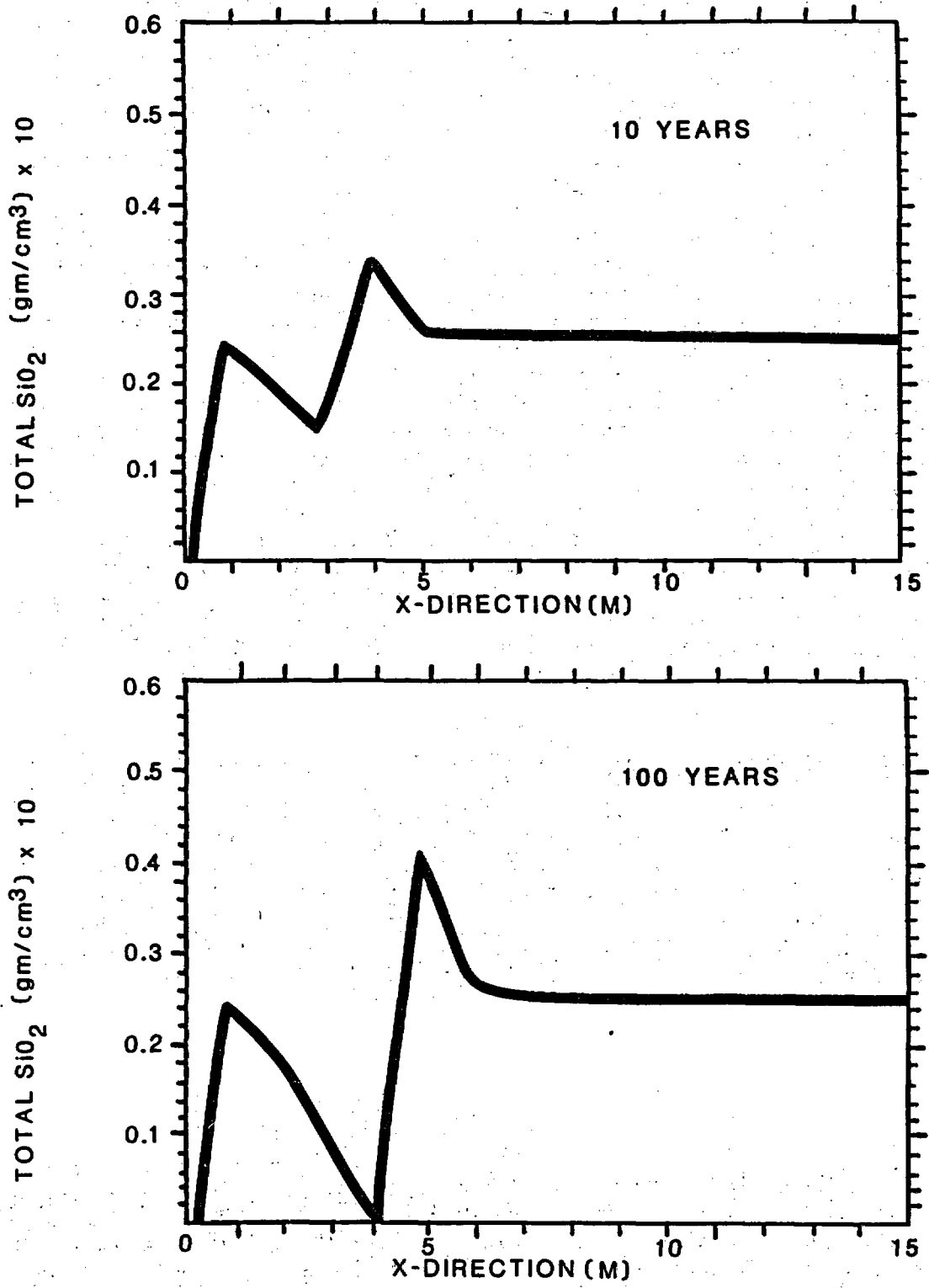
Figure 4-20. Calculated total silicon dioxide (dissolved and precipitated) at selected times. Modified from Travis and Nuttall (1987).

Figure 4-21 shows the calculated distribution for the transient chloride concentration. Initially, the chloride concentration increases in the hottest region because of a decrease in water saturation from a loss of water through vaporization. The concentration of chloride in the higher saturation region decreases because of the addition of liquid water as the vapor condenses. The chloride concentration is a minimum where x = 4 m. This region corresponds to a region of elevated saturation. As the saturation returns to ambient levels, so, too, does the chloride concentration profile.

Significant changes in the amount of dissolved or precipitated silica can lead to large permeability changes. Assuming that permeability is related to the pore diameters and that a silica precipitate will coat pore walls uniformly, then permeability change as a function of porosity change can be calculated (Travis and Nuttall, 1987). Figure 4-22 shows the permeability change predicted for the end of the heat decay period by the WAFE calculation. The silica-precipitate distribution leads to an elevated-permeability region close to the container and a reduced-permeability region immediately outside the elevated-permeability region. Both of these regions are only a few centimeters thick. The outer reduced permeability shell will tend to deflect the downward-flowing water away from the container region rather than through the region. In addition, the inner elevated permeability ring will tend to channel water that had penetrated the low permeability shell, also around the container rather than through it. By reducing the amount of available water, the amount of radionuclides dissolved and transported will be decreased. The exact magnitude of this effect depends on the details of the hydrologic behavior of the host rock, and, in particular, on the presence or absence of fractures.

The numerical calculation of Travis and Nuttall (1987), summarized above, did not treat the full complexity of the water composition and reactions. Instead, the calculations were simplified by considering only silica dissolution, transport, and precipitation. As the potential hydrologic behavior of the Topopah Spring Member is better estimated (Section 8.3.1.2), the information concerning the presence or absence of fractures is obtained (Section 8.3.1.2), and as the ground-water transport models are further developed (Section 8.3.1.3.7), the effects of thermal pulses on radionuclide migration due to all significant changes in transport processes will be further investigated (Section 8.3.1.3.7).

4.3 NATURAL ANALOGS AND RELATED FIELD TESTS

The long period of time over which a repository must provide waste isolation and the large volume of rock present between a repository and the accessible environment pose particularly difficult problems in the prediction and assessment of repository performance. Although laboratory studies provide data on fundamental chemical and physical processes, modeling of the total repository system will require the extrapolation of these data in space and time. However, the study of natural systems possessing one or more features that mimic critical parts of a repository environment may provide
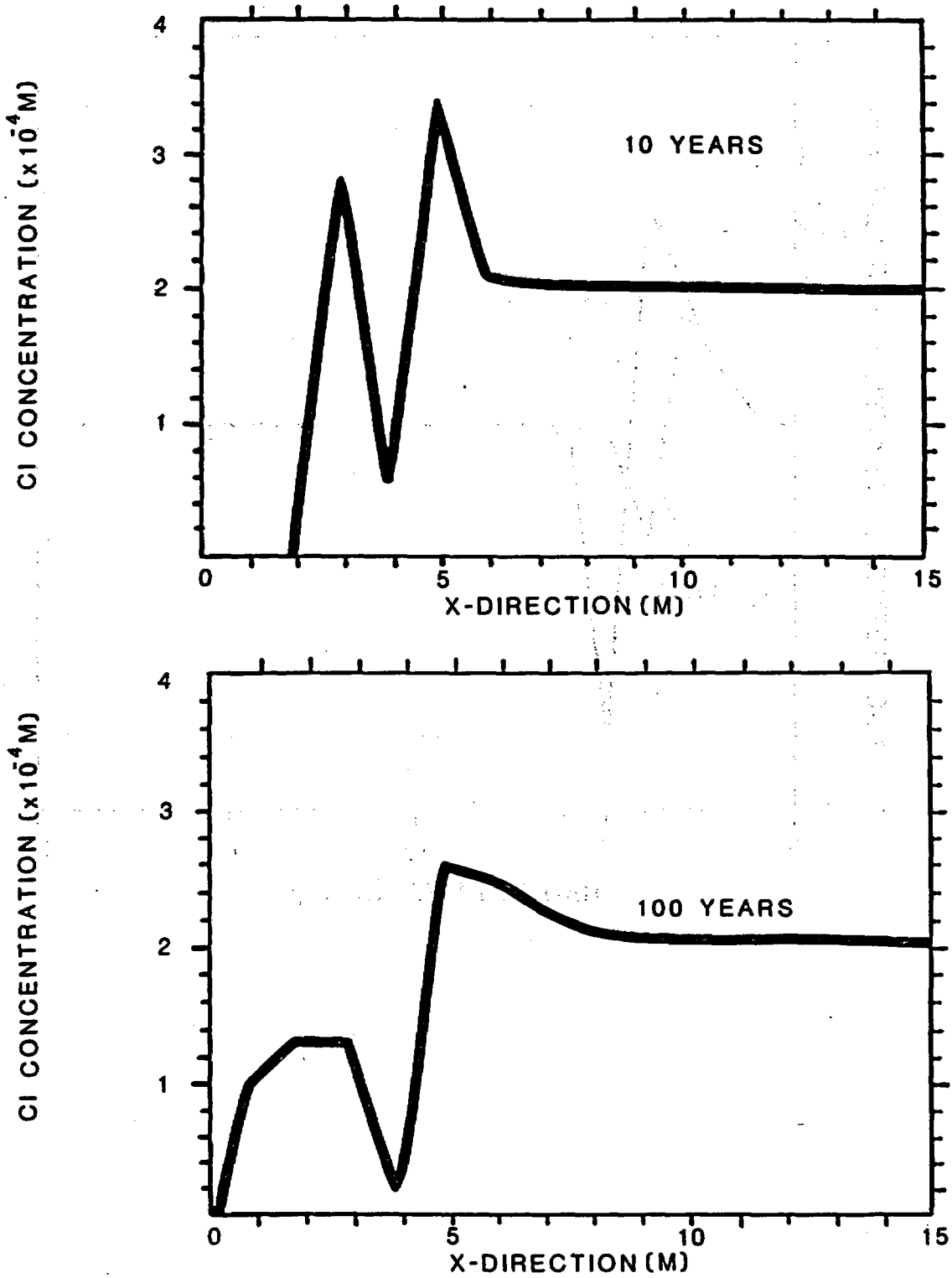
Figure 4-21. Calculated chloride distribution at selected times. Modified from Travis and Nuttall (1987).
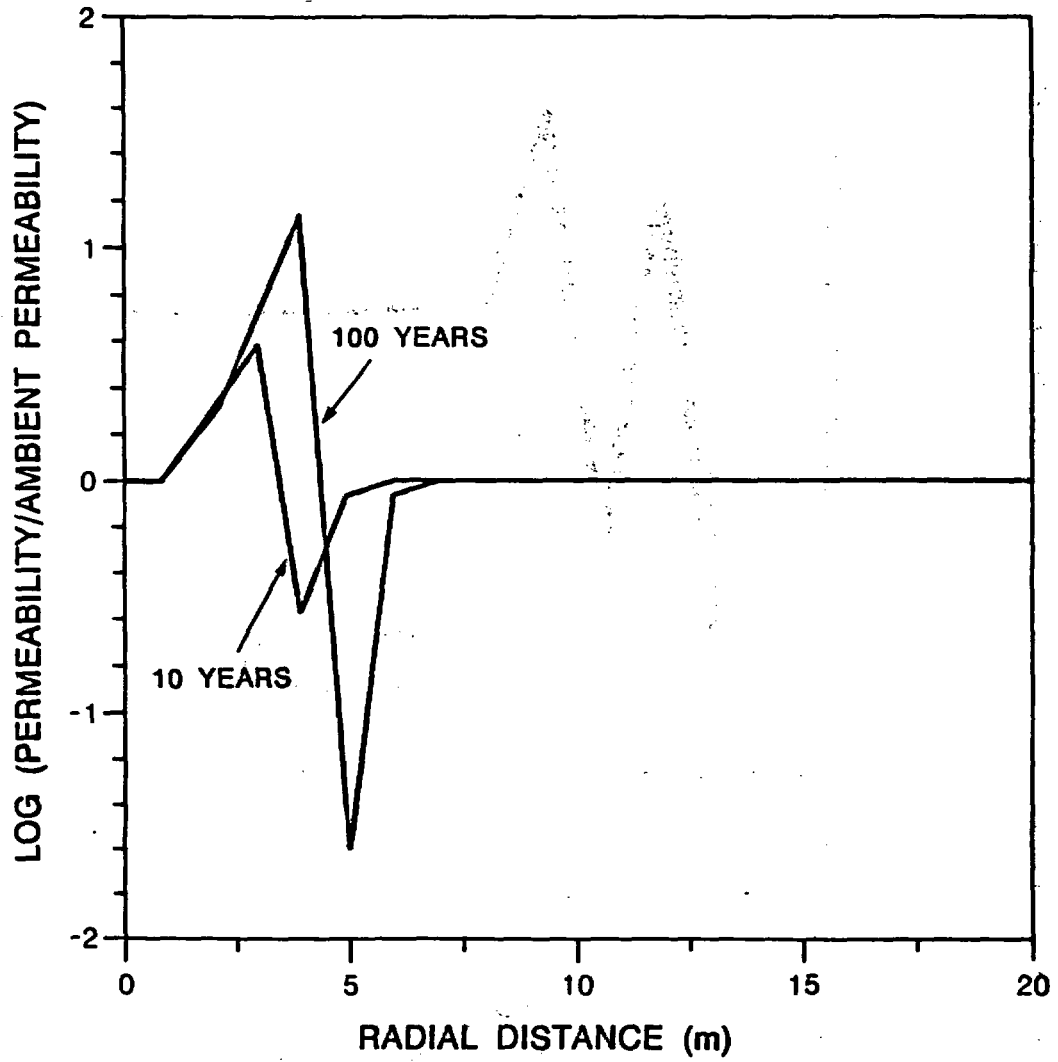
Figure 4-22. Calculated permeability assuming relationships between pore volume and permeability. Modified from Travis and Nuttall (1987).

additional confidence in the required extrapolations. This section describes natural analogs and related field tests that possess these attributes.

4.3.1 NATURAL ANALOGS

Although there are no natural systems available for study that are totally analogous to a repository environment, the following systems possess features that are pertinent to a repository in tuff: (1) warm and hot springs in tuffaceous rocks, and (2) uranium and thorium ore bodies and their host rocks. Only a small group of potentially analogous sites are discussed in this section.

4.3.1.1 Warm and hot springs

The study of warm and hot springs in tuffaceous rocks provides information about several important aspects of a repository environment in tuffaceous rock including (1) the effect of the thermal pulse on the chemistry of ground water; (2) the effect of heated ground water on the host rock including dissolution and precipitation reactions; (3) the transport of certain elements (e.g., strontium, cesium, uranium, thorium, etc.) found in radioactive waste in a hydrothermal environment; and (4) hydrothermal fluid flow in fractured tuff. In addition, the studies will provide case studies for testing computer codes like EQ3/6.

Warm and hot springs are present in tuffaceous rocks at many locations in the western United States. Several of the locations have been studied in detail, including (1) the geyser basins in Yellowstone National Park (Honda and Muffler, 1970; Thompson et al., 1975; Keith and Muffler, 1978; Keith et al., 1978; Thompson and Yadav, 1979; Bargar and Beeson, 1981; Bargar and Muffler, 1982; Keith et al., 1983; Barger and Beeson 1984a,b); (2) the Valles caldera in northern New Mexico (Goff and Sayer, 1980; Goff et al., 1981; Goff and Grigsby, 1982; Goff et al., 1982; Phillips et al., 1984; Hulen and Nielson, 1985); and (3) the Newberry Volcano in central Oregon (Bargar and Keith, 1984; Keith et al., 1984a,b). Although the Newberry Volcano is not composed of typical silicic ash-flow tuff, it contains intermediate to silicic lavas and tuffs of the type that also occur in and around Yucca Mountain. The results obtained from the studies have been largely empirical and have included (1) descriptions of the petrography and the primary and secondary mineralogy of core and surface samples, (2) chemical analyses of rocks and thermal waters, and (3) temperature profiles.

The warm and hot springs of the geyser basins in the Yellowstone National Park are discussed here because they have been studied in the most detail. The springs emerge from silicic volcanic rocks and volcanogenic sediments that are less than 1 million years old. In fact, the springs are likely surface manifestations of recent igneous activity. The USGS has drilled 13 drillholes (75 to 320 m) to investigate the hydrothermal systems in the Yellowstone National Park. These holes have penetrated volcanogenic sediments (partly glacial), rhyolitic lava flows, volcanic breccias, and various types of silicic tuffs. Because the drillholes are located in parts

of the Yellowstone caldera that have been filled in with postcaldera rhyolite flows, ash-flow tuffs are not the dominant rock type encountered (Keith and Muffler, 1978). However, drillholes Y-5 (Keith and Muffler, 1978) and Y-9, Y-12, and Y-11 (Bargar and Muffler, 1982) do contain ash-flow tuffs (part of the Lava Creek Tuff of the Yellowstone Group; Christiansen and Blank, 1972) similar in composition and texture to the tuffs exposed at Yucca Mountain.

The warm and hot springs have altered the Lava Creek Tuff in drillholes Y-5 and Y-11 to a suite of secondary minerals including alpha-cristobalite, beta-cristobalite, quartz, chalcedony, opal, hematite, goethite, pyrite, manganese oxides, clays, zeolites, calcite, gypsum, and other minor phases. Because data are available on the alteration paragenesis, compositions of the secondary minerals, present day temperature profiles, and the compositions of water in the drillholes, the relative stabilities of the secondary mineral assemblages in the Yellowstone drillholes can be derived. In this context, the capability of the EQ3/6 code will be used and tested. Kinetic effects should be apparent in comparisons of the code predictions with the observed mineral assemblages.

Once the dominant chemical controls on the secondary mineral assemblages in the Yellowstone drillholes have been identified, this information can be used to characterize the stability ranges of the secondary minerals (e.g., silica, polymorphs, and zeolites) in Yucca Mountain under ambient conditions as well as in the thermal regime resulting from waste emplacement. In addition, the modeling will result in a better understanding of the effects of the thermal pulse on the chemistry of ground water in the near field. Plans for additional studies are described in Sections 8.3.1.3.1, and 8.3.1.3.3.

4.3.1.2 Uranium and thorium ore deposits and their host rocks

Uranium and thorium ore deposits, are a source of data on the following: (1) the long-term stability of radioactive solids (Naudet, 1978); (2) the long-term release of radionuclides from these solids (Curtis, 1985); (3) the transport of radionuclides under various pH, Eh, temperature, and pressure conditions, ground-water and host rock compositions, and hydrologic regimes (Ruffenach et al., 1980); and (4) the long-term effects of radiolysis (Curtis and Gancarz, 1983). Items 1, 2, and 4 relate to near-field conditions in a repository environment while Item 3 relates to near- and far-field conditions under which radionuclides may be transported from a repository to the accessible environment.

Known uranium and thorium ore deposits are separated into two types for the discussion that follows: those that reached nuclear criticality (i.e., experienced a sustained nuclear fission reaction), and those that did not reach criticality. The first type yields information on many of the radio- nuclides present in modern radioactive waste, while the second type yields information on a more limited number of radionuclides. Only one of the first type of deposit has been identified to date, the Oklo uranium deposit in the Republic of Gabon, Africa. Although there are many deposits of the second type, only a few have been studied from the viewpoint of the four items

listed above (e.g., Osmond and Cowart, 1981; Eisenbud et al., 1984; Airey et al., 1984, 1985).

4.3.1.2.1 The Oklo uranium deposit

Studies of the Oklo deposit indicate that, under the conditions in which the deposit was formed and subsequently evolved, uraninite remained generally stable over a period of 2.0 billion yr (Gancarz, 1978). The critical stage for the deposit lasted only 100 to 800 thousand yr (Ruffenach et al., 1980). Tellurium, uranium, thorium, niobium, zirconium, yttrium, the rare-earth elements, tin, plutonium, and the noble metals ruthenium, rhodium, and palladium, either remained in the uraninite lattice or were partly redistributed within the critical reaction zones over time (Table 4-20). The low solubility of most of these elements in aqueous fluids under the ambient chemical conditions was largely the reason for their retention in the zones. Chalcophyllic elements such as cadmium, molybdenum, silver, and lead were transported out of the critical reaction zones by hydrothermal fluids and deposited in the surrounding host rocks at distances dictated by the solubilities of their respective sulfide or oxide phases under the temperature, pressure, and chemical conditions in the surrounding rocks. The alkali and alkaline earth elements and the noble gases were largely transported out of the Oklo deposit. Annual release rates cannot be derived for these elements because the timing of the losses cannot be constrained.

The effects of radiolysis in the Oklo ore deposit are discussed by Curtis and Gancarz (1983). The authors calculated the alpha- and beta-particle doses in the critical reaction zones during criticality and the energy imparted to the fluid phase by these particles. The energy caused radiolysis of water and the production of reductants and oxidants. The effect of these reductants and oxidants on the transport of radionuclides within and outside the reactors has been difficult to quantify. Analysis of iron(III)/iron(II) ratios in bulk rock samples from the reactor zones (Branche et al., 1975) indicate that the iron in these zones is generally more reduced than the iron in the host rocks well away from the reactor zones. In fact, iron is most reduced in the samples that show the greatest uranium-235 depletion. This suggests that the reduction of iron in the reactor zones was contemporaneous with the nuclear reactions and not a later supergene phenomenon of secondary enrichment. Curtis and Gancarz (1983) suggest that radiolysis of water resulted in the reduction of iron(III) in the reactor zones and the oxidation of uranium(IV) in uraninite. Furthermore, Curtis and Gancarz suggest that the oxidized uranium was transported out of the critical reaction zones and precipitated through reduction processes in the host rocks immediately outside the zones. The reduction processes likely involved organics or sulfides present in the host rocks. However, if the host rocks around the natural reactor cores had not contained species capable of reducing the oxidized uranium transported out of the cores, the uranium could have been transported much farther from the critical reaction zones. The important point is that even with intensive radiolysis very little of the uranium in the natural reactors was mobilized (several percent--Naudet, 1978).

Table 4-20. Behavior of fission products in industrial reactors and in the Oklo natural reactors[a]

Chemical state	Elements	Ionic radius (A)	Industrial reactors Retention in the fuel	Localization in the free volume of the cladding	Oklo natural reactors Retention	Migration
Gaseous compounds	Kr	1.8^b		x		x
	Xe	2.0^b		x		x
Volatile compounds	I_2	2.5^b		x		x
	Te	0.60		x	x	
	Cs	1.8		x		x
Oxides insoluble in the matrix	Sr	1.21		x		x
	Ba	1.44		x		x
	Mo	0.73		x		x
Metallic inclusions	Tc	0.72		x	x	
	Ru	0.70		x	x	
	Rh	0.71	x		x	
	Pd	0.70	x		x	
Oxides soluble in the matrix	Y	0.98	x		x	
	Nb	0.72	x		x	
	Zr	0.92	x		x	
	Rare-earths	1.02–1.13	x		x	
	Pb	1.02				
	Th	1.12				
	U	1.08				
	Pu	1.04				

[a]Source: Ruffenach et al. (1980).
[b]Molecular radius (Johnston, 1966).

4.3.1.2.2 Other uranium and thorium deposits

Studies of uranium and thorium deposits that have not undergone a critical reaction phase have provided data on the mobility of various shortlived radionuclides in the uranium and thorium decay series. The deposits may also yield data on the mobility of technetium, neptunium, and plutonium, although

no such data have been reported to date. The ore deposits of Alligator Rivers are discussed here because they have been studied in considerable detail. Other deposits that have been investigated are the Colorado Plateau uranium deposits (e.g., Osmond and Cowart, 1981) and the Morro de Ferro thorium deposit in Brazil (Eisenbud et al., 1984).

The Alligator Rivers region of northern Australia is underlain by lower Proterozoic sediments and tuffs that overlie late-Archean granitic complexes. Approximately 1,800 million yr ago, these rocks were subjected to regional metamorphism and deformation. After subsequent uplift and some retrograde metamorphism, the rocks were covered by middle-Proterozoic and younger units (Needham and Stuart-Smith, 1980).

The uranium deposits of the Alligator Rivers area are found mainly in the lower Proterozoic Cahill Formation. The formation has a lower member of carbonate rock and carbonaceous schists that is overlain by an upper member composed of mica-quartz schist and gneiss. It was metamorphosed to amphibo-lite facies and subsequently retrograded to greenschist facies assemblages. Uranium mineralization is found in zones of brecciation, faulting, and ferromagnesian alteration within the formation (Needham and Stuart-Smith, 1980). The primary uranium mineralization appears to have occurred approxi-mately 1,400 million yr ago. It consists mainly of uraninite that is locally replaced by coffinite and brannerite.

Because the Alligator Rivers region has a monsoonal climate, deep lateritic weathering profiles with anomalous uranium concentrations overlie the primary ore bodies. The profiles are generally composed of four zones (Airey et al., 1985): (1) a zone of oxidized ferricrete or a ferruginous zone grading into a mottled zone (these zones are unsaturated in the dry season and generally have an oscillating water table at other times - uranium is leached in these zones); (2) a pallid zone from which iron has been leached (some uranium is deposited in this zone - this and the following zones are all permanently saturated); (3) a transition zone between weathered and unweathered rock (conditions are generally oxidizing in the zone with some uranium leaching); and (4) unweathered rock of the Cahill formation.

The Australian Atomic Energy Commission under a contract with the NRC has conducted studies (Airey et. al., 1984, 1985) of radionuclide transport in the rocks, sediments, and waters in and around the Alligator Rivers uranium deposits. The results of the studies include the following: (1) in the zone of weathering, uranium and thorium are associated principally with iron minerals; (2) ground waters in the region are generally oxidizing (+60 to +400 mV) and contain dissolved oxygen; (3) although uranium and thorium are mobilized in solution, a more significant mode of transport is by erosion; (4) the concentration of uranium in ground water ranges from approximately 0.25 to 190 ppb; (5) the rate at which uranium is leached or deposited in and around the ore bodies in percent per 1,000 yr ranges from a deposition rate of 0.4 to a leach rate of 2.5; and (6) colloidal transport does not contribute significantly to uranium transport but is important for the transport of thorium.

4.3.2 RELATED FIELD TESTS

Field tests at other sites have yielded data relevant to migration of radionuclides and to evaluation of models to be used for performance assessment. The following sections discuss the results of studies of radionuclide migration at (1) the site of the underground Cambric nuclear explosion on the Nevada Test Site, and (2) the DP site at Los Alamos National Laboratory where liquid radioactive waste has infiltrated downward into Bandelier Tuff.

4.3.2.1 Cambric site

Data from a field experiment at the site of the Cambric underground nuclear test have provided direct information on the transport rates of radionuclides through alluvium. The data can help confirm that the transport model in the performance assessment code TRACR3D can accurately model radionuclide transport in tuffaceous media. The data also provide some indication of the limitations of laboratory sorption measurements; however, no further work is planned.

A field study of the distribution of radionuclides around the Cambric underground cavity was initiated in 1974, about 9 yr after detonation of the Cambric nuclear test. The field study provides an actual in situ field test in rocks that have some of the same sorption characteristics as those at or along flow paths from the potential repository at Yucca Mountain. Additionally, although the medium is dominantly tuffaceous alluvium, the reactive surface area is higher and effective porosity lower than is expected for the rocks in and around the exploratory block at Yucca Mountain.

The following information was taken from Hoffman and Daniels (1981). The explosion at the Cambric site was a 0.75-kiloton test fired in May 1965, at a depth of 294 m beneath the water table in tuffaceous alluvium (Figure 4-23). Tests began after the cavity and chimney were predicted to be filled with ground water to the preshot static water level, 73 m above the detonation point. It was assumed that tritium, plutonium, and uranium fission products would be present in the cavity and in the ground water within the cavity and could be used to study possible migration from the cavity.

The field study began with the completion of a satellite well (RNM-2S) 91 m from the Cambric cavity followed by drilling of a reentry well (RNM-1) into the cavity itself. Both solid and liquid samples were taken from well RNM-1 to determine the distribution of radionuclides between the solid material and the ground water. Water was then pumped from the satellite well to induce an artificial gradient sufficient to draw water from the Cambric cavity through the surrounding rocks. Pumping from well RNM-2S began in October 1975. The original pump rate was 1 m^3/min until October 1977 when the pump rate was increased to about 2.3 m^3/min.

The various radionuclides present in water drawn from well RNM-2S reflect the extent of radionuclide migration. Approximately 2 yr after pumping started, significant amounts of tritiated water were found in water from the satellite well, signaling the arrival of water from the Cambric cavity region. By that time, approximately 1.44 million m^3 of water had been
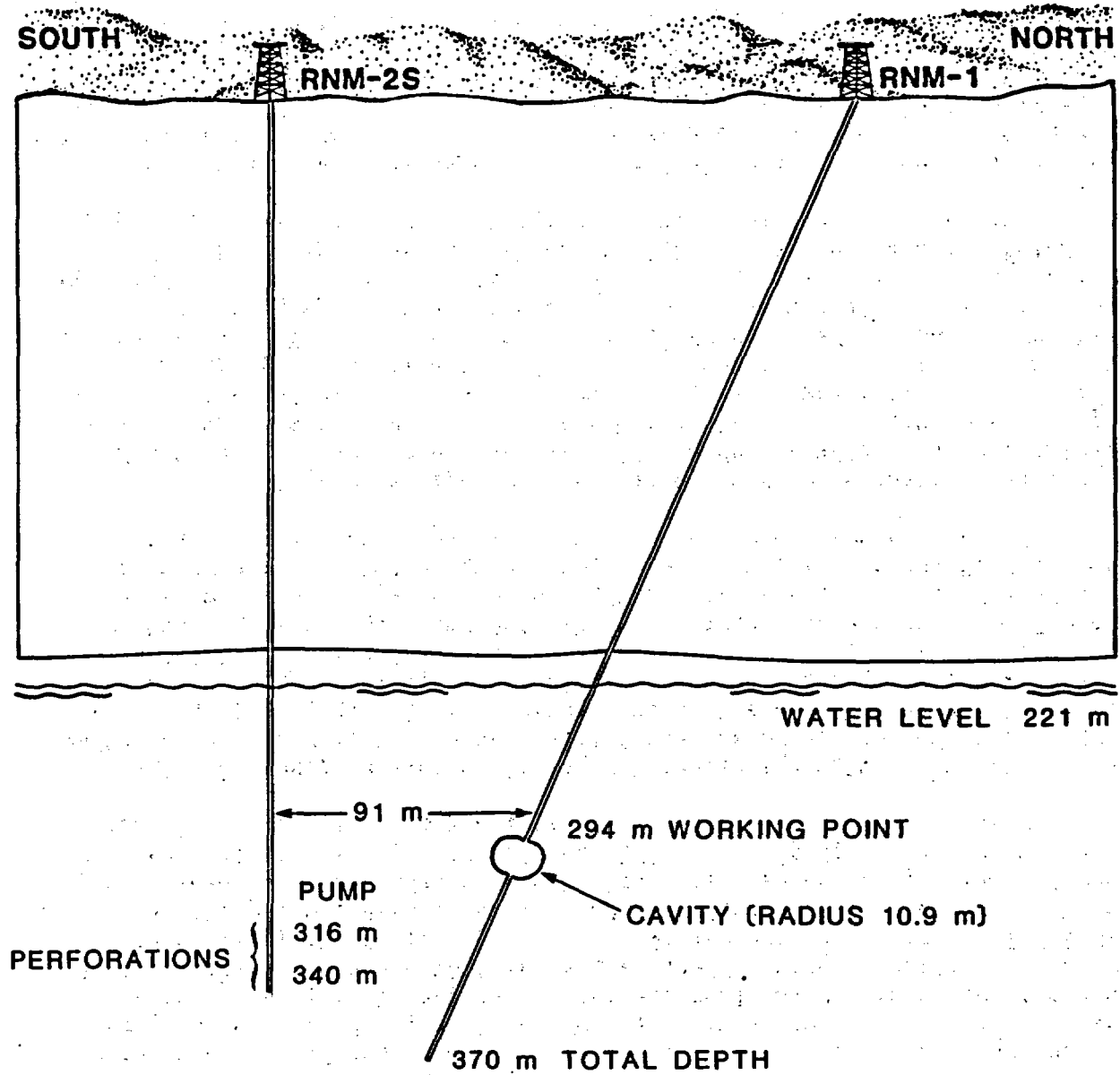
SOUTH   RNM-2S   NORTH   RNM-1

WATER LEVEL   221 m

←———91 m———→   294 m WORKING POINT

PERFORATIONS { PUMP
              316 m
              340 m

CAVITY (RADIUS 10.9 m)

370 m TOTAL DEPTH

Figure 4-23.   Schematic of Cambrian explosion cavity and drillholes RNM-1 and RNM-2S. Modified from Hoffman and Daniels (1981).

pumped from the satellite well. After almost 6 yr of pumping, the tritium concentration in the pumped water reached a maximum. The original amount of tritium produced during the Cambric event was about 6×10^4 curies (Hoffman et al., 1977). By the end of September 1984, slightly more than 3.7×10^4 curies of tritium had been pumped out through well RNM-2S (about 60 percent of the initial inventory). The result of a transport calculation based on Sauty's model for hydrodispersive transfer in aquifers (Sauty, 1980) was presented by Thompson (1985). Travis (1984) has modeled the tritium elution at Cambric using the TRACR3D code. According to Travis (1984), the difference between the calculated and observed breakthrough curves is approximately equal to the margin of error in the input parameters used in the code.

Other radionuclides have also been measured in water from well RNM-2S including chlorine-36, krypton-85, ruthenium-106, and iodine-129. Radionuclides present in the Cambric cavity in cationic form (e.g., strontium-90 and cesium-137) have not been detected to date in well RNM-2S water (Thompson, 1985). The chlorine-36 results presented in Figure 4-24 indicate that the chlorine-36 pulse preceded the tritium pulse in well RNM-2S. This suggests that tritiated water is exchanging with water in the pores in the tuffaceous alluvium which, to some degree, exclude chlorine-36 due to the repulsion of the negative ion by negative surface charges. This suggests that matrix diffusion of water does occur in tuffaceous alluvium.

Krypton is a noble gas and might be expected to show very little retention in the alluvial aquifer. Although the krypton data show more scatter than the tritium data, the behavior of the elements is correlated. The observations are compatible with the hypothesis that some krypton is sorbed on the alluvium and is therefore retarded relative to water (Thompson, 1985). The fact that the krypton-tritium ratios in well RNM-2S water are lower than the calculated source term ratio of 1.22×10^{-4} while they are higher than the calculated krypton-tritium ratio in well RNM-1, also suggests krypton is sorbed onto the alluvium relative to tritium (Thompson, 1985).

Ruthenium-106 has been detected in well RNM-2S water (Daniels, 1981; Coles and Ramspott, 1982). Although the data are limited, it is clear that some ruthenium from the Cambric cavity has been transported to well RNM-2S. Sorption measurements for ruthenium on tuffaceous alluvium indicate ruthenium has a high sorption coefficient (K_d = 10 to 30; Wolfsberg, 1978) under ambient conditions, which suggests ruthenium should not have migrated more than a fraction of a meter from the Cambric cavity since 1965. However, batch sorption measurements may not distinguish which species of a given element sorb or to what extent the species sorbs. Therefore, there may be species present in the batch sorption experiments which sorb very little, if at all. Daniels (1981) suggests that the ruthenium-106 present in well RNM-2S water exists as an anionic species which does not sorb on the alluvium.

Analyses of iodine-129 in water from well RNM-2S show that iodine, like chlorine, appears to have arrived at well RNM-2S sooner than tritium. However, the calculated fraction of iodine-129 that has been eluted is only 39 ± 11 percent in comparison with approximately 60 percent for tritium. The cause for this difference has not been determined (Thompson, 1985).
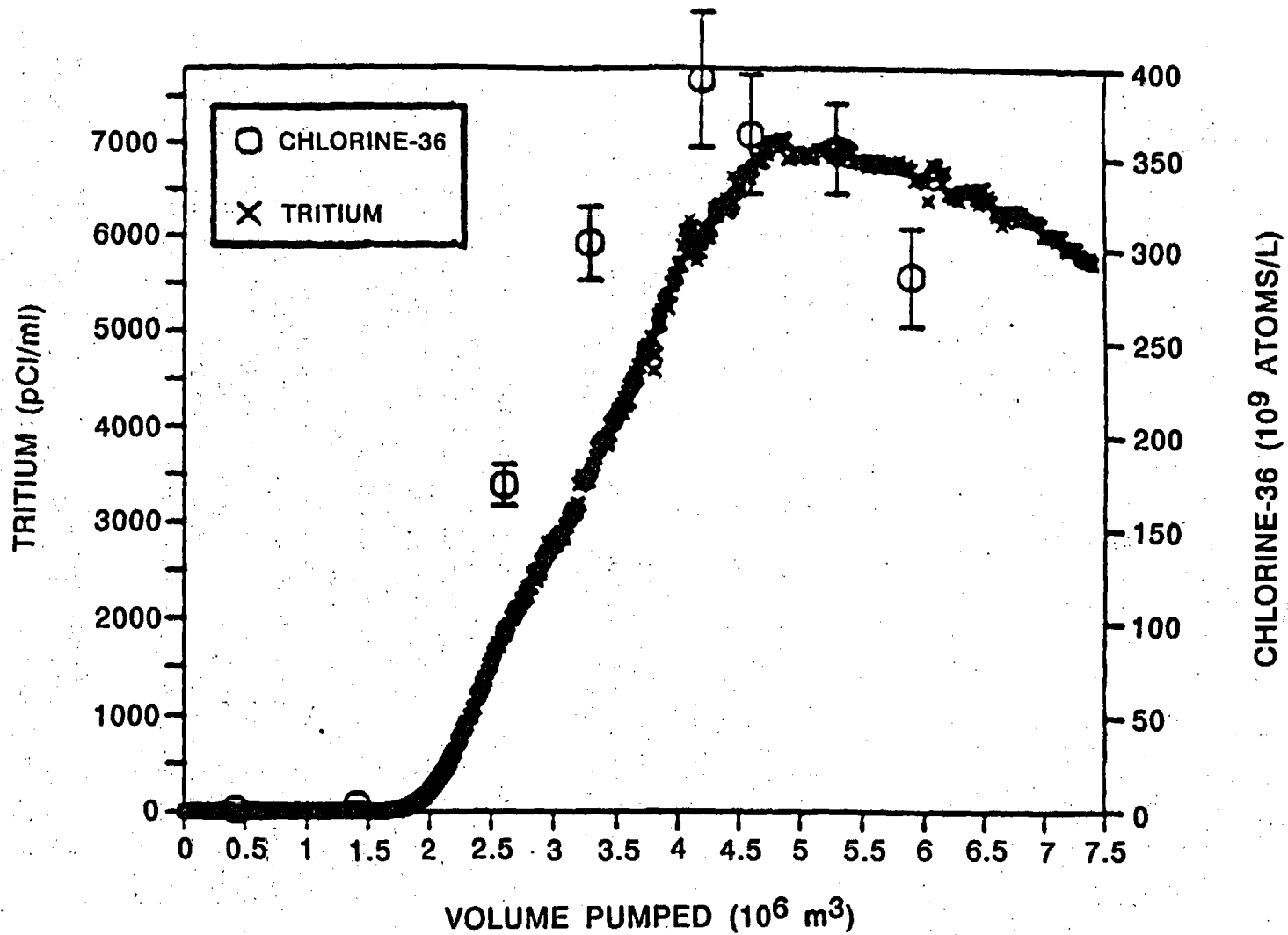
Figure 4-24. Chlorine-36 and tritium concentrations in well RNM-2S water. The error bars are the standard deviations for single measurements; they were obtained from the errors associated with measurements and estimated uncertainties for the various parameters entering into the calculation. The estimated uncertainties were propagated in quadrature. Modified from Daniels and Thompson (1984).

4.3.2.2 Los Alamos DP site

The distribution of radionuclides and water beneath a liquid waste disposal site at the Los Alamos National Laboratories was investigated by Nyhan et al. (1985). The site, known as the DP West site, was used from 1943 to 1951 to dispose of untreated radioactive liquid wastes resulting from plutonium-purification operations. A liquid-waste-treatment plant was installed in 1952 to handle the increased load but discharges continued until 1967, when a new treatment plant was built. The liquid wastes were discharged into absorption beds 36.6 by 6.1 m and 1.2 m deep. Approximately 69,260 m^3 of liquid effluent was discharged into the beds, with 89 percent added between 1945 and 1960. An estimated 10 curies of plutonium was discharged, with about 98 percent of the figure having been discharged, as untreated waste between 1945 and 1952. In August 1961, 10.8 m^3 of plutonium-bearing effluent followed by 9.7 m^3 of tap water were added to absorption bed 1. The fluid pulse resulted in formation of a saturation front that subsequently traveled downward through the unsaturated zone beneath the site.

The absorption beds consist of 60 cm of stone cobbles overlain by 15 cm of gravel, 15 cm of sand, and 30 cm of soil that were excavated out of the Tshirege Member of the Bandelier Tuff. The Bandelier Tuff at this location consists of an upper 3.6 m of moderately welded, light-brownish-gray tuff underlain by a 3-m-thick layer of reworked tuff and pumice which fills a channel (or cut) in the underlying tuff unit and is separated by a sharp contact zone. The underlying unit consists of 33 m of moderately welded, light-gray tuff. It is in turn underlain by a moderately to densely welded zone that forms the lower portion of the 250 m of the Bandelier Tuff at this location. The zone of water saturation is 350 m below the surface of the site. Therefore, at this location the Bandelier Tuff is entirely in the unsaturated zone.

Nyhan et al. (1985) drilled two 30.5 m drillholes through absorption beds 1 and 2 in area T of the DP West site. Continuous core samples were obtained and water samples were collected. A total of 800 samples were analyzed for americium-241 and plutonium. The results are shown in Figures 4-25 and 4-26. In drillhole 1 of bed 1, plutonium and americium-241 were detected to a sampling depth of 30.0 m and 30.5 m, respectively, while in drillhole 2 of the bed plutonium and americium-241 were detected to a depth of 14.5 m and 30.8 m, respectively. In bed 2, plutonium and americium-241 did not penetrate as far into the tuff because the bed did not receive the water pulse added to bed 1 in 1961. Plutonium penetrated 6.55 m in drillhole 1 and americium-241 penetrated 13.41 m. In drillhole 2 of bed 2, plutonium was detected only to a depth of 5.2 m and americium-241 to a depth of 12.8 m. The observations indicate that americium-241 has a higher mobility in this setting than does plutonium.

The spikes in the radionuclide-concentration profiles (Figures 4-25 and 4-26) are to some degree associated with geologic conditions. For instance, at 4 to 5.5 m in bed 1, a highly weathered, light orange-gray tuff layer with a high clay content was found, while at 8 to 9 m a contact zone was found separating a brownish-gray, moderately welded tuff from an underlying light gray, moderately welded tuff. Both the clay-rich layer and the contact zone have decreased hydraulic conductivities. Fractures, though present, did
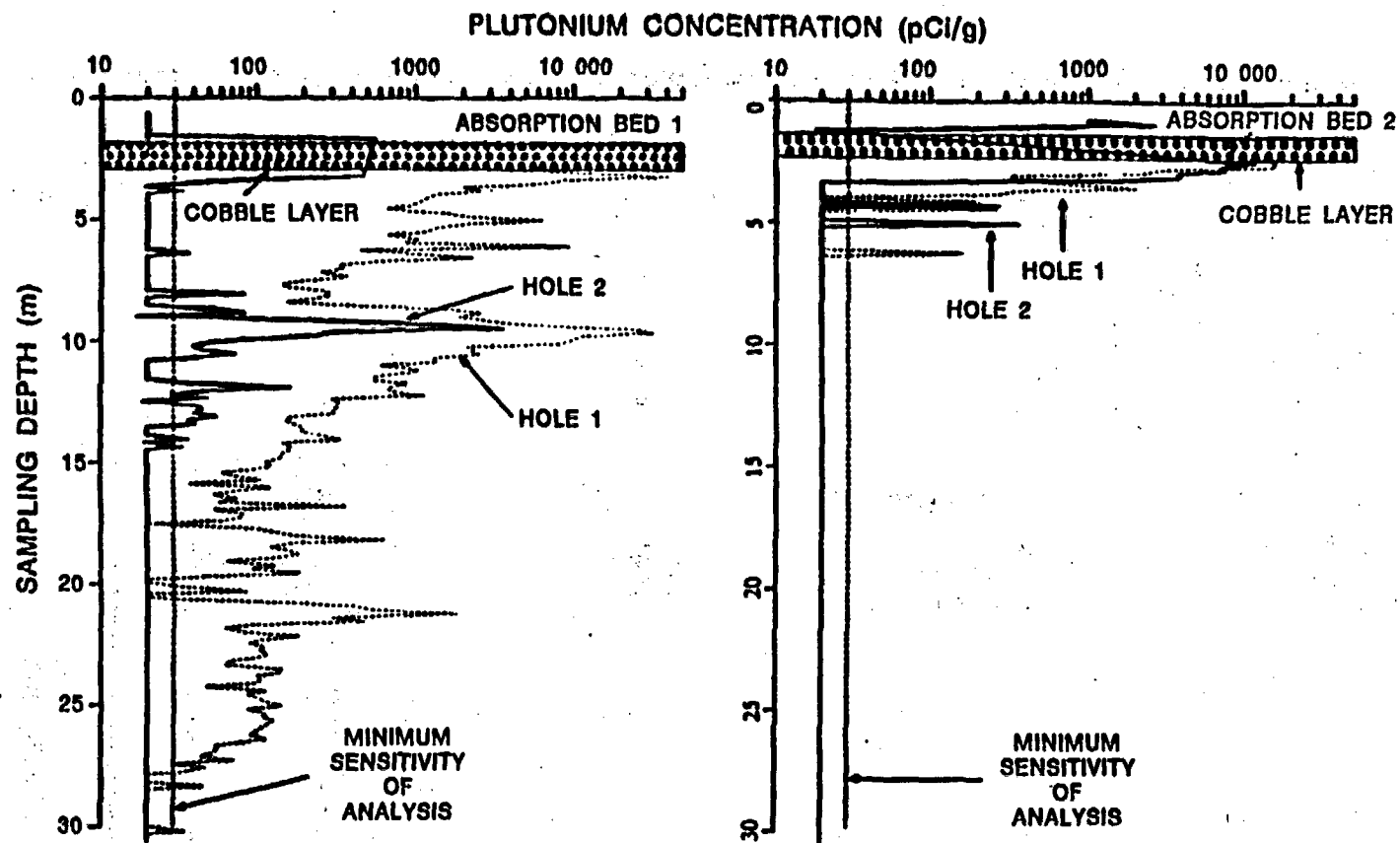
PLUTONIUM CONCENTRATION (pCi/g)

Figure 4-25. Concentration of plutonium as a function of sampling depth for absorption beds 1 and 2 in 1978. Modified from Nyhan et al. (1985).
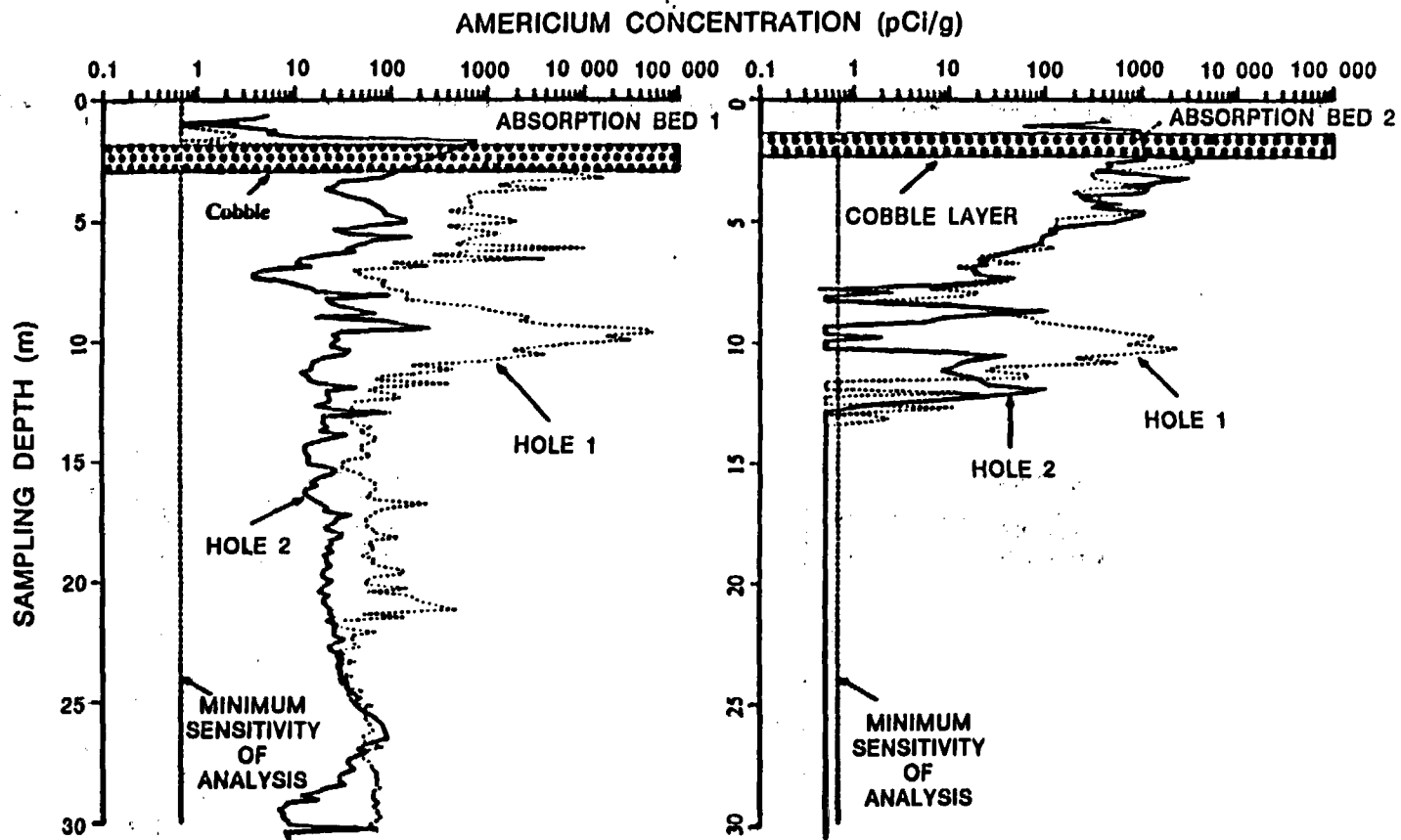
Figure 4-26. Concentration of americium-241 as a function of sampling depth for absorption beds 1 and 2 in 1978. Modified from Nyhan et al. (1985).

not appear to be associated with enhanced radionuclide transport. In fact, the fractures appeared to be barriers to unsaturated flow. Overall, Nyhan et al. (1985) concluded that "from 0.3 to 5.1 percent of the plutonium and from 3.0 to 49.0 percent of the americium-241 initially absorbed can be mobilized with the addition of less than 1 column volume of water."

Travis (1985) has attempted to model the migration of radionuclides at the DP West site with the TRACR3D code. He compared concentration profiles calculated on the basis of a constant adsorption coefficient and a colloid-population-balance approach. His results are shown in Figure 4-27. The colloid-population-balance approach clearly produces a better fit to the observed profile. This is consistent with the laboratory results of Fried et al. (1975) in which a rapidly migrating form of plutonium was found in experiments on Bandelier Tuff. Unfortunately, insufficient data exist on the forms of plutonium and americium likely to be released from waste packages at a repository at Yucca Mountain for extrapolating the results of Travis (1985) and Fried et al. (1975).

4.4 GEOCHEMICAL STABILITY

Man-induced factors that could potentially affect the geochemical stability of the site include mining, exploring for minerals, drilling unrelated to NNWSI Project operations, and withdrawing ground water. Natural changes that could affect the geochemical stability of the site include changes in the water regime as a result of tectonic or climatic variations and the introduction of magmatic fluids into the area. However, natural chemical buffers present in the water and rock help to resist changes in the geochemistry. The geochemical stability of the Topopah Spring tuff can be understood from the data presented in Section 4.1.1; chemical interaction between water and rock are discussed in detail in Section 4.1.1.3.

4.4.1 MAN-INDUCED EFFECTS

The potential for mining at the Yucca Mountain site is discussed in Section 1.7. As there is no compelling evidence that major, significant, or unique deposits of mineral or energy resources exist in the vicinity of the repository, the potential for mining is not considered important for geochemical stability.

The record of subsurface drilling is discussed in Section 1.6. Injection disposal wells are not present in the vicinity of the Yucca Mountain repository site. There is no reason to expect that the site has particularly favorable characteristics so that future injection disposal wells would be located in the area. Therefore, this factor is not a consideration for geochemical stability. Further discussion of this topic can be found in the Yucca Mountain environmental assessment (EA) (DOE, 1986).

Pumping of ground water may cause changes, usually minor, in groundwater chemistry by modifying flow paths or by inducing drainage of poorly permeable beds in which stored water has higher concentrations of solutes
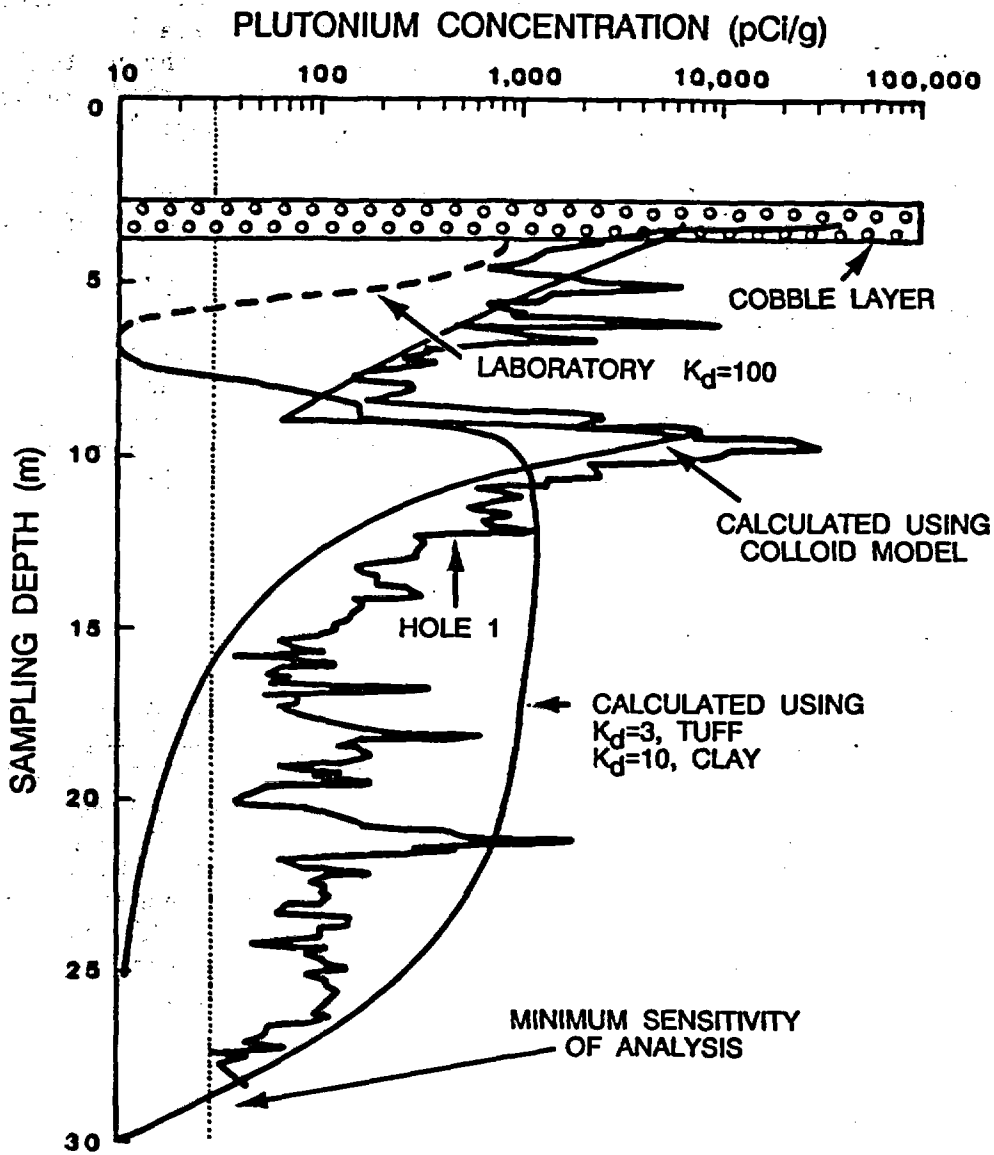
Figure 4-27. The measured and simulated plutonium concentration profiles for the region below bed 1 at the DP West sites. Kd = distribution coefficient. Modified from Nyhan et al. (1985).

than actively flowing water. In the region around Yucca Mountain, ground water is used primarily for irrigation. Lesser uses include municipal, domestic, livestock, mining, and support of operations at the Nevada Test Site.

Projections of future ground-water withdrawal in the region are discussed in Section 3.8. Although these projections and simulations of their effects at Yucca Mountain have not been completed, the effects of long-term pumping close to Yucca Mountain have been insignificant. Extensive pumping from well J-13, which produces from tuffs correlative with those at Yucca Mountain, has supported operations at Jackass Flat for more than two decades without significant changes in water levels or water chemistry (Thordarson, 1983). Although small, the hydraulic stresses around well J-13 are very likely greater than those resulting at Yucca Mountain from reasonably expectable future ground-water development. Therefore, disruption of geochemical stability by hydraulic stresses seems highly unlikely.

The construction and operation of the repository could affect radio-nuclide transport in two ways: first, the introduction of drilling fluids may provide a nutrient source for microbes; therefore, the effect of microbial activity on radionuclide migration is being assessed (Section 8.3.1.3.4); and second, the construction of the repository will produce particulates. The sorption and transport of radionuclides by particulates and colloids will also be studied (Section 8.3.1.3.4). Plans for studying the filtration of particulates by Yucca Mountain tuff are discussed in Section 8.3.1.3.6.

4.4.2 POTENTIAL EFFECTS OF NATURAL CHANGES

Natural processes of potential importance for geochemical stability include tectonism and volcanism (Section 1.3), flooding (Section 3.2), glass or mineral alteration that have effects on water composition (Sections 4.1 and 4.2), and climatic changes (Section 5.2). Where appropriate, specific processes that require further study are indicated.

Tectonism, volcanic activity, and structural features have already been treated in terms of possible physical disruption of the repository (Section 1.3.2); the displacement of flow paths by such processes could alter the effectiveness of natural geochemical barriers at the site. Among structural features, faults are important in bounding the exploration block at Yucca Mountain. Because variably mineralized faults may act either to enhance or retard ground-water flow, it is important to know not only what types of faults occur, but also what changes in flow and geochemical retardation might occur as a result of seismic activity and fault movement (Section 1.4). The problem will be addressed among the site characteristics contributing to performance assessment (Section 8.3.5.2.3), based on data obtained from the site geohydrology program (Section 8.3.1.2). The potential effects of igneous intrusion have been evaluated by Link et al. (1982), and the probabilities of volcanic activity have been estimated by Crowe et al. (1982). The risk from future igneous activity is low, but risk assessment is continuing (Section 8.3.1.8).

Because the potential repository horizon at Yucca Mountain is in the unsaturated zone, there are some conceivable changes in saturation that would affect geochemical processes. First, any possible flooding of the repository would affect geochemical stability. A future rise in the water table is one possibility that has been evaluated, and it is considered that inundation of the repository is improbable (Chapter 3, DOE, 1986). Zones below the repository that were previously unsaturated may become saturated, however, and such a change will be considered in assessing the balance between saturated- and unsaturated-zone processes of retardation. Another possible mechanism of repository saturation would be through hydrothermal activity. There is some record of past hydrothermal activity at depth, well below the present water table. Current studies indicate that hydrothermal activity is old (Bish, 1987) and is related to the Timber Mountain igneous activity about 11 million yr ago (Kistler, 1968). Minerals with moderately high temperatures of formation (between ambient temperature and 200°C) (Levy, 1987) do occur in some voids and fractures above the water table; the timing of formation for such minerals will be evaluated to determine whether they formed during the waning stages of tuff cooling or whether they may have formed from later hydrothermal fluids (Section 8.3.1.3.2). The test will determine whether post-Miocene hydrothermal activity will have to be considered to be a potential risk at the site. Finally, the possibility of deep-seated spring activity transgressing the repository horizon at some time in the past is being assessed by the study of fault-related mineral deposits (Section 8.3.1.3.2).

The geochemistry (nonhydrothermal) of rock and water interactions at Yucca Mountain involves a number of metastable mineral phases. As such, the chemical rock and water system will change toward more stable assemblages. The changes, however, have been occurring for several million years and can be expected to continue so slowly that there will be no significant effect on repository performance. In particular, it is important to note that the potential repository horizon is located in devitrified tuff with a relatively stable assemblage of feldspar minerals and quartz and some metastable cristobalite and opal along with very small amounts of other metastable minerals. The impact of the natural evolution of silica activity on the metastable assemblages is the major factor of concern. This natural change has been investigated (Section 4.1.1.4), and will be a part of future studies (Investigation 8.3.1.3.3).

Long-term climatic changes are discussed in Section 5.2. In terms of geochemical effects that influence repository performance, a renewed pluvial episode like those of the Pleistocene Epoch could result in increased recharge through Yucca Mountain, a higher water table, or the expansion or appearance of zones of perched water (Winograd and Doty, 1980). Any of these changes could affect flow rates or flow pathways that are important for integrating the site geochemistry into performance assessment. For example, a recharge-related transition from matrix flow to fracture flow may result in more rapid transport, along with changes in colloid retardation properties and dispersion/diffusion properties. The bounds on effects from such potential changes are a part of the performance-assessment program plan (Section 8.3.5).

4.5 SUMMARY

4.5.1 SUMMARY OF SIGNIFICANT RESULTS

The results summarized here are those related to the geochemical retardation processes that are considered the most significant in terms of the performance objectives and conceptual models. Thus a comprehensive summary of Chapter 4 is not presented. Sections 4.1.1 (Mineralogy and petrology), 4.1.2 (Ground-water chemistry), and 4.1.3 (Geochemical retardation processes) are briefly summarized with emphasis on performance objectives.

The mineral and petrologic results, as related to performance objectives and conceptual models, are best summarized by describing the distribution of sorptive zeolites at Yucca Mountain. The sorptive zeolites in the units surrounding the host rock provide part of the geochemical barrier for the retardation of radionuclides. Four principal intervals of zeolitization have been identified: (1) the clinoptilolite-heulandite-smectite zone at the top of the lower Topopah Spring vitrophyre; (2) the relatively thick zone of clinoptilolite that occurs in the bedded, nonwelded, and poorly welded tuffs that form the base of the Topopah Spring Member and the underlying tuffs of the Calico Hills, and extends into the top of the Prow Pass Member of the Crater Flat Tuff; (3) the partly welded and bedded tuffs at the base of the Prow Pass Member and at the top of the underlying Bullfrog Member; and (4) the poorly welded and bedded tuffs at the base of the Bullfrog Member compound cooling unit and at the top of the underlying cooling unit within the uppermost Tram Member.

The ground-water chemistry of the site is summarized from the results obtained from the saturated-zone wells on and near Yucca Mountain. Analyses of ground water from the drillholes that penetrate the host rock and surrounding units in the area of the exploration block indicate that they are principally sodium bicarbonate waters with low total dissolved solid content (200 to 400 mg/L). However, water from the carbonate aquifer contains over 1,000 mg/L total dissolved solids. Yucca Mountain ground waters are oxidizing. The dominant cations in the Yucca Mountain ground water are sodium, calcium, potassium, and magnesium with sodium the most abundant, ranging from 65 to 95 percent of the cations present. The concentrations of iron and manganese are generally low. The anionic constituents of the ground water show a relatively uniform distribution in the wells with about 80 percent bicarbonate and the remainder as sulfate and chloride (usually present in nearly equal molar concentrations) and fluoride (in varying concentrations). Overall, only minor variations in ground-water compositions occur in and adjacent to Yucca Mountain. Temporal variations in ground-water composition are also minor. Finally, the water from well J-13 has been chosen as the reference ground water that will represent the ground-water conditions along the transport pathways from the repository to the accessible environment.

The geochemical retardation processes described in Section 4.1.3 include sorption, precipitation, and matrix diffusion. Sorption data have been obtained with samples representative of Yucca Mountain strata. The variables include time, temperature, particle size, oxidation-reduction conditions, element concentration, ground-water composition, and test method (batch,

column, or circulating system). The radionuclides investigated were americium, cesium, neptunium, plutonium, uranium, thorium, strontium, technetium, tin, barium, radium, cerium, europium, and selenium. A correlation of sorptive behavior with mineralogy has been identified. Sorption of alkali metals (e.g., cesium) and alkaline earths (strontium, barium, radium) is directly correlated with the presence of minerals with exchangeable cations such as the zeolite clinoptilolite and potentially the smectite clays. Sorption ratios on these minerals vary from 1,000 to more than 10,000 ml/g. The correlation of sorption of cesium, europium, plutonium, and americium with mineralogy exists, but the relation is not as clear as for the alkali metals. However, sorption ratios are high for the elements listed above (100 to more than 1,000 ml/g); therefore, the lack of correlation is not critical. The sorption of these elements though, is undoubtedly influenced by the formation of hydroxy and carbonate complexes. It appears that sorption on tuff will not offer much retardation for such anionic species as an oxidized technetium species (i.e., TcO_4^-). Precipitation processes (i.e., solubility) will limit the concentration of radionuclides in water that moves from the repository toward the accessible environment. The solubility of americium, plutonium, neptunium, uranium, curium, thorium, strontium, radium, carbon, cesium, technetium, iodine, tin, zirconium, samarium, and nickel in well J-13 water has been compiled from available measurements and calculations. Diffusion of radionuclides from fracture water into the pore water in the rock matrix is important for retarding the transport of dissolved waste elements through fractures in tuff.

4.5.2 RELATION TO DESIGN

The geochemical characteristics of the backfill materials and the anticipated chemical interactions among the waste container, backfill, ground water, and the host rock under assumed waste emplacement conditions are described in Sections 6.3.3 and 7.4. The geochemical characteristics of the seal material as well as the anticipated chemical interactions among the seal materials, ground water, host rock, and backfill under assumed emplacement conditions are described in Section 6.3.5. Waste container design and geochemical interactions are described in Section 7.4. The mineral stability studies may have an impact on design considering that there is a reported volume change as minerals undergo transitions. This volume change should be assessed in order to determine whether the change is significant to design.

4.5.3 IDENTIFICATION OF INVESTIGATIONS

The investigations under the geochemistry program are listed below and will be discussed in detail in Section 8.3.1.3. Investigations 8.3.1.3.1 (ground water chemistry), 8.3.1.3.2 (mineralogy, petrology and rock chemistry) and 8.3.1.3.3 (stability of minerals and glasses) will provide the base site characterization data on the natural geochemical environment at Yucca Mountain. Investigations 8.3.1.3.4 (radionuclide sorption), 8.3.1.3.5 (radionuclide solubility), 8.3.1.3.6 (radionuclide dispersion, diffusion, and advection), and 8.3.1.3.8 (gaseous radionuclide transport) will investigate the geochemical processes that are acting and may potentially act at Yucca

Mountain. Finally, Investigation 8.3.1.3.7 will support the listed investigation and assess the physical/chemical processes through integrated transport calculations. This investigation will synthesize the geochemistry test program data and provide a geochemical/physical model of Yucca Mountain. The investigations are the following:

Investigation 8.3.1.3.1 Water chemistry within the potential emplacement horizon and along potential flow paths.

The water chemistry within the saturated zone has been well characterized, but more data are needed for the unsaturated zone (Section 8.3.1.2.2). A model of the ground-water chemistry for Yucca Mountain relating composition to the geologic location along potential pathways is also needed.

The information needed is as follows:

1.   Water chemistry of the unsaturated zone.

2.   Additional baseline data on naturally occurring radionuclides in Yucca Mountain ground water.

3.   Particulate content of Yucca Mountain ground water and collection.

4.   More data on the mineralogic controls on Yucca Mountain ground water.

5.   Model of the ground-water chemistry at Yucca Mountain.

Investigation 8.3.1.3.2 Mineralogy, petrology, and rock chemistry within the potential emplacement horizon and along potential flow paths.

The host rock in the Topopah Spring Member has been described, including the primary phenocryst and vapor-phase constituents. The discussion is found mostly in Chapter 1. Also discussed are the secondary minerals within fractures. The data were assessed for usefulness in indicating stratigraphic position and in characterizing the mineralogy along potential radionuclide travel paths. The chemistry and mineralogy of the surrounding units were detailed including a discussion of the secondary minerals with emphasis on the sorptive zeolites and clays.

More data are still needed to assess (1) how the mineral distributions at Yucca Mountain are going to affect retardation by sorption , (2) what processes account for the minerals found at Yucca Mountain, (3) whether those processes have been completed or are still operating, and (4) how the projected processes would affect a repository at Yucca Mountain. The following list of parameters address these needs:

1.   Mineral distributions in bulk rock.
2.   Mineral distributions in fractures.
3.   Bulk rock chemistry.
4.   Fracture chemistry.

   5.   Mineral origins and alteration history.
   6.   Mineralogy of transport pathways.

Investigation 8.3.1.3.3   Stability of minerals and glasses.

     Mineral stability in Yucca Mountain was considered in two ways. The
first consideration was whether the present mineral assemblages in Yucca
Mountain are stable under present conditions and, if they are not, what
mineralogic changes are probable. The presence or absence of clays, cristo-
balite, glass, and zeolites was studied to assess past thermal gradients.
The transformation of cristobalite to quartz was studied in order to under-
stand the evolution of silica activity, which controls the stability of
clinoptilolite, a sorbing mineral. The second consideration was what effect
repository heating will have on mineral stability, due to both increased
temperature and possible dehydration of the rock. The hydrothermal altera-
tions of zeolites, smectites, and rhyolitic glasses were studied to determine
alteration products, volume changes, and to understand the kinetics of these
mineral reactions. More work is needed to further define the stability of
minerals and glasses in every area mentioned previously.

     The information needed is as follows:

   1.   Data on mineral assemblages and temperatures in active hydrothermal
        systems in vitric tuff.

   2.   Data on dehydration in smectites, zeolites, and glasses. (From
        8.3.1.3.2)

   3.   Data on the kinetics of silica phase transformations and
        correlations to aqueous silica activity.

   4.   Data on the kinetics of transformations in smectites, zeolites, and
        related tektosilicates.

   5.   Data for constructing thermodynamic models of clinoptilolite,
        analcime, and albite.

   6.   Development of a conceptual model of mineral evolution.

**Investigation 8.3.1.3.4   Radionuclide retardation by sorption processes along
                            flow paths to the accessible environment.**

     The retardation process of sorption has been thoroughly considered in
this chapter. Sorption as a function of ground-water composition, mineral-
ogy, pH, temperature, oxidation-reduction conditions, sorbing species, and
waste element concentrations have been considered. Detail was provided on
the analytical techniques used to determine sorptive coefficients and a
discussion of the techniques for elucidating dynamic processes and how they
are coupled to sorption.

     Work must continue on all the previously discussed process parameters in
order to assess the interrelationships of water chemistry, mineralogy,

solubility, and speciation, and the effect of these processes on the retardation process of sorption in expected and unexpected conditions.

The information needed is as follows:

1. Data on sorption as a function of ground-water composition, mineralogy, and sorbing element concentration.

2. Extension of the sorption data base, specifically sorption coefficients correlated with stratigraphy.

3. Data on sorption on particulates and colloids and its relation to transport.

4. Data on the affects of microbial activity on sorption and the subsequent relation to transport.

5. Work on the statistical analysis of sorption data.

6. Model for sorptive behavior of important waste elements.

Investigation 8.3.1.3.5 Radionuclide retardation by precipitation along flow paths to the accessible environment.

Precipitation processes will limit radionuclide transport when the solubility limits of waste elements are exceeded in water as it moves toward the accessible environment. Speciation, defined as the formation of various complexes and oxidation states in the aqueous phase, in turn affects the solubility. This chapter briefly discussed speciation, solubility, radio-colloid formation, and radiolysis, all processes important in understanding concentration limits of elements in solution. The few solubility measurements that have been conducted were discussed along with the modeling work needed to further calculate waste-element solubilities.

To continue the experimental work it is necessary to define the conditions that control solubility (water chemistry, temperature, radiation field) and to define the waste element behavior in order to best understand precipitation processes.

The information needed is as follows:

1. Experimental data on solubility or concentration limits of important waste elements.

2. Experimental data on the ability of waste elements to form natural colloids.

3. Data on, or theoretical understanding of, the sensitivity of solubility limits in controlling parameters. Theory will be developed from speciation measurements and solubility modeling.

4. Solubility calculations.

Investigation 8.3.1.3.6   Radionuclide retardation by dispersive, diffusive, and advective transport processes along flow paths to the accessible environment.

The retardation of radionuclides by dispersive, diffusive, and advective processes was discussed in this chapter in relation to the anticipated and unanticipated conditions at Yucca Mountain. The chapter discussed the processes of radionuclide transport (diffusion, fracture flow, anion exclusion, hydrodynamic dispersion, and particulate (colloids or solids) transport. Some of the transport processes retard the rate of radionuclide transport. Matrix diffusion was discussed along with matrix diffusion coupled with fracture flow. Although dispersion is not a transport mechanism, the process also retards radionuclides by channeling (Non-Fickian dispersion) and the broadening effect of heterogeneously distributed material properties. The transport processes are also intimately associated with sorption and with geochemical processes that result in precipitation.

The transport of tracers in geohydrologic systems is not simple and the simplifying assumptions must be tested by laboratory and field experiments to understand fully the relationship of these processes to the retardation of radionuclides. Extensive laboratory work is needed to successfully model the processes.

The information needed is as follows:

1.   Data on diffusion processes (advection and no advection).

2.   Data on matrix diffusion and its relationship to fracture flow.

3.   Data on the relationship of adsorption to these transport processes.

4.   Data on sorption kinetics.

5.   Data on anion exclusion.

6.   Data on colloidal movement and particulate transport.

7.   Data on dispersion (hydrodynamic, channeling).

Investigation 8.3.1.3.7   Radionuclide retardation by all processes along flow paths to the accessible environment.

The modeling of radionuclide transport requires that chemical reactions of radionuclides occurring between the solid phase (minerals or precipitates) and aqueous phase (fracture or pore water) be coupled with the hydrologic flow and physical processes like diffusion and dispersion. The combination of all processes can be used to assess the retardation of radionuclides. This chapter discussed geochemical retardation in the host rock for anticipated and unanticipated conditions. The computer models discussed have the capability to include most of the known physical and geochemical transport processes. The preliminary work on radionuclide retardation was reported. Also discussed was the effect of the thermal load on radionuclide migration.

A conceptual geochemical-geophysical model must be developed to provide the baseline data needed for integrated radionuclide transport calculations. This baseline data set is incomplete; however, the calculation can be an iterative process as better and more complete data from geochemical, mineralogical-petrological, hydrological, and other pertinent NNWSI Project tasks are obtained. The significance and relative importance of each physical and geochemical process affecting transport also needs to be assessed.

The information needed is as follows:

1. Data from previous investigations listed and other NNWSI Project tasks (geochemical characteristics, source terms, rock characteristics, and geohydrologic characteristics).

2. Geochemical-geophysical model of Yucca Mountain.

3. Integrated transport calculations.

4. Significance and relative importance of processes affecting transport (sensitivity analysis).

5. Continued development of transport models.

6. Integration of field test results (geochemical).

Investigation 8.3.1.3.8 Retardation of gaseous radionuclides along flow
                         paths to the accessible environment.

Because the repository may be in the unsaturated zone, this chapter discussed gaseous transport as a potentially significant mechanism for the transport of volatile radionuclide. Two mechanisms are likely to be effective: (1) isotopic exchange between the gas phase and aqueous phase, and (2) the solubility of the gaseous species in the aqueous phase. No experimental work has been done to date on the geochemical aspects of gaseous transport.

The information needed is as follows:

1. Gaseous species.

2. Gas-phase composition.

3. Physical transport mechanisms and rates.

4. Retardation mechanisms and transport with retardation.

5. Gaseous radionuclide transport calculations.

6. Experimental verification of gaseous transport calculations (gas-transport measurements).

4.5.4 RELATION TO REGULATORY GUIDE 4.17

Regulatory Guide 4.17, Part B, Section 6 (NRC, 1987) provides generic guidance for geochemical topics to be addressed in a site characterization report to the NRC. All of the geochemical topics called for in Regulatory Guide 4.17 are relevant and applicable to the Yucca Mountain site. Most of these are addressed primarily in this chapter, although some are discussed only briefly and with reference to more complete treatments in Chapters 3, 7, and 8 of this document.

Nuclear Waste Policy Act
(Section 113)

Consultation Draft

Site Characterization
Plan

Yucca Mountain Site, Nevada Research
and Development Area, Nevada

Volume II

January 1988

REFERENCES FOR CHAPTER 4

Airey, P. L., D. Roman, C. Golian, S. Short, T. Nightingale,
     R. T. Lowson and G. E. Calf, 1984. Radionuclide Migration
     Around Uranium Ore Bodies - Analogue of Radioactive Waste
     Repositories, Annual Report, 1982-83, AAEC/C40, Australian
     Atomic Energy Commission Research Establishment, Lucas
     Heights Research Laboratories, University of Sydney.

Airey, P. L., D. Roman, C. Golian, S. Short, T. Nightingale,
     T. Payne, R. T. Lowson and P. Duerden, 1985. Radionuclide
     Migration Around Uranium Ore Bodies - Analogue of Radioactive
     Waste Repositories, Annual Report 1983-84, AAEC/C45,
     Australian Atomic Energy Commission Research Establishment,
     Lucas Heights Research Laboratories, University of Sydney.

Allard, B., 1983. Actinide Solution Equilibria and Solubilities
     in Geologic Systems, KBS-TR-83-35, Svensk
     Karnbransleforsorjning AB/Avdelning KBS, Stockholm, Sweden.

Allard, B., and B. Torstenfelt, 1983. On the Solubility of
     Technetium in Geochemical Systems, KBS-TR-83-60, Svensk
     Karnbransleforsorjning AB/Avdelning KBS, Stockholm, Sweden.

Apps, J. A., C. L. Carnahan, P. C. Lichtner, M. C. Michel,
     D. Perry, R. J. Silva, O. Weres, and A. F. White, 1983.
     Status of Geochemical Problems Relating to the Burial of
     High-Level Radioactive Waste, 1982, NUREG/CR-3062,
     U.S. Nuclear Regulatory Commission, Washington, D.C.

Ausloos, P., 1969. Fundamental Processes in Radiation Chemistry,
     Interscience Publishers, New York, pp. 651-685.

Avogadro, A., and G. De Marsily, 1984. "The Role of Colloids in
     Nuclear Waste Disposal," Scientific Basis for Nuclear Waste
     Management VII, Materials Research Society Symposia
     Proceedings, Boston, Massachusetts, November 1983,
     G. L. McVay (ed.), Vol. 26, North-Holland, Elsevier Science
     Publishing Co., Inc., New York, pp. 405-505.

Avogadro, A., and F. Lanza, 1982. "Relationship Between Glass
     Leaching Mechanism and Geochemical Transport of
     Radionuclides," Scientific Basis for Nuclear Waste Management
     V, Materials Research Society Symposia Proceedings, Berlin,
     Germany, June 7-10, 1982, W. Lutze (ed.), Vol. 5,

North-Holland, Elsevier Science Publishing Co., Inc.,
New York, pp. 103-112.

Baes, C. F., and R. E. Mesmer, 1976. The Hydrolysis of Cations,
A Wiley-Interscience Publication, John Wiley and Sons,
New York, pp. 1, 6-7, 176-177, 180-181, 184-191.

Bargar, K. E., and M. H. Beeson, 1981. "Hydrothermal Alteration
in Research Drill Hole Y-2, Lower Geyser Basin, Yellowstone
National Park, Wyoming," The American Mineralogist, Vol. 66,
No. 5-6, Mineralogical Society of America, pp. 473-490.

Bargar, K. E., and M. H. Beeson, 1984a. "Hydrothermal Mineralogy
in Research Drill Hole Y-3, Yellowstone National Park,
Wyoming," Geothermal Resources Council Transactions, Vol. 8,
pp. 111-117.

Bargar, K. E., and M. H. Beeson, 1984b. Hydrothermal Alteration
in Research Drill Hole Y-6, Upper Firehole River, Yellowstone
National Park, Wyoming, U.S. Geological Survey Professional
Paper 1054-B, U.S. Government Printing Office,
Washington, D.C.

Bargar, K. E., and T. E. C. Keith, 1984. Hydrothermal Alteration
Mineralogy in Newberry 2 Drill Core, Newberry Volcano,
Oregon, USGS-OFR-84-92, Open-File Report, U.S. Geological
Survey, Denver, Colo.

Bargar, K. E., and L. J. P. Muffler, 1982. "Hydrothermal
Alteration in Research Drill Hole Y-11 from a Vapor-Dominated
Geothermal System at Mud Volcano, Yellowstone National Park,
Wyoming," Thirty-Third Annual Field Conference, Wyoming
Geological Association Guidebook, pp. 139-152.

Bazan, F., and J. Rego, 1985. Parametric Testing of a DWPF
Glass, UCRL-53606, Lawrence Livermore National Laboratory,
Livermore, Calif.

Benson, L. V., and L. S. Teague, 1980. A Tabulation of
Thermodynamic Data for Chemical Reactions Involving 58
Elements Common to Radioactive Waste Package Systems,
LBL-11448, Lawrence Berkeley Laboratory, Berkeley, Calif.

Benson, L. V., J. H. Robison, R. K. Blankennagel, and
A. E. Ogard, 1983. Chemical Composition of Ground Water and
the Locations of Permeable Zones in the Yucca Mountain Area,
Nevada, USGS-OFR-83-854, Open-File Report, U.S. Geological
Survey, Denver, Colo.

Bentley, C. B., J. H. Robison, and R. W. Spengler, 1983.
Geohydrologic Data for Test Well USW H-5, Yucca Mountain
Area, Nye County, Nevada, USGS-OFR-83-853, Open-File Report,
U.S. Geological Survey, Denver, Colo.

Bernkopf, M. F., and J. I. Kim, 1984. Hydrolysereaktionen und
Karbonatkomplexierung von Dreiwertigem Americium in
Naturlichen Aquatischen System, RCM-02884, Institut fur
Radiochemie der Technischen Universitat Munchen, Federal
Republic of Germany.

Bidoglio, G., A. De Plano, and A. Chatt, 1983. "Studies on
Speciation of Americium, Technecium, and Neptunium in
Simulated Vitrified-Waste Leachates," Scientific Basis for
Nuclear Waste Management VI, Materials Research Society
Symposia Proceedings, Boston, Massachusetts, November, 1982,
G. Brookins (ed.), Vol. 15, North-Holland, Elsevier Science
Publishing Co., Inc., New York, pp. 373-382.

Bish, D. L., 1981. Detailed Mineralogical Characterization of
the Bullfrog and Tram Members in USW-G1, with Emphasis on
Clay Mineralogy, LA-9021-MS, Los Alamos National Laboratory,
Los Alamos, N. Mex.

Bish, D. L., 1984. "Effects of Exchangeable Cation Composition
on the Thermal Expansion/Contraction of Clinoptilolite,"
Clays and Clay Minerals, Vol. 32, No. 6, pp. 444-452.

Bish, D. L., 1985. "Effects of Composition on the Dehydration
Behavior of Clinoptilolite and Heulandite," Proceedings of
the International Conference on the Occurrence, Properties,
and Utilization of Neutral Zeolites, Budapest, Hungary,
August 1985.

Bish, D. L., 1987. Evaluation of Past and Future Alterations in
Tuff at Yucca Mountain, Nevada Based on the Clay Mineralogy
of Drill Cores USW G-1, G-2, and G-3, LA-10667-MS, Los Alamos
National Laboratory, Los Alamos, N. Mex.

Bish, D. L., and S. J. Chipera, 1986. Mineralogy of Drill Holes J-13, UE-25A 1, and USW G-1 at Yucca Mountain, Nevada, LA-10764-MS, Los Alamos National Laboratory, Los Alamos, N. Mex.

Bish, D. L., and D. T. Vaniman, 1985. Mineralogic Summary of Yucca Mountain, Nevada, LA-10543-MS, Los Alamos National Laboratory, Los Alamos, N. Mex.

Bish, D. L., F. A. Caporuscio, J. F. Copp, B. M. Crowe, J. D. Purson, J. R. Smyth, and R. G. Warren, 1981. Preliminary Stratigraphic and Petrologic Characterization of Core Samples from USW-G1, Yucca Mountain, Nevada, A. C. Waters and P. R. Carroll (eds.), LA-8840-MS, Los Alamos National Laboratory, Los Alamos, N. Mex.

Bish, D. L., D. T. Vaniman, F. M. Byers, Jr., and D. E. Broxton, 1982. Summary of the Mineralogy-Petrology of Tuffs of Yucca Mountain and the Secondary Phase Thermal Stability in Tuffs, LA-9321-MS, Los Alamos National Laboratory, Los Alamos, N. Mex.

Bish, D. L., A. E. Ogard, D. T. Vaniman, and L. Benson, 1984. "Minerology-Petrology and Groundwater Geochemistry of Yucca Mountain Tuffs," Scientific Basis for Nuclear Waste Management VII, Materials Research Society Symposia Proceedings, Boston, Massachusetts, November 1983, G. L. McVay (ed.), Vol. 26, North-Holland, Elsevier Science Publishing Co., Inc., New York, pp. 283-291.

Blacic, J. D., D. T. Vaniman, D. L. Bish, C. J. Duffy, and R. C. Gooley, 1986. Effects of Long-Term Exposure of Tuffs to High-Level Nuclear Waste Repository Conditions: Final Report, LA-9330-MS, Los Alamos National Laboratory, Los Alamos, N. Mex.

Blake, C. A., C. F. Coleman, K. B. Brown, D. G. Hill, R. S. Lowrie, and J. M. Schmitt, 1956. "Studies in the Carbonate-Uranium System," Journal of American Chemical Society, Vol. 78, pp. 5978-5983.

Boersma, M. D., 1984. Letter from M. D. Boersma (Savannah River Laboratory) to J. F. Kerrisk (Los Alamos National Laboratory), October 8, 1984; with enclosure tables of "DWFP product glass isotopes and radioactivity."

Branche, G., F. Chantret, A. Guillemaut, and R. Pouget, 1975. "Donnees Chimiques et Mineralogiques sur le Gisement d'Oklo," Le Phenomene d'Oklo, STI/PUB/405, International Atomic Energy Agency, pp. 119-132.

Breck, D. W., 1974. Zeolite Molecular Sieves, John Wiley and Sons, New York, pp. 529-592.

Broxton, D. E., D. T. Vaniman, F. Caporuscio, B. Arney, and G. Heiken, 1982. Detailed Petrographic Descriptions and Microprobe Data for Drill Holes USW-G2 and UE25b-1H, Yucca Mountain, Nevada, LA-9324-MS, Los Alamos National Laboratory, Los Alamos, N. Mex.

Broxton, D. E., R. G. Warren, R. C. Hagan, and G. Luedemann, 1986. Chemistry of Diagenetically Altered Tuffs at a Potential Nuclear Waste Repository, Yucca Mountain, Nye County, Nevada, LA-10802-MS, Los Alamos National Laboratory, Los Alamos, N. Mex.

Bryant, E. A., and D. T. Vaniman (comps.), 1984. Research and Development Related to the Nevada Nuclear Waste Storage Investigations, July 1-September 30, 1983, LA-10006-PR, Los Alamos National Laboratory, Los Alamos, N. Mex.

Byers, F. M., Jr., 1985. Petrochemical Variation of Topopah Spring Tuff Matrix with Depth (Stratigraphic Level), Drill Hole USW G-4 Yucca Mountain, Nevada, LA-10561-MS, Los Alamos National Laboratory, Los Alamos, N. Mex.

Byers, F. M., Jr., and R. G. Warren, 1983. Revised Volcanic Stratigraphy of Drill Hole J-13, Fortymile Wash, Nevada, Based on Petrographic Modes and Chemistry of Phenocrysts, LA-9652-MS, Los Alamos National Laboratory, Los Alamos, N. Mex.

Byers, F. M., Jr., W. J. Carr, P. P. Orkild, W. D. Quinlivan, and K. A. Sargent, 1976. Volcanic Suites and Related Cauldrons of the Timber Mountain-Oasis Valley Caldera Complex, Southern Nevada, U.S. Geological Survey Professional Paper 919, U.S. Government Printing Office, Washington, D.C.

Caporuscio, F. A., and D. T. Vaniman, 1985. Iron and Manganese in Oxide Minerals and in Glasses: Preliminary Consideration of Eh Buffering Potential at Yucca Mountain, Nevada, LA-10369-MS, Los Alamos National Laboratory, Los Alamos,

N. Mex.

Caporuscio, F. A., D. Vaniman, D. Bish, D. Broxton, D. Arney,
    G. Heiken, F. Byers, R. Gooley, and E. Semarge, 1982.
    Petrologic Studies of Drill Cores USW-G2 and UE25b-1H, Yucca
    Mountain, Nevada, LA-9255-MS, Los Alamos National Laboratory,
    Los Alamos, N. Mex.

Carlos, B. A., 1985. Minerals in Fractures of the Unsaturated
    Zone from Drill Core USW G-4, Yucca Mountain, Nye County,
    Nevada, LA-10415-MS, Los Alamos National Laboratory,
    Los Alamos, N. Mex.

Carroll, P. I., F. A. Caporuscio, and D. L. Bish, 1981. Further
    Description of the Petrology of the Topopah Spring Member of
    the Paintbrush Tuff in Drill Holes UE25a-1 and USW-GI and of
    the Lithic-Rich Tuff in USW-G1, Yucca Mountain, Nevada,
    LA-9000-MS, Los Alamos National Laboratory,
    Los Alamos, N. Mex.

Champ, D. R., W. F. Merritt, and J. L. Young, 1982. "Potential
    for the Rapid Transport of Plutonium in Groundwater as
    Demonstrated by Core Column Studies," Scientific Basis for
    Nuclear Waste Management V, Materials Research Society
    Symposia Proceedings, Berlin, Germany, June 7-10, 1982,
    W. Lutze (ed.), Vol. 5, North-Holland, Elsevier Science
    Publishing Co., Inc., New York, pp. 745-754.

Christiansen, R. L., and H. R. Blank, Jr., 1972. Volcanic
    Stratigraphy of the Quaternary Rhyolite Plateau in
    Yellowstone National Park, Geological Survey Professional
    Paper 729-B, U.S. Geological Survey, Washington, D.C.

Claassen, H. C., 1973. Water Quality and Physical
    Characteristics of Nevada Test Site Water-Supply Wells,
    USGS-474-158, U.S. Geological Survey, Lakewood, Colo.

Claassen, H. C., 1985. Sources and Mechanisms of Recharge for
    Ground Water in the West-Central Amargosa Desert, Nevada--A
    Geochemical Interpretation, U.S. Geological Survey
    Professional Paper 712-F, U.S. Government Printing Office,
    Washington, D.C.

Coles, D. G., and L. D. Ramspott, 1982. "Migration of
    Ruthenium-106 in a Nevada Test Site Aquifer: Discrepancy
    Between Field and Laboratory Results," Science, Vol. 215,
    pp. 1235-1237.

Couture, R. A., 1985. "Rapid Increases in Permeability and
    Porosity of Bentonite-Sand Mixtures Due to Alteration by
    Water Vapor," Scientific Basis for Nuclear Waste Management
    VIII, Materials Research Society Symposia Proceedings,
    Boston, Massachusetts, November 26-29, 1984, C. M. Jantzen,
    J. A. Stone, and R. C. Ewing (eds.), Materials Research
    Society, Pittsburgh, Penn., pp. 515-522.

Craig, R. W., R. L. Reed, and R. W. Spengler, 1983.
    Geohydrologic Data for Test Well USW H-6, Yucca Mountain
    Area, Nye County, Nevada, USGS-OFR-83-856, Open-File Report,
    U.S. Geological Survey, Denver, Colo., 35 p.

Crank, J., 1975. The Mathematics of Diffusion, Second Edition,
    Oxford University Press, London, pp. 121-146, 331-333.

Croff, A. G., and C. W. Alexander, 1980. Decay Characteristics
    of Once-Through LWR and LMFBR Spent Fuels, High-Level Wastes,
    and Fuel-Assembly Structural Material Waste, ORNL/TM-7431,
    Oak Ridge National Laboratory, Oak Ridge, Tenn.

Crowe, B. M., and D. T. Vaniman, (comps.), 1985. Research and
    Development Related to the Nevada Nuclear Waste Storage
    Investigations, January 1 - March 31, 1984, LA-10154-PR,
    Los Alamos National Laboratory, Los Alamos, N. Mex.

Crowe, B. M., M. E. Johnson, and R. J. Beckman, 1982.
    "Calculation of the Probability of Volcanic Disruption of a
    High-Level Radioactive Waste Repository within Southern
    Nevada, USA," Radioactive Waste Management and the Nuclear
    Fuel Cycle, Vol. 3, No. 2, pp. 167-190.

Curtis, D. B., 1985. The Chemical Coherence of Natural Spent
    Fuel at the Oklo Nuclear Reactors, Technical Report 85-04,
    Svensk Karnbranslenhantering AB., Swedish Nuclear Fuel and
    Waste Management Co.

Curtis, D. B., and A. J. Gancarz, 1983. Radiolysis in
    Nature: Evidence from the Oklo Natural Reactors, Technical
    Report 83-10, Svensk Karnbransleforsorjning/Avdelning KBS.

DOE (U.S. Department of Energy), 1986. Final Environmental Assessment: Yucca Mountain Site, Nevada Research and Development Area, Nevada, DOE/RW-0073, Washington, D.C.

Daniels, W. R. (comp.), 1981. Laboratory and Field Studies Related to the Radionuclide Migration Project, October 1, 1979-September 30, 1980, LA-8670-PR, Los Alamos National Laboratory, Los Alamos, N. Mex.

Daniels, W. R., and J. L. Thompson (comps.), 1984. Laboratory and Field Studies Related to the Radionuclide Migration Project, October 1, 1982-September 30, 1983, LA-10121-PR, Los Alamos National Laboratory, Los Alamos, N. Mex.

Daniels, W. R., K. Wolfsberg, R. S. Rundberg, with others, 1982. Summary Report on the Geochemistry of Yucca Mountain and Environs, J. Heiken (ed.), LA-9328-MS, Los Alamos National Laboratory, Los Alamos, N. Mex.

Daniels, W. R., B. R. Erdal, and D. T. Vaniman (comps.), 1983. Research and Development Related to the Nevada Nuclear Waste Storage Investigations: July 1-September 30, 1982, LA-9577-PR, Los Alamos National Laboratory, Los Alamos, N. Mex.

Drever, J. I., 1982. "Colloid Properties," The Geochemistry of Natural Waters, Prentice Hall, New Jersey, pp. 78-89.

EPA (U.S. Environmental Protection Agency), 1976. Environmental Monitoring Report for the Nevada Test Site and Other Test Areas Used for Underground Nuclear Detonations, January through December, 1975, EMSL-LV-539-4, Las Vegas, Nev., p. 82.

Eisenbud, M., K. Krauskopf, E. P. Franca, W. Lei, R. Ballad, P. Linsalata, and K. Fujimori, 1984. "Natural Analogues for the Transuranic Actinide Elements: An Investigation in Minas Gerais, Brazil," Environmental Geological Water Science, Vol. 6, No. 1, pp. 1-9.

Freeze, R. A., and J. A. Cherry, 1979. Groundwater, Prentice-Hall, Inc., Englewood Cliffs, N.J. pp. 389-390, 551-552

Fried, S. M., A. M. Friedman, J. J. Hines, and L. A. Quarterman, 1975. Annual Report on DWMT Project ANO115A, FY 1975, ANL-75-64, Argonne National Laboratory, Argonne, Ill.

Gancarz, A. J., 1978. "U-Pb age (2.05 x 10-9 years) of the Oklo Uranium Deposit," Natural Fission Reactors, Symposium Proceedings, Paris, 1977, STI/PUB/475, International Atomic Energy Agency, Vienna, Austria, pp. 513-520.

Garrels, R. M., and C. L. Christ, 1965. Solutions, Minerals, and Equilibria, Freeman, Cooper, and Company, San Francisco, Calif., pp. 12-15, 50-51, 70-71, 262-263.

Gayer, K. H., and H. Leider, 1955. "The Solubility of Uranium Trioxide, UO_3H_2O, in Solutions of Sodium Hydroxide and Perchloric Acid at 25 degrees C," Journal of American Chemical Society, Vol. 77, pp. 1448-1450.

Goff, F. E., and C. O. Grigsby, 1982. "Valles Caldera Geothermal Systems, New Mexico, U.S.A.," Journal of Hydrology, Vol. 56, pp. 119-136.

Goff, F. E., and S. Sayer, 1980. A Geothermal Investigation of Spring and Well Waters of the Los Alamos Region, New Mexico, LA-8326-MS, Los Alamos National Laboratory, Los Alamos, N. Mex.

Goff, F. E., C. O. Grigsby, P. E. Trujillo, Jr., D. Counce, and A. Kron, 1981. "Geology, Water Chemistry and Geothermal Potential of the Jemez Springs Area, Canon de San Diego, New Mexico," Journal of Volcanology and Geothermal Research, Vol. 10, Elsevier Scientific Publishing Company, Amsterdam, pp. 227-244.

Goff, F. E., T. McCormick, P. E. Trujillo, Jr., D. Counce, and C. O. Grigsby, 1982. Geochemical Data for 95 Thermal and Nonthermal Waters of the Valles Caldera - Southern Jemez Mountains Region, New Mexico, LA-9367-OBES, Los Alamos National Laboratory, Los Alamos, N. Mex.

Hay, R. L., 1978. "Geologic Occurrence of Zeolites," Natural Zeolites: Occurrence, Properties, Use, L. B. Sand and F. A. Mompton (eds.), Pergamon Press, New York, pp. 135-143.

Hay, R. L., and R. A. Sheppard, 1977. "Zeolites in Open Hydrologic Systems," Mineralogy and Geology of Natural Zeolites, F. A. Mumpton (ed.), Mineralogical Society of America Short Course Notes, Vol. 4, pp. 93-102.

Heiken, G. H., and M. L. Bevier, 1979. Petrology of Tuff Units from the J-13 Drill Site, Jackass Flats, Nevada, LA-7563-MS, Los Alamos National Laboratory, Los Alamos, N. Mex.

Hoffman, D. C., and W. R. Daniels, 1981. Assessment of the Potential for Radionuclide Migration From a Nuclear Explosion Cavity, LA-UR-81-3181; CONF-811211--1; Los Alamos National Laboratory, Los Alamos, N. Mex.

Hoffman, D. C., R. Stone, and W. W. Dudley, Jr., 1977. Radioactivity in the Underground Environment of the Cambric Nuclear Explosion at the Nevada Test Site, LA-6877-MS, Los Alamos National Laboratory, Los Alamos, N. Mex.

Honda, S., and L. J. P. Muffler, 1970. "Hydrothermal Alteration in Core from Research Drill Hole Y-1, Upper Geyser Basin, Yellowstone National Park, Wyoming," The American Mineralogist, Vol. 55, pp. 1714-1737.

Hulen, J. B., and D. L. Nielson, 1985. "Hydrothermal Alteration in the Baca Geothermal System, Redondo Dome, Valles Caldera, New Mexico," Journal of Geophysical Research.

Isherwood, D., 1985. Application of the Ruthenium and Technetium Thermodynamic Data Bases Used in the EQ3/6 Geochemical Codes, UCRL-53594; Lawrence Livermore National Laboratory, Livermore, Calif.

Johnston, H. S., 1966. Gas Phase Reaction Rate Theory, The Ronald Press Company, New York, pp. 102-103.

Keith, T. E. C., and L. J. P. Muffler, 1978. "Minerals Produced during Cooling and Hydrothermal Alteration of Ash Flow Tuff from Yellowstone Drill Hole Y-5," Journal of Volcanology and Geothermal Research, Vol. 3, pp. 373-402.

Keith, T. E. C., D. E. White, and M. H. Beeson, 1978. Hydrothermal Alteration and Self-Sealing in Y-7 and Y-8 Drill Holes in Northern Part of Upper Geyser Basin, Yellowstone National Park, Wyoming, Geological Survey Professional Paper 1054-A, U.S. Geological Survey, Washington, D.C.

Keith, T. E. C., J. M. Thompson, and R. E. Mays, 1983.
"Selective Concentration of Cesium in Analcime during
Hydrothermal Alteration, Yellowstone National Park, Wyoming,"
Geochimica et Cosmochimica Acta, Vol. 47, pp. 795-804.

Keith, T. E. C., K. E. Bargar, S. S. Howe, W. W. Carothers, and
I. Barnes, 1984a. "Mineralogical Studies of the Hydrothermal
System in Newberry Volcano Drill Hole 2, Oregon," Geothermal
Resources Council Transactions, Vol. 8, pp. 125-128.

Keith, T. E. C., R. H. Mariner, K. E. Bargar, W. C. Evans, and
T. S. Presser, 1984b. "Hydrothermal Alteration in Oregon's
Newberry Volcano No. 2: Fluid Chemistry and Secondary
Mineral Distribution," Geothermal Resources Council Bulletin,
pp. 9-17.

Kerrisk, J. F., 1983. Reaction-Path Calculations of Groundwater
Chemistry and Mineral Formation at Rainier Mesa, Nevada,
LA-9912-MS, Los Alamos National Laboratory, Los Alamos,
N. Mex.

Kerrisk, J. F., 1984a. Americium Thermodynamic Data for the
EQ3/6 Database, LA-10040-MS, Los Alamos National Laboratory,
Los Alamos, N. Mex.

Kerrisk, J. F., 1984b. Solubility Limits on Radionuclide
Dissolution at a Yucca Mountain Repository, LA-9995-MS,
Los Alamos National Laboratory, Los Alamos, N. Mex.

Kerrisk, J. F., 1985. An Assessment of the Important
Radionuclides Nuclear Waste, LA-10414-MS, Los Alamos National
Laboratory, Los Alamos, N. Mex.

Kerrisk, J. F., 1987. Groundwater Chemistry at Yucca Mountain,
Nevada, and Vicinity, LA-10929-MS, Los Alamos National
Laboratory, Los Alamos, N. Mex.

Kim, J. I., CH. Lierse, and F. Baumgartner, 1983. "Complexation
of Plutonium(IV) Ion in Carbonate-Bicarbonate Solutions,"
Plutonium Chemistry, W. T. Carnall and G. R. Choppin (eds.),
American Chemical Society Symposium Series 216, pp. 317-334.

Kim, J. I., G. Backua, F. Baumgartner, H. C. Moon, and D. Lux,
1984a. "Colloid Generation and Actinide Migration in
Gorleben Groundwaters," Scientific Basis for Nuclear Waste
Management VII, Materials Research Society Symposia

Proceedings, Boston, Massachusetts, November 1983,
G. L. McVay (ed.), Vol. 26, North-Holland, Elsevier Science
Publishing Co., Inc., New York, pp. 31-40.

Kim, J. I., M. Bernkopf, CH. Lierse, and F. Koppold, 1984b.
"Hydrolysis Reactions of Am(III) and Pu(VI) Ions in
Near-Neutral Solutions," Geochemical Behavior of Disposed
Radioactive Waste, 185th Meeting of the American Chemical
Society, Seattle, Wash., March 20-25, 1983, G. S. Barney,
J. D. Navratil and W. W. Schulz (eds.), ACS Symposium Series
246, American Chemical Society, Washington, D.C.,
pp. 115-134.

Kistler, R. W., 1968. "Potassium-Argon Ages of Volcanic Rocks in
Nye and Esmeralda Counties," Nevada Test Site, E. B. Eckel
(ed.), Geological Society of America Memoir 110, Boulder,
Colo., pp. 251-262.

Knauss, K. G., and W. B. Beiriger, 1984. Report on Static
Hydrothermal Alteration Studies of Topopah Spring Tuff Wafers
in J-13 Water at 150 deg. C, UCRL-53576, Lawrence Livermore
National Laboratory, Livermore, Calif.

Koster van Groos, A. F., and S. Guggenheim, 1984. "The Effect of
Pressure on the Dehydration Reaction of Interlayer in
Na-Montmorillonite (SWy-1)," American Mineralogist, Vol. 69,
pp. 872-879.

Koster van Groos, A. F., and S. Guggenheim, 1986. "Dehydration
of K-Exchanged Montmorillonite at Elevated Temperatures and
Pressures," Clays and Clay Minerals, Vol. 34, No. 3,
pp. 281-286.

Krupka, K. M., D. Rai, R. W. Fulton, and R. C. Strickert, 1984.
Solubility Data for U(VI) Hydroxide and Np(IV) Hydrous
Oxide: Application of MCC-3 Methodology, PNL-SA-12324,
Pacific Northwest Laboratory, Richland, Wash.

Le Page, Y., and G. Donnay, 1976. "Refinement of the Crystal
Structure of Low-Quartz," Acta Crystallographica, Vol. B32,
pp. 2456-2459.

Lemire, R. J., and P. R. Tremaine, 1980. "Uranium and Plutonium
in Equilibria in Aqueous Solutions to 200 degrees C," Journal
of Chemical and Engineering Data, Vol. 25, No. 4,
pp. 361-370.

Levy, S. S., 1984a. Petrology of Samples from Drill Holes USW H-3, H-4 and H-5, Yucca Mountain, Nevada, LA-9706-MS, Los Alamos National Laboratory, Los Alamos, N. Mex.

Levy, S. S., 1984b. "Studies of Altered Vitrophyre for the Protection of Nuclear Waste Repository-Induced Thermal Alteration at Yucca Mountain, Nevada," Scientific Basis for Nuclear Waste Management VII, Materials Research Society Symposia Proceedings, Boston, Massachusetts, November 1983, G. L. McVay (ed.), Vol. 26, North-Holland, Elsevier Science Publishing Co., Inc., New York, pp. 959-966.

Levy, S. S., 1987. Alteration Products and Processes in the Lower Topopah Spring Member of the Paintbrush Tuff, Yucca Mountain, and Vicinity, Nevada, LA-10677-MS, Los Alamos National Laboratory, Los Alamos, N. Mex.

Lindberg, R. D., and D. D. Runnells, 1984. "Ground Water Redox Reactions: An Analysis of Equilibrium State Applied to Eh Measurements and Geochemical Modeling," Science, Vol. 225, pp. 925-927.

Link, R. L., S. E. Logan, H. S. Ng, F. A. Rockenbach, and K. J. Hong, 1982. Parametric Studies of Radiological Consequences of Basaltic Volcanism, SAND81-2375, Sandia National Laboratories, Albuquerque, N. Mex., pp. 4-347.

Lipman, P. W., R. L. Christiansen, and J. T. O'Connor, 1966. A Compositionally Zoned Ash-Flow Sheet in Southern Nevada, Geological Survey Professional Paper 525-F, U.S. Geological Survey, Washington, D.C.

Lundqvist, R., 1982. "Hydrophilic Complexes of the Actinides. I. Carbonates of Trivalent Americium and Europium," Acta Chemica Scandinavica, Vol. A 36, pp. 741-750.

Means, J. L., A. S. Maest, and D. A. Crerar, 1983. Organic Geochemistry of Deep Ground Waters and Radionuclide Partitioning Experiments Under Hydrothermal Conditions, ONWI-448, Office of Nuclear Waste Isolation, Battelle Memorial Institute, Columbus, Ohio.

Meyer, R. E., W. D. Arnold, J. G. Blencoe, G. D. O'Kelley, R. I. Case, J. F. Land, and G. K. Jacobs, 1986. Progress in Evaluation of Radionuclide Geochemical Information Developed by DOE High-Level Nuclear Waste Repository Site

Projects: Semi-Annual Report for October 1985 - March 1988, NUREG/CR-4708, Vol. 1, No. 1, U.S. Nuclear Regulatory Commission, Washington, D.C.

Miller, L. J., 1958. "The Chemical Environment of Pitchblende," Economic Geology, Vol. 53, pp. 521-545.

Montazer, P., and W. E. Wilson, 1984. Conceptual Hydrologic Model of Flow in the Unsaturated Zone, Yucca Mountain, Nevada, USGS-WRI-84-4345, Water-Resources Investigations Report, U.S. Geological Survey, Lakewood, Colo.

Mumpton, F. A., 1960. "Clinoptilolite Redefined" American Mineralogist, Vol. 45, pp. 351-369.

NRC (U.S. Nuclear Regulatory Commission), 1984. Determination of Radionuclide Solubility in Groundwater for Assessment of High-Level Waste Isolation, U.S. Nuclear Regulatory Commission Technical Position.

NRC (U.S. Nuclear Regulatory Commission), 1987. Standard Format and Content of Site Characterization Plans for High-Level-Waste Geological Repositories, Regulatory Guide 4.17, Washington, D.C.

Naudet, R., 1978. "Synthese Des Donnees Concernant La Stabilite Et Les Remobilisations De L'Uranium Et Des Terres Rares," in Le Ruacteurs de Fission Naturels, Symposium Proceedings, Paris, 1977, STI/PUB/475/IAEA-TC-119/25 International Atomic Energy Agency, Vienna, Austria, pp. 643-676.

Needham, R. S., and P. G. Stuart-Smith, 1980. "Geology of the Alligator Rivers Uranium Field," in Proceedings of the International Uranium Symposium on the Pine Creek Geosyncline, Sydney, 1979, J. Ferguson and A. B. Goloby (eds.), STI/PUB/555, International Atomic Energy Agency, Vienna, Austria, pp. 233-257.

Neretnieks, I., 1980. "Transport Mechanisms and Rates of Transport of Radionuclides in the Geosphere as Related to the Swedish KBS Concept," in Underground Disposal of Radioactive Wastes, Vol. II, Proceedings of a Symposium, Otaniemi, 2-6 July 1979, IAEA-SM-243/108, International Atomic Energy Agency (IAEA), Vienna, Austria, pp. 315 339.

Newton, T. W., and V. L. Rundberg, 1984. "Disproportionation and Polymerization of Plutonium(IV) in Dilute Aqueous Solutions," Scientific Basis for Nuclear Waste Management VII, Materials Research Society Symposia Proceedings, Boston, Massachusetts, November 1983, G. L. McVay (ed.), Vol. 26, North-Holland, Elsevier Science Publishing, Inc., New York, pp. 867-873.

Nitsche, H., and N. M. Edelstein, 1985. Determination of Solubilities and Complexation of Waste Radionuclides Pertinent to Geologic Disposal at the Nevada Tuff Site, LBL-18900, Lawrence Berkeley Laboratory, Berkeley, Calif.

Nyhan, J. W., B. J. Drennon, W. V. Abeele, M. L. Wheeler, W. D. Purtymun, G. Trujillo, W. J. Herrera, and J. W. Booth, 1985. "Distribution of Plutonium and Americium Beneath a 33-yr-old Liquid Waste Disposal Site," Journal of Environmental Quality, Vol. 14, pp. 501-509.

Ogard, A. E., and J. F. Kerrisk, 1984. Groundwater Chemistry Along Flow Paths Between a Proposed Repository Site and the Accessible Environment, LA-10188-MS, Los Alamos National Laboratory, Los Alamos, N. Mex.

Ogard, A. E., and D. T. Vaniman (comps.), 1985. Research and Development Related to the Nevada Nuclear Waste Storage Investigations, July 1-September 30, 1984, LA-10299-PR, Los Alamos National Laboratory, Los Alamos, N. Mex.

Ogard, A. E., W. R. Daniels, and D. T. Vaniman (comps.) 1983a. Research and Development Related to the Nevada Nuclear Waste Storage Investigations, October 1-December 31, 1982, LA-9666-PR, Los Alamos National Laboratory, Los Alamos, N. Mex.

Ogard, A. E., K. Wolfsberg, and D. T. Vaniman (comps.) 1983b. Research and Development Related to the Nevada Nuclear Waste Storage Investigations, April 1-June 30, 1983, LA-9846-PR, Los Alamos National Laboratory, Los Alamos, N. Mex.

Olofsson, U., B. Allard, K. Andersson, and B. Torstenfelt, 1981. Formation and Properties of Radiocolloids in Aqueous Solution—A literature Survey, National Council for Radioactive Waste Report Prav 4.25, Department of Nuclear Chemistry, Chalmers University of Technology, Goteborg, Sweden.

Olofsson, U., B. Allard, B. Torstenfelt, and K. Andersson,
    1982a. "Properties and Mobilities of Actinide Colloids in
    Geologic Systems," Scientific Basis for Nuclear Waste
    Management V, Materials Research Society Symposia
    Proceedings, Berlin, Germany, June 7-10, 1982, W. Lutze
    (ed.), Vol. 5, North-Holland, Elsevier Science Publishing
    Co., Inc., New York, pp. 755-764.

Olofsson, U., B. Allard, K. Andersson, and B. Torstenfelt,
    1982b. "Formation and Properties of Americium Colloids in
    Aqueous Systems," Scientific Basis for Nuclear Waste
    Management, Materials Research Society Symposia Proceedings,
    Boston, Massachusetts, November 1981, S. Topp (ed.), Vol. 6,
    North-Holland, Elsevier Science Publishing Co., Inc.,
    New York, pp. 191-198.

Olofsson, U., M. Bengtsson, and B. Allard, 1984. "Generation and
    Transport Properties of Colloidal Tri- and Tetravalent
    Actinide Species in Geologic Environments," Scientific Basis
    for Nuclear Waste Management VII, Materials Research Society
    Symposia Proceedings, Boston, Massachusetts, November 1983,
    G. L. McVay (ed.), Vol. 26, North-Holland, Elsevier Science
    Publishing Co., Inc., New York, pp. 859-866.

Orkild, P. P., 1965. "Paintbrush Tuff and Timber Mountain Tuff
    of Nye County, Nevada," Changes in Stratigraphic Nomenclature
    by the U.S. Geological Survey 1964, G. V. Cohee and
    W. S. West (eds.), U.S. Geological Survey Bulletin 1224-A,
    Washington, D.C., pp. A44-A51.

Osmond, J. K., and J. B. Cowart, 1981. Uranium-Series
    Disequilibrium in Ground Water and Core Composite Samples
    from the San Juan Basin and Copper Mountain Research Sites,
    Report GJBX 364(81), Department of Geology, Florida State
    University, Tallahassee.

Peacor, D. R., 1973. "High-Temperature Single-Crystal Study of
    the Cristobalite Inversion," Zeitschrift fur
    Kristallographie, Vol. 138, pp. 274-298.

Perkins, B., B. Travis, and G. DePoorter, 1985. Validation of
    the TRACR3D Code for Soil Water Flow Under
    Saturated/Unsaturated Conditions in Three Experiments,
    LA-10263-MS, Los Alamos National Laboratory, Los Alamos,
    N. Mex.

Phillips, F. M., F. Goff, F. Vautaz, H. W. Bentley, D. Elmore, and H. E. Gove, 1984. "36-Cl as a Tracer in Geothermal Systems: Example from Valles Caldera, New Mexico," Geophysical Research Letters, Vol. 11, No. 12, pp. 1227-1230.

Rai, D., 1984. "Solubility Product of Pu(IV) Hydrous Oxide and Equilibrium Constants of Pu(IV)/Pu(V), Pu(IV)/Pu(VI), and Pu(V)/Pu(VI) Couples," Radiochimica Acta, Vol. 35, pp. 97-106.

Rai, D., and J. L. Ryan, 1982. "Crystallinity and Solubility of Pu(IV) Oxide and Hydrous Oxide in Aged Aqueous Suspensions," Radiochimica Acta, Vol. 30, pp. 213-216.

Rai, D., and J. L. Ryan, 1984. "Solubility Constraint: An Important Consideration in Safety Assessment of Nuclear Waste Disposal," Scientific Basis for Nuclear Waste Management VII, Materials Research Society Symposia Proceedings, Boston, Massachusetts, November, 1983, G. L. McVay (ed.), Vol. 26, North-Holland, Elsevier Science Publishing Co., Inc., New York, pp. 805-815.

Rai, D., and R. J. Serne, 1978. Solid Phases and Solution Species of Different Elements in Geologic Environments, PNL-2651, Pacific Northwest Laboratory, Richland, Wash.

Rai, D., and J. L. Swanson, 1981. "Properties of Plutonium (IV), Polymer of Environmental Importance," Nuclear Technology, Vol. 54, No. 1, pp. 107-112.

Rai, D., R. J. Serne, and D. A. Moore, 1980. "Solubility of Plutonium Compounds and Their Behavior in Soils," Soil Science Society of America Journal, Vol. 44, pp. 490-495.

Rai, D., R. G. Strickert, D. A. Moore, and J. L. Ryan, 1983. "Am(III) Hydrolysis Constants and Solubility of Am(III) Hydroxide," Radiochimica Acta, Vol. 33, pp. 201-206.

Rard, J. A., 1983. Critical Review of the Chemistry and Thermodynamics of Technetium and Some of Its Inorganic Compounds and Aqueous Species, UCRL-53440, Lawrence Livermore National Laboratory, Livermore, Calif.

Robins, R. G., 1966. "Hydrolysis of Uranyl Nitrate Solutions at
   Elevated Temperatures," Journal of Inorganic and Nuclear
   Chemistry, Vol. 28, pp. 119-123.

Rossotti, F. J. C., and H. Rossotti, 1961. The Determination of
   Stability Constants and Other Equilibrium Constants in
   Solution, McGraw-Hill Book Company, New York, pp. 270-271.

Ruffenach, J. C., R. Hagemann, and E. Roth, 1980. "Isotopic
   Abundances Measurements a Key to Understanding the Oklo
   Phenomenon," Z. Naturforsch, Vol. 35a, pp. 171-179.

Rundberg, R. S., 1985. Assessment Report on the Kinetics of
   Radionuclide Adsorption on Yucca Mountain Tuff, Los Alamos
   National Laboratory, Los Alamos, N. Mex.

Rundberg, R. S., A. E. Ogard, and D. T. Vaniman, 1985. Research
   and Development Related to the Nevada Nuclear Waste Storage
   Investigations, April 1-June 30, 1984, LA-10297-PR,
   Los Alamos National Laboratory, Los Alamos, N. Mex.

Sass, J. H., and A. H. Lachenbruch, 1982. Preliminary
   Interpretation of Thermal Data from the Nevada Test Site,
   USGS-OFR-82-973, Open-File Report, U.S. Geological Survey,
   Denver, Colo.

Sauty, J.-P., 1980. "An Analysis of Hydrodispersive Transfer in
   Aquifers," Water Resources Research, Vol. 16, No. 1,
   pp. 145-158

Scott, R. B., and J. Bonk, 1984. Preliminary Geologic Map of
   Yucca Mountain, Nye County, Nevada, with Geologic Sections,
   USGS-OFR-84-494, Open-File Report, U.S. Geological Survey,
   Denver, Colo.

Scott, R. B., R. W. Spengler, S. Diehl, A. R. Lappin, and
   M. P. Chornak, 1983. "Geologic Character of Tuffs in the
   Unsaturated Zone at Yucca Mountain, Southern Nevada," Role of
   the Unsaturated Zone in Radioactive and Hazardous Waste
   Disposal, J. W. Mercer, P. S. C. Rao, and I. W. Marine
   (eds.), Ann Arbor Science Publishers, Ann Arbor, Mich.,
   pp. 289-335.